Smart Energy Solutions to Smart Grid Challenges

by

Nelson Xuntuo Wang

M.B.A. Minor, Harvard University (2019)
S.M., Massachusetts Institute of Technology (2014)
B.S., General Motors Institute, UMich (2012)

Submitted to the Department of Electrical Engineering and Computer Science
in partial fulfillment of the requirements for the degree of

Doctor of Philosophy in Electrical Engineering and Computer Science

at the

MASSACHUSETTS INSTITUTE OF TECHNOLOGY

September 2020

Author .....
Department of Electrical Engineering and Computer Science
August 28, 2020

Certified by .....
James L. Kirtley Supervisor
Professor of Electrical Engineering and Computer Science
Thesis Supervisor

Accepted by .....
Leslie A. Kolodziejski
Professor of Electrical Engineering and Computer Science
Chair, Department Committee on Graduate Students

Smart Energy Solutions to Smart Grid Challenges

by

Nelson Xuntuo Wang

Submitted to the Department of Electrical Engineering and Computer Science
on August 28, 2020, in partial fulfillment of the
requirements for the degree of
Doctor of Philosophy in Electrical Engineering and Computer Science

Abstract

The smart micro-grid is an energy network, and researchers have spent decades working on technology development. Among most existing solutions, they focus on dynamic operation and stability issues, however the smart grid still exhibit these challenges: the electric energy network has complicated system structure, high cost, and low energy efficiency in operation. In light of popular applications, this thesis analyzes the smart grid at the local (residential) level into two categories: high-power network - electric network dealing with electric vehicles (EVs), and low-power network - electronics network dealing with smart mobile phones.

This thesis proposes a centralization approach to tackle these addressed problems. On the electric network side, current micro-grid systems with high penetration of electric vehicles (EVs) have a bulky and low energy efficiency system to connect solar panels and the utility with EV batteries. This work proposes a smart and efficient EV charger to be the hub to make the system more energy efficient; On the electronics network side, multi-use application requires multiple power converters, this work proposes a centralized wireless power transfer system to be the hub charging multiple phones and low power devices using the grid power. Data mining is applied to the operation analysis of the electric network on economics where optimization strategies are discussed.

Thesis Supervisor: James L. Kirtley Supervisor
Title: Professor of Electrical Engineering and Computer Science

Acknowledgments

My doctoral work is a special one, especially after I was diagnosed with sleep apnea in 2015, an illness has very similar symptoms on hard breathing as COVID-19. With a 15-pound sleep machine for 3 years then a major operation at a hospital, I suffered, survived, and felt reborn. This work is impossible without your support.

First, I would like to thank my dear parents and family for their generous support throughout my entire life. My significant other Celia, has been supporting and challenging me in various ways.

Prof. James Kirtley, my thesis supervisor and life mentor, who has been guiding me in many different perspectives, your support has raised me up to more than I can be. Prof. Jeffrey Lang, my academic advisor, always being patient and humble, your wisdom really inspired me on everything. Dr. Robert Stoner, thanks for your generous time providing directions from your busy schedule, your keen insights on energy systems for developing countries inspired me with a vision of making portable yet cost-effective technologies.

I would like to thank my co-founders, advisors, and employees of my tech start-up companies in energy and healthcare, and fellow entrepreneurs at Forbes community.

I would like to thank the beloved LEES members for contributing to such a lovely community, groups of Professor Kirtley, Professor Perreault, Professor Kassakian, Professor Lang and Professor Leeb, my collaborators Chris, Jamey, Sajjad, Jin, and my mentees through Undergraduate Research Opportunities (UROP) Program, Henry on wireless power transfer system project, PJ, and Jackson on battery management system project .

I would like to thank my Chinese basketabll team members, Wujie, Yu, Xiangming, Yongbin, Hongyu, Rong, Kaichao, Jiexi, the best championship team and all-star plays.

Last but not least, I would like to thank project sponsors - MITEI, MIT Innovation Initiative, and Mac McQuown, owner of Stone Edge Farm in Sonoma, CA.

Thank you for all of your support. I am deeply grateful.

Contents

List of Figures

List of Tables

Chapter 1

Introduction

1.1 Background

. Smart micro-grid applications [12–28] have grown enormously in the past decade, but the industry lacks a device that is smart enough to interact with each component of this system. This thesis focuses on developing a centralized methodology to tackle this challenge, so that people in the future will be able to use solar energy to power their homes and electric car and use batteries for multi-purpose tasks more effectively and efficiently. The information cluster processing energy transfer on solar energy, the grid, and batteries is referred to as energy internet, in which the internet collects all the data, it is imperative to have a device to absorb energy information so that the system features the most efficient architecture. The ultimate goal is that clean energy will be used anywhere and anytime. Then a problem arises: clean energy is a complex system which has various energy sources. How do we connect them more effectively and efficiently? In order to solve the increasing need for the renewable energy world, this work proposes developing a smart hub that can connect electric vehicle, solar, energy storage, and the grid together. This work focuses on the micro-grid with high penetration of electric vehicles (EVs): solar power, EVs, batteries, and the utility. As the Internet needs information routers, the energy world will need energy routers. With respect to this energy router, we can apply smart AI machine learning techniques. With the AI tools, can we let the machine learn scalable supervi-

sion? Can we train the machine to have a strong robustness to the complicated input network? An extensive study in this interdisciplinary field is conducted. This work will combine the traditional knowledge of the power system and power electronics with data mining to train the system to be smarter, in a way that it can operate the complex network effectively and efficiently. Data Mining, a statistical way to analyze the numerical data and optimize the system performance, is a highly useful tool in the energy domain.

The high-power electric network is discussed above, what about low-power electronic network where massive cellphones, tablet computers and electronic watches are used? This network will be much more efficient if something can serve as a hub connecting these them with the grid. While 5G wireless communication is coming around the corner, a multi-charging wireless power transfer system that can provide uniform magnetic field in the 3-D space is the problem-solver.

To sum up, this thesis investigates innovative tools that can centralize the system structure to make the energy network easier to operate and function, resulting in higher energy efficiency, lower cost, and enhanced flexibility.

1.2 Motivation

The key challenges for smart-grids at the distribution levels are summarized as high cost (both materials cost and maintenance cost) and low energy efficiency operation, which are determined by their complicated structures - multiple separated power electronics systems dealing with power conversion.

This thesis proposes a smart methodology that can integrate all power electronics systems into one single system. This can be implemented through bi-directional power flow and multi-user wireless power transfer techniques.

Therefore, this work summarizes two approaches based on a hybrid AC-DC system architecture: Electric Network (High Power) - developing an integrated system to connect the system efficiently Electronic Network (Low Power) - developing a wireless power transfer system that can charge multiple electronic loads simultaneously.

1.3 Electric Vehicles

Electric Vehicles (EVs) have been around for over one hundred years, but their recent development and deployment has been significantly increased due to radical government regulations and reduced cost of batteries in the past decade. EV is essentially an electric system that contains energy storage which provides energy, energy drive (includes electric motor) which consumes energy, and auxiliary parts for interface.

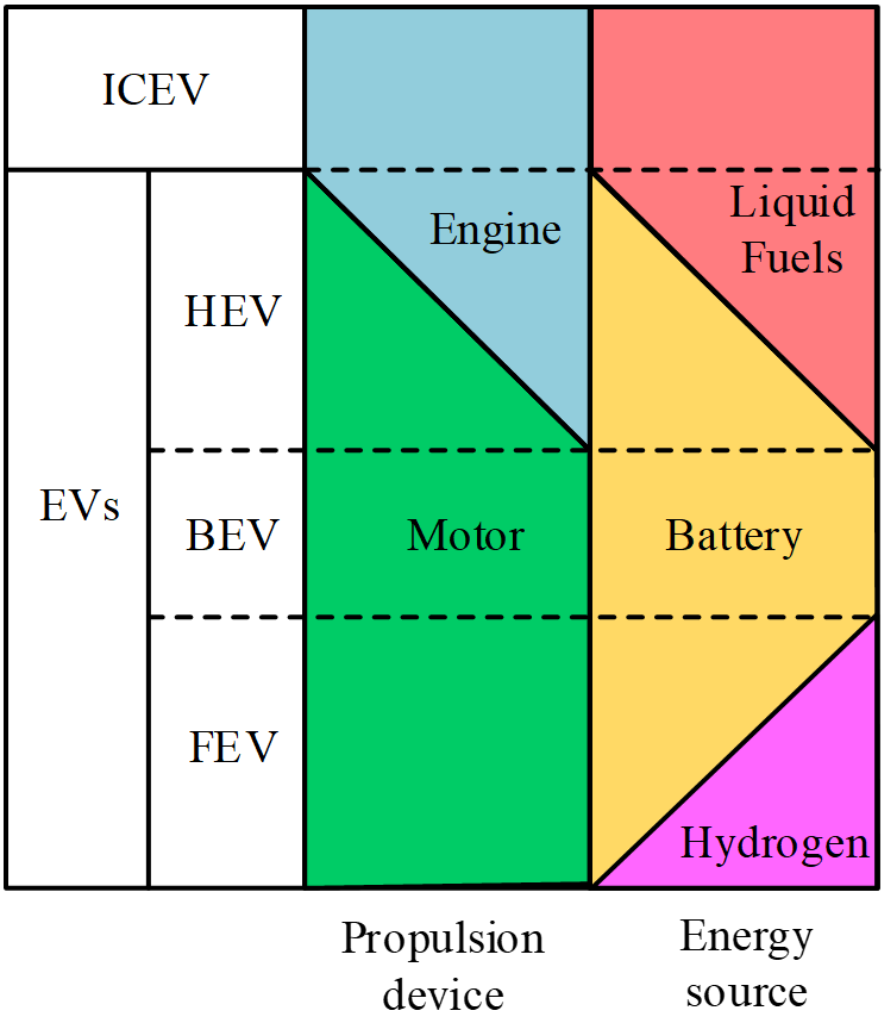

Figure 1-1: Classification of EV. ICEV - Internal Combustion Engine Vehicle, HEV - Hybrid Electric Vehicle, BEV - Battery Electric Vehicle, PEV - Plug-In Electric Vehicle. Picture Sourced from our paper "Electric Drives and Power Chargers: Recent Solutions to Improve Performance and Energy Efficiency for Hybrid and Fully Electric Vehicles", 2020 [1].

The class of EVs, shown in Fig. 1-1, includes all type of vehicles where at least

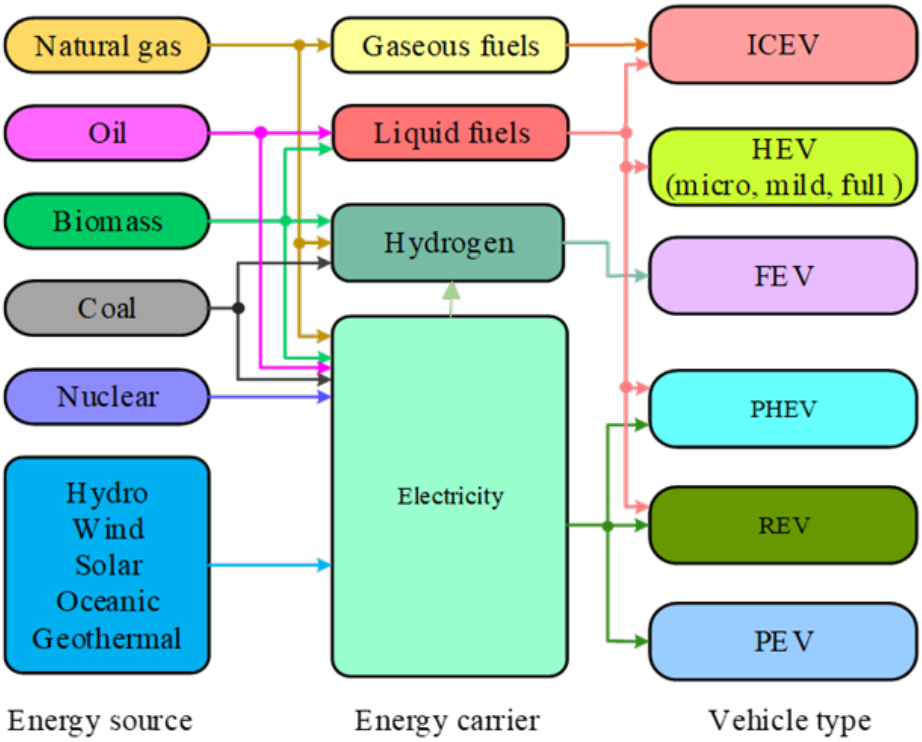

Figure 1-2: Energy Source Diversification of EV. Picture Sourced from our paper "Electric Drives and Power Chargers: Recent Solutions to Improve Performance and Energy Efficiency for Hybrid and Fully Electric Vehicles", 2020 [1].

part of the propulsion energy comes from an electric motor. Depending on the energy source (batteries, hydrogen, fuel) and the propulsion device (ICE or electric motor) many types of EV can be defined. In Fig. 1-1 the three main EV types are highlighted, namely battery EV (BEV), Fuel-cell EV (FEV) and Hybrid EV (HEV). Due to many production and distribution issues of hydrogen, the main interest today is on HEV and BEV, on which the thesis is focused. In case the on-board energy storage unit is re-charged by "plugging it in" to a charging station, the vehicle is named plug-in HEV (PHEV) or EV (PEV). Hereafter, the main reasons for the current trend on vehicle electrification are discussed: - Energy source diversification. The electrification of vehicles allows for a diversification of energy sources, including the exploitation of renewable sources (e.g. hydro, solar, wind) to obtain the electricity, see Fig. 1-2(in such case the acronym REV-Renewable Electric Vehicle is introduced).

EVs have two advantages over conventional ICEVs: First, pollutant emission re-

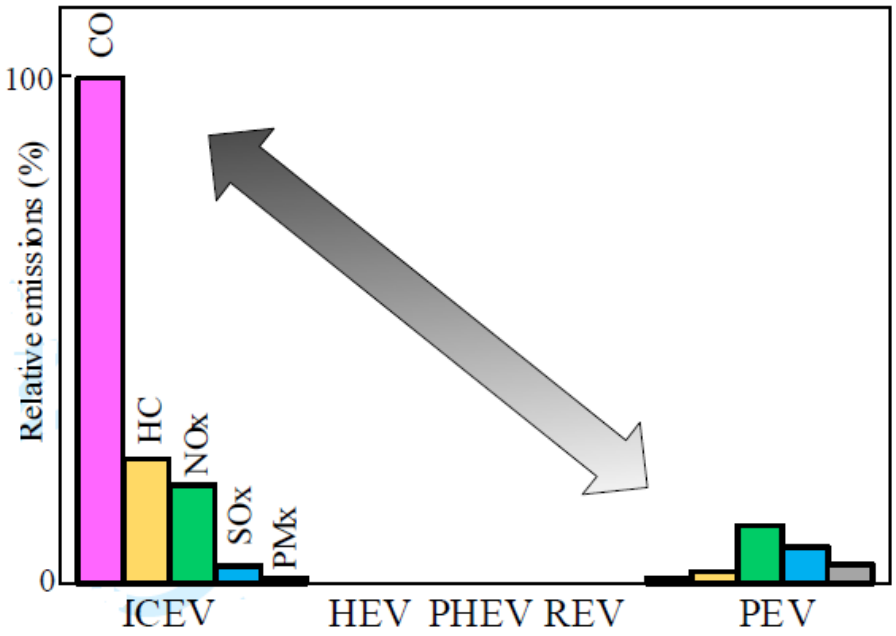

Figure 1-3: Relative Emission of ICEV vs PEV on Percentage Scale, date used from [2–9]. CO - Carbon Monoxide, HC - Hydrocarbons, NOx - Nitrogen Oxides, SOx - Sulfur Oxides, PMx - Particulate matters. Picture Sourced from Our Paper [1].

duction. As presented in Fig. 1-3, the emissions are dramatically reduced moving from ICEV to PEV. Second, energy efficiency increase. The efficiency in the use of energy, considering for a fair comparison in both cases of ICEV and BEV crude oil as initial energy source, is increased from about 13% of ICEV to 18% of PEV in Fig. 1-4.

The trend in vehicle design for the 21st century is the electrification of propulsion [2–9], mainly to reduce the emission of pollution (e.g. CO, NOx, CO2, SOx) in the air, and to reduce the use of fossil fuels. The evolution towards electric and hybrid mobility has been accelerated by the "dieselgate" in Europe and US [29], and by the high economic cost, for cars equipped with conventional internal combustion engines (ICE), to face restrictive regulations about greenhouse gases. Key components to enable such revolution in the electrification are power converters [30], as well as electric machines and energy storage components [31–33]. Allowed CO2 emissions in US, EU, Japan and China have been reduced from about 200 g of CO2 per travelled km in the 2000s to less than 100 g/km in 2020, for example. With EURO 6.2 regulation CO2

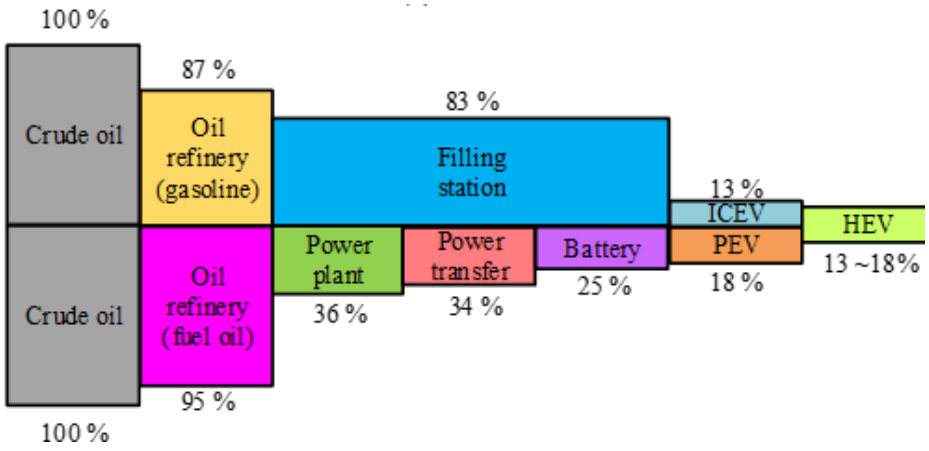

Figure 1-4: Energy efficiency of EV vs Conventional ICEV without renewable sources, some waste can be eliminated with renewable sources. Picture Sourced from Our Paper [1].

emissions in Europe should be reduced within the limit of 95 g/km [31]. Moreover, homologation cycles have been also modified, increasing more deceleration and acceleration phases. Indeed, from the NEDC (New European Driving Cycle) in 1997 to the new WLTP (Worldwide Harmonized Light Vehicles Test Procedure) developed by the United Nations Economic Commission for European (UN/ECE/WP29) in 2017 ,the percentage of the cycle in acceleration and deceleration modes have been increased from 15.5% and 22.4% in NEDC to 41.5% and 42.2% in WLTP, respectively [31]. Full Electric Vehicles (EV) are already a reality for low-volume premium car brands, like Tesla, but several large-volume car makers have announced a reduction in the number of all petrol/diesel vehicles. For example, in Europe the take rate (visitor to offer taker conversion rate) of diesel cars is predicted to decrease from 48% in 2014 to 15% (worst case) in 2024 [32].

Fig. 1-5 shows electric vehicle architecture. Concerning positioning of electric motor in a HEV or full EV, in HEV the electric machine can be placed directly on the ICE, position PO in Fig. 6, this is the case of Belt-driven Starter Generator (BSG), or between the ICE and the gearbox, eventually separated by a clutch, (positions P1 and P2) or on the gearbox (position P3) or beyond such as rear axle or tightly coupled with the driving wheels (position P4). In Full EV mainly the last types of positioning are considered.

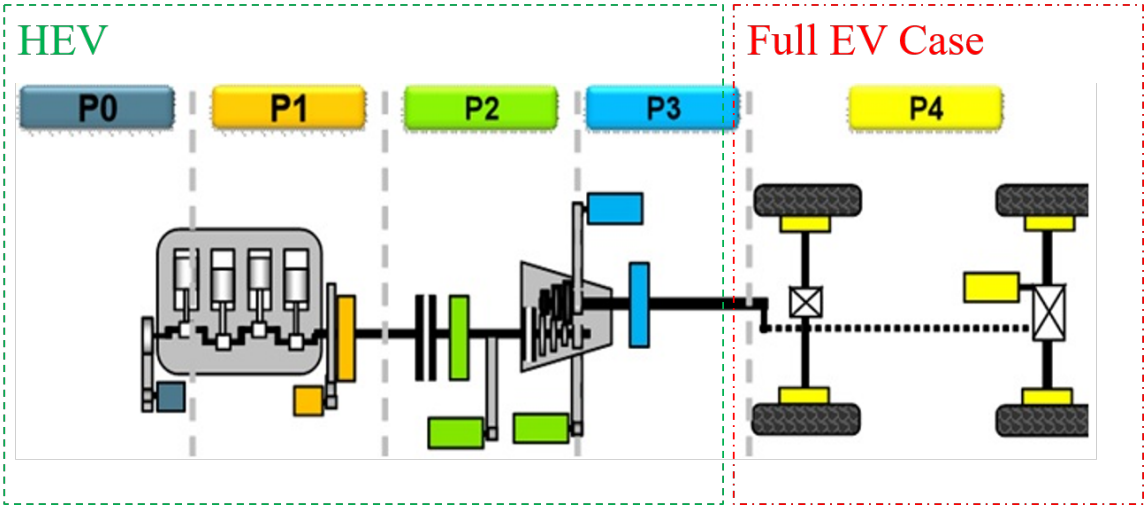

Figure 1-5: Hybrid EV Architecture. Picture Sourced from Our Paper [1]. P - Position.

Besides electric motors, power electronics plays an important role in battery charging/discharging and interaction with the grid, and further renewable energy sources (RES). Hence, a bidirectional EV charger described in chapter 3 is developed to achieve the addressed topics in the context of smart grid that has RES. Li-ion batteries are widely used due to their high power and energy density, and they serve as an energy storage unit connecting to the smart grid and to a RES such as PV panels in our focused application. This leads to a hub connection discussion: the current industry lacks an efficient integrated connection system since PV panels are not directly connected to the EV charger, see Fig. 2-3a. They are firstly connected to the grid via an inverter, then a traditional EV charger is used to connect the grid with the EV. This means that two routes are taken for a solar-powered EV charging system, resulting in extra power loss and higher system cost. In this section, a novel bi-directional EV charger system using all wide-bandgap devices is proposed to build a direct connection between PV panels and the EV as shown in Fig. 2-3b, and also introduces V2G (Vehicle to Grid) path. Therefore, reduced power loss and lower system cost features are achieved from a highly integrated power electronics system with high efficiency and high power density.

1.4 Wireless Power Transfer

In the low-power electronics network, wireless power transfer (WPT) can be viewed as an effective tool to centralize the system by charging multiple electronic loads remotely and wirelessly, Fig. 1-7 shows future wireless charging concept in the 5G network where radio frequency (RF) wireless charging is promoted. Researchers have spent considerable efforts to develop wireless power transfer (WPT) systems over the past decade. Following the first demonstration of efficient long-distance WPT in [10] shown in Fig. 1-6 achieved by making the inductive circuits resonate at the same frequency.

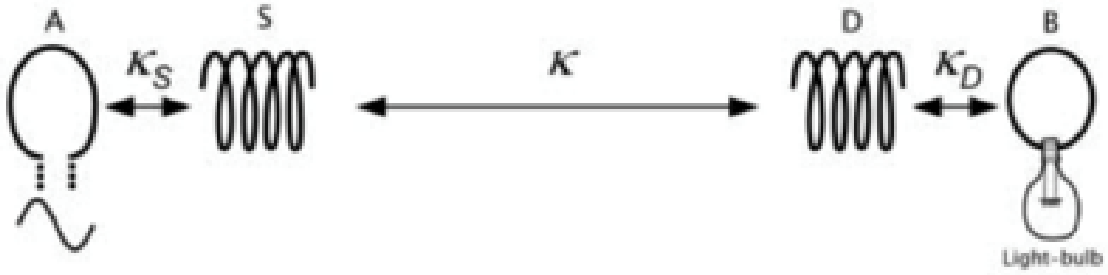

Figure 1-6: Past Wireless Charging Developed at MIT. Picture Sourced from Soljacic's Paper [10].

Subsequent papers [34–44] investigated this approach, especially strengthening the resonant charging concept. Later, researchers developed multi-user charging [45, 46] to meet the increasing need for charging more than one electronic device at the same time. Due to their ubiquity, smart phones, for example, are increasingly in need of group charging in venues ranging from coffee shops to airports. In such multi-user scenarios, the location of the smart phone with respect to the charging transmitter cannot be adjusted. Correspondingly, the objective is to provide for quasi-uniform charging efficiency throughout all space around the transmitter, enabling multiple users to receive power efficiently regardless of their locations.

Resonant WPT, which has been applied to various applications, is fundamental to achieving high-efficiency power transfer between two sets of coils. For example, [38] focuses on the biomedical applications, [39] focuses on flying drone applications,

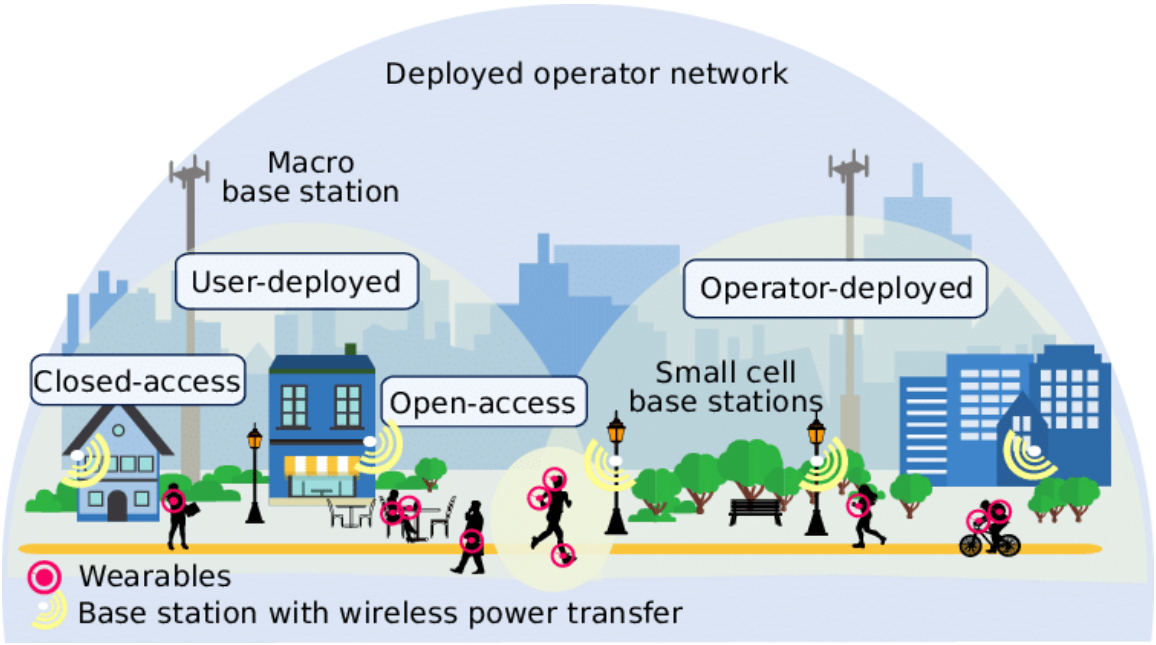

Figure 1-7: Future Wireless Charging for Electronics Network. Pictures Sourced from [11].

[41, 42] focuses on electric motor applications, [47, 48] introduce several methods to track and increase system efficiency, and [49, 50] focus on network applications. The WPT system proposed here is distinct from those discussed above. In particular, it employs rotating magnetic fields so as to improve spatial uniformity, and is applicable to smart phones, tablets, multimedia devices, and even low-power laptops. Magnetic MIMO [51, 52] has been adopted for position-free charging applications. To enable charging by multiple users, adaptive algorithms based on user-detection are developed in [45], but the uniformity of power distribution is not considered. Thus, even though overall efficiency is maximized, some users might be incapable of receiving power. The single-user efficiency distribution using phase-shifted current is studied in [53]. The current control to achieve optimized power efficiency is studied in [54, 55] The rotational and directional magnetic field of an omnidirectional WPT system is studied in [54]. However, the efficiency uniformity and power distribution among multiple users are not studied.

To overcome these addressed issues above, we developed a novel uniform wireless power transfer method in Chapter 4. An advantage is quasi-uniform efficiency in

3-D space by employing rotating fields, which follows the similar principle of multi-phase electric machines [55–58]. Two different types are developed and studied: a 2-coil system with a phase shift of 90 degrees between the coil currents, and a 3-coil system with a phase shift of 120 degrees between the coil currents. The phase-shifted currents create a uniform rotating magnetic field around the coils and provides a seamless power transfer to the multiple receivers in the charging space. This phase-shifting method creates uniform efficiency in the space, which cannot be achieved by using traditional non-phase shifting method. [59] introduced a 2-transmitter method, but it only works in 2-D quasi-uniform with >10% fluctuation while the proposed methods in this thesis verify uniform field in 2-D and quasi-uniform field in 3-D, and a much more robust system up to 88% reduction on efficiency variance with a 3-coil transmitter structure.

1.5 Impact

The economic impact of these cutting-edge technologies are significant in numbers, with proposed electric vehicle and renewable power sources, the carbon dioxide emission can be reduced up to 45% [60] in Massachusetts, the home state of the author's institute - MIT. Moreover, the cost can be saved up to 50% as discussed in Chapter 2.2 against existing technologies on solar-powered EV charging.

Chapter 2

Preliminary Work

2.1 System Overview - Hybrid AC-DC Architecture (Local)

A complete structure of the local (residential) system in Chapter 1 is described in Fig. 2-1, connecting to the distribution line. It compromises two networks: electric and electronics which depends on the power rating. The high-power system is categorized as electric network circled in red color, and the low-power system is categorized as electronic network circled in blue color. The city level has similar structure except the residential appliance section, but it usually has higher power limit - up to 200kW versus 20kW for the local level.

Since there are AC and DC –powered electric loads in the system, a hybrid AC-DC architecture can improve the system efficiency by reducing the number of power conversions. Due to the increasing need of DC power, researchers have proposed a DC Microgrid over the past few years. This work proposes a hybrid AC-DC micro grid, by combining traditional AC Microgrid and DC Microgrid, which is believed by us to be the most viable solution. The essential issue is to determine the regulated DC bus voltage level, [61] analyzes a systematic methodology in the automotive application. This work proposes a study in the residential application and presents a systematic study to recommend the DC bus voltage in the hybrid AC-DC network. Thee-phase

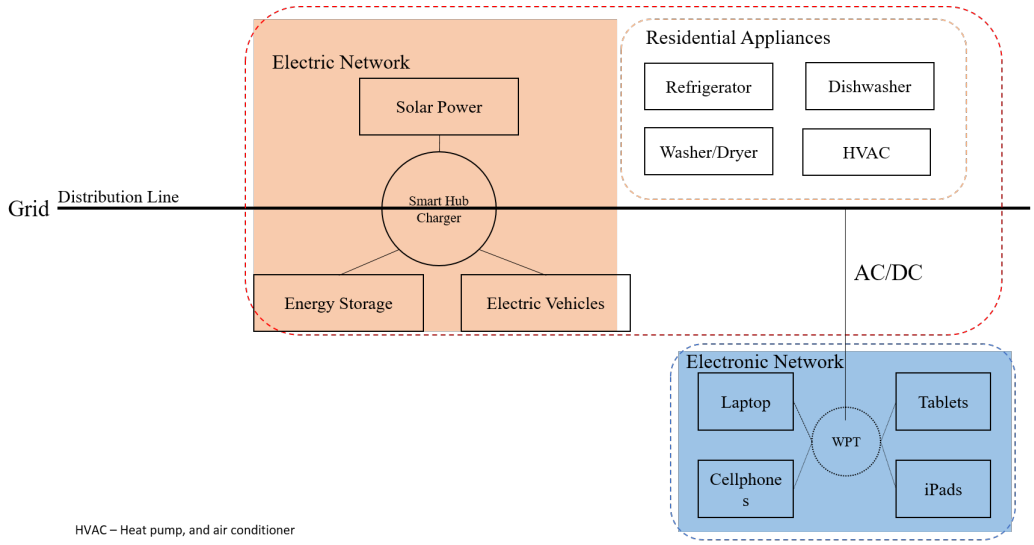

Figure 2-1: Network Diagram

AC grid voltage for larger users have different standards, USA uses 480V 60Hz (single phase 240V, center capped for most residential cases), Europe uses 400V 50Hz, and China uses 380V 50Hz. This thesis assumes the US standard.

2.2 Electric Network

For the electrical network which consists of solar power, EV, and the AC three-phase grid shown in Fig. 2-2, there exists a traditional structure which uses two separated systems - solar inverter and EV charger as shown in Fig. 2-3a to process power electronics that convert DC solar power to AC power feeding the grid, then either uses that generated power or power from the grid to charge the EV. This means that two routes are taken for a solar-powered EV charging system, resulting in extra power loss and higher system cost, a third route is employed by some technologies has developed V2G which allows power transfer from the vehicle's battery to the grid.

(a) Solar-Powered EV Network Concept, Picture Sourced from Google.

(b) Solar-Powered EV Network at Stone Edge Farm, Picture Taken by the Author Using An iPhone.

Figure 2-2: Solar-Powered EV Network.

In this thesis, a bi-directional EV charger shown in Fig. 2-3b of [62] is proposed to serve as the hub to connect both solar panel and the utility. This novel bi-directional method with all wide-bandgap semiconductor devices is analyzed in detail in Chapter 3. As we learn from industry data, a solar inverter costs roughly the same as an EV charger, thus our proposal results in 50% cost saving on hardware with this single novel EV charger.

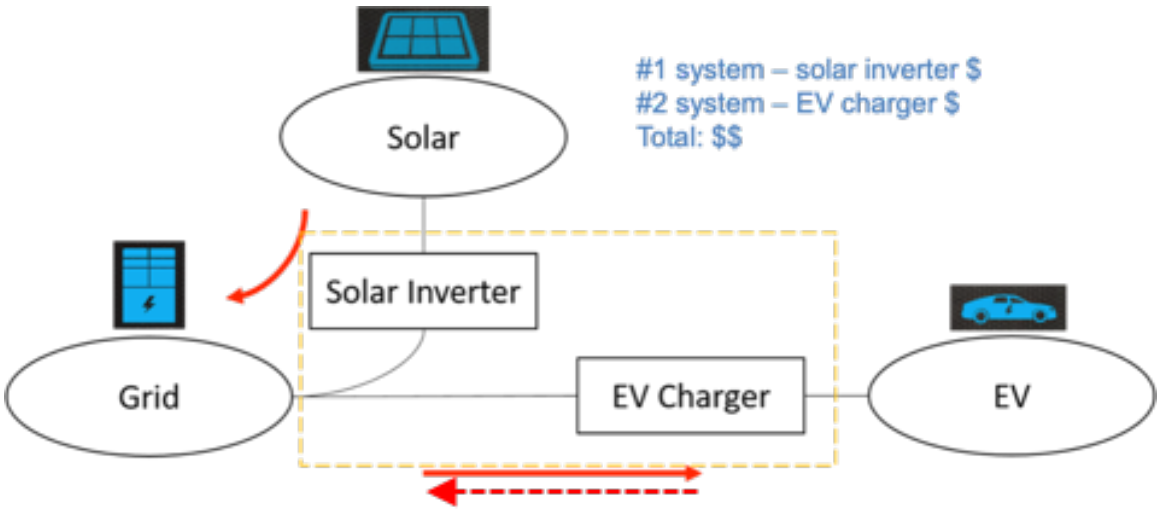

(a) Traditional Structure of Solar-Powered EV Network in [63–69].

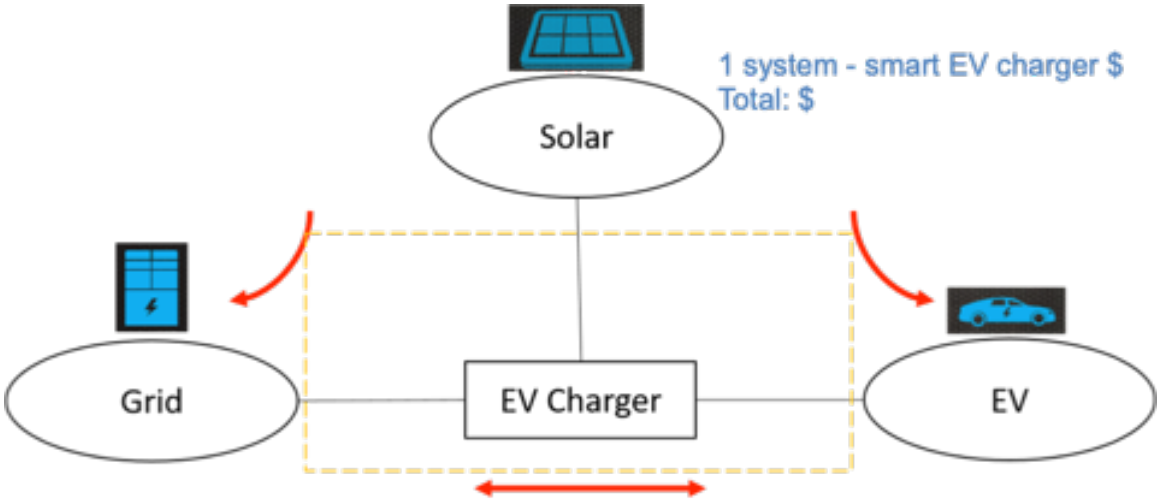

(b) Proposed Structure of Solar-Powered EV Network.

Figure 2-3: Comparison of Technical Structure in Solar-Powered EV Network.

Fig. 2-3b shows the bi-directional power flow diagram, representing two power flows, namely Grid-to-Vehicle (G2V) and Vehicle-to-Grid (V2D) modes. In G2V

mode, the battery is in the charging process, during which power flows from the three-phase grid through the power factor correction (PFC) and DC Bus to the battery. In V2G mode, the battery is in the discharging process, during which power flows from the battery through the DC Bus and PFC to the grid. In addition, with the injection of solar power, there is an additional power flow route to charge the battery from the solar panel. A power adapter system is designed to regulate the solar output power. The output power levels of state-of-the-art EV chargers are from a few to tens of kilowatts, the dc power bus levels are from Vdc up to 840V with 400V being a typical value, the converter switching frequencies are from tens of kilohertz when using Si-powered MOSFETs or insulated-gate bipolar transistors up to 500 kHz; in the case of widebandgap power devices, SiC and GaN are used. [62] firstly used all wide bandgap devices to achieve high-efficiency bidirectional EV charger, later publications on EV charger design followed this bi-directional concept.

As EV's battery capacity is growing larger for each individual EV, the power flow between the EV and the grid is examined in a bidirectional fashion. This is especially useful in applications using Renewable Energy Sources (RESs), e.g., the solar panels in [62]. The bidirectional flowchart is shown in Fig. 2-3b. During the bidirectional power-flow interaction, the solar power can flow either from the PV panel to the grid or to the EV, and the battery charging power can flow G2V or vice versa. Two additional power flows are provided compared to that of the unidirectional mode, which increases system flexibility. In [70], V2G power flow implies that the power can be drawn from the battery serving as the electric source, which has significant benefits in future applications, such as powering a house during electricity shut down or powering electric equipment during a road trip once EV batteries have become bigger and more powerful. The system becomes simpler after applying the bidirectional power flow method, and its benefits can be summarized as 1) direct access to solar generation and the EV's battery and 2) efficiency maximization. Concerning the direct access to solar generation and the EV's battery thanks to two additional power flow paths - solar power to EV charging and the EV's back feed to the grid, as depicted in Fig. 2-3b versus Fig. 2-3a, the system becomes more flexible for the

usage and transfer of energy. The system integrates the functionality of solar inverters and battery charging into one unit by providing direct access between each power element, which reduces system size. The overall average efficiency is improved by 5%, comparing the bidirectional power flow method with the traditional unidirectional one with the PV-to-car efficiency of 91%, based on the same efficiency data for power electronics - an averaged EV charger efficiency of 94% and a solar inverter efficiency of 97% at the time of development. When using RESs, the unidirectional approach where two steps are needed from the solar PV panels to the EV charger and from the EV charger to the EV has an overall efficiency of 91%. Instead, for the bidirectional solution, the overall efficiency is 96%. This 5% is a substantial savings of electricity usage, in addition to the material cost savings derived from one compact integrated system versus two bulky separated systems. The only requirement for the system in Fig. Fig. 2-3b, as discussed in [62], is the use of bidirectional switches where power can flow either way through switches.

2.3 Electronic Network

For the electronic network, a quasi-uniform wireless power transfer (WPT) system is proposed to serve as the hub to connect the multiple electronics devices – tablets, cellphones and even low-power laptops. the main objective is to provide convenience and simplicity when compared with wired chargers. Their charging power ranges from 5W to 20W per unit. This thesis focuses on stationary application where all the electronic devices are relatively stationary in a place such as table, but allowing them to be moved around within a certain radius of the center therefore flexibility is considered. For instance, during a casual meeting, attendees can use their phones to check messages and browse the Internet while sitting. The goal is to have all these electronic devices being charged with one single wireless power transfer system. The edge is enabling 3-D position-free charging against exiting WPT technologies shown in Fig. 2-4.

This work proposes an innovative WPT technology to use phase-shift driven cur-

WPT Technologies	Multi-Charging	Distanced Charging	2-D Position-Free	3-D Position-Free
Our Approach	Y	Y	Y	Y
Witricity	N	Y	N	N
MagMIMO, Pi	Y	Y	Y	N
Apple's Charging Mat	Y	N	Y	N
Best Charging Pad on Amazon	N	N	Y	N

Figure 2-4: Benchmark Comparison of WPT Technologies.

rents to create rotating magnetic fields for the multi-user application that can eliminate blind spot and provide uniform efficiency. Its system overview is shown in Fig. 2-5.

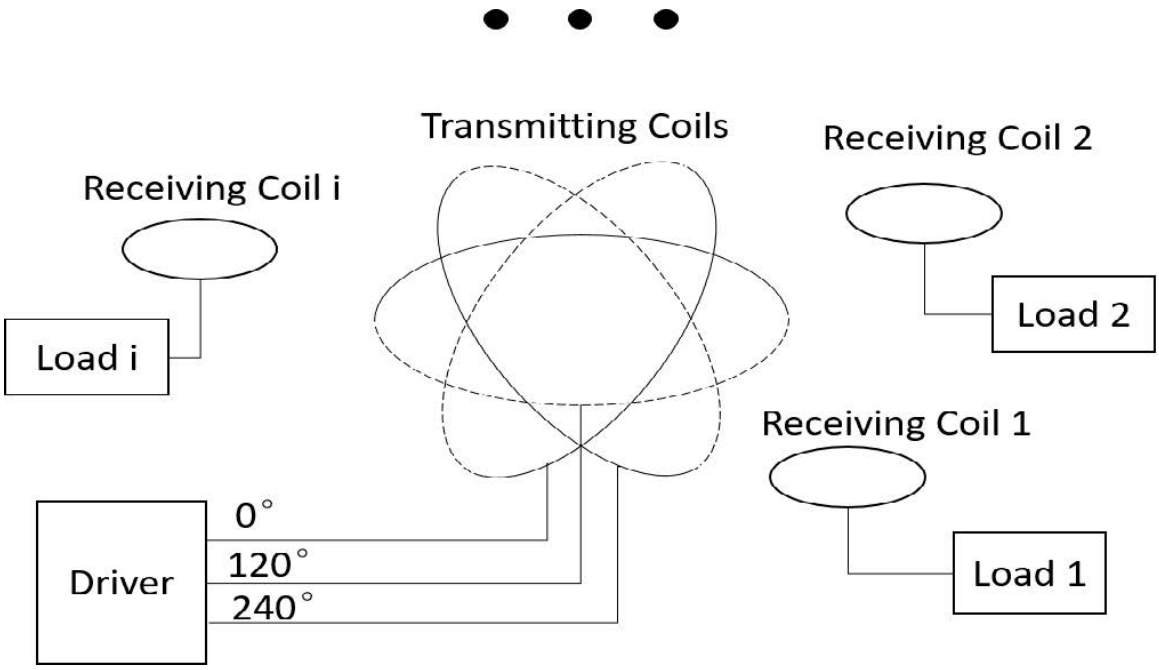

Figure 2-5: Electronic Network Diagram.

This wireless power transfer systems for multi-user charging is proposed to demonstrate a robust quasi-uniform power efficiency in 3-D space. It employs a set of balanced magnetic coils excited with phase-shifted currents on the transmitting side to feature omnidirectionality. In this thesis, two transmitter structures, 2-coil and 3-coil systems are discussed and compared. These systems produce a quasi-uniform magnetic field magnitude regardless of the location of the receiving coils provided that

the receiving coils point to the center of the transmitting system sphere at the same distance. A simulation platform is established for the proposed method. Experimental results at 2MHz substantiate uniform spatial efficiency, and bound the average error of analytical calculations within 10%. Furthermore, the proposed method with rotating fields based on phase-shifted currents shows that 3-coil system yields a higher and much more stable efficiency range, 6.8% improvement on average efficiency and 88.7% reduction on efficiency variance compared to the 2-coil system.

Chapter 3

Centralization of Electric Network (Local)

Centralization is to create a centralized structure of the system by using a power hub to connect with the remaining components of the system. In the electric network, particularly with the application of electric vehicles, alternative power sources are needed when the traditional grid cannot meet the increasing demand of charging electric vehicles, solar photovoltaic(PV) is a great candidate and will contribute to 16 percent of the electricity as the largest source by 2050 [71]. Thus, we focus on a three-component network: electric vehicles, solar PV, and the grid.

3.1 Smart Hub - Bi-Directional EV Charger

A power hub is a universal power electronics devices that can handle all sorts of power conversions - ac-dc rectification, ac-ac conversion, dc-ac inversion, and dc-dc conversion, this means all of these four addressed functions are being implemented on one single device. If we look at the current power electronics for the EV industry, EV charger, solar inverter and etc., after a careful review we can conclude that EV charger essentially consists of ac-dc rectification and dc-dc conversion already, so we just need two more functions - ac-ac conversion and dc-ac inversion to form this power hub which can handle all four power conversions to be universal. An electric

transformer essentially does ac-ac conversion, and it provides electric isolation for the safety purpose. Now only one is missing - dc-ac inversion. It sounds interesting that dc-ac inversion can be realized just by reversing the power flow of ac-dc rectification. Therefore, designing a bi-directional EV charger can integrate all of these functions into one single device.

The circuit diagram of a candidate device is shown in Fig. 3-1. This circuit can be viewed as two main parts: power factor correction (PFC) and also a dc-ac inverter at reverse power flow mode, and isolated dc-dc converter which has an ac-ac transformer in the middle. PFC is power-factor correction increases the power factor of a load which measures the ratio of the real power absorbed by the load to the apparent power flowing in the circuit, thus improving efficiency for the distribution system to which it is attached. A simple boost circuit that that does DC-DC voltage increase is auxiliary. PFC converts three-phase 480VAC (Phase to Phase) via three-phase full-bridge rectifier to 400V DC bus voltage, then a DC-DC converter converts and isolates this 400VDC to 600VDC for the battery charging of EV. The voltage from solar power is boosted to 400VDC bus to offset the input from the grid. EV's voltage ranges from 400-800VDC depends on manufacturer and battery capacity.

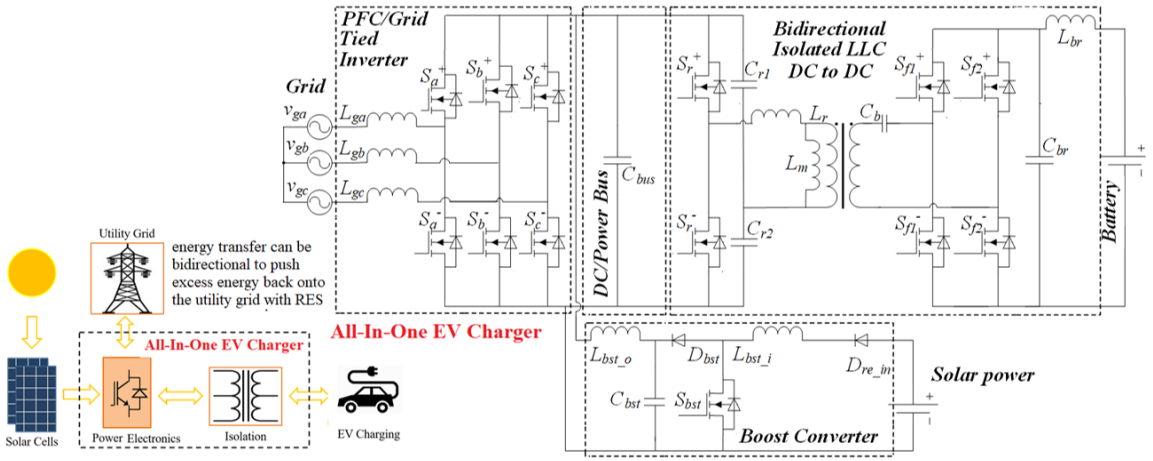

Figure 3-1: Circuit Diagram of Bi-Directional EV Charger. PFC - Power Factor Correction, LLC - Inductor Inductor Capacitor.

With the rapid increasing demand of electric vehicles, bi-directional power flow represents the future trend. Thus, to realize vehicle-to-grid (V2G) and grid-to-vehicle

(G2V) technology, a high-efficiency bidirectional charger needs to be integrated into the power grid. Fig. 3-1 shows a general structure of an EV battery charging system, which is often composed of a bidirectional power factor control (PFC) rectifier, a bidirectional isolated dc/dc converter, and a unidirectional dc/dc converter for solar panels if renewable energy is incorporated. The charger accommodates three-phase 380 V ac for European and Asian markets and single-phase 120-240 V ac (center capped) for North America. Recent work [72–81] demonstrates some high-performance single-phase EV chargers. To receive the three-phase 380 V ac input, the conventional two-level topology requires high-voltage switches (>600 V). However, nearly all 1200 V Si insulated gate bipolar transistors (IGBTs) or 900 V CoolMOS have worse performance compared with 600 V switches, e.g., slower switching transition, higher forward voltage drop, and larger reverse recovery loss. The high channel resistance and large gate charge of Si MOSFETs result in a high conduction loss and switching loss. A multilevel topology is a possible solution [77], which reduces the voltage stress of switching devices, thereby allowing the use of lower voltage MOSFETs or IGBTs. The major drawback is the large number of switches and gate-drive circuits, which potentially lowers the power density. While nearly all present systems are based on conventional silicon semiconductors, [75–78] discussed the application of widebandgap (WBG) devices like silicon-carbide (SiC) MOSFETs and gallium-nitride (GaN) high electron mobility transistors(HEMTs) shown in Fig. 3-12. However, the impact of WBG devices on EV battery chargers, especially the efficiency increment, has not been quantitatively discussed yet.

To enhance the system efficiency and power density, the SiC MOSFET is an excellent candidate, which is known for its low channel resistance, high-voltage withstanding capability, low reverse recovery charge, and better thermal characteristics compared with Si devices. With the superior performance of 1200 V SiC MOSFETs, power electronics engineers could use a simple topology with the smallest number of switches. As shown in Fig. 2, an all-SiC-MOSFET-based three-phase boost-type PFC with a half-bridge LLC resonant converter contains fewer semiconductors compared with a three-level power factor correction (PFC) or dual-active-bridge topology [9].

The dc/dc part adopts the LLC resonance technology to realize zero-voltage-switching (ZVS) turn ON, though it remains uncertain how such topology could realize the bidirectional power flow with ZVS for the whole power range, which is the scope of this work. On the other hand, to precisely estimate the system efficiency, an accurate circuit behavior model must be established prior to the prototyping. At the present time, first harmonic approximation (FHA) method is widely used in the LLC resonant converter design [21]–[34], which is an attempt to simplify the loss calculation. However, due to the wide voltage range of the on-board battery pack, the system usually does not work exactly at the resonant frequency, which results in the resonant current waveform being far from the ideal sinusoidal waveform and makes the FHA method no longer accurate. Reference [20] uses a MOSFET datasheet for the loss evaluation, while [29] relies on the simulation model. In the reality, the semiconductor switching performance might vary drastically under different operational conditions, e.g., gate-drive voltage, current, and temperature. To estimate the loss accurately, a double pulse test (DPT) needs to be conducted first.

This work presents an in-depth and comprehensive analysis of SiC devices based bidirectional EV charger. Section 3.1.1 presents operational principles of the system in G2V and V2G modes. The steady-state analysis of the bidirectional LLC resonant converter is processed based on state-space equations. An accurate power-loss model is derived in Section 3.1.2, which indicates that the system reaches the peak efficiency when the LLC converter is operated at the resonant frequency. Based on such characteristics, a variable dc-bus control to maximize the efficiency. The control method varies the PFC output voltage to achieve the highest system efficiency at any given battery charging power.

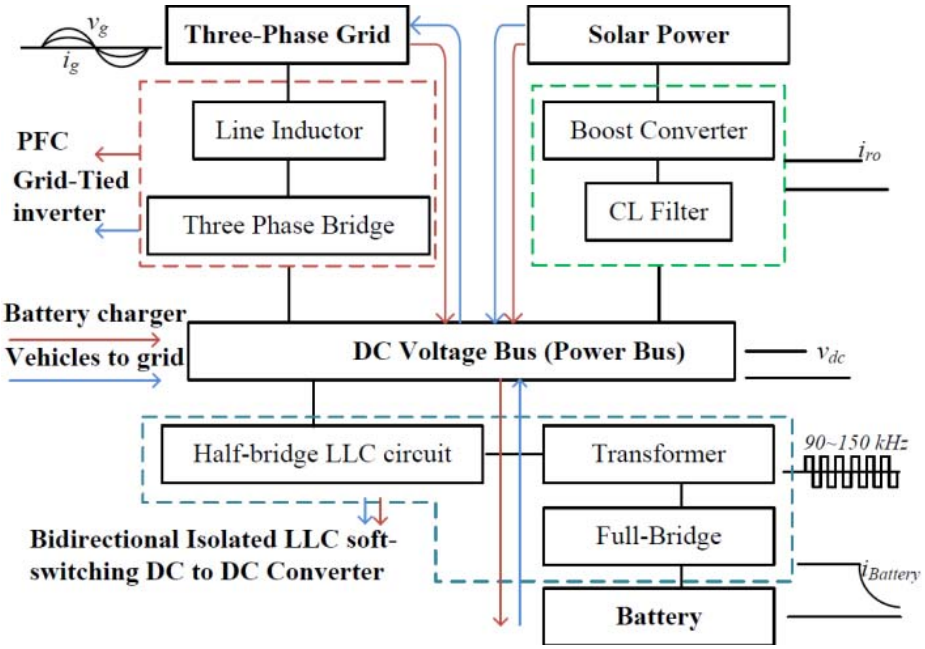

Figure 3-2: Power-flow diagram of the SiC bidirectional charger.

3.1.1 Operation Principles of Bi-Directional Power Flow

0. Principle of Space Vector Pulse Width Modulation (SVPWM).

Space Vector Pulse Width Modulation (SVPWM) is a brilliant vector control algorithm to generate desired PWM signals through Park transformation and rotating (d-q-0) to stationary (α-β-0) frame transformation. Each switch status is represented by 1(on) or 0(off), its space vector diagram and duty cycle for each phase is shown in Fig. 3-3 and Fig. 3-4, respectively.

When implementing the voltage vectors, different sequence could be selected to form various control strategies, here we compare symmetric control with traditional control,

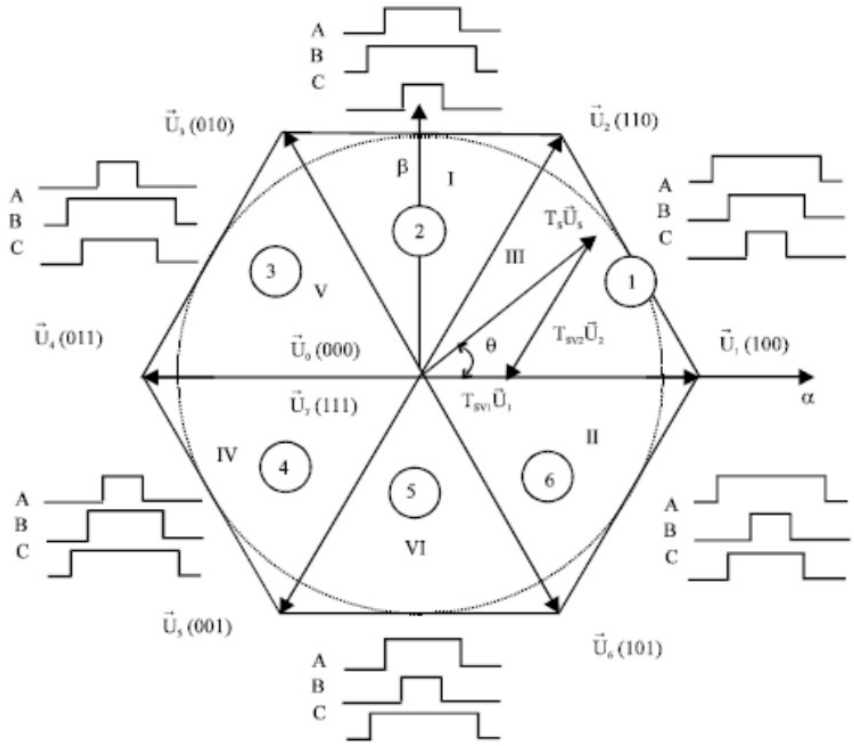

Figure 3-3: Space Vector Diagram Representing All Possible Switch Combinations. A-C Represent Upper Switch in Each Leg, Turn-On is 1 While Turn-Off is 0.

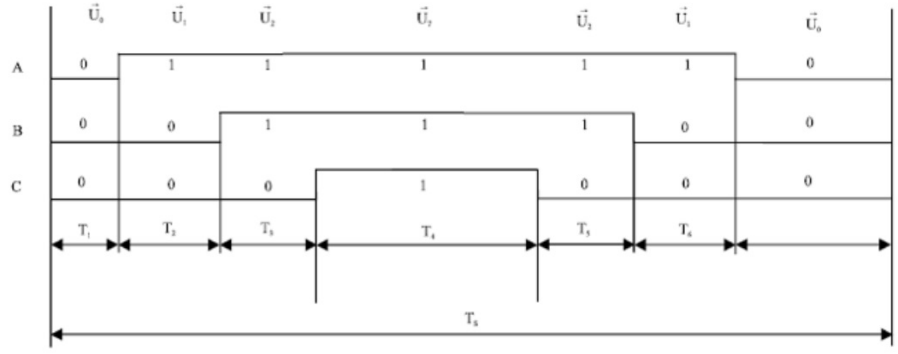

Figure 3-4: Diagram of Duty Cycle For All Six Switches.

Seen from Fig. 3-9b, duty cycles of symmetric (also interpreted as discontinuous) SVPWM can reach to values of both zero and one hundred percent, however in Fig. 3-9b duty cycles of traditional symmetric never reach to a value of zero and one hundred percent. This means, for the symmetric control, there is always 1/6 of the period when the switch is forever on and another 1/6 when the switch is forever off. So it is expected to have 16.67% less switching loss. This figure comparison indicate loss saving.

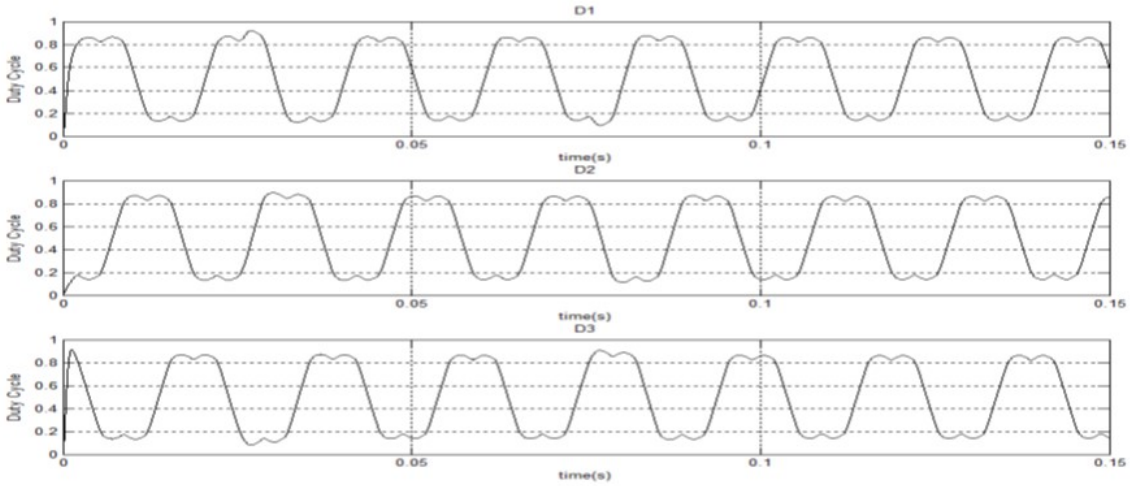

Figure 3-5: Traditional SVPWM where D never reaches to 0/1. Duty cycle pattern is related to output power due to switching actions.

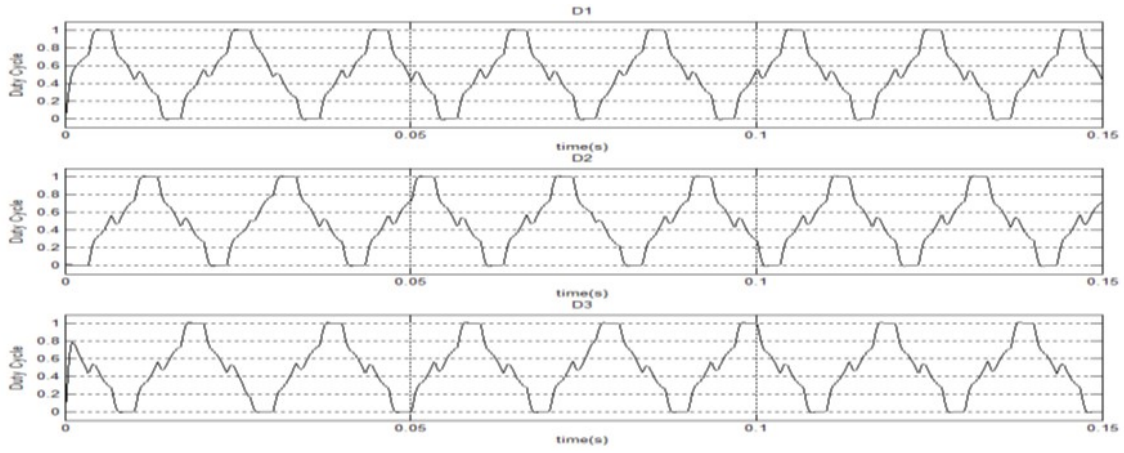

Figure 3-6: Symmetric (Discontinuous) SVPWM where D reaches both 0 and 1, hence saving switching loss.

A. G2V Mode

In the G2V mode, the three-phase PFC rectifies the grid input to a dc output. The isolated LLC resonant converter then delivers the power to the high-voltage EV battery. The solar boost converter tied to the PFC dc output can intake the solar power to reduce the overall electricity cost. The red lines in Fig. 3-2 indicate the power flow in the G2V mode. Fig. 3-7 shows the control block diagram of the PFC. To minimize the switching loss of six switches, a discontinuous pulsewidth modulation is used to minimize the switching actions [35]. The closed-loop PI controller regulates the PFC output voltage, as shown in Fig. 3-7. All secondary switches are OFF. Fig. 3-8 shows the operation of the solar panel boost converter, which will not be detailed here. The LLC dc/dc converter uses a closed-loop feed-forward controller to regulate the battery charging current.

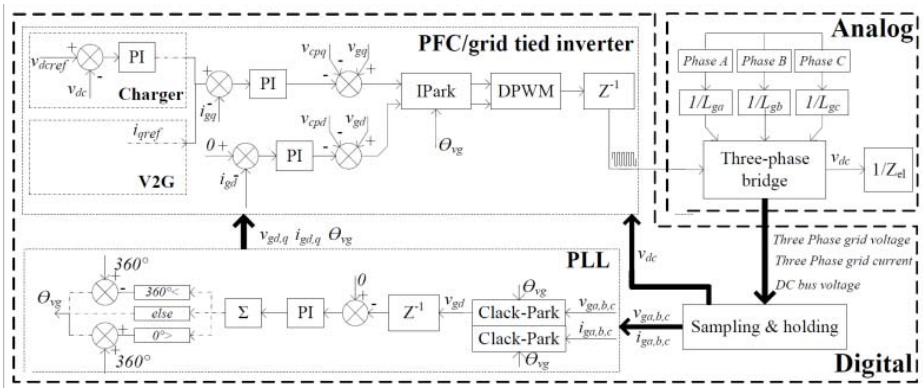

Figure 3-7: Control diagram of the three-phase boost-type PFC rectifier.

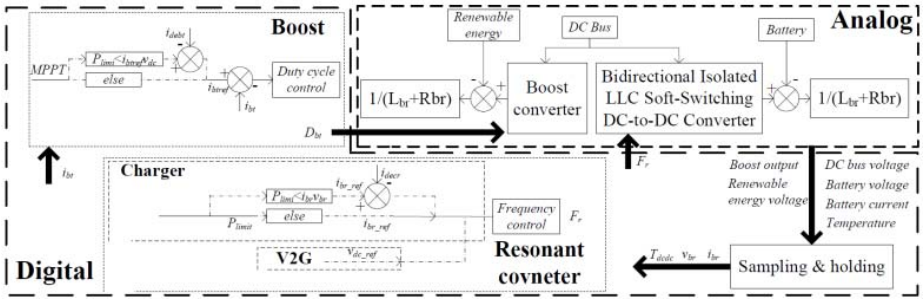

Figure 3-8: DC/DC converter control diagram.

To calculate the system loss, operational principles of the LLC converter must be addressed to obtain the exact switching current waveforms. In this work, a half-bridge

series resonant topology is used instead of the full-bridge LLC converter to simplify our structure. This topology is advantageous in the resonant capacitor design since the voltage across the capacitor is reduced to half with reduced number of gate drivers. This LLC resonant circuit can be operated in either the discontinuous current mode (DCM) or the continuous current mode (CCM), depending on the load condition and switching frequency. Regardless of the operational modes, there are three possible equivalent circuits during the half switching period, i.e., state 1, state 2, and state 0 shown in Fig. 3-9a to Fig. 3-9c, respectively.

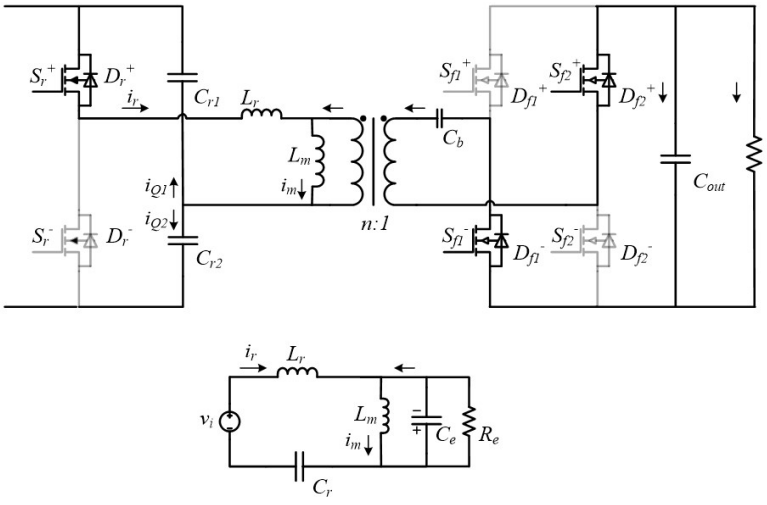

(a)

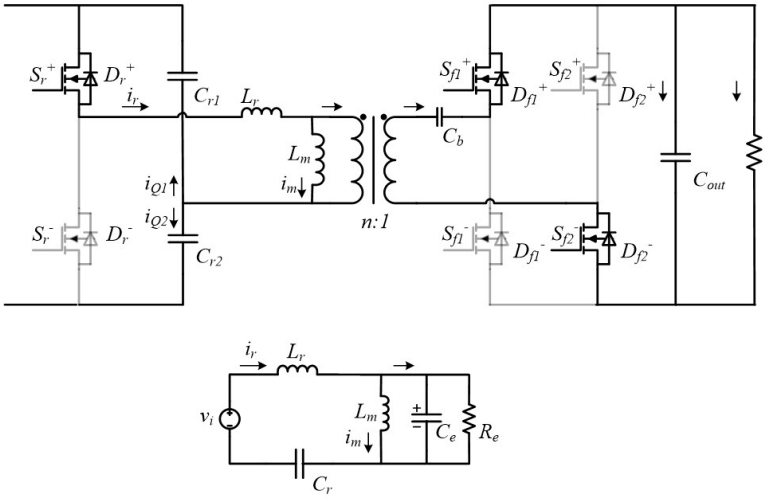

(b)

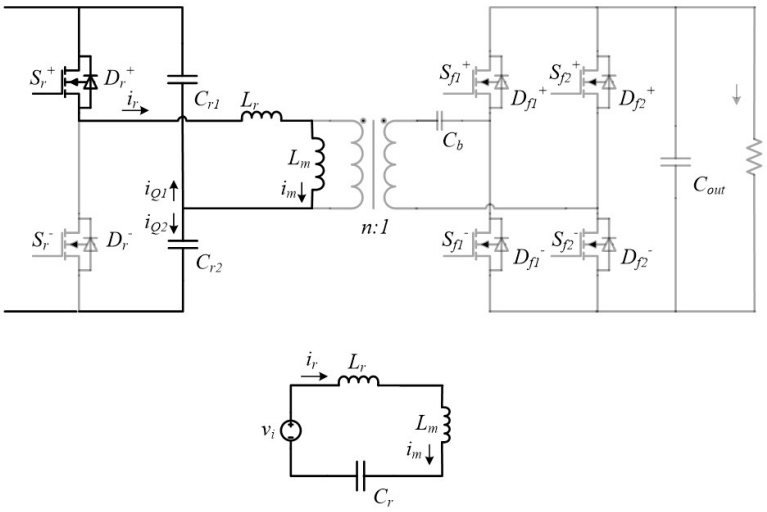

(c)

Figure 3-9: Equivalent circuits of the LLC converter. (a) State 1. (b) State 2. (c) State 0.

Fig. 3-10(a) to Fig. 3-10(c) shows the waveforms when operated under the resonant frequency in DCMB1, DCMB, and CCMB modes, respectively. The output voltage is not modeled as an ideal constant voltage source, but a parallel RC load where C_{out} is the output capacitance and R_L is the output resistance determined by the battery voltage/current. V_2 is the output voltage. In state 1 shown in Fig. 3-9a, secondary diodes D_{f2}^{+} and D_{f1}^{-} are ON. The voltage across the transformer magnetizing inductance V_m is clamped to nV_2. In state 2 shown in Fig. 3-9b, secondary diodes D_{f1}^{+} and D_{f2}^{-} are ON. V_m is clamped to -nV_2. In state 0 shown in Fig. 3-9c, all secondary diodes are OFF. V_m is independent of the output voltage.

A1. DCMB1 Mode ($f < f_r$)

When the load is light, the circuit is first operated in state 1 starting at t = 0. During state 1, the inductor L_r resonates with C_r. V_m is equal to nV_2, resulting in the continuously increasing magnetizing current I_m. At $t = t_0$, the resonant current is equal to the magnetizing current, i.e., $I_r = I_m$, which makes the circuit switch from state 1 $\rightarrow$ state 0 because all secondary diodes turned OFF. The output current is supplied through discharging the output capacitor C_{out}. During state 0, V_m is determined by the resonant circuit and gradually decreases. If $|V_m| < |nV_2|$, the circuit remains in state 0. At $t = (T_s/2)$, the input voltage changes the polarity. The circuit changes to state 2 since V_2 = -V_m. To summarize the DCMB1 mode, the circuit is operated in the following sequence within the half switching period $t \in [0, (T_s/2)]$: state 1 $\rightarrow$ state 0.

Define the secondary current reflected to the primary side as I_{sec}. It can be calculated as

$$I_{sec} = \begin{cases} |I_r(t) - I_m(t)| & 0 < \mathrm{t} < t_0 \\ 0 & t_0 < \mathrm{t} < \frac{T_s}{2} \end{cases} \tag{3.1}$$

A2. DCMB Mode ($f < f_r$)

If the load becomes heavier, the circuit starts to work in the DCMB mode. The circuit begins with state 1 at t = 0. Then the circuit changes to state 0 when $I_r = I_m$. At t = $t_2 < (T_s/2)$, the magnetizing inductance voltage $|V_m| = |nV_2|$. Secondary diodes D_{f1}^{+} and D_{f2}^{-} turn ON clamping V_m to nV_2. The circuit starts to operate in state 2. To summarize the DCMB mode, the circuit is operated in the following sequence within the half switching period $t \in [0, (T_s/2)]$: state 1 $\rightarrow$ state 0 $\rightarrow$ state 2. I_{sec} can be calculated as

$$I_{sec} = \begin{cases} |\ \mathrm{I}_r(t) - I_m(t)| & 0 < \mathrm{t} < t_0 \quad or \quad \mathrm{t}_2 < \mathrm{t} < \frac{T_s}{2} \\ 0 & t_0 < \mathrm{t} < t_2 \end{cases} \tag{3.2}$$

A3. CCMB Mode ($\mathbf{f} < \mathbf{f}_r$)

As the load continues to increase, state 0 disappears. At the end of state 1 where $t = t_2$, $i_r = i_m$, the circuit no longer switches back to state 0. Instead, it switches to state 2 directly, i.e., the circuit operates according to the following sequence in the half switching period $t \in [0, (T_s/2)]$: state 1 $\rightarrow$ state 2. I_{sec} is calculated as

$$I_{sec} = |I_r(t) - I_m(t)| \quad 0 < \mathrm{t} < \frac{T_s}{2} \tag{3.3}$$

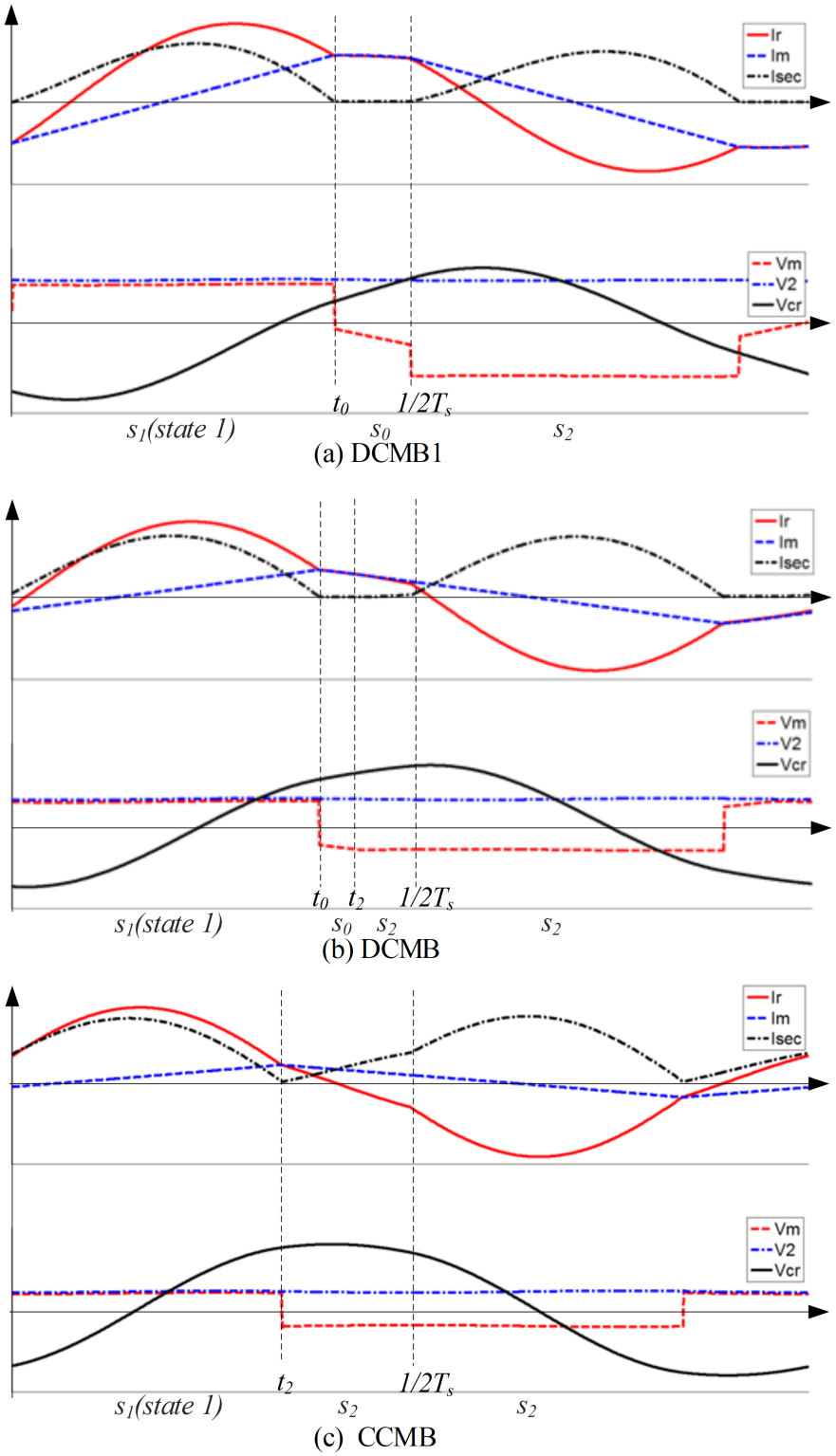

Figure 3-10: Matlab Simulation Waveforms of each LLC converter mode in G2V mode. X-axis time label, state 1 starts(at t=0), state 0 starts at t_0, and state 2 starts at t_2 for the half switching cycle [0, $(T_s/2)$].

B. V2G Mode

In the V2G mode, shown as the blue line in Fig. 3-2, the LLC resonant converter transfers the power to the primary side dc bus. Power factor correction (PFC) circuit regulates the desired three-phase grid feedback currents. The boost converter from the solar cells tied to the PFC dc output can contribute to the power intake, reducing the energy consumption of the EV battery. Here the LLC converter behaves differently from the G2V mode. S_{f1}^{+}, S_{f1}^{-} and S_{f2}^{+}, S_{f2}^{-} are all switched at 50% duty cycle with a 180^{o} phase shift. The secondary winding voltage is clamped to the output voltage. Hence the magnetizing voltage Vm is clamped to |nV2| regardless of the circuit state. Im is only determined by the battery voltage. The magnetizing inductance Lm does not participate in any resonance or the power transfer. Fig. 3-11(a) and (b) shows the circuit waveform when operated in the CCMB and CCMA modes, respectively. Possible operation modes are state 1 and state 2, state 0 no longer exists since all secondary switches cannot be turned off simultaneously when power flows from vehicle to grid.

When switching frequency is below the resonant frequency $f < f_r$, the circuit follows the sequence of state 1 $\rightarrow$ state 2 in the half switching period for the CCMB mode as shown in Fig. 3-11(a). When operated above the resonant frequency, the circuit follows the sequence of state 2 $\rightarrow$ state 1 in the half switching period for continuous current mode A (CCMA) mode as shown inFig. 3-11(b).

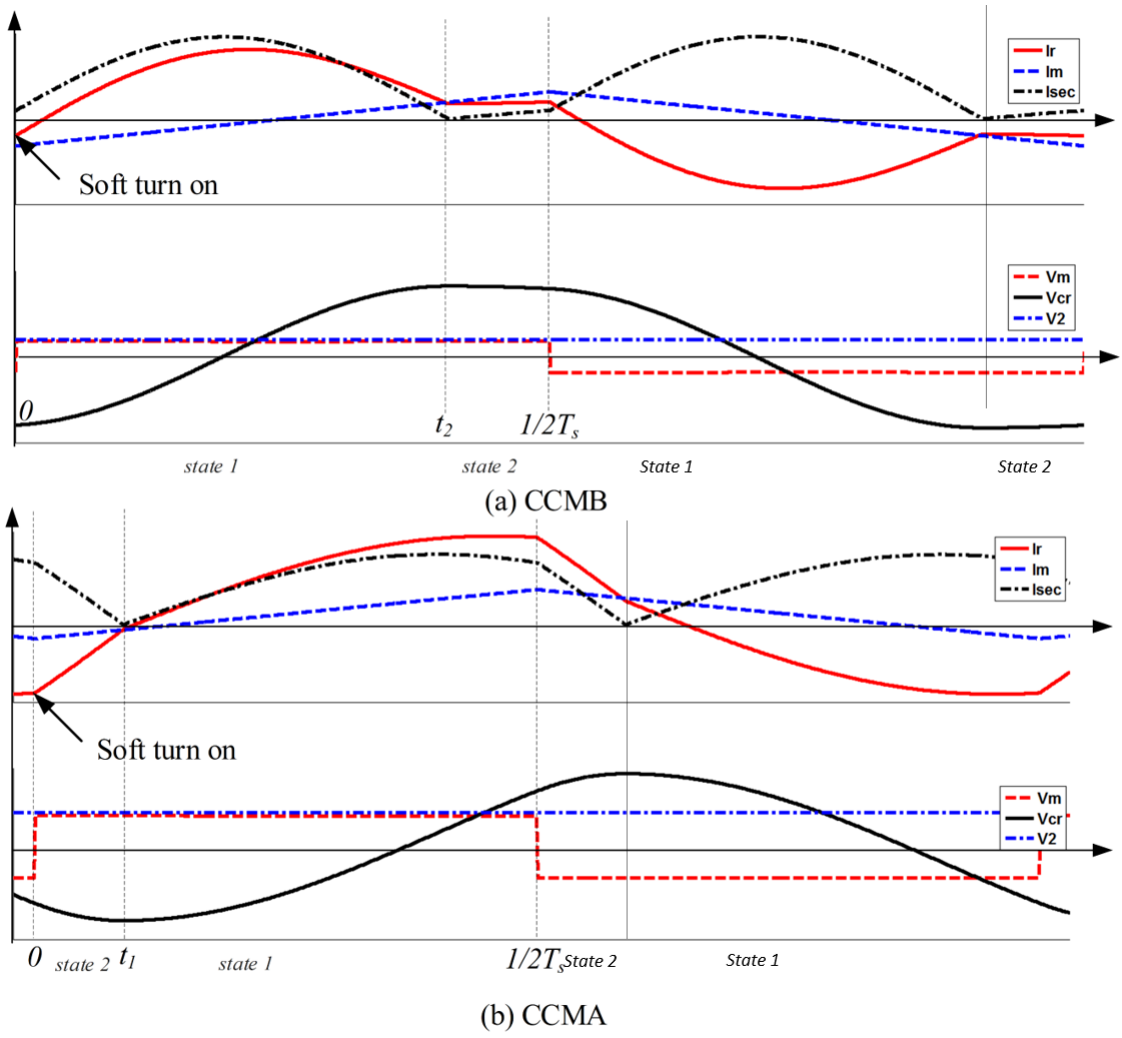

Figure 3-11: Matlab Simulation Waveforms of the LLC converter in the V2G mode. (a) CCMB. (b) CCMA. X-axis time label, state 1 starts at t_1, and state 2 starts at t_2, no state 0, and this pattern repeats every $1/2T_s$.

Semiconductor devices play a critical role in power conversion as they make high-performance switches to turn on or off with certain duty cycle to do the power conversion. Three materials are discussed here: Silicon(Si), Silicon Carbide(SiC), and Gillium Nitride(GaN) as shown in Fig. 3-12. We can see that GaN generally operates in higher frequency (0.1M-100MHz) versus SiC and Silicon (800-10MHz).

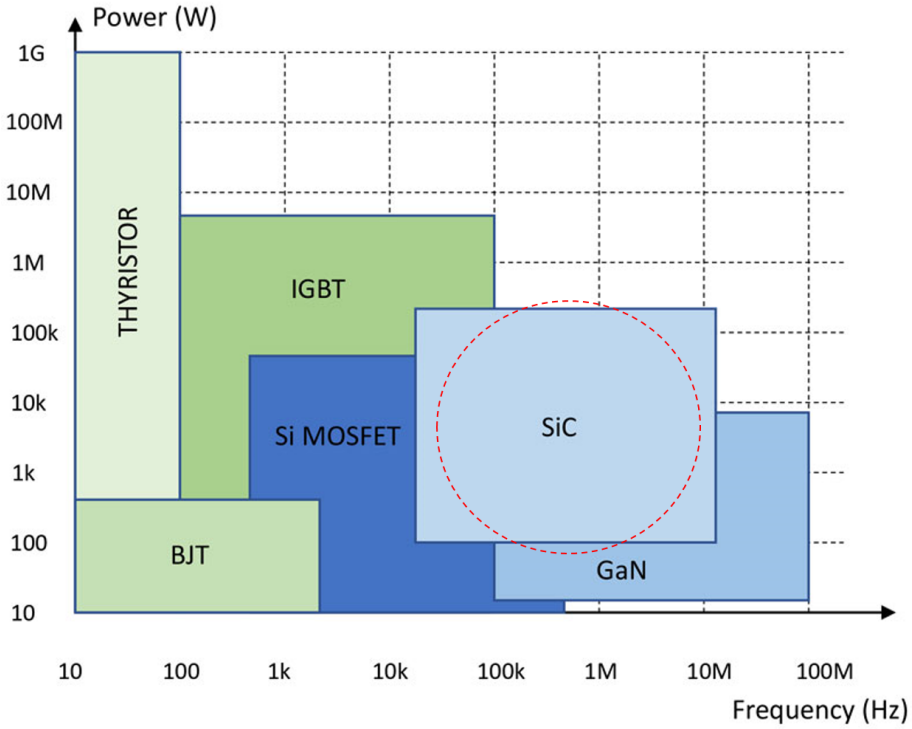

Figure 3-12: Graph of Semiconductor Materials. Sourced from UnitedSiC.

Table 3.1: Material Properties.

Materials Property	Si	SiC	GaN
Band Gap (eV)	1.1	3.2	3.4
Critical Field $10^6 V/cm$	0.3	3	3.5
Electron Mobility (cm2/V-sec)	1450	900	2000
Electron Saturation Velocity ($10^6 cm/sec$)	10	22	25
Thermal Conductivity (Watts/cm2 K)	1.5	5	1.3

Considering the system parameters on voltage(380V AC), power (10kW), and switching frequency(50-400kHz) in Fig. 3-14, we omit GaN since the system does not operate below 100kHz, and omit Si since SiC has high thermal conductivity shown in Table 3.2 which leads to lower losses, a feature summary can be generated as shown in Fig. 3-13. GaN is an excellent material, came out after SiC, and it is theoretically capable of higher switching speed than SiC or Si, with its much higher electron mobility, but it has a lower thermal conductivity compared with SiC therefore suffering higher loss due to higher current from bigger temperature rise, which is a

trade-off. Thus, SiC MOSEFT 1200V C2M0040120D made by CREE is chosen.

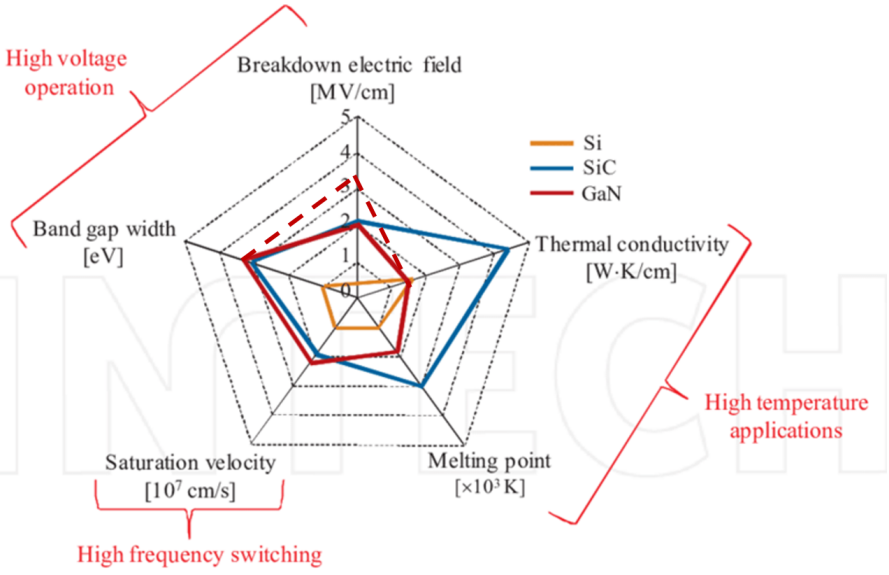

Figure 3-13: Feature summary of Si-SiC-GaN semiconductor materials. This picture is revised based from O. Deblecker's paper in comparative study of power semiconductor devices.

Symbol	Parameter	Value
V_{grid}	Grid voltage	3-phase 380VAC
f_{sw_PFC}	PFC switching frequency	50kHz
f_{sw_LLC}	LLC converter switching frequency	90kHz~150kHz
f_r	LLC resonant frequency	120kHz
f_{sw_Boost}	Boost converter switching frequency	$400kHz$

Figure 3-14: System Parameters.

3.1.2 Power Loss Analysis

The semiconductor loss of the whole charger can be categorized as the power factor correction (PFC) circuit loss, the LLC circuit converter loss, and the solar boost converter circuit loss. For the PFC circuit, the semiconductor loss can be further divided

into the switching loss, conduction loss, and gate-drive loss, denoted by P_{sw_PFC}, $P_{con\_PFC}, and P_{g\_PFC}$, respectively. For the LLC converter circuit, there are switching loss, conduction loss, diode rectifier loss, and gate-drive loss, denoted by P_{sw_LLC}, P_{con_LLC}, P_{rec_LLC}, and P_{g_LLC}, respectively. Here we use a typical Double-Pulse Test (DPT) circuit shown in Fig. 3-15, DPT is a standard method for measuring the switching parameters of MOSFETs or IGBT power devices, which is done with an inductive load and a power supply. The inductor is used to replicate circuit conditions in a converter design. The power supply is used to provide voltage to the inductor. An arbitrary function generator is used to output pulses that triggers the gate of the MOSFET and thus turns it on to start conduction of current. The energy switching waveform of SiC MOSEFT as device under test (DUT) is shown in Fig. 3-16.

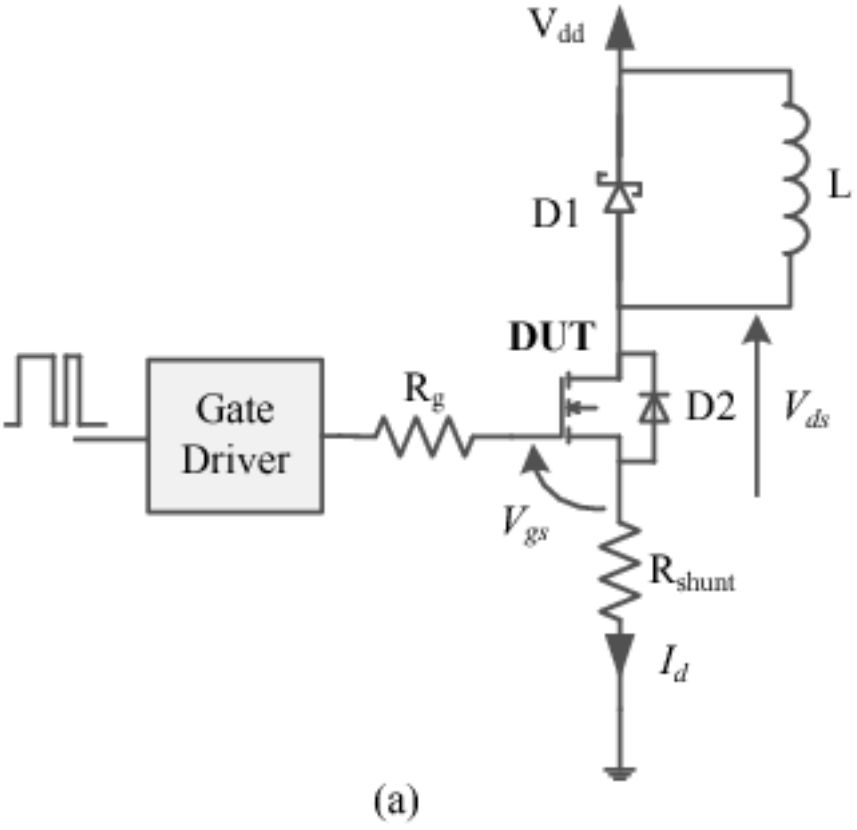

Figure 3-15: DPT Test Circuit.

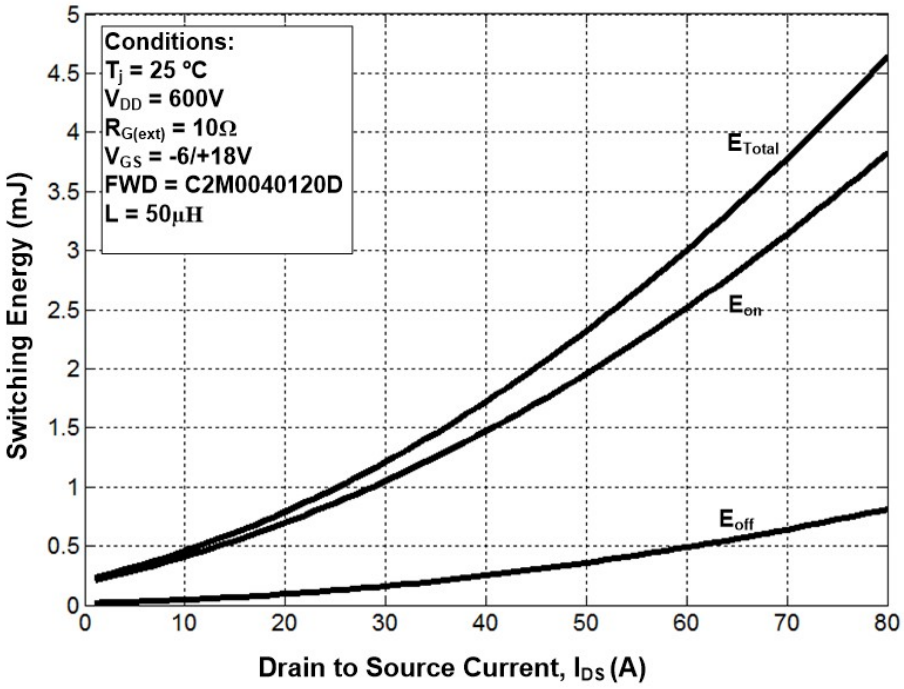

Figure 3-16: SiC MOSFET switching-energy curve, Source from Manufacturer Cree's Datasheet C2M0040120D.

As mentioned above, the SiC MOSFET used in this charger is rated at 1200 V/60 A. Double-Pulse Test (DPT) was conducted to obtain the first-hand data on the turn–ON energy (EON) and turn-OFF energy (EOFF). The curve fitted EON and EOFF are shown as Fig. 3-16. The test result is shown in Fig. 3-17a and 3-17b.

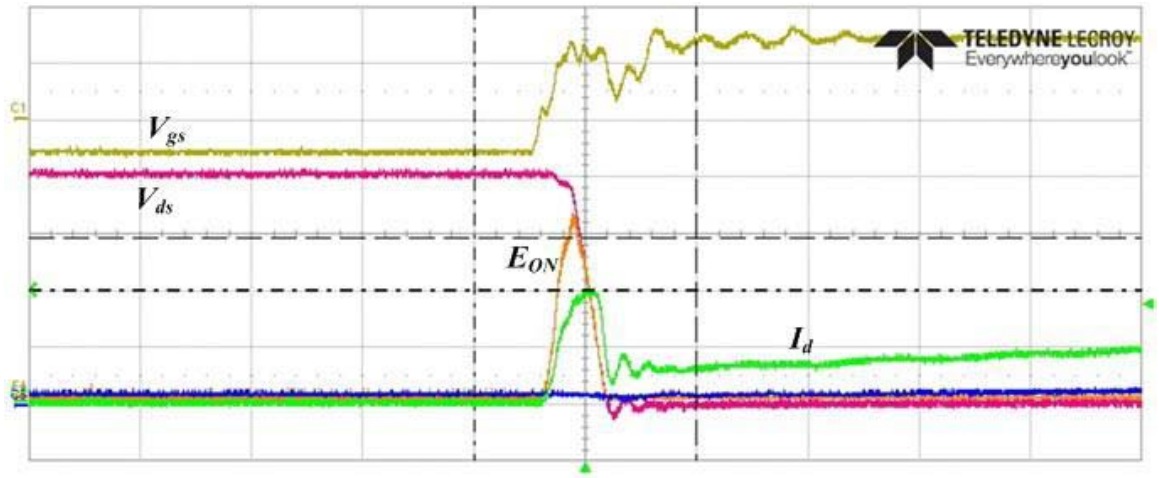

(a) SiC MOSFET switching transient waveform turn-ON process. Gate–source voltage: Vgs (10 V/div); drain–source current: Id (10 A/div); drain–source voltage: Vds (100 V/div); turn-ON energy: EON.

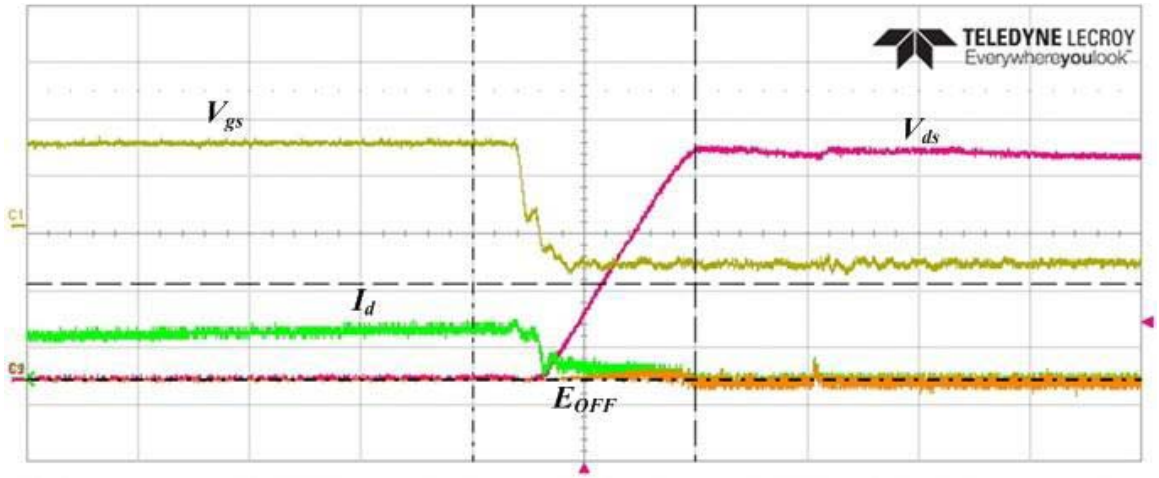

(b) SiC MOSFET switching transient waveform turn-OFF process. Gate–source voltage: Vgs (10 V/div); drain–source current: Id (10 A/div); drain–source voltage: Vds (100 V/div); turn-OFF energy: EOFF.

Figure 3-17: SiC MOSFET switching transient waveform turn-ON and turn-OFF processes from our DPT test using Teledyne LeCroy-manufactured scope.

The switching energy EON and EOFF ofthe switches can be described using curve fitting as

$$E_{ON}(V_{ds}, I_{d\_ON}) = \frac{V_{ds}}{V_{ds_{test}}}(A_1 I_{d\_ON}^2 + B_1 I_{d\_ON} + C_1) \tag{3.4}$$

$$E_{OFF}(V_{ds}, I_{d\_OFF}) = \frac{V_{ds}}{V_{ds_{test}}}(A_2 I_{d\_OFF}^2 + B_2 I_{d\_OFF} + C_2) \tag{3.5}$$

where V_{ds} is the drain–source voltage of the MOSFET, Vdstest is the dc-bus voltage used in the DPT, I_{d_ON} is the current when the switch turns ON, and I_{d_OFF} is the current when the switch turns OFF. Once the LLC circuit is operated under ZVS turn-ON modes, $E_{ON} = 0$. In the PFC circuit, since the switching period is very small compared with the grid period, the PFC inductor current can be assumed constant during one switching period. Overall I_{d_ON} and I_{d_OFF} follow the grid current 50/60 Hz waveform. A similar approach could be adopted for the SiC MOSFET body diode forward voltage drop Vf

$$V_f(t) = A_3 I_{diode}(t)^2 + B_3 I_{diode} + C_3 \tag{3.6}$$

PFC losses can be calculated as

$$\mathrm{P}_{SW\_PFC}(V_{ds}, I_{d\_ON}(t), I_{d\_OFF}(t)) = 6(\int_0^{\pi/3} E_{OFF}(V_{ds}, I_{d\_OFF}(t)))f_{SW\_PFC}dt + \int_{\frac{2}{3}\pi}^{\pi}(E_{ON}(V_{ds}, I_{d\_ON}(t)) + E_{OFF}((V_{ds}, I_{d\_OFF}(t)))f_{SW\_PFC}dt)/2\pi \tag{3.7}$$

Meanwhile

$$I_{d\_ON} = I_{d\_OFF} = I_{grid\_peak}sin(\omega t) \tag{3.8}$$

$$P_{CON\_PFC}(R_{ds}, I_d(t) = 3\int_0^{\pi} I_d(t)^2 R_{ds}dt/\pi \tag{3.9}$$

$$P_{g\_PFC} = Q_g V_{gs} f_{sw\_PFC} \tag{3.10}$$

Using the state-space model proposed in Section II, the turn ON/OFF current of SiC MOSFETs can be obtained for the switching loss calculation in both V2G and

G2V modes. The resonant current waveform can be used for the conduction loss calculation. The secondary diode current can be used for the diode loss calculation. The LLC converter loss can be calculated as

$$P_{SW\_PFC}(V_{ds}, I_{d\_ON}, I_{d\_OFF}) = 2((E_{ON}(V_{ds}, I_{d\_ON}) + E_{OFF}(V_{ds}, I_{d\_OFF}))f_{SW\_PFC} \tag{3.11}$$

$$I_{d\_ON} = I_r(0) \tag{3.12}$$

$$I_{d\_ON} = I_r(\frac{T_s}{2}) \tag{3.13}$$

$$P_{CON\_LLC}(R_{ds}, I_d) = 2\int_0^{\frac{T_s}{2}} I_d^2 R_{ds} dt / \frac{T_s}{2} \tag{3.14}$$

$$I_d(t) = I_r(t) \tag{3.15}$$

$$P_{REC\_LLC}(V_f, I_{REC}) = 4\int_0^{\frac{T_s}{2}} I_{REC} V_f dt / \frac{T_s}{2} \tag{3.16}$$

The above equations can be further summarized in Fig. 3-18, N/A means data is negligible for calculating the system loss.

Type	Part	Switching Loss	Conduction Loss	Secondary Diode Loss	Gate-Drive Loss
Active	PFC	$P_{sw_{PFC}}(V_{ds}, I_{d_{on}}(t), I_{d_{off}}(t)) = 6(\int_0^{\frac{\pi}{2}}(E_{on}(V_{ds}, I_{d_{on}}(t)) + E_{off}(V_{ds}, I_{d_{off}}(t)))f_{sw_{PFC}}dt + \int_{\frac{\pi}{2}}^{\pi}(E_{on}(V_{ds}, I_{d_{on}}(t)) + E_{off}(V_{ds}, I_{d_{off}}(t)))f_{sw_{PFC}}dt)/2\pi$	$P_{con_{PFC}}(R_{ds}, I_d(t)) = 3\int_0^{\pi} I_d(t)^2 R_{ds} dt/\pi$	N/A	$P_{g\_PFC} = Q_g V_{gs} f_{sw\_PFC}$
	LLC	$P_{sw_{LLC}}(V_{ds}, I_{d_{on}}, I_{d_{off}}) = 2((E_{on}(V_{ds}, I_{d_{on}}) + E_{off}(V_{ds}, I_{d_{off}}))\, f_{sw_{LLC}}$	$P_{con_{LLC}}(R_{ds}, I_d) = 2\int_0^{\frac{T_s}{2}} I_d^2 R_{ds} dt/\frac{T_s}{2}$	$P_{sec_{LLC}}(V_f, I_{rec}) = 4\int_0^{\frac{T_s}{2}} I_{rec} V_f dt/\frac{T_s}{2}$	N/A
		Copper Loss	Iron Loss		
Passive	Resonant Capacitor	$P_{copper_{Cr,Lr,Ls}}(R_{ESR}, I_r) = \int_0^{T_s} {I_r}^2 R_{ESR} dt/T_s$	N/A		
	Resonant Inductor		N/A		
	Transformer		$P_v = k f^{\alpha} \hat{B}^{\beta}$		

Figure 3-18: Overview of System Power Loss.

Using the power loss model above, the system efficiency can be derived as a function of component parameters, system operating conditions, and MOSFET characteristics. The related parameters include the system gain M, quality factor Q, ac equivalent resistance R_{ac}, load resistance R_L, LLC switching frequency f_{sw}, and circuit current/voltage waveform. Other conditions such as the grid voltage and the

PFC switching frequency are either uncontrollable or assumed to be constant. In general

$$P_{loss\_total} = f(V_{dc}, V_{bat}, I_{bat}) \tag{3.17}$$

Here we propose to further optimize the system efficiency by varying V_{dc}. Due to the complexity of the LLC converter operating modes, every battery charging condition can be realized by various combinations of f_{sw} and V_{dc}, which exhibits different efficiency. A conventional PFC is controlled to output a constant dc-bus voltage (V_{dc}), where the controller can only modify the switching frequency slightly to maintain a desired charging profile. By varying the dc bus voltage, we have the potential to gain an even higher efficiency.

3.2 System Test of Electric Network

After the system modeling and simulations, it's the time to prove the concept by building and testing a research prototype. The proposed control algorithm is experimentally validated on the designed 10 kW 250–400 V SiC-based EV charger. The designed 250–450 V/10 kW three-phase EV charger is used to verify the proposed control method and the power-loss model. Two TI F28335 digital signal processor (DSP) controllers are used to control the PFC/LLC/boost circuit. DSP1 controls the boost PFC. DSP2 controls the LLC converter and the solar boost converter.

Tested efficiency using the variable dcbus control method and constant dc-bus control method is shown in Figs. 3-19 and 3-20 by measuring voltages and currents at the system input and output.

The dc-bus voltage is limited to 510–850 V to ensure safe operation. The simulated efficiency is very close to the experimental efficiency. It is of note that these efficiency curves included the loss of passive components. The tested efficiency also verified the effectiveness of such variable dc-bus control over the load range in Fig. 3-21. The efficiency curve is achieved from tests using constant 400V battery with 1 to 10kW charging power.

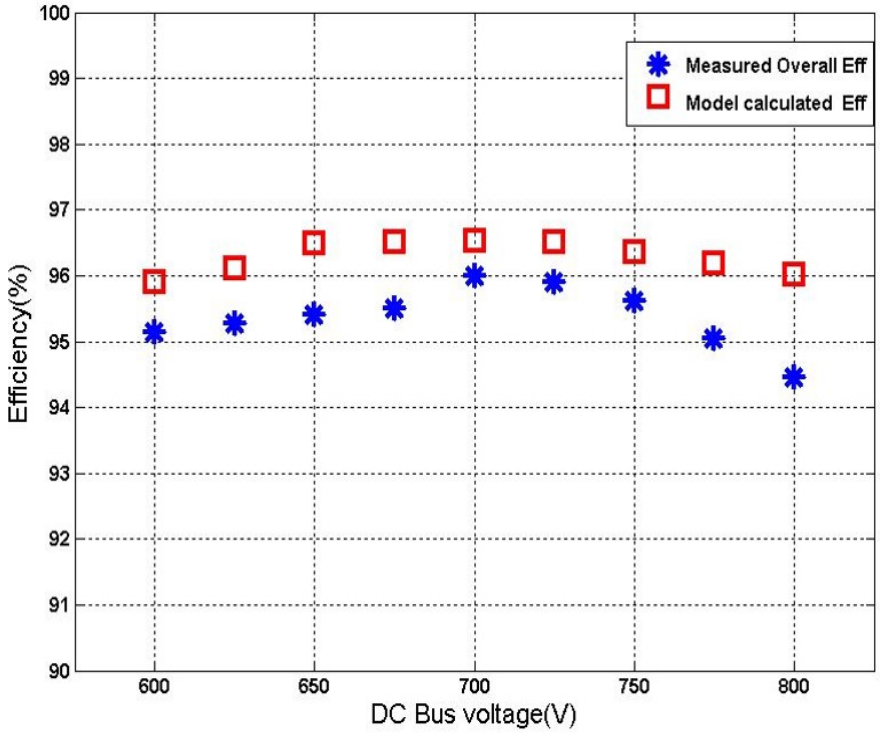

Figure 3-19: Efficiency curve at 400 V/17 A output with variable dc-bus voltages (G2V). Measured Eff. is obtained from measured voltages and currents at the system input and output.

The optimal dc-bus voltage is calculated and set at 715 V by the PFC controller. The LLC converter maintains the switching frequency at 120 kHz. As the load current target changes, software fine-tunes the voltage set point to regulate the output current.

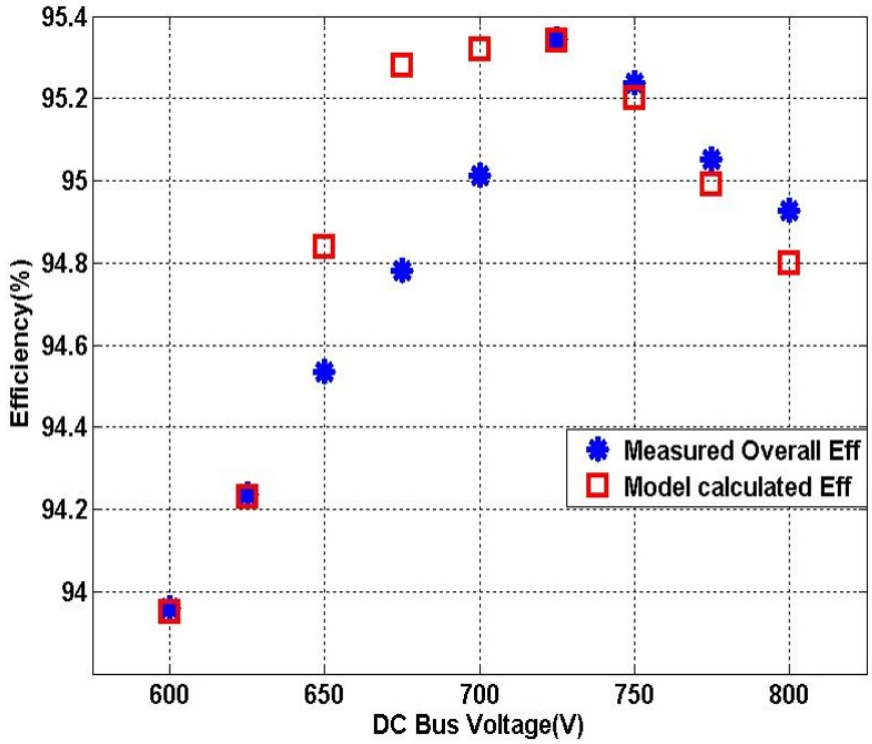

Figure 3-20: Efficiency curve at 400 V/8 A output with variable dc-bus voltages (G2V).

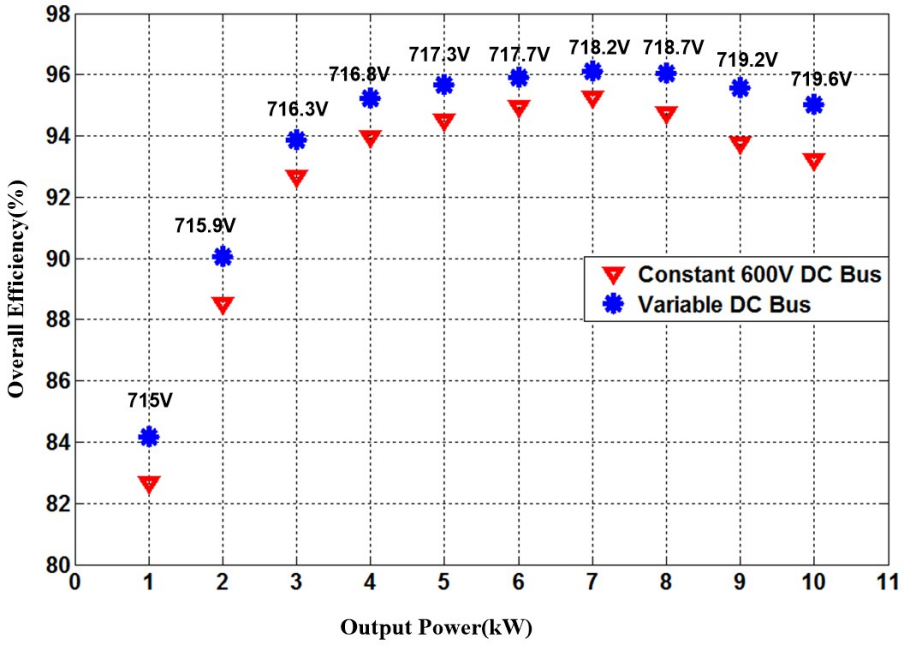

Figure 3-21: Overall system efficiency curve comparison over a load range at 400 V/2.5–25 A between optimal dc-bus voltage control and constant 600 V dc-bus control (G2V).

To conclude, a SiC-based three-phase EV charger made of a bidirectional PFC, a bidirectional LLC converter, and a unidirectional solar boost converter. It is well known that the LLC topology could realize the ZVS when charging the battery; however, it is not very well explored that it could reach ZVS as well when used in the V2G mode, which has been verified in this work. The double pulse test was first used to measure the SiC MOSFET power loss. Based on that, the power conversion efficiency is estimated using the current and voltage information derived from the LLC converter statespace model. Compared with the conventional FHA method, state-space models used in this work are more accurate when calculating the switching-ON/OFF losses. The simulation results show that the overall system efficiency reaches its peak value at the LLC resonant frequency.

Table 3.2: Our approach versus the state of the art in EV chargers.

Reference	Efficiency	Maximum Power(kW)	V2G Capable	Year of Completion
our work	96.0%	10	Yes	2016
[63]	90.0%	3.7	No	2014
[64]	95.0%	6.1	No	2014
[65]	94.0%	8	No	2014
[66]	95.0%	2	No	2015
[67]	93.8%	3.3	Yes	2015
[68]	94.5%	3.3	Yes	2015
[69]	94.6%	2	No	2016
[82]	95.2%	10	Yes	2019
[83]	95.3%	6.6	Yes	2019

The experimental results based on an all-SiC 10-kW EV charger prototype verified the simulation results. Compared to existing state-of-art technologies [63–69, 82, 83] shown in Table 3.2, our approach provides the efficiency increment of up to 2% in average, shown in Fig. 3-22. Also, we achieved V2G by using controlled SiC MOSEFT switches in our bi-directional circuit topology.

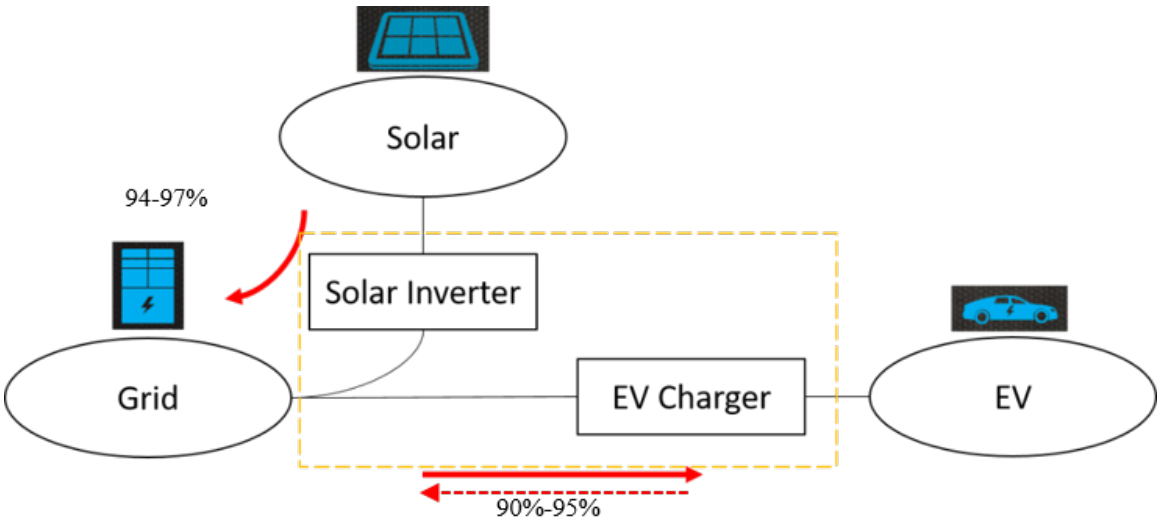

(a) State of Art Technologies in [63–69, 82, 83].

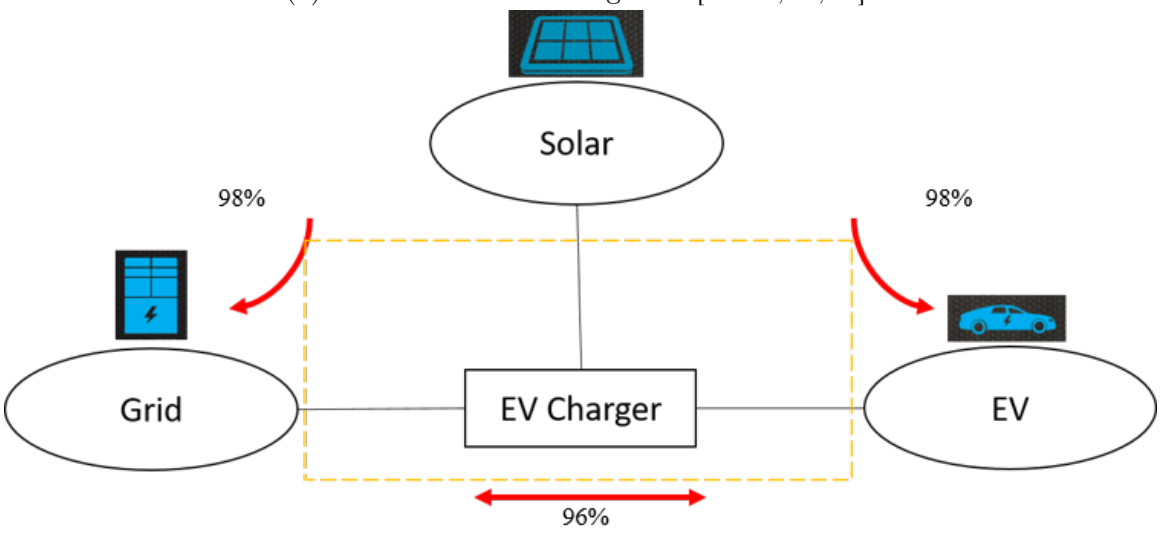

(b) Our Work with Smart EV Charger.

Figure 3-22: Comparison of Technologies in Solar-Powered EV Network.

Chapter 4

Centralization of Electronic Network

A wireless power transfer systems for multi-user charging is proposed to demonstrate a robust quasi-uniform power efficiency in 3-D space. It employs a set of balanced magnetic coils excited with phase-shifted currents on the transmitting side to feature omnidirectionality. In this work, two transmitter structures, 2-coil and 3-coil systems are discussed and compared. These systems produce a quasi-uniform magnetic field magnitude regardless of the location of the receiving coils provided that the coils point to the center of the transmitting system sphere at the same distance. A simulation platform is established for the proposed method. Experimental results at 2MHz substantiate uniform spatial efficiency, and bound the average error of analytical calculations within 10%. Furthermore, the proposed method with rotating fields based on phase-shifted currents shows that 3-coil system yields a higher and much more stable efficiency range, 6.8% improvement on average efficiency and 88.7% reduction on efficiency variance compared to the 2-coil system.

4.1 3-D Quasi-Uniform Wireless Power Transfer System

4.1.1 Modeling and Control

A. Circuit Model

A1. Single-Transmitter Single-Receiver (STSR) System

Consider first the single-transmitter and single-receiver (STSR) case shown in Fig. 4-1. The magnetic coupling of the circuit is described as below

$$\begin{bmatrix} v_1 \\ v_2 \end{bmatrix} = j\omega \begin{bmatrix} L_t & M \\ M & L_r \end{bmatrix} \begin{bmatrix} i_1 \\ i_2 \end{bmatrix} \tag{4.1}$$

As determined by the load, the secondary voltage is therefore

$$v_2 = -(R_r + R_{r-rad} + R_L + \frac{1}{j\omega C_r})i_2 \tag{4.2}$$

where R_r is resistance of the receiving coil, R_L is load resistance, C_r is a resonant capacitance, and R_{r-rad} is the equivalent radiation resistance of the receiving coil. The radiation resistance, caused by the radiation of electromagnetic waves, is defined as the ratio of radiation power over current squared. Since the radius of the transmitting (Tx) coil (10cm) is much smaller than the wavelength of radiation (150m), Rr-rad can be approximated as a magnetic dipole. The radiation power of the magnetic dipole is $\frac{\mu_0 \omega^4 |m|^2}{12^3}$ where μ_0 is the permeability of free space, ω is the angular frequency, c is speed of light, and m is the magnetic dipole moment [84]. For the Tx coil, the magnetic dipole moment is proportional to its winding turns n, coverage area $\pi\alpha^2$ namely $n\pi\alpha^2$. Thus R_{r-rad} can be further obtained as

$$R_{r-rad} = \frac{n\mu_0\pi\alpha^4}{12c^3}\omega^4 \tag{4.3}$$

where α is radius of the coil, and n is the number of winding turns. When the frequency ω is on the order of 1MHz, α is on the order of 10 cm, and n is on the order of 10, R_{r-rad} becomes on the order of $10^{-7}\Omega$, and is thus negligible at single digit MHz frequencies; however, R_{r-rad} is proportional to the 4th power of the frequency ω, thus if the frequency increases to 10 MHz for example, the radiation resistance increases to the mΩ level, and becomes comparable to the coil resistance.

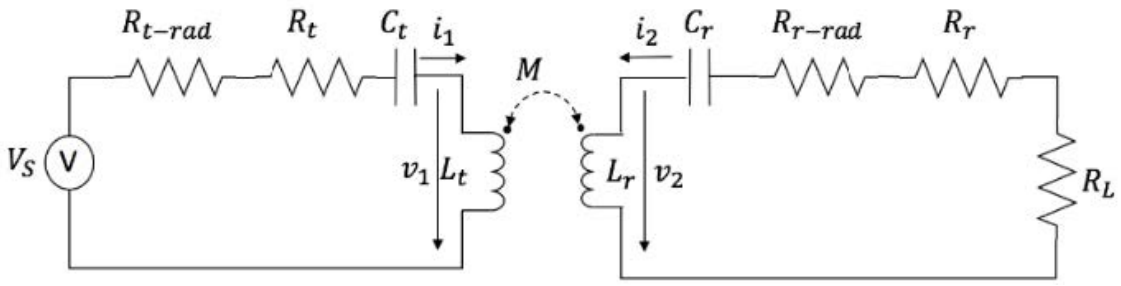

Figure 4-1: Circuit Model of STSR System.

When working at the resonance frequency of the transmitting coil and receiving coil, combining 4.1 and 4.2 yields

$$\frac{i_1}{i_2} = \frac{R_r + R_{r-rad} + R_L}{\omega M} \tag{4.4}$$

as the ratio of transmitting-coil to receiving-coil coil current. Efficiency is defined as the ratio of the output power to the power input to the transmitting system, which is given by

$$\eta = \frac{i_2 i_2^* R_L}{i_1 i_1^* (R_t + R_{t-rad}) + i_1 i_2^* (R_r + R_{r-rad} + R_L)} \tag{4.5}$$

where Rt is the resistance of transmitting coil, and Rt-rad is the equivalent resistance of the transmitting coil radiation. Combining Eq. (4.4) and Eq. (4.5) then allows the efficiency to be expressed as

$$\eta = \frac{R_S}{R_S + R_t + R_{t-rad}} \frac{R_L}{R_L + R_r + R_{r-rad}} \tag{4.6}$$

where

$$R_S = \frac{\omega^2 M^2}{R_L + R_r + R_{r-rad}} \tag{4.7}$$

The efficiency expression shown in Eq. (4.6) is therefore the product of the transmitting-side efficiency $\frac{R_S}{R_S+R_t+R_{t-rad}}$ and the receiving-side efficiency $\frac{R_L}{R_L+R_r+R_{r-rad}}$.

A2. Multi-Transmitter Multi-Receiver (MTMR) System

The proposed system layout shown in Fig. 3 includes a transmitting subsystem with phase-shifted current drives, a receiving-coil subsystem comprising multiple receiving coils with electric loads, and a power electronics subsystem including the DC/AC inverter and power amplifiers. The transmitting subsystem is a balanced coil structure so that the amplitude of the resulting magnetic field can be approximately uniform with proper angle settings, as motivated by the rotating magnetic field of electric machines. Current sources with proper phase shift drive the transmitting coils, with each coil having its own current source. Two balanced structures are proposed and found to achieve a uniform-amplitude magnetic field, and hence a nearly-uniform efficiency at the resonant frequency. These two structures are a 2-coil system and 3-coil system. A practical objective is to use the fewest possible coils to achieve uniform efficiency, thereby maintaining competitive cost. Circuit models of the 2-coil and 3-coil WPT systems are shown in Fig. 4-3 and Fig. 4-4, respectively. On the transmitting side, each coil has the same model, and the mutual inductances among them is zero owing to the orthogonal structure. Therefore, no mutual inductance exists on the transmitting side. Between the transmitting side and receiving side, mutual inductances are created by the interaction of the transmitting coils and multiple receiving coils, denoted as M1i, M2i, (M3i), respectively. A general case is discussed here: MTMR with n transmitting coils and m receiving coils. Similar to the STSR case, the relation between the coil voltage and currents can be described by

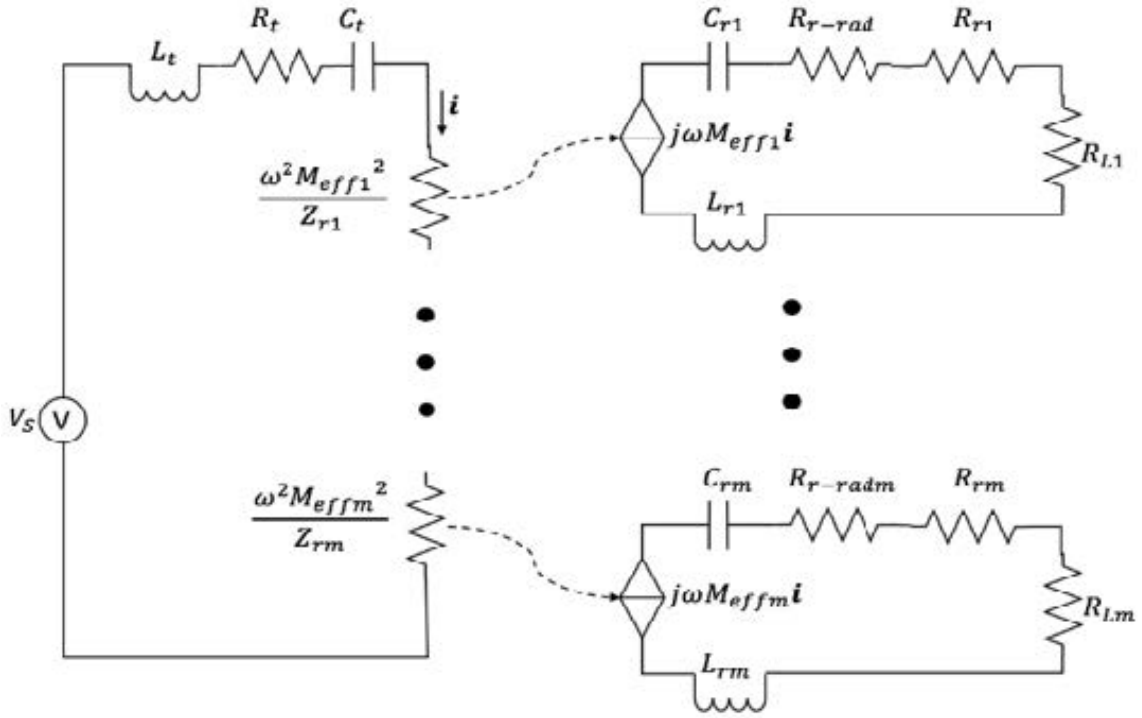

Figure 4-2: Equivalent Circuit Model for MTMR System.

$$\begin{bmatrix} v_{t1} \\ \vdots \\ v_{tn} \\ \vdots \\ v_{r1} \\ \vdots \\ v_{rm} \end{bmatrix} = j\omega \begin{bmatrix} L_{t1} & \dots & M_{t1n} & M_{11} & \dots & M_{1m} \\ \vdots & & \vdots & \vdots & \ddots & \vdots \\ M_{tn1} & \dots & L_{tn} & M_{n1} & \dots & M_{nm} \\ M_{11} & M_{1n} & \dots & L_{r1} & \dots & M_{r1m} \\ \vdots & \ddots & \vdots & \vdots & \ddots & \vdots \\ M_{m1} & \dots & M_{mn} & M_{rm1} & \dots & L_{rm} \end{bmatrix} \begin{bmatrix} i_{t1} \\ \vdots \\ i_{tn} \\ i_{r1} \\ \vdots \\ i_{rm} \end{bmatrix} \tag{4.8}$$

where M_{tij} represents mutual inductance between the transmitting coils, M_{rij} represents mutual inductance between the receiving coils, L_{ti} represents self-inductance of the transmitting coils, and L_{ri} represents self-inductance of the receiving coils. In this case, because the transmitting coils are orthogonal, $M_{tij} = 0$.

As taken from 4.8, the voltages of the receiving coils are

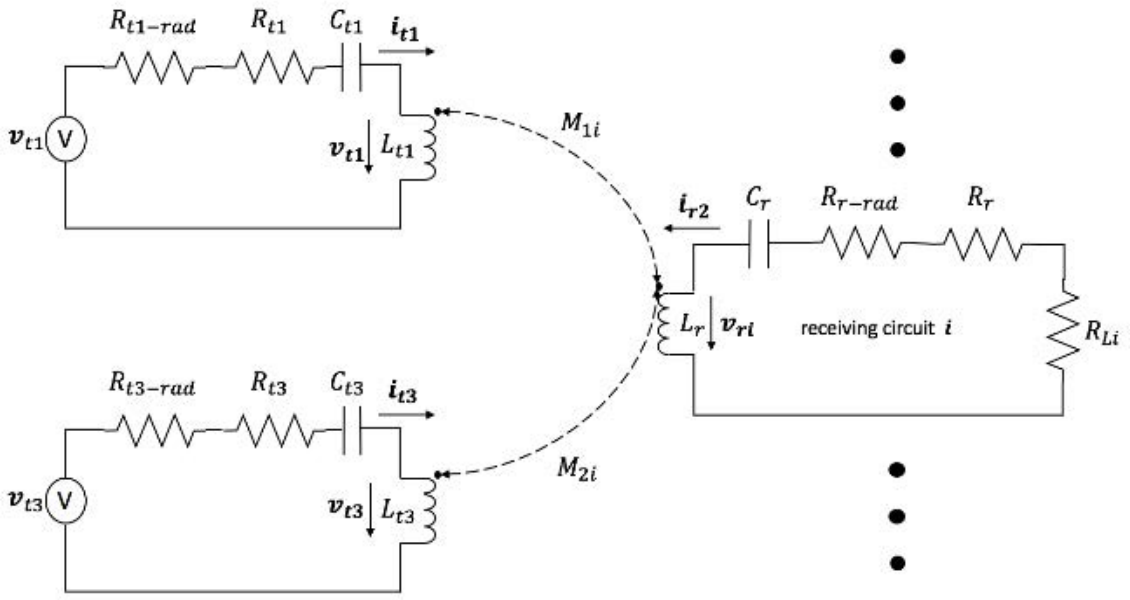

Figure 4-3: Circuit Model of MTMR System of 2-coil system

$$\begin{bmatrix} v_{r1} \\ \vdots \\ v_{rm} \end{bmatrix} = j\omega \begin{bmatrix} M_{11} & \dots & M_{1n} & L_{r1} & \dots & 0 \\ \vdots & \ddots & \vdots & \vdots & \ddots & \vdots \\ M_{m1} & \dots & M_{mn} & 0 & \dots & L_{rm} \end{bmatrix} \begin{bmatrix} i_{t1} \\ \vdots \\ i_{tn} \\ i_{r1} \\ \vdots i_{rm} \end{bmatrix} \tag{4.9}$$

Separately, the voltage of each receiving coil can be represented by

$$v_{ri} = -(R_{ri} + R_{r-radi} + R_{Li} + \frac{1}{j\omega C_{ri}})i_{ri} \tag{4.10}$$

where i is from 1 to m. Let the currents of transmitting coils to be

$$i_{ti} = i_t \beta_i e^{\alpha i} \tag{4.11}$$

where it is the normal current of the transmitting coil-set, and β_i and α_i the normalized amplitude coefficient and phase of corresponding transmitting coils. When all transmitting and receiving coils resonate at the same frequency, similar to the

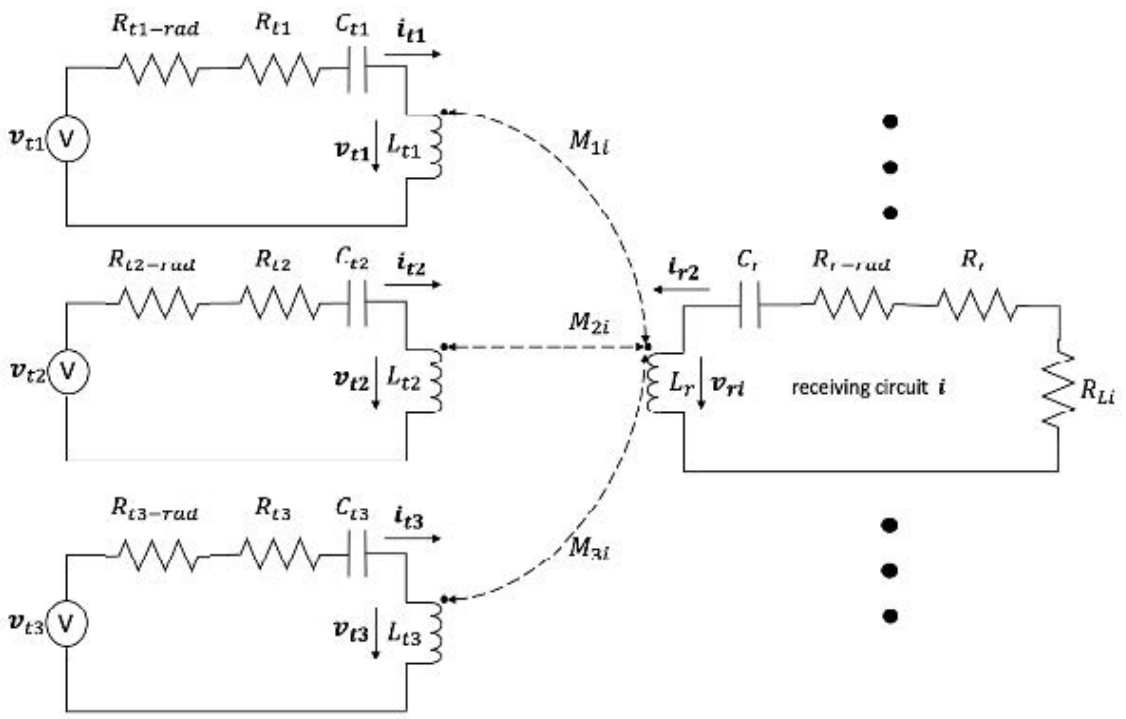

Figure 4-4: Circuit Model of MTMR System of 3-coil system

STSR case, the ratio of the norm of the transmitter currents and receiving coil current is

$$\frac{i_t}{i_{ri}} = \frac{R_{ri} + R_{r-radi} + R_{Li}}{\omega M_{effi}} \tag{4.12}$$

Efficiency is again defined as

$$\eta = \frac{\sum_{i=1}^{m} i_{ri} i_{ri}^* R_{Li}}{\sum_{i=1}^{m} i_{ti} i_{ti}^* (R_{ti} + R_{t-radi}) + \sum_{i=1}^{m} i_{ri} i_{ri}^* (R_{ri} + R_{r-radi} + R_{Li})} \tag{4.13}$$

Substituting Eq. (4.12), efficiency becomes

$$\eta = \frac{R_S}{R_S + R_t} \sum_{i=1}^{n} \frac{R_{Si}}{R_S} \frac{R_{Li}}{R_{Li} + R_{ri} + R_{r-radi}} \tag{4.14}$$

where

$$R_t = \sum_{i=1}^{n} \beta_i^2 (R_{ti} + R_{t-radi}) \tag{4.15}$$

$$R_s = \sum_{i=1}^{m} R_{si} \tag{4.16}$$

$$R_{si} = \frac{\omega^2 M_{effi}^2}{R_{Li} + R_{ri} + R_{r-radi}} \tag{4.17}$$

$$M_{effi} = \sum_{j=1}^{n} M_{ji} \beta_j \exp^{\alpha j} \tag{4.18}$$

which is defined as the effective mutual inductance of corresponding receiving coil. Substituting Eq. (4.15) - Eq. (4.18), Eq. (4.14) becomes

$$\eta = \frac{\sum_i k_{1i} M_{effi}^2}{R_r + \sum_i k_{2i} M_{effi}^2} \tag{4.19}$$

where

$$k_{2i} = \frac{\omega^2}{R_{Li} + R_{ri} + R_{r-radi}} \tag{4.20}$$

$$k_{1i} = \frac{\omega^2 R_{Li}}{(R_{Li} + R_{ri} + R_{r-radi})^2} \tag{4.21}$$

Although Eq. (4.19) shows a non-linear relationship between efficiency and effective mutual inductance, it shows that the relationship depends on a combination of resistances which are constant at a given frequency ω. Thus, the efficiency has a positive relationship with the effective mutual inductance of multiple receivers at a given frequency. Finally, the ratio of a user's power to the total power input to the transmitting coil is

$$\frac{P_i}{P_t} = \frac{R_{Si}}{R_S + R_t} \frac{R_{Li}}{R_{Li} + R_{ri} + R_{r-radi}} \tag{4.22}$$

The expressions for efficiency and receiver power can be understood by the equiv-

alent circuit of the MTMR WPT system shown in Fig. 3, where $Z_{Li} = R_{ri} + R_{r-radi} + R_{Li} + \frac{1}{j\omega C_{ri}} + j\omega L_{ri}$.

B. Effective Mutual Inductance

The mutual inductance between two coils [55] is

$$M = \frac{\mu_0}{4\pi} \oint_{L'} \oint_{L} \frac{Idl}{r} \, dl' \tag{4.23}$$

where L and L' are curve following the two coils, and r is the distance between the two coil segments. The effective mutual inductance can be calculated by Eq. (4.18) thereafter. The 2-coil system in Fig. 4-5 comprises two vertical coils, and the 3-coil system in Fig. 4-6 comprises three tilted coils. The tableplane shows transmitting coils are orthogonal in both of the structures. The normal vectors of the 2-coil system are (1,0,0) and (0,1,0); and of the 3-coil system are ($-\frac{1}{\sqrt{2}}$, $\frac{1}{\sqrt{6}}$,$-\frac{1}{\sqrt{3}}$), ($\frac{1}{\sqrt{2}}$,$\frac{1}{\sqrt{6}}$, $-\frac{1}{\sqrt{3}}$), and (0, $-\frac{2}{\sqrt{6}}$, $-\frac{1}{\sqrt{3}}$). To measure the mutual inductance distribution, consider the tableplane with the receiving coil facing the z axis (coil A in Fig. 4-5) and the sphere with the receiving coil facing the radial direction (coil B in Fig. 4-6). Fig. 4-7 shows the flowchart of the phase-shift control method. The operating mode is automatically selected between 2-phase and 3-phase based on environmental parameters.

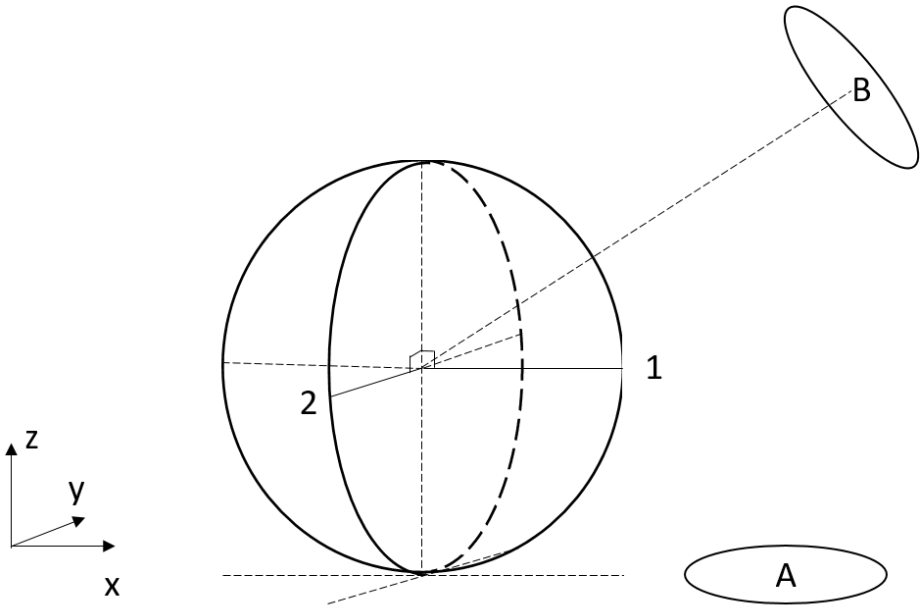

Figure 4-5: Placement of the transmitting and receiving coil:2-Coil system.

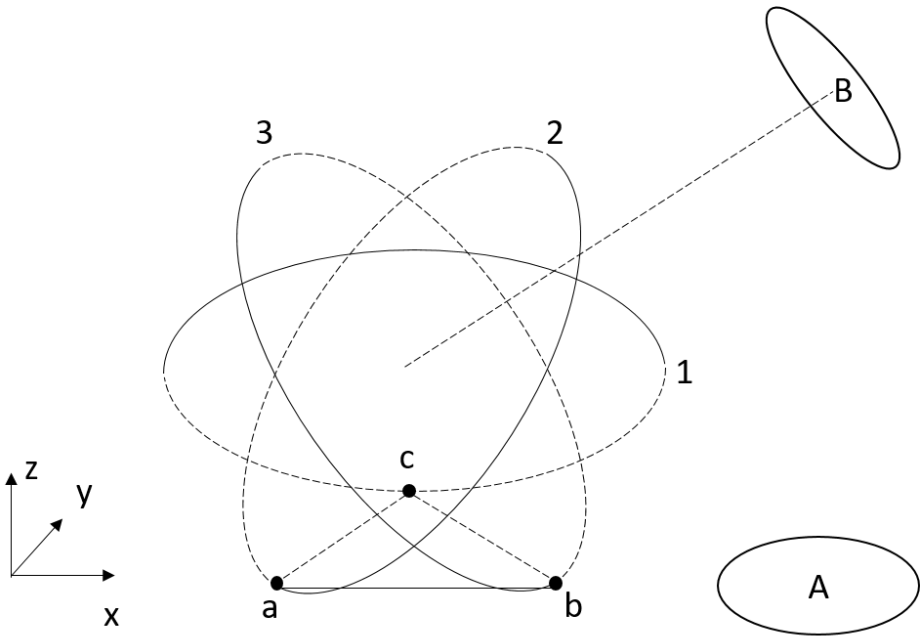

Figure 4-6: Placement of the transmitting and receiving coil: 3-Coil system.

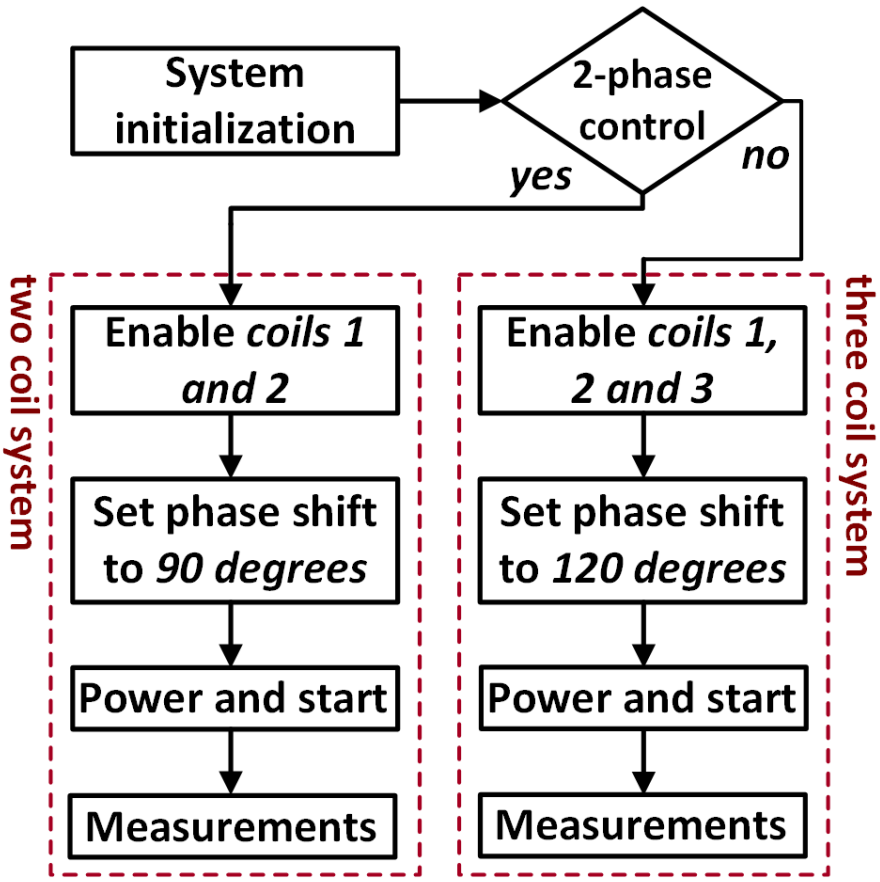

Figure 4-7: Flowchart of phase-shift control.

For evaluation purposes, let the radius of each transmitting coil be 7.5 cm, and each receiving coil be 5 cm. The effective mutual inductance for driven currents with and without phase shift for the 2-coil structure and 3-coil structure are compared, respectively. First, 2-coil structure has two coils, coil 1 and coil 2's effective mutual inductance shown in Fig. 4-8 has the same shape but different direction since they are placed in different position as shown in Fig. 4-5. The sum of these two vectors results in the effective mutual inductance shown in Fig. 4-9.

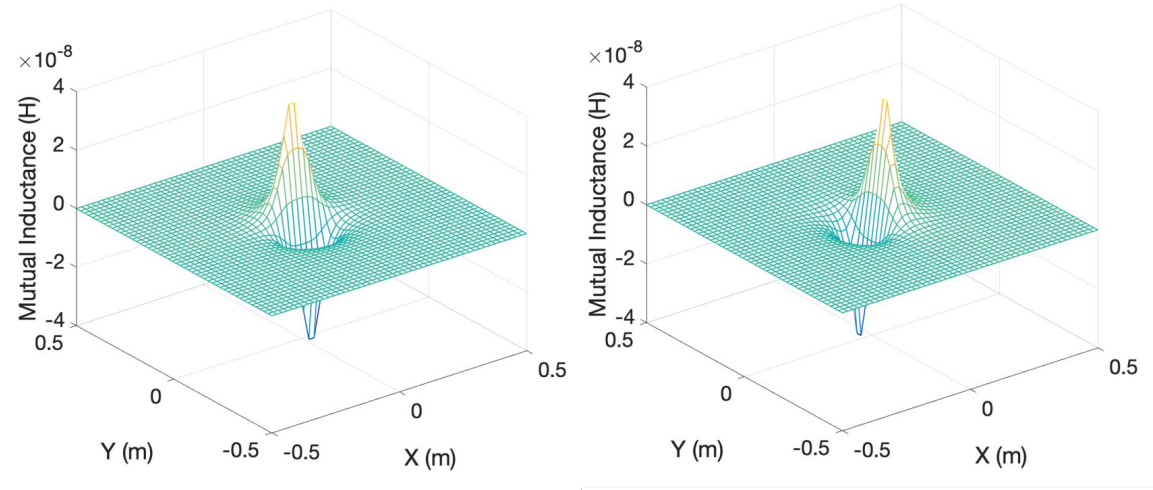

Figure 4-8: Planar mutual inductance distribution of 2-Coil structure: effective mutual inductance without phase shift of each coil.

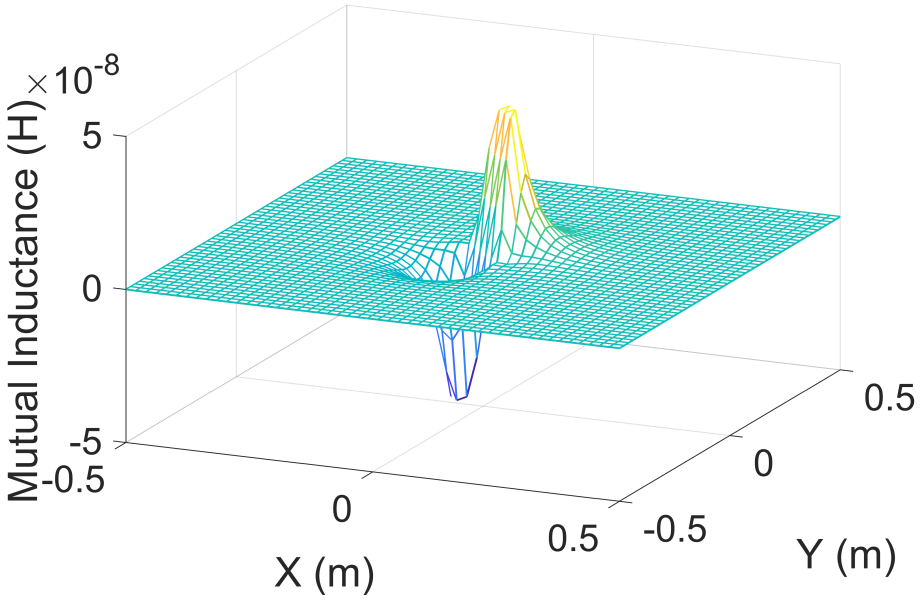

Figure 4-9: Planar mutual inductance distribution of 2-Coil structure: effective mutual inductance without phase shift of vector sum.

Similarly, 3-coil structure has three coils, coil 1, coil 2 and coil 3's effective mutual inductance shown in Fig. 4-10 has the same shape but different direction since they are placed in different position as shown in Fig. 4-6. The sum of these three vectors results in the effective mutual inductance shown in Fig. 4-11. These graphs explain the condition without phase shift.

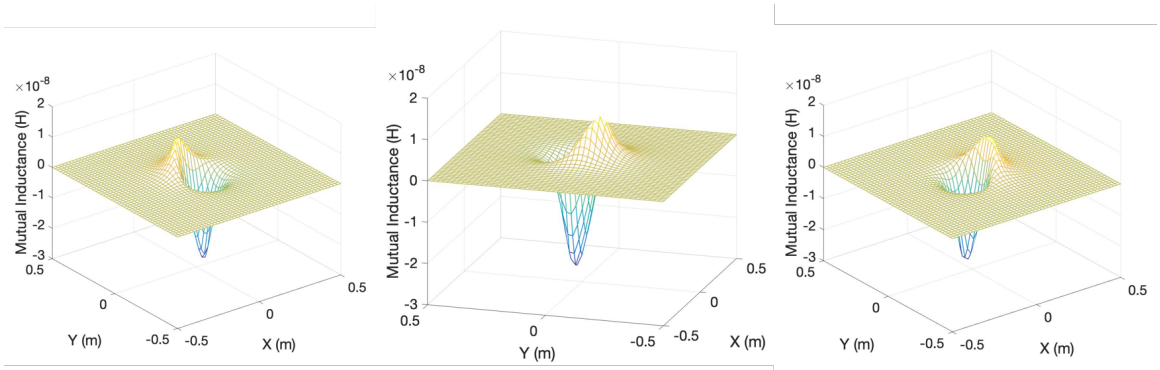

Figure 4-10: Planar mutual inductance distribution of 3-Coil structure: effective mutual inductance without phase shift of each coil.

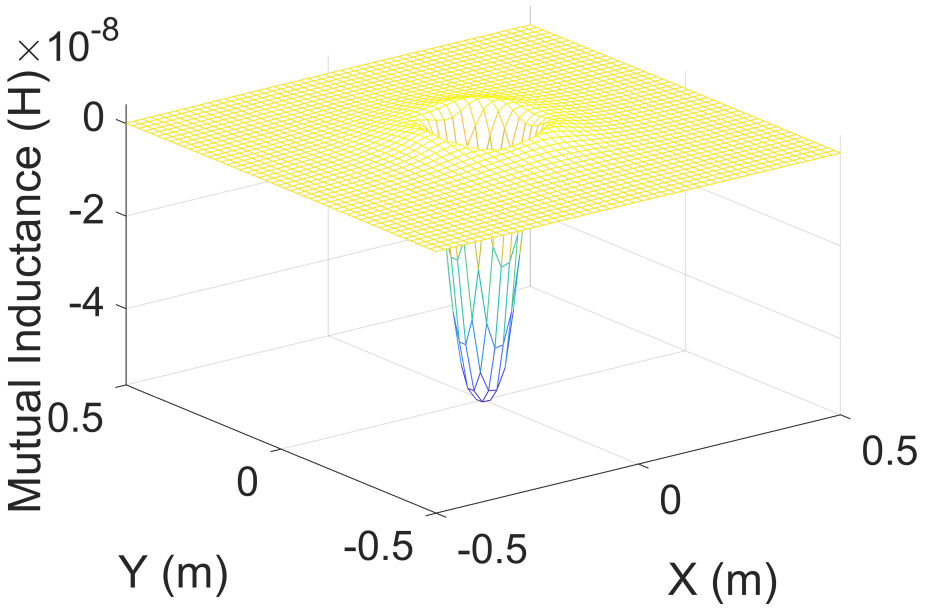

Figure 4-11: Planar mutual inductance distribution of 3-Coil structure: effective mutual inductance without phase shift of vector sum.

Second, we introduce the phase shift method for each structure, 2-coil structure has 90degrees phase shift between each coil, and 3-coil structure has 120degrees between each coil. The vector sum of them are in complex form, and its magnitude of planar view are shown in Fig. 4-12 for the 2-coil structure and Fig. 4-13 for the 3-coil structure. The value of magnitude for the 3-coil case is smaller because the relatively laying position as shown in Fig. 4-6.

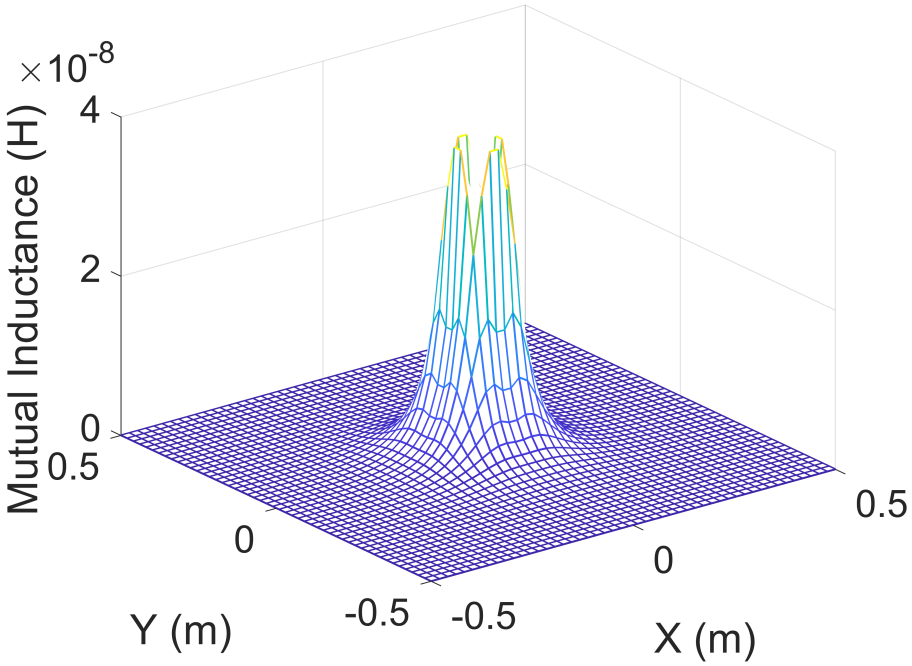

Figure 4-12: Planar mutual inductance distribution of 2-Coil structure: magnitude of effective mutual inductance with 90 degrees phase shift.

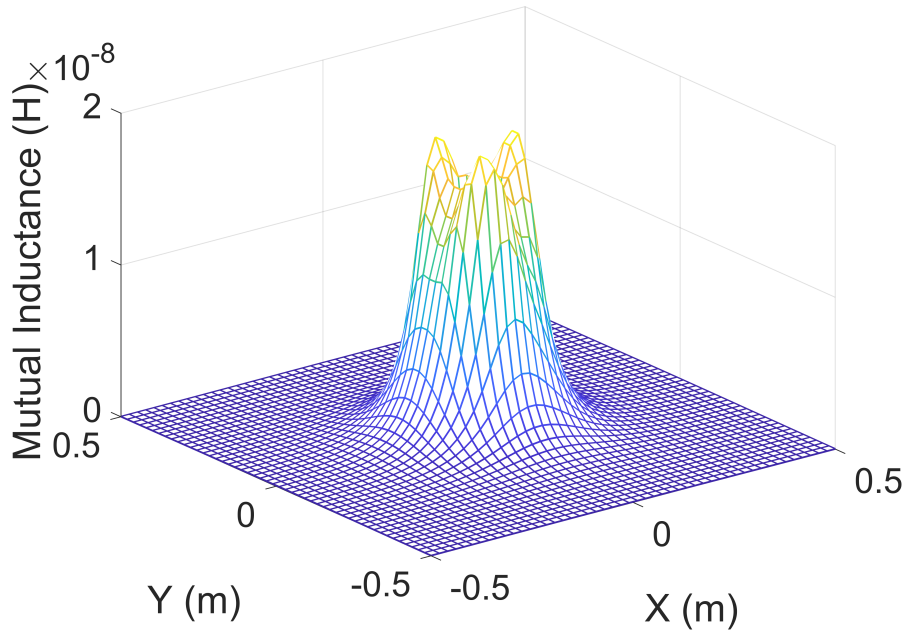

Figure 4-13: Planar mutual inductance distribution of 3-Coil structure: magnitude of effective mutual inductance with 120 degrees phase shift.

These figures show that, when the currents are in phase, the effective mutual inductance only has high intensity at two quadrants for the 2-coil structure, and at the center where receiver cannot reach for the 3-coil structure. Comparing Fig. 4-9 and Fig. 4-12, andFig. 4-11 and Fig. 4-13 it is apparent that proper phase shift of the driven currents can generate nearly equal strong effective mutual inductance all around the transmitter if the receiving coil is placed on the table plane.

The 3-D diagram of mutual inductance distribution on the sphere with 20 cm radius for the 2-coil and 3-coil structures are shown in Fig. 4-14 - Fig. 4-19, respectively. In a manner analogous to the radiation pattern of an antenna, under the spherical coordinates, the radii to the surfaces represent the absolute value of mutual inductance of the receiving coil placed at corresponding angle with radial orientation. By comparing Fig. 4-15 and Fig. 4-18, and Fig. 4-17 to Fig. 4-19, it is apparent that the use of proper phase-shifts for drive currents can enhance the mutual inductance around the entire 3-D space in the vicinity.

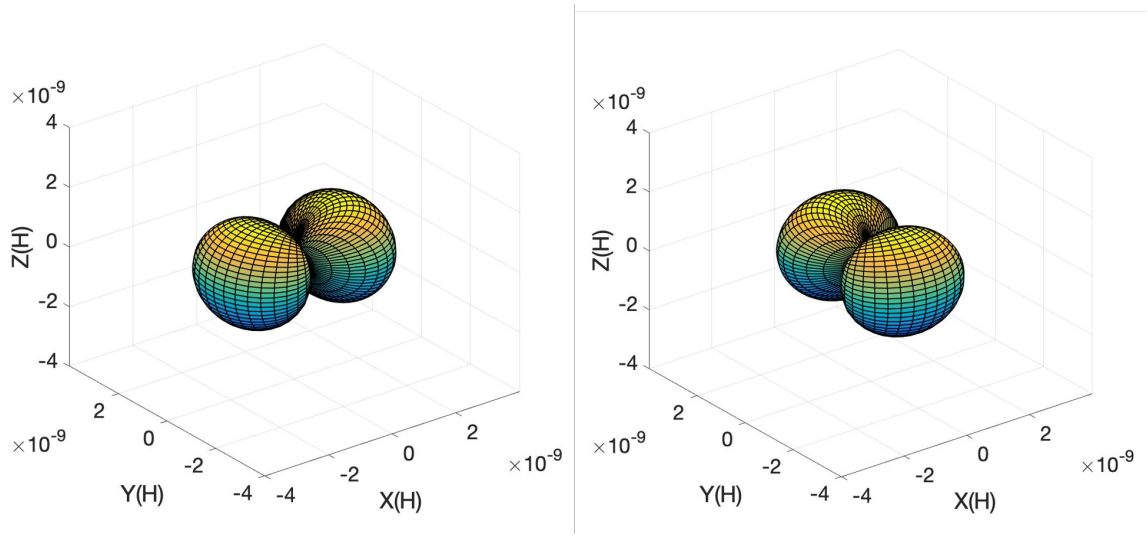

Figure 4-14: 3D mutual inductance distribution of 2-Coil structure: effective mutual inductance without phase shift of each coil.

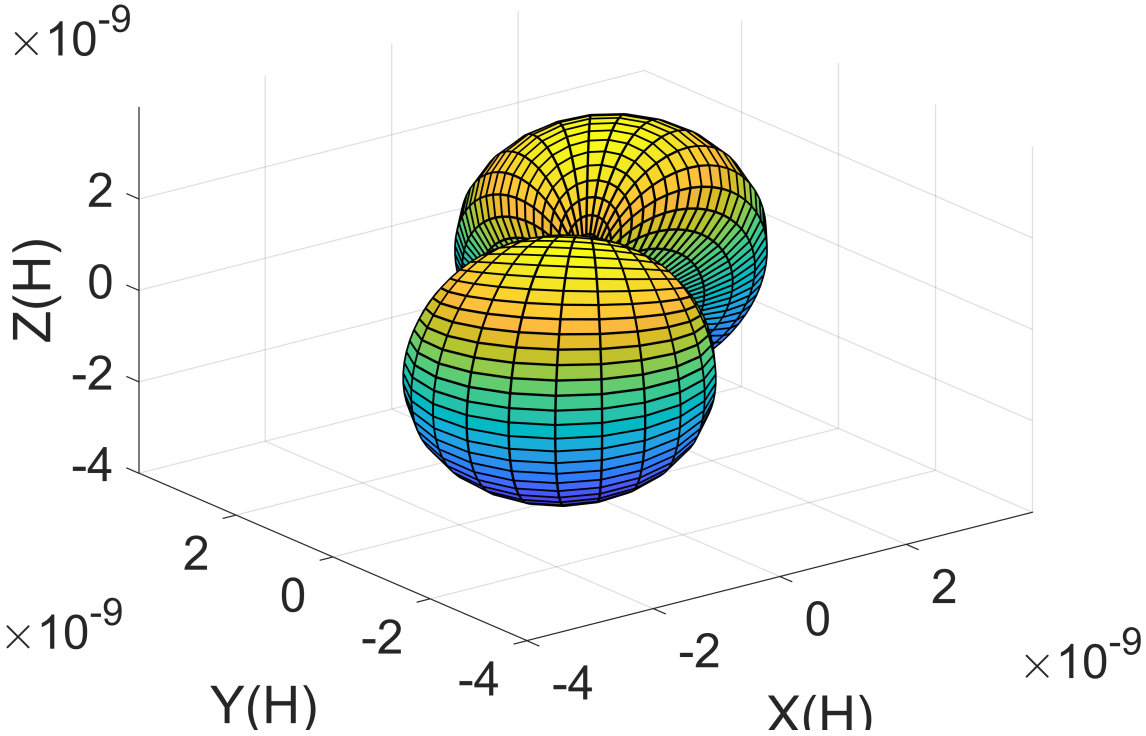

Figure 4-15: 3D mutual inductance distribution of 2-Coil structure: effective mutual inductance without phase shift of vector sum.

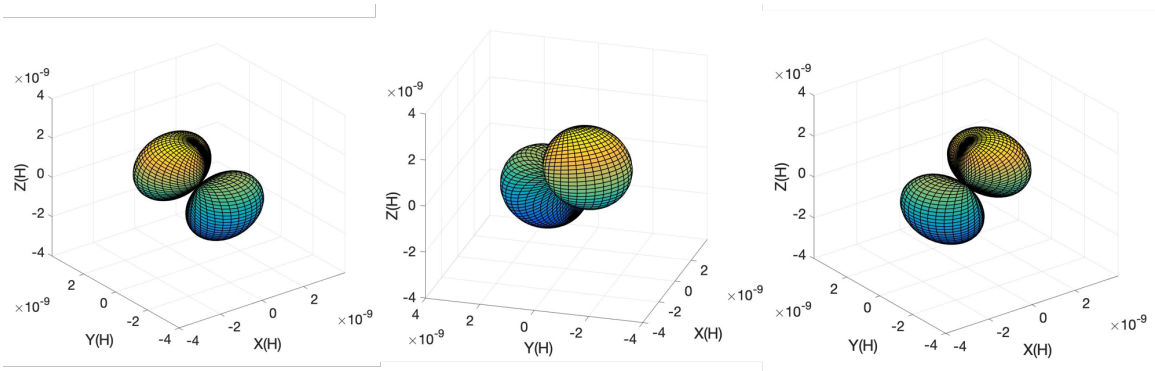

Figure 4-16: 3D mutual inductance distribution of 3-Coil structure:effective mutual inductance without phase shift of each coil.

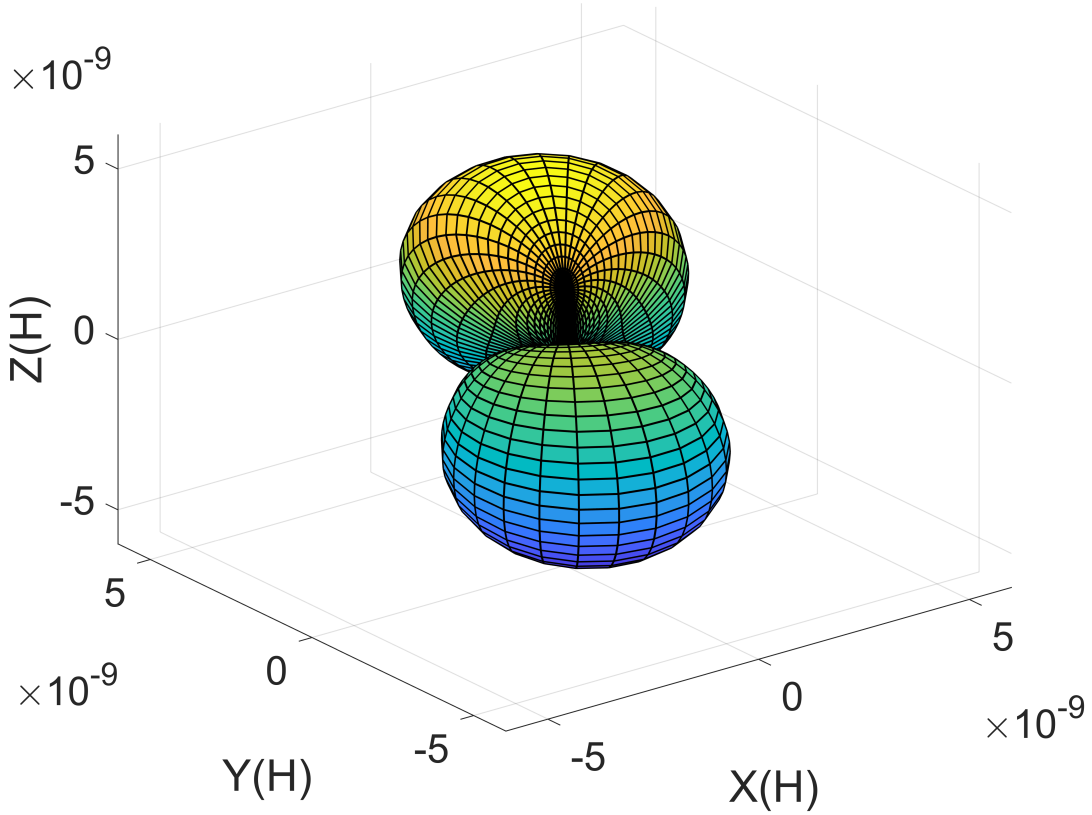

Figure 4-17: 3D mutual inductance distribution of 2-Coil structure: effective mutual inductance without phase shift of vector sum.

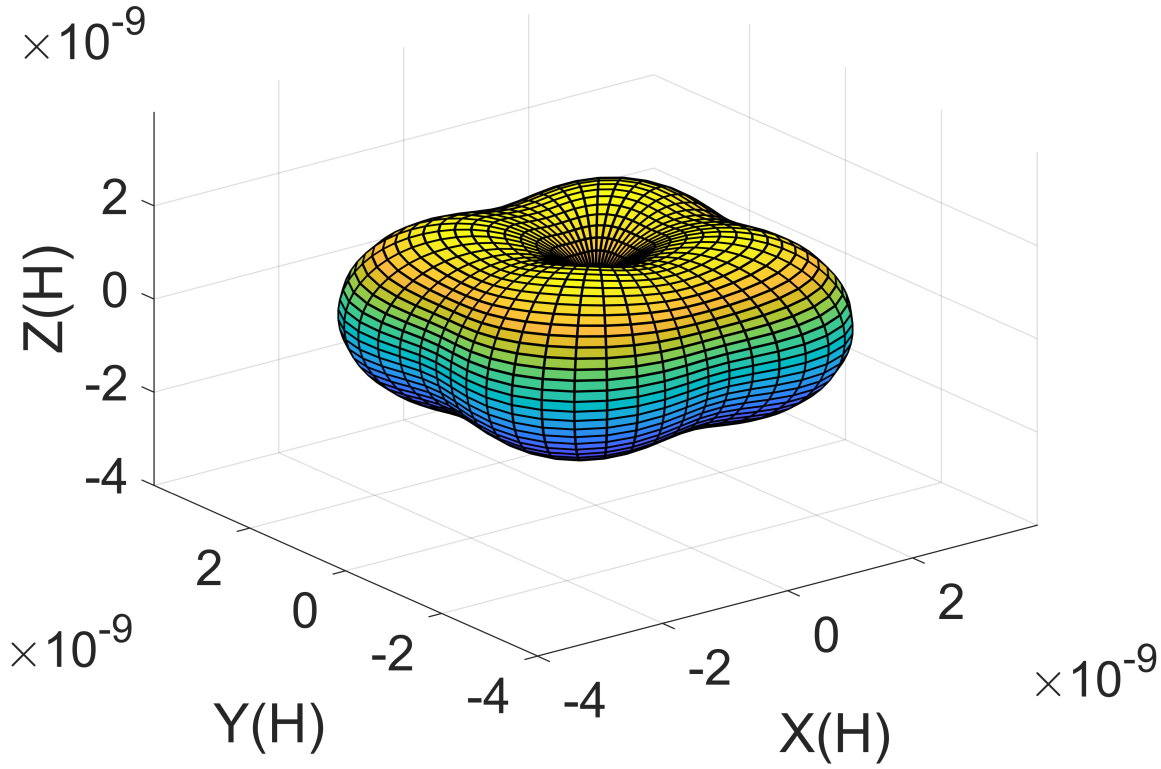

Figure 4-18: 3D mutual inductance distribution of 2-Coil structure: magnitude of effective mutual inductance with 90degrees phase shift of vector sum.

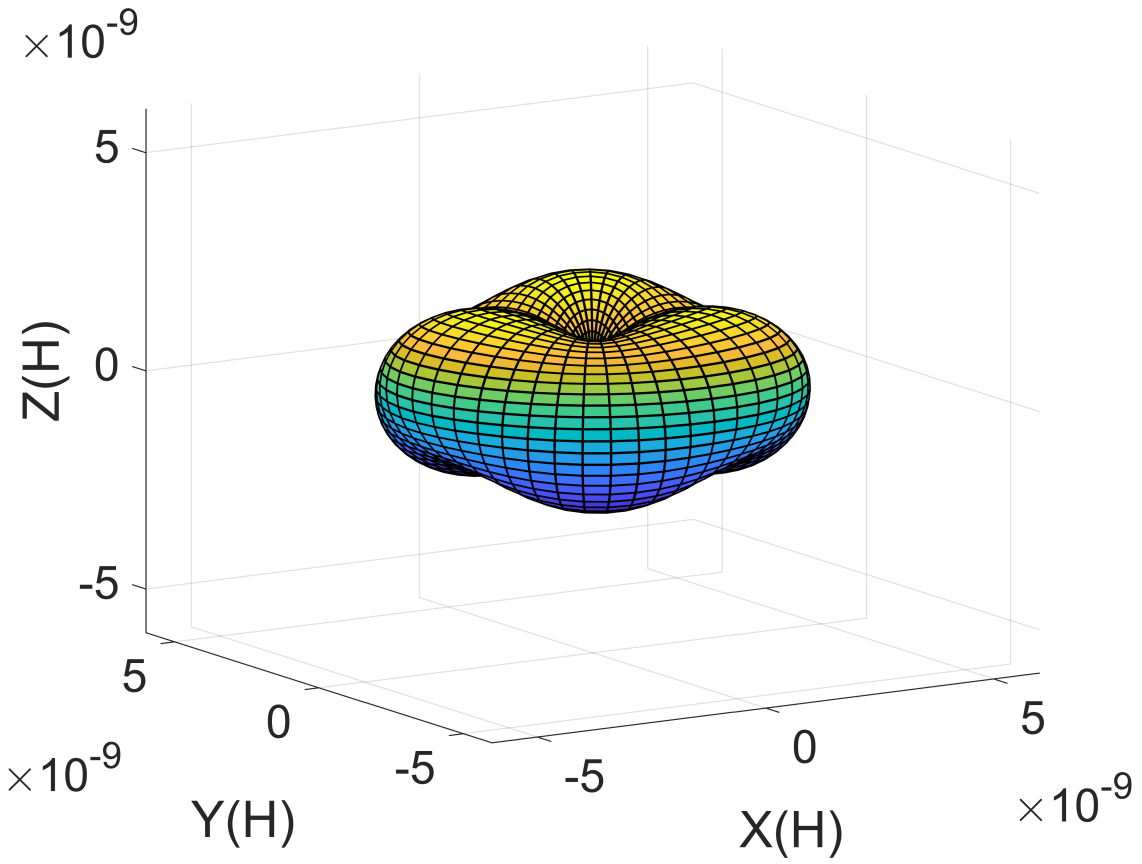

Figure 4-19: 3D mutual inductance distribution of 3-Coil structure: magnitude of effective mutual inductance with 120degrees phase shift of vector sum.

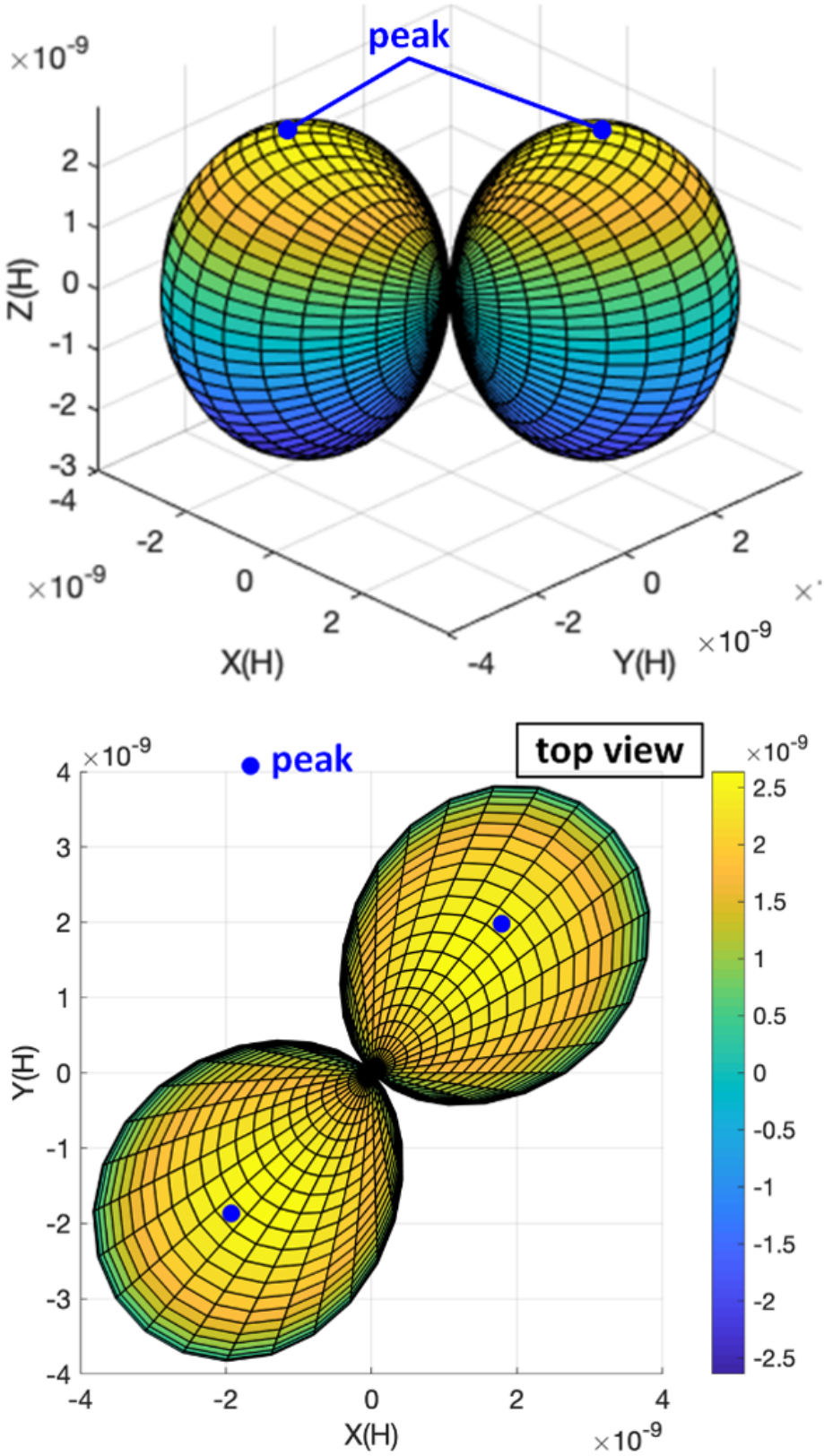

Figure 4-20: Another View for Fig. 4-15.

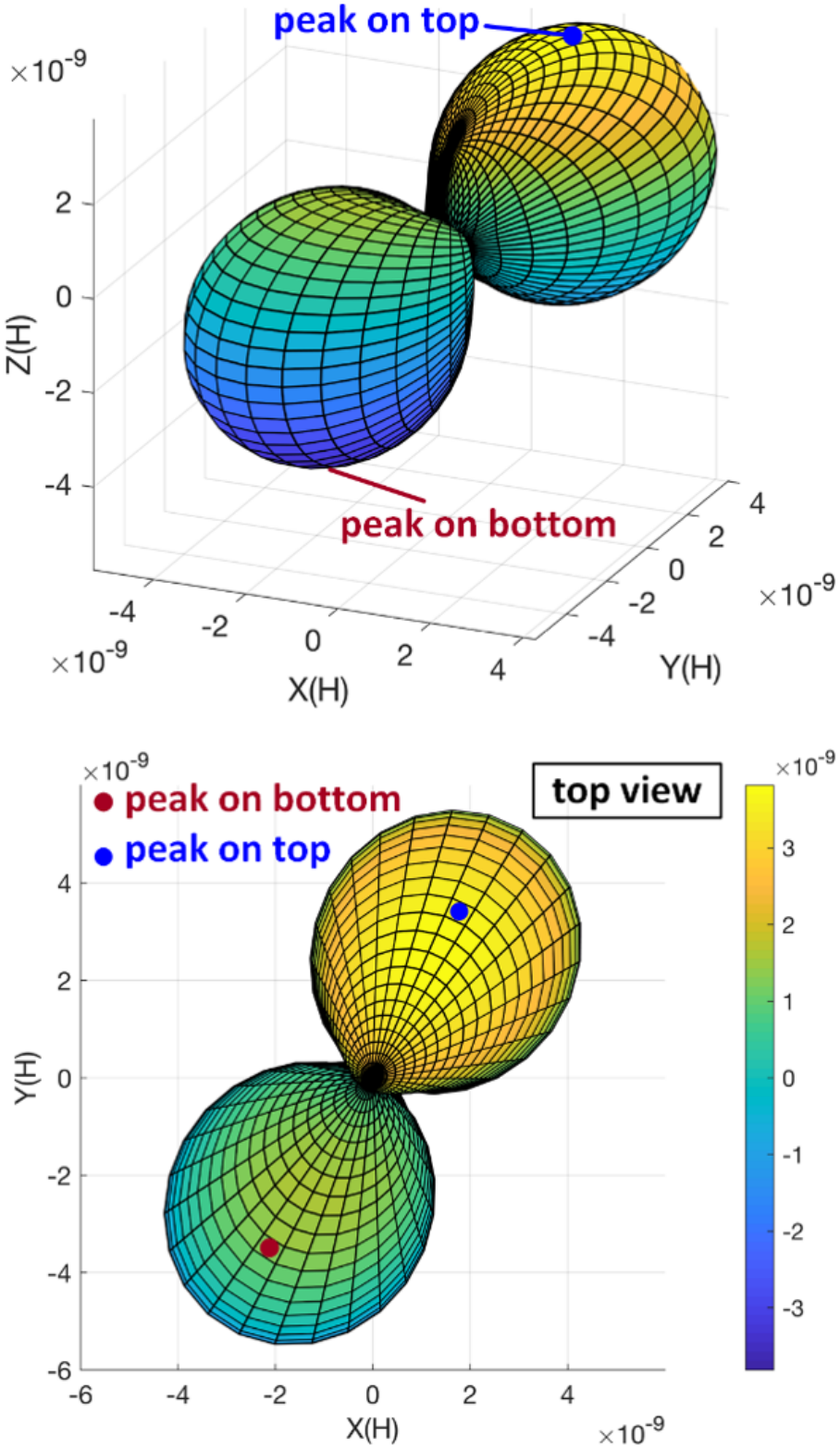

Figure 4-21: Another View for Fig. 4-17.

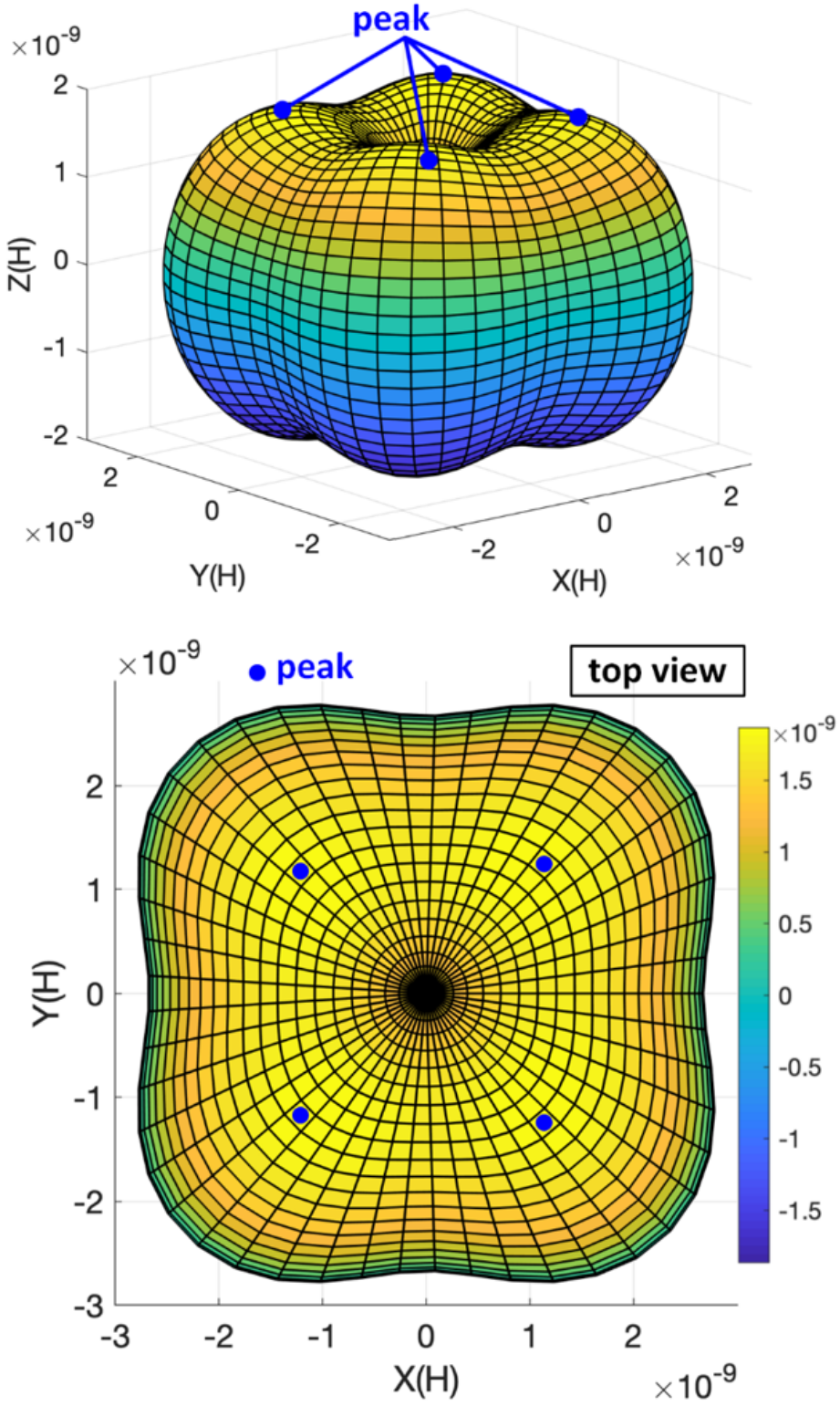

Figure 4-22: Another View for Fig. 4-18.

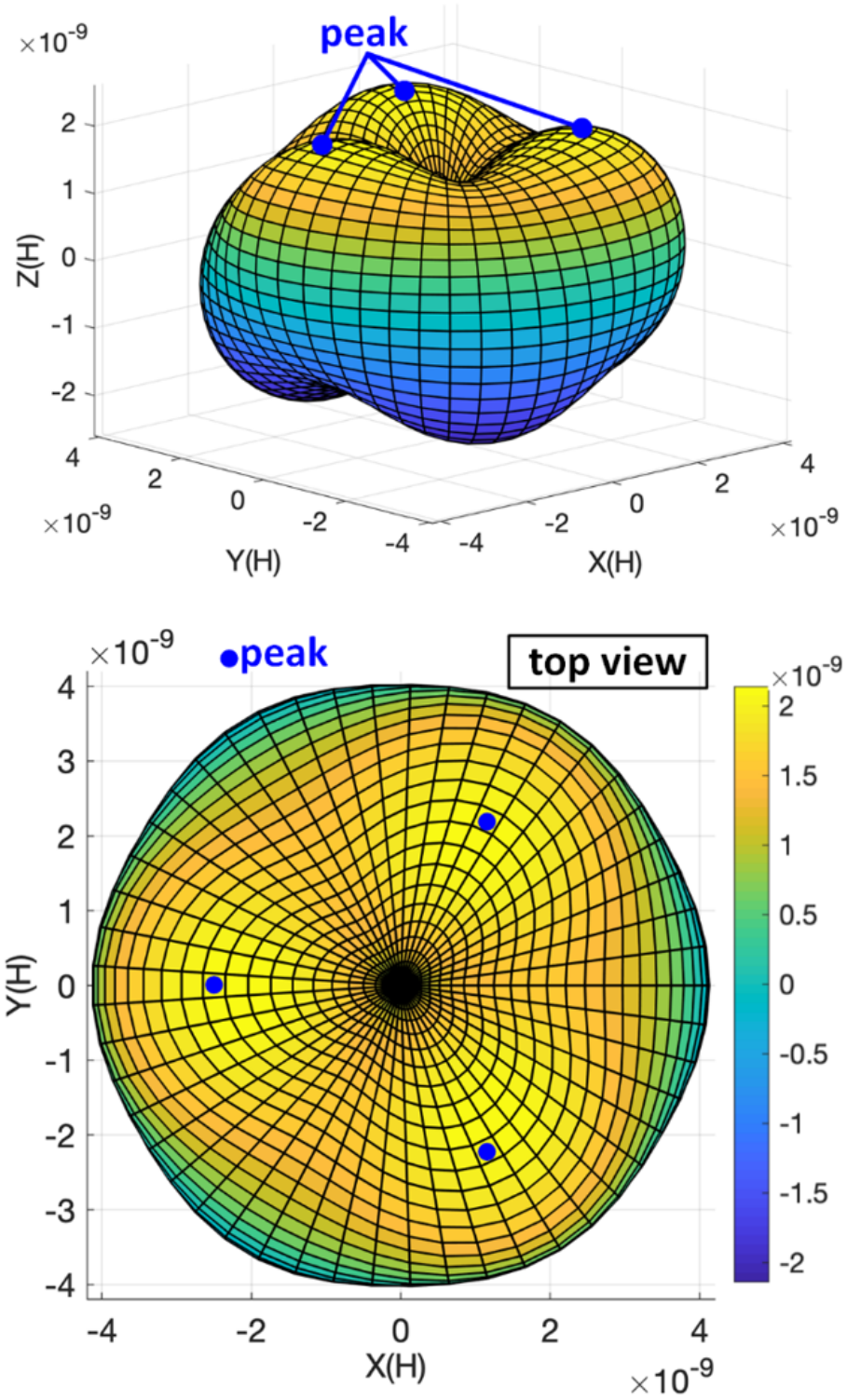

Figure 4-23: Another View for Fig. 4-19.

C. Efficiency

C1. Efficiency Distribution of Single Receiver

The number of turns for each transmitting and receiving coil of the two structures are set to 20 and 10, respectively. In this case, the resistance density of the wire is 0.51 Ω/m at 2 MHz for Litz wire with a diameter size of 1.5mm , and the appropriate load resistance is

$$R_L = \sqrt{(R_r + R_{r-rad})^2 + \frac{(R_r + R_{r-rad})(\omega M)^2}{R_t + R_{t-rad}}} \tag{4.24}$$

Correspondingly, the optimized efficiency distributions for a single receiver at 2 MHz for the two structures driven by phase-shifted current are shown in Fig. 4-27 and Fig. 4-29.

C2. Efficiency of Multiple Receivers and Minimum Receiving Power among Users

The efficiency of multiple receivers and minimum receiving power among users are two important factors measuring the charging quality of WPT, efficiency is the sum of each receiving power over the input power while minimum receiving power is the minimal one of receiving powers over the input power. Referring to Fig. 9, three cases are analyzed below: (i) 4 receivers placed at 1, 3, 5 and 7; (ii) 4 receivers placed at 2, 4, 6, and 8; and (iii) 8 receivers placed at all positions. At 2 MHz, the receivers are both 15 cm away from the transmitter, and all load resistances are 5 Ω. TABLE I show the minimum power ratio (minimum receiving power over input power) and overall power efficiency of the 2-coil structure and 3- coil structure. C. V. stands for current vector, which is the vector of normalized current coefficients β. As can be seen from the rightmost column in Table I, which introduces appropriate phase shifts, the power transfer is drastically increased on efficiency with proper phase shifts, availing simultaneous power delivery to all users. Fig. 4-24 and Fig. 4-25 shows the vertical view.

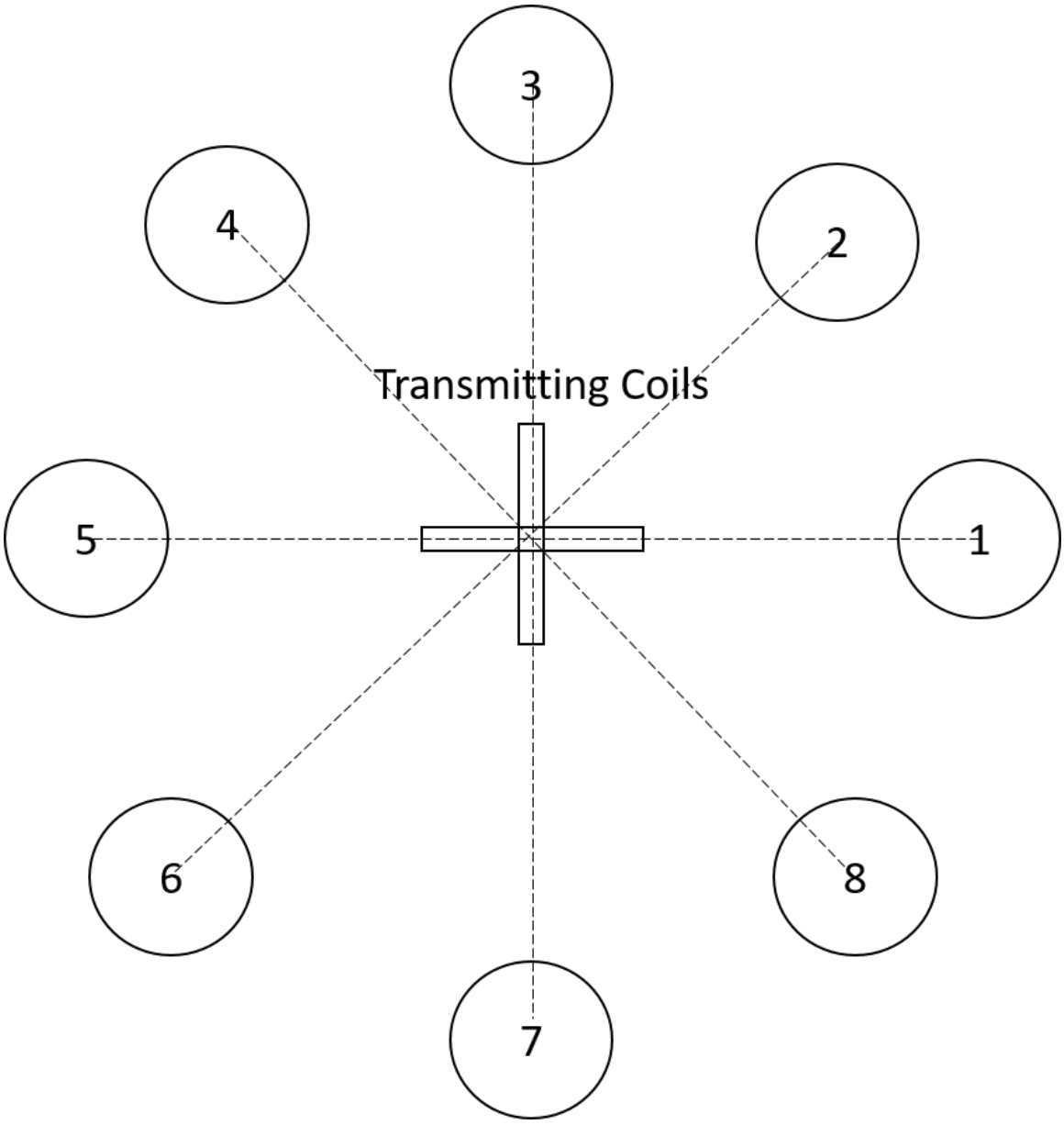

Figure 4-24: Vertical View of WPT with Multiple Receivers: 2-Coil Structure.

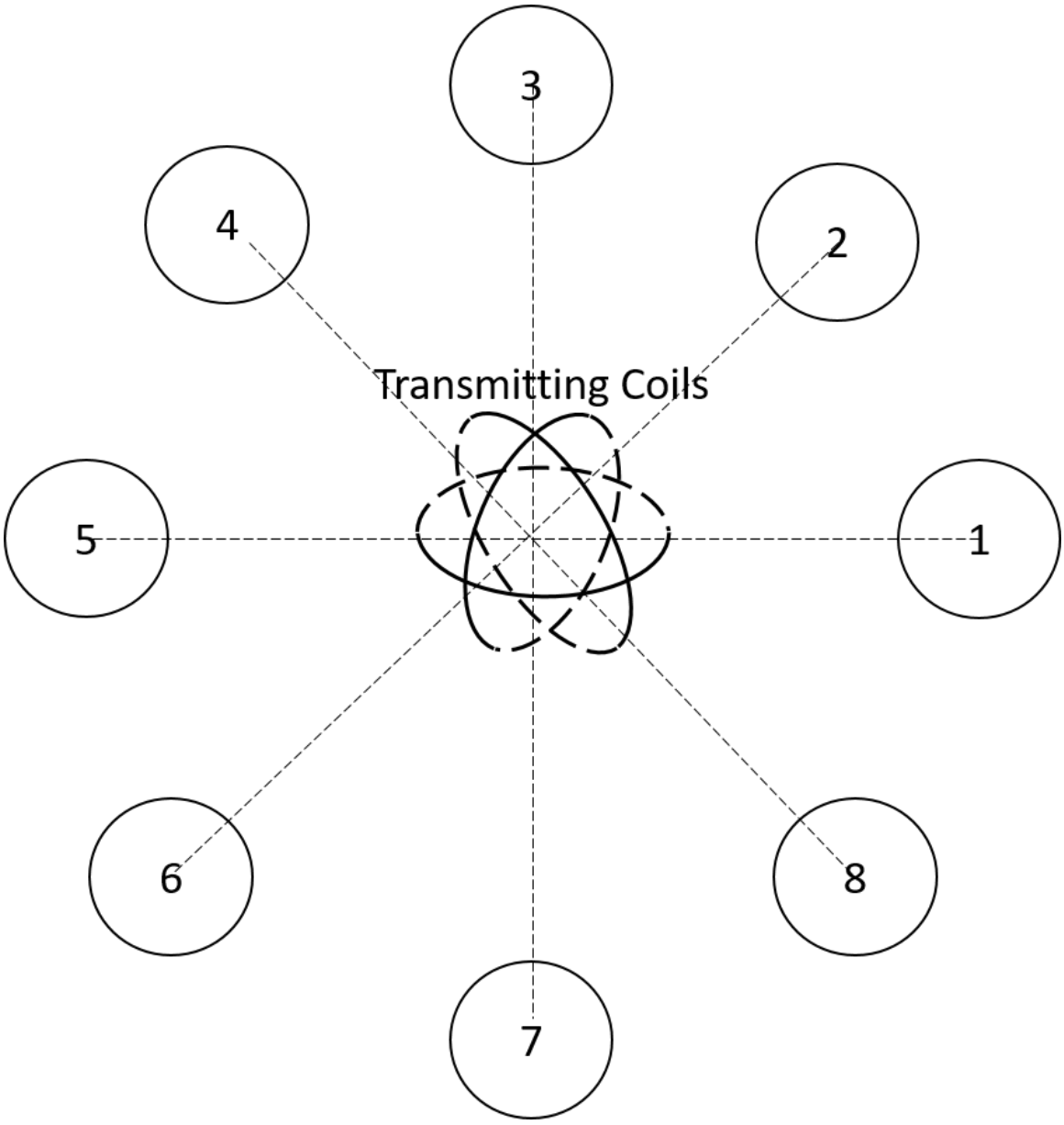

Figure 4-25: Vertical View of WPT with Multiple Receivers: 3-Coil Structure.

D. Benchmark Comparison

Current WPT technologies are discussed in [85]. The representative methods [34–39, 51, 86–90] as mentioned in the Introduction section are Witricity (resonant inductive charging), MagMIMO (position-free charging), and Qi (contacted). A detailed list below in Table 4.2 shows the advantages of the proposed system over multiple features, 2D means 2D position-free, 3D means 3D position-free. Our proposed method shows the greatest convenience by providing 3D charging regardless of the receivers' position.

Table 4.1: Benchmark Comparison.

Methods	Multi-Charge	Dist. Charge	2D	3D	Uniform Eff.
Proposed	Y	Y	Y	Y	Y
Witricity [10]	N	Y	N	N	N
MagMIMO [51]	N	Y	Y	Y	N
Qi Charging [34–39]	Y	N	N	N	N
2-Coil [86]	Y	Y	Y	N	N
3-Coil [87, 88]	Y	Y	Y	N	N
4-Coil [89, 90]	Y	Y	Y	N	N

4.2 System Test of Electronic Network

The 3-D diagram of mutual inductance distribution on the sphere with 20 cm radius for the 2-coil and 3-coil structures are shown in Fig. 4-14 - Fig. 4-19, respectively. In a manner analogous to the radiation pattern of an antenna, under the spherical coordinates, the radii to the surfaces represent the absolute value of mutual inductance of the receiving coil placed at corresponding angle with radial orientation. By comparing Fig. 4-15 and Fig. 4-18, and Fig. 4-17 to Fig. 4-19, it is apparent that the use of a proper drive-current phase shift can reduce the low effective mutual inductance region.

4.2.1 Experiment Setup

The proposed system consists a transmitting subsystem which is configured either as 2-coil structure or 3-coil structure, receiving subsystem which includes multiple receiving coils with loads, and power electronics system comprising a signal generator and power amplifiers. The experiment setup is shown in Fig. 10. We use two power amplifiers, power amp1 is made by Amplifier Research, model 150A100B, 150Watts output, 10kHz -100 MHz, 55dB gain (nominal), power Amp 2: ENI, model 3100LA RF Power Amplifier, 100Watts output, 250kHz – 1500 MHz, 55dB (nominal). We use scope of Tektronix 4-Channel 1GHz. Signal generator is high precision dual-channel signal source generator with sampling rate 200MsA/S, 25MHz, model number is KKmoon MHS-5200A.

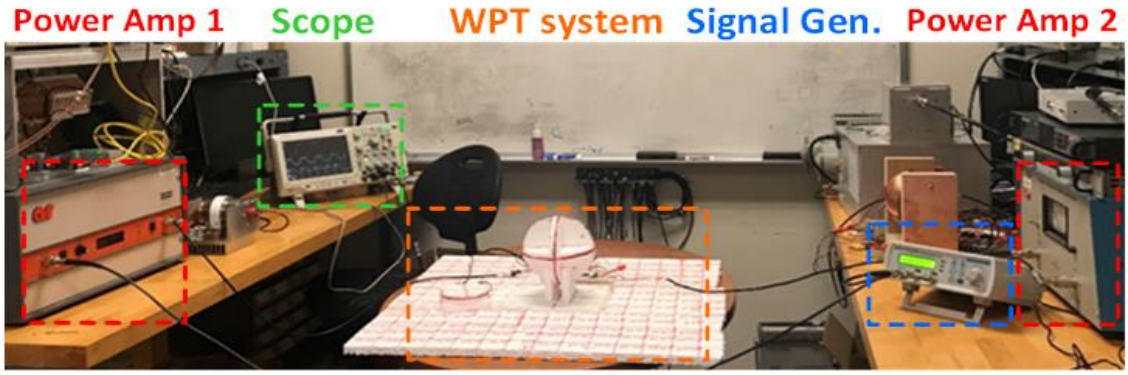

Figure 4-26: Experiment Test Bench. Receiving coils on the table with 40cm away from the center of transmitting coils in this picture.

Case 1: 2-Coil Structure, 90degrees phase shift (2MHz)

From Eq. (4.9), the open-circuit voltage of a single receiver can be regarded as having a linear relationship with the normal transmitting current given a fixed frequency, so the effective mutual inductance between one loop of transmitting coil and one loop of receiving coil is measured by the ratio of open-circuit voltage of the receiving coil V_{r-open} and normal current of the transmitting coil i_t.

The measurement results of the effective mutual inductance are shown in Fig. 4-27.

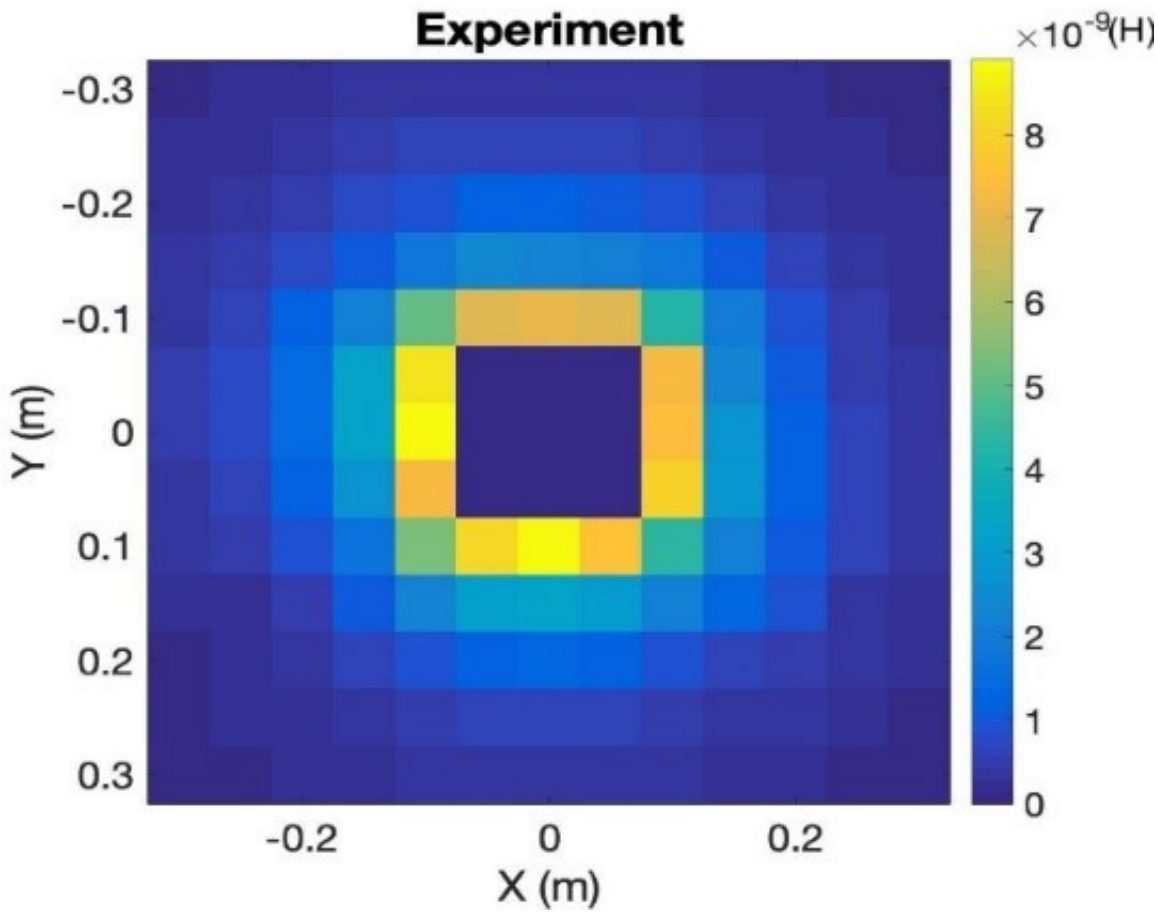

Figure 4-27: Experimental results of effective mutual inductance for the 2-Coil structure.

The error rate, namely the difference between the experimental results and theoretical calculations based on the model of section II, ranges from -21% to 16% with an average of 10.3% as shown in Fig. 4-28. This error rate demonstrates the close match between experiment and theory.

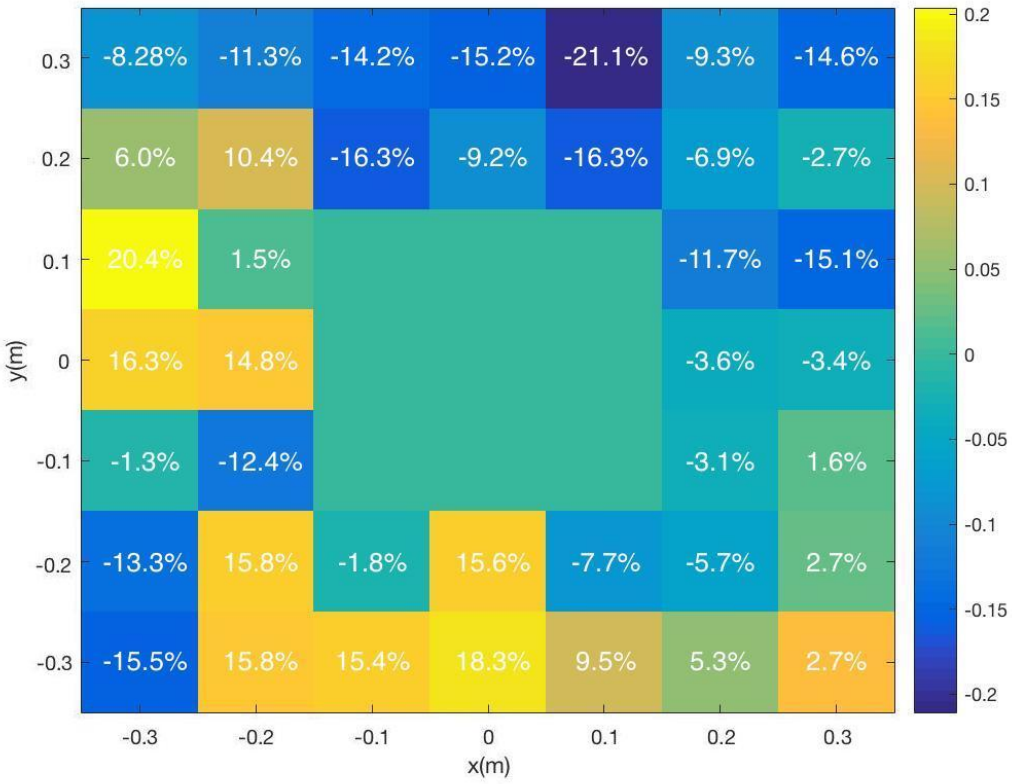

Figure 4-28: Error Rate of Experiment Versus Theory.

The efficiency distribution of a single receiving coil with optimized load resistance by Eq. (4.24) is measured by the ratio of receiving power to transmitting power, which is shown in Fig. 4-29.

Case 2: 3-Coil Structure, 120degress phase shift (2MHz)

The effective mutual inductance for the 3-coil structure is shown in Fig. 4-30.

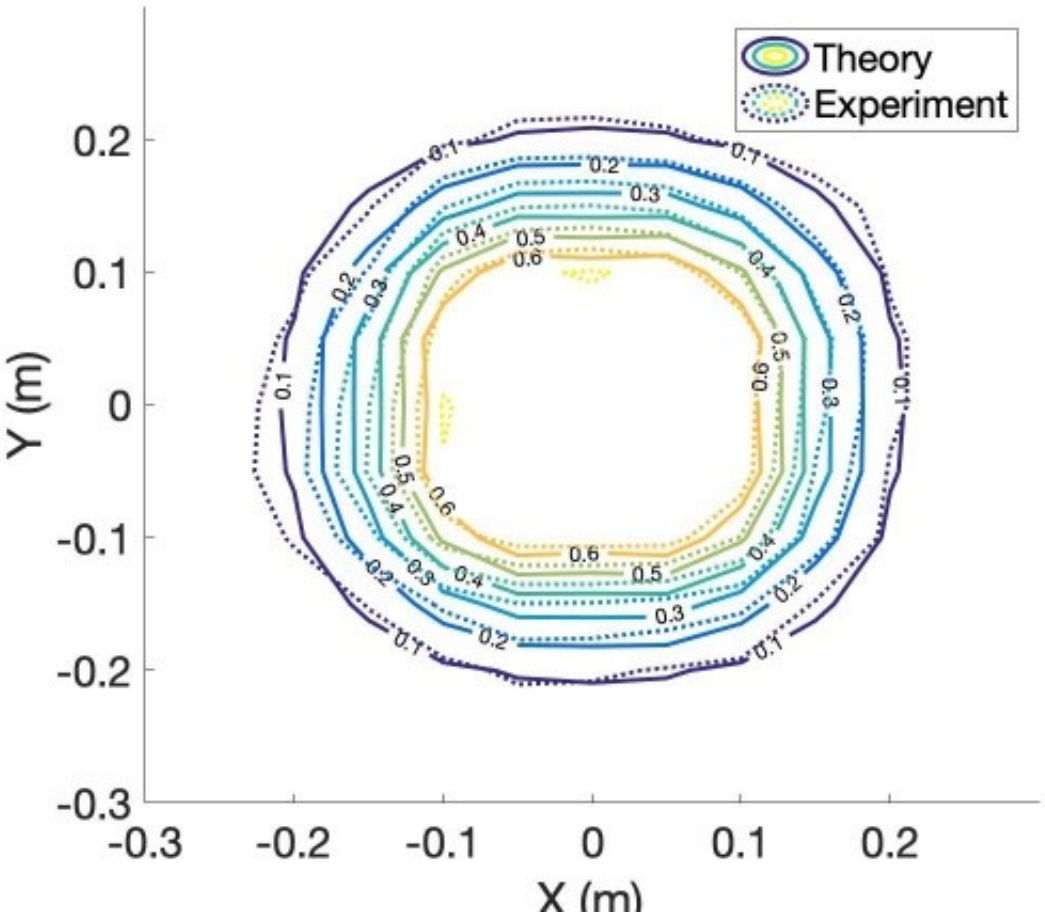

Figure 4-29: Efficiency distribution of the 2-coil structure.

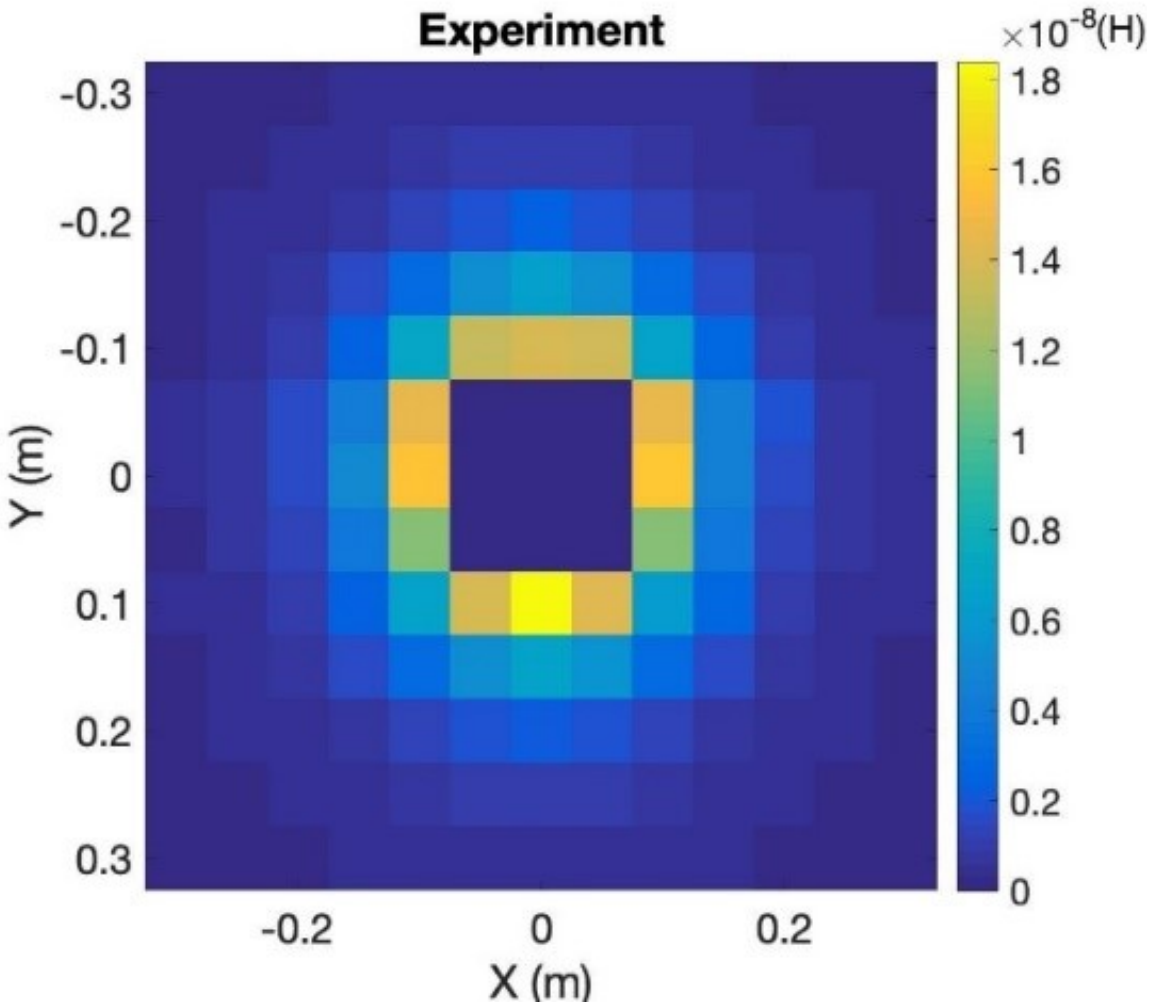

Figure 4-30: Experimental results of effective mutual inductance for the 3-Coil structure.

The error rate ranges from –24.4% to 17.5% with an average of 8.03% as shown in Fig. 4-31.

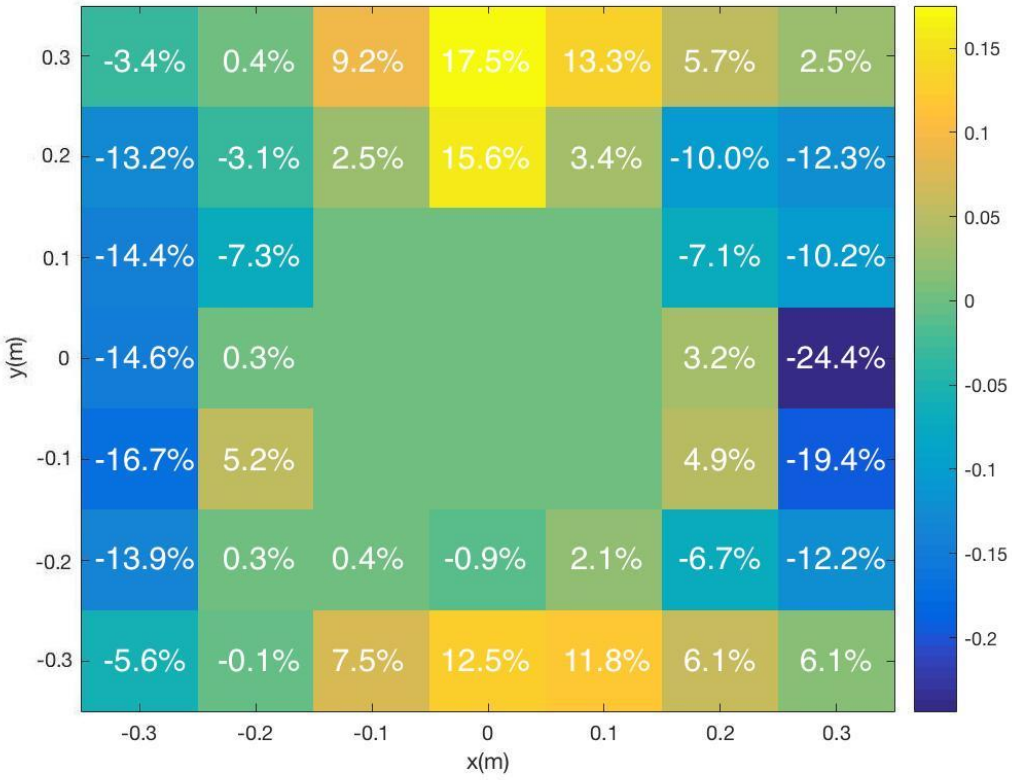

Figure 4-31: Error Rate of Experiment Versus Theory.

The efficiency distribution of a single receiving coil with optimized load resistance by Eq. (4.24) is shown in Fig. 4-32. The overall efficiency and minimum receiving power is shown in Table 4.2.

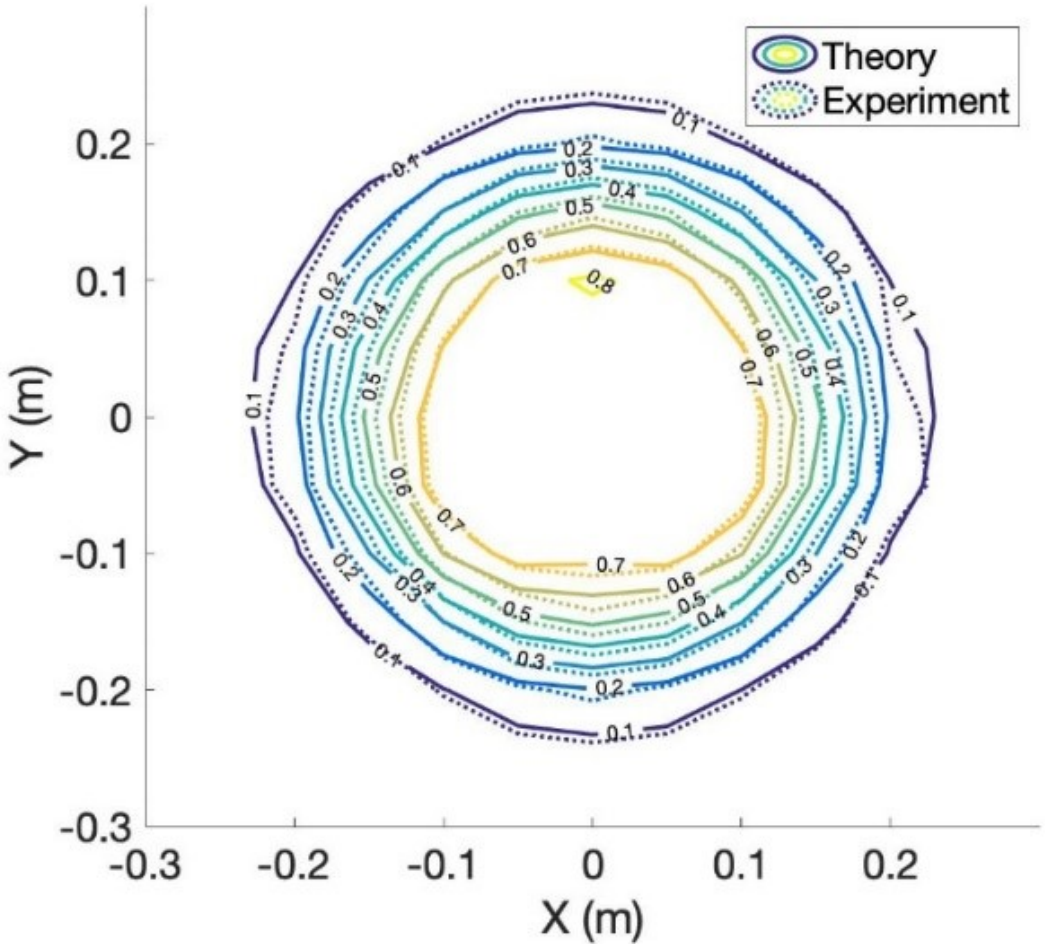

Figure 4-32: Efficiency distribution of the 3-coil structure.

Case 2 with phase-shifts of 120 degrees shows an even higher efficiency in the 3-D space, ensuring the broader and more uniform high-efficiency charging range. It may lead to extra material in comparison to Case 1 with a phase-shift of 90 degrees. Depending on the coil material, the extra cost may be significant.

The overall efficiency and minimum receiving power with 4 and 8 receivers with load resistance of 5 placed in the positions shown in Fig. 4-29 with the distance of 15 cm to the center is shown in Table 4.2 in regards to C2 in section C, where the minimum receiving power ratio is defined as ratio of the lowest receiving power over the total input power, different from the efficiency defined as ratio of power of all receiving coils over the input power, further calculations yield the average efficiency

of 66.04% and variance of 0.26 for the 2-coil system, average efficiency of 70.53% and variance of 0.03 for the 3-coil system, which means 6.8% improvement on average efficiency and 88.7% reduction on its variance for the 3-coil system as the winner.

Table 4.2: Experimental Result of the 2-Coil 3-Coil Structure.

*		2-Coil		3-Coil	
Case	Measure	Efficiency	Min. Rec. Power Ratio	Efficiency	Min. Rec. Power Ratio
i	Theory	57.66%	14.42%	68.61%	15.85%
	Experiment	58.97%	12.02%	68.54%	12.81%
ii	Theory	68.11%	17.03%	70.89%	15.89%
	Experiment	68.64%	13.79%	70.37%	15.19%
iii	Theory	70.08%	4.70%	72.89%	6.77%
	Experiment	70.52%	3.13%	72.69%	4.39%

4.2.2 Demonstration

For the purposes of best illustration, colorful LEDs are used to emulate the electric load as shown in Fig. 4-33. The performance of the 2-coil structure and 3-coil structure is shown respectively.

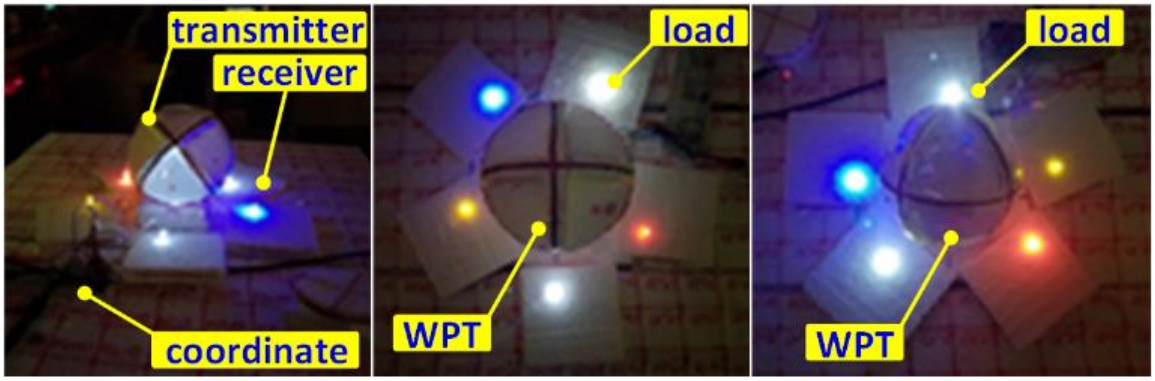

Figure 4-33: Demonstration experiment: a) WPT set-up; b) 2-coil structure; c) 3-coil structure.

To conclude, For WPT systems, an effective method to create quasi-uniform efficiency in 3-D space around the transmitting system is proposed and examined theoretically. The key novelty is the application of phase-shifting method on balanced

magnetic coil structures, which clearly show the distinct outcome compared with traditional non-phase shifting method. The 3-coil structure is verified to have a more robust efficiency delivery with 88.7% reduction on the variance when compared with the 2-coil structure. Experimental results have verified the theoretical calculations with less than 10% average error rate. The study shows that: (1) the effective mutual inductance distribution around the transmitter is quasi-uniform when the transmitting coil-set is driven by properly phase-shifted currents; (2) the rotating magnetic field proved by phase-shifted current driving will form a quasi-uniform efficiency distribution for single user, and higher minimum receiving power ratio for multiple users; and (3) the 3-coil structure driven by 120 degrees phase-shift current shows better performance – a higher and much more stable efficiency, compared with the 2-coil structure driven by 90 degrees phase-shift current, variation reduced by 88.7%, average efficiency improved by 6.8%. However, the 2-coil system is more economic with 33% reduction on the material cost. To summarize, the proposed WPT system shows robustness and flexibility to the receivers' position and orientation in a complicated multi-user environment.

Chapter 5

System Modeling and Operation Analysis

This section summarizes system operation at the Stone Edge Farm micro-grid site from January through December, 2017. The primary objective of data mining for micro-grid site is to validate the claimed merits of our proposed methods in Chapter 3 by analyzing usage of renewable sources and economics of the operation. After a study on data analysis, solar plants on the rooftops of the farm generate an average of 342kWh energy per day, and electric loads (excluding the storage - batteries) of this site consumes an average range of 360-480kWh energy (15-20kW for 24 hours) per day, hence the renewable energy usage ratio is 71% - 95%. Moreover, this site is able to achieve 100% renewable energy supply with proper electricity use on sunny days. With quantitative analysis, we can conclude the combination of solar power and battery storage system (BSS) can provide the most economic saving of up to 29% compared with the traditional system which has no solar power and storage. The analysis is based on the data acquisition sources from Enphase, a leading solar micro-inverter company headquartered in Petaluma, CA, and Wattsworth, an on-line data management site developed at MIT. Mr. Craig Wooster oversaw the operation staff at the farm.

5.1 Mathematical modeling and system characterization

The Micro-Grid site at Stone Edge Farm is made up of five nodes, in other words, switching points - DER (no node number), node 1 through 4 as shown in Fig. 5-1. Although the latest updates add another plant – node 5 located in Napa, since node 5 is not in the research scope, we still consider five nodes for the site. Its system layout is described as follows: DER is equipped with hydrogen electrolyzers and Aquion's Sodium-ion batteries; Node 1 is equipped with a 65kW Capstone's micro-turbine, Node 2 is equipped with Energy Storage Systems (ESS)'s iron flow batteries and the main network server powered by Sony's LiFePO4 batteries; Node 3 is equipped with a common box, a chicken coop and some dining shops; Node 4 is equipped with Tesla's energy storage system, a garage with large PV plant on the roof. Every power plant has electric transformer(s) to convert the voltage to proper values. Each node is equipped with solar arrays which are detailed in part A of Section 5.1.1.

Figure 5-1: Micro-Grid Site at Stone Edge Farm, Sonoma, Cali., Overview of Each Node Described Above.

5.1.1 System Parameters

Various power components are utilized in this micro-grid system: solar photovoltaic arrays, a gas fired micro-turbine provided by Capstone, fuel cells, hydrogen electrolyzers, and batteries. Hydrogen generator and storage is in conjunction with the fuel cells energy storage. Four types of batteries are used: sodium-ion batteries from Aquion, iron flow batteries from ESS, LiFePO 4 batteries from Sony, and Lithium-Ion batteries from Tesla. The power details of each component are summarized in Fig. 5-2.This section describes the primary components, their functions and operation constraints, in the real MCESS, Stone Edge Farm, to be further analyzed. The main components of Stone Edge Farm MCESS include solar photovoltaic arrays, combined heat and power system (CHP), electric heat pump (EHP), absorption chiller, boiler,

BSS, HSS, and load, which will be illustrated in detailed throughout this section.

A. Solar Arrays

Solar arrays serve as the major power generation source in the system, with its current capacity of 140kW. Solar photovoltaic arrays (PVs) are installed into eight sections spanning the five power nodes as defined above. Eight sections, ranking from the highest power rating to the lowest one, are as follows: Autobarn, AG-SHED, ZEN/SPA, Bulter Building, Guest House, Gate House, Garage, and Glide House. The locations are marked in the geographic map in Fig. 5-3. Please note that this map was captured by the satellite in the earlier time when only a few solar PVs were installed. Solar photovoltaic arrays in this Multi-Carrier Energy Storage Systems(MCESS) serve as a primary electric power source, with maximum output electric power capability of 122kW converted by Enphase M250 and S280 micro-inverters. The solar photovoltaic arrays are installed on the roofs of eight buildings in the MCESS as shown in Fig. 2. The electric power injected to the MCESS from the solar photovoltaic arrays should be less than the maximum available solar power at each time point. In order to maintain system reliability, solar power will be stored to BSS firstly as in Eq. (5.1) below.

$$0 \leq S(t) \leq S_{Max}(t) \tag{5.1}$$

B. Combined Heat and Power System (CHP)

The electric and heating systems are coupled by CHP in the MCESS, which uses natural gas to produce electricity, and the waste heat from the Capstone turbine is a power generation source for balancing the heat loads in the heating system [91, 92].CHP can meet heating power demand with less cost than EHP when local natural gas price is relatively lower than electricity price. CHP in Stone Edge Farm MCESS is mainly driven by a Capstone Gas turbine C65 natural gas-fired variable external combustion engine as shown in Fig.1 below. The combined heat and power efficiency is up to 90%. Among the converted power from natural gas, 68% goes to heating power and the remaining becomes electric power, which would be the maximum

available heating and electric power from CHP at different time point given certain amount of natural gas input. The Capstone Gas turbine uses natural gas to produce electricity, and waste heat from the turbine is a power generation source for a heater system, with a power rating of 65kW. It is equipped with an absorption cooler. It is located next to the owner's house. Considering CHP limitations, the maximum output heating power H_{CHP} is 52kW and maximum output electric power E_{CHP} is 65kW as in Eq. (5.2) below.

$$0 \leq H_{CHP}(t) \leq min\{G_{CHP}(t)\eta_{CHP,Com}\eta_{CHP,H}, H_{CHPMax}\} \tag{5.2a}$$

$$0 \leq E_{CHP}(t) \leq min\{G_{CHP}(t)\eta_{CHP,Com}\eta_{CHP,E}, E_{CHPMax}\} \tag{5.2b}$$

C. Electric Heat Pump(EHP)

EHP system Jandy Pro Series Hi-E2 with water supply in Stone Edge Farm. The EHP system is capable of generating maximum heating power 80kW and maximum cooling power 80kW. Since EHP system cannot generate both heating and cooling power at the same time, binary variables $I_{EHP,C}$ and $I_{EHP,H}$ are adopted in this research to indicate the corresponding operation status and put the constraint at different time as in Eq. (5.3).

$$0 \leq H_{EHP}(t) \leq H_{EHPMax}I_{EHP,P} \tag{5.3a}$$

$$0 \leq C_{EHP}(t) \leq C_{EHPMax}I_{EHP,C}(t) \tag{5.3b}$$

$$0 \leq I_{EHP,C}(t) + I_{EHP,H}(t) \leq 1 \tag{5.3c}$$

D. Absorption Chiller

The absorption chiller is equipped on CHP capstone turbine system. The maximum output cooling power is 65kW with efficiency of 80% from converting the received natural gas as formulated in Eq. (5.4)

$$C_C(t) = G_C(t)\eta_C \tag{5.4a}$$

$$0 \leq C_C(t) \leq C_{CMax} \tag{5.4b}$$

E. Boiler

The boiler equipped on CHP capstone turbine system in Stone Edge Farm MCESS. The maximum output heating power is 80kW from converting the received natural gas as formulated in Eq. (5.5) below.

$$H_B(t) = G_B(t)\eta_B \tag{5.5a}$$

$$0 \leq H_B(t) \leq H_{BMax} \tag{5.5b}$$

F. Battery Storage System (BSS)

Five types of batteries are used in the system for energy storage purpose of electric power supply, electric vehicles, and network servers. Here we focus on Tesla Lithium-Ion batteries 250kW/475kWh since they are the major electric power storage system in Stone Edge Farm as shown in Fig. 6. This utility-scale battery consists of five 50kW/95kWh cabinet-and-rack units, each containing 16 individual pods of lithium cobalt ion batteries. The BSS charging efficiency is 92% with maximum charging power 250kW, and the discharging efficiency is 90% with maximum discharging power 250kW as in Eq. (5.6). Besides, since BSS can only work in either charging or discharging status, binary variables IBSS, Cha and IBSS, Dis are adopted here to put this constraint and indicate the corresponding operation status at different time.

$$E_{BSS,S}(t+1) = E_{BSS,S}(t) + E_{BSS,Cha}(t)\Delta T\eta_{BSS,Cha} - \frac{E_{BSS,Dis}}{\eta_{BSS,Dis}}\Delta T \tag{5.6a}$$

$$0 \leq E_{BSS,Cha}(t) \leq E_{BSS,ChaMax} I_{BSS,Cha}(t) \tag{5.6b}$$

$$0 \leq E_{BSS,Dis}(t) \leq E_{BSS,DisMax} I_{BSS,Dis}(t) \tag{5.6c}$$

$$0 \leq I_{BSS,Cha}(t) \leq E_{BSS,Dis}(t) <= 1 \tag{5.6d}$$

$$0 \leq E_{BSS,S} \leq E_{BSS,Smax} \tag{5.6e}$$

G. Hydrogen Storage System(HSS)

Millennium Reign Energy Series 3 hydrogen storage and fueling station SHFA model 300 are applied in the HSS. Hydrogen is stored here in 24 one-kg red carbon fiber and steel tanks at 6,000psi to supply demands from Toyota Mirai fuel cell cars. Hydrogen electrolyzer, by its name, generates hydrogen that can later produce electricity through the electro-chemical reactions in fuel cells or that can be used by fuel cell cars. The equivalent maximum HSS capacity is 800kWh.The maximum charging power is 400kW with efficiency of 60%, and the maximum discharging power is also 400kW with efficiency of 60%. Similarly, as HSS can only work in either charging or discharging status, binary variables IHSS, Cha and IHSS, Dis are adopted for indicating the corresponding operation status and put the constraint at different time as in Eq. (5.7). If direct charging is applied for HVs instead of using the storage, the efficiency of electric-to-hydrogen is 65%.

$$E_{HSS,S}(t+1) = E_{HSS,S}(t) + E_{BSS,Cha}(t)\Delta T\eta_{HSS,Cha} - \frac{R_{HSS,Dis}}{\eta_{HSS,Dis}}\Delta T \tag{5.7a}$$

$$0 \leq E_{HSS,Cha}(t) \leq E_{HSS,ChaMax} I_{HSS,Cha}(t) \tag{5.7b}$$

$$0 \leq R_{HSS,Dis}(t) \leq R_{HSS,DisMax} I_{HSS,Dis}(t) \tag{5.7c}$$

$$0 \leq I_{HSS,Cha}(t) \leq E_{HSS,Dis}(t) <= 1 \tag{5.7d}$$

$$0 \leq R_{HSS,S} \leq R_{HSS,Smax} \tag{5.7e}$$

H. Fuel Cells

Fuel cells use hydrogen from electrolyzers to generate electricity, some of them are used to feed an emergency bus called critical bus. Their power rating is 30kW.

Hydrogen Electrolyzers

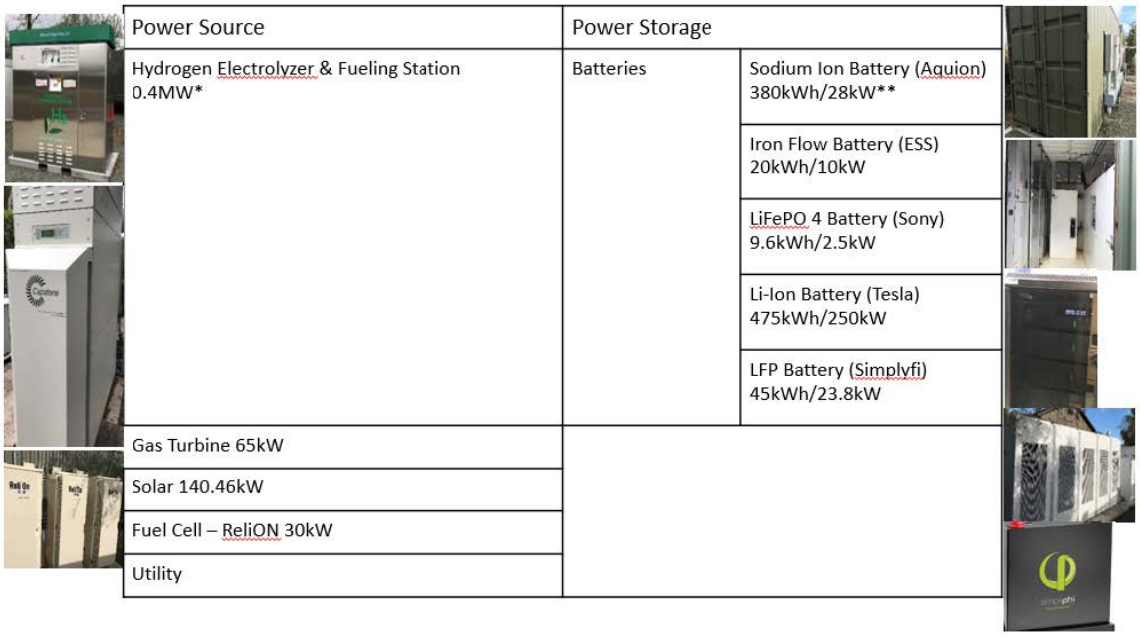

Figure 5-2: Power Table of Electric Components.

5.1.2 Renewable Energy Source - Solar Power

Solar generations at the farm contribute the majority of the electricity as a renewable energy source. With an installed power of 140kW, the farm is, in principle, capable of performing normal operations without the use of the grid during the sunny days. However, due to the ongoing construction and technical issues such as partial shading and cross-talk communications as shown in Fig. 5-4, the major solar plants generate 65KW (observed peak value) per day by our measurement, which means only 53.5% of the installed power (121.59kW as detailed in the following sentence) is actually being used. The current solar installation has four major sites: Zen Spa (23.1kW), Main House/Butler Building (8.67kW), Autobarn (58.2kW) which is divided into two

portions: AutobarnNorth and Autobarn-node 4, and AG-SHED(31.62kW), totaling of 121.59kW. The rest of solar plants are located in Garage, Guest, Gate, and Slide Houses, they are not on the data monitoring list, which can be viewed in Fig. 5-3.

Solar Location

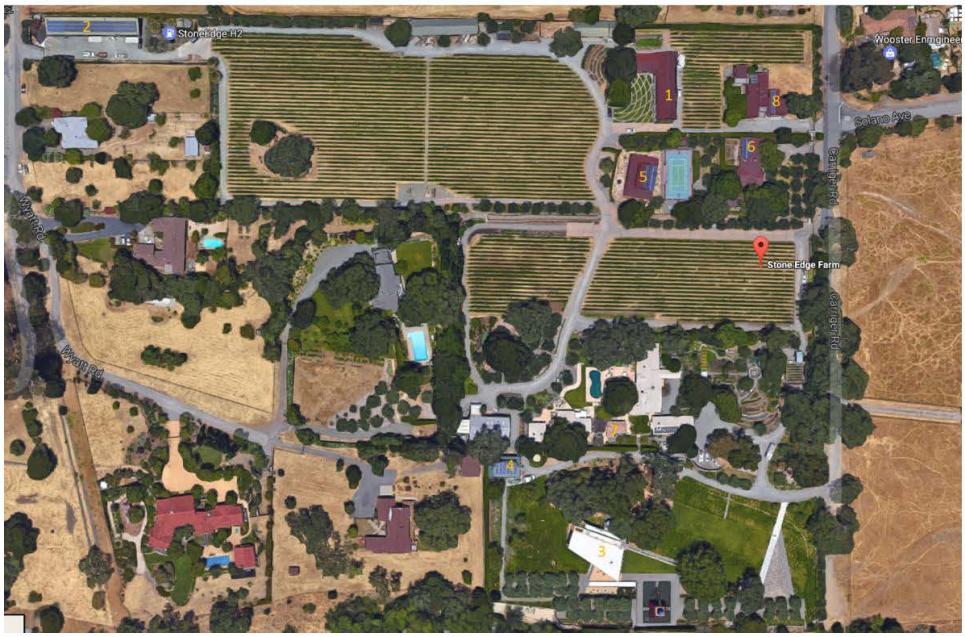

No	Location	Node
1	AutoBarn	N4
2	AG-HED	DER
3	ZEN/SPA	N1
4	BULTER	N2
5	GUEST HOUSE	N4
6	GATE HOUSE	N4
7	GARAGE	N1
8	GLIDE HOUSE	N4

Figure 5-3: Map View of the Solar Locations. Picture Sourced From Google 2016.

The solar system is managing by Enphase, a micro-inverter supplier company. Enphase has a data acquisition platform for the solar generation. Wattsworth, a technology developed at MIT to measure electrical properties by magnetic sensing, also has an access to the operation data. For the better credibility, we use both platforms to analyze the data. The tables below detail the performance of four major solar generating elements as mentioned above. The first table shows the operating condition of the solar panels by using % percentage to indicate the ratio of working solar cells among the total cells; description term full means full system were operating, partial means either only some of solar panels were operating or the data acquisition stopped for a few days of a month, N/A means the system data is not available shown in Table 5.1.

Table 5.1: Overview of Solar Planets.

Solar Label	Location	Installed Power(kW)	Measured Power in Average(kW)
1	ZEN/SPA	23.1	20
2	Main/Butler Bldg	8.67	7.56
3	AutobarnNorth Autobarn-node4	58.2	7.74
4	AG-SHED	31.62	29.7

Table 5.2: Operating Condition of Each Solar Location.

Loc \ Mon	3	4	5	6	7	8	9	10	11
1	87%	87%	87%	87%	87%	87%	87%	N/A	87%
2	N/A	N/A	N/A	86%	86%	89%	89%	89%	89%
3	94%	94%	Partial	Partial	Partial	Partial	Partial	N/A	Partial
3	Partial	Partial	N/A	N/A	N/A	Partial	Partial	N/A	Partial
4	98%	98%	95%	94%	94%	94%	94%	N/A	98%

From the above tables, we can conclude that Autobarn's solar panels has been experiencing system malfunction issues which include partial shade problem with trees and some non-operative solar panels as shown below in Fig. 5-4, which contribute to the major loss of solar energy generation.

(a) Partial Shade Problem with Trees (b) Cross-Talk between Arrays (Out of Operation)

Figure 5-4: Technical Issues Causing Insufficient Solar Energy Generation.

Due to the malfunction issues, we filter the data by considering the solar panels operating condition, which means the data in May through July is removed since a major solar plant Autobarn-node 4 has zero value and the data in October and

November is removed since the October's wild fire has impacted the Sonoma region. Therefore, the months being analyzed are March, April, August, and September. These four months' total power generation is 41.0644MWh, which gives an average of 10.2661MWh per month, that is 342kWh per day. Using a quick check on this calculation, we can approximate the average value from the sinusoidal-shape power curve during the sun is up.

$$P_{avg} = \frac{2}{\pi} P_p \tag{5.8}$$

5.1.3 Case Analysis – Tesla Operation

A system test has been performed to analyze the operation of the Tesla batteries when only the utility 1 is connected. The Tesla system, 250kW power converter is connected to 475kWh battery packs. The single-line diagram is shown in Fig. 5-7 and the power flow diagram is shown in Fig. 5-8 reflecting the calculation results in the following section

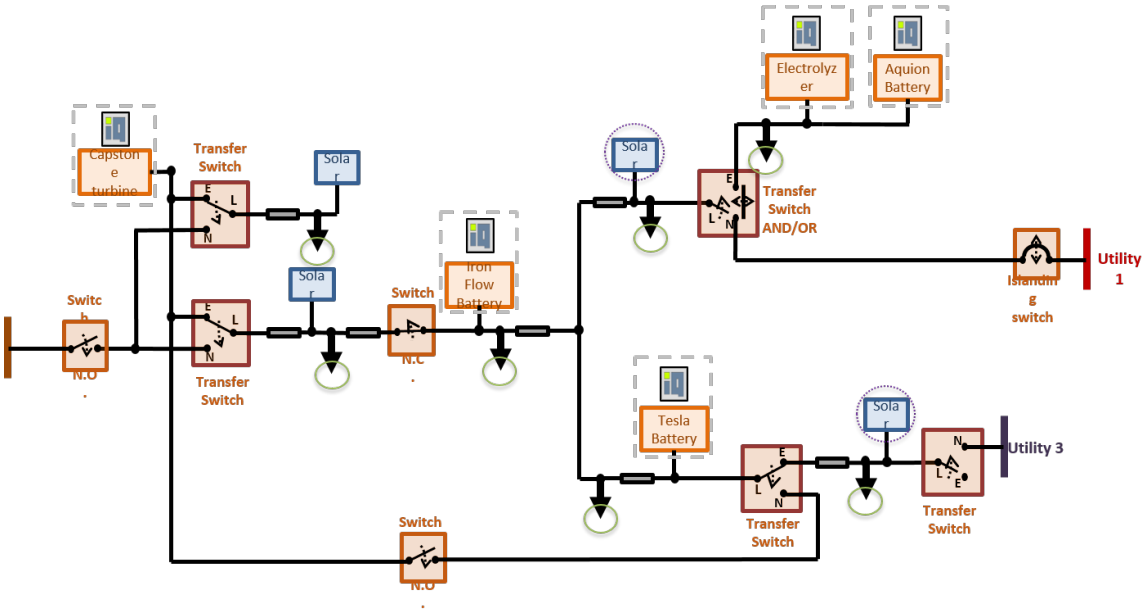

Figure 5-5: Micro-Grid System Topology.

Figure 5-6: Tesla's Batteries and Power Converter System.

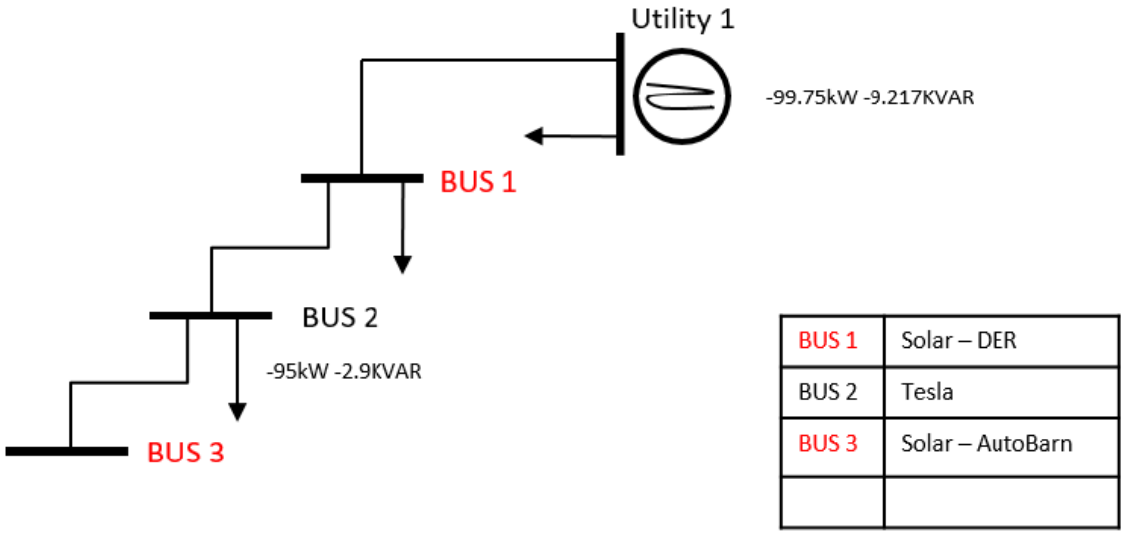

Figure 5-7: Single-Line Diagrams of Tesla Case.

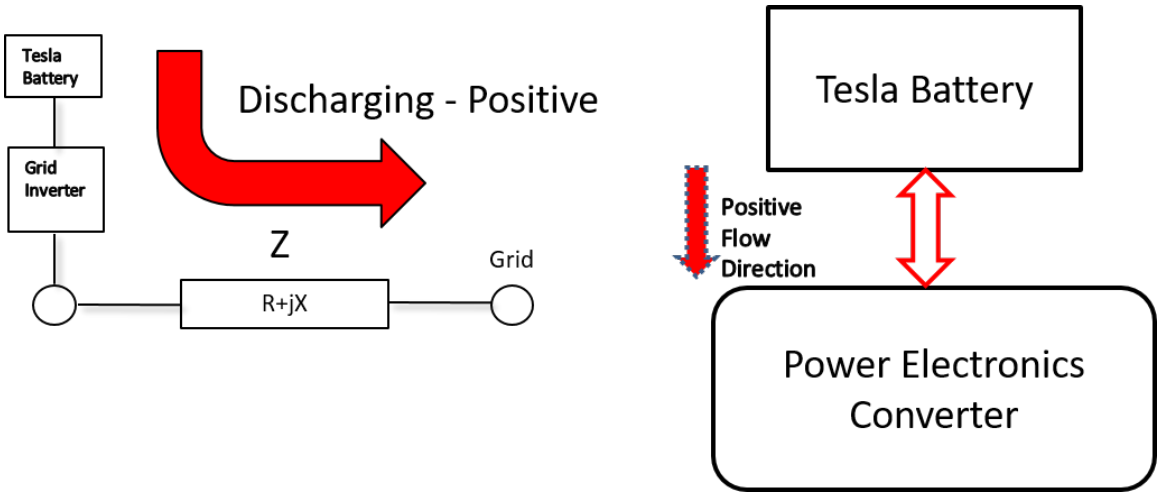

Figure 5-8: System's Power Flow Diagrams.

Analyzing the unknown variables of the system, we need to find grid voltage, inverter voltage, and impedance, namely resistance and reactance. The only known variables are the magnitude of the inverter voltage, real power and reactive power of the inverter; therefore, we have more unknown variables than the number of normal voltage and power equations. This condition reminds us of the complex form, which divide the voltage and current in its real and imaginary values, respectively.

$$v = V_d + jV_q \tag{5.9a}$$

$$i = I_d + I_q \tag{5.9b}$$

Applying Kirchhoff's Circuit Laws (KVL) to the circuit above, we obtain

$$v_i - v_g - i(R + jX) = 0 \tag{5.10}$$

Then, we use the d-q frame to divide one equation into two:

$$\frac{(V_i d - V_g d)}{\sqrt{3}} - I_d R + I_q X = 0 \tag{5.11}$$

$$\frac{(V_i q - V_g q)}{\sqrt{3}} - I_q R - I_d X = 0 \tag{5.12}$$

We know the inverter voltage's magnitude based on its d-q value.

$$V_i = \sqrt{V_{id}^2 + V_{iq}^2} \tag{5.13}$$

The real and reactive power of the inverter system in d-q frame are derived

$$P = \sqrt{3}(V_{id} I_d + V_{iq} I_q) \tag{5.14}$$

$$Q = \sqrt{3}(V_{iq} I_d - V_{id} I_q) \tag{5.15}$$

We set the utility voltage as reference, so the q-axis value is zero.

$$V_{gq} = 0 \tag{5.16}$$

Furthermore, three sets of data points are extracted to build the 15 non-linear equations with 15 unknown variables.

All the 15 unknown variables Vid1, Viq1, ... impedance R and X are calculated in Fig. 5-9, and the vector representation of the voltages is shown in Fig. 5-10. During the battery charge mode, the power flows from the grid to the battery, hence the grid power is higher than the inverter power. The grid power is lower when the battery discharge, its real power shown in Fig. 5-12 and reactive power shown in Fig. 5-13 with line loss and efficiency data are in Fig. 5-11.

Calculation – Finding the unknown data				Background Information	
Variables		Value	Relative angle to the grid voltage (°)	Real Power (W)	Reactive Power (VAR)
Grid Voltage v_g		507.2832 ∠0^0	e.g., at data point 1, Current i_1 = 197.474∠174.72^0 A	$99{,}750_1$ - point 1	$9{,}217.6_1$
Resistance R		0.0703		$2{,}741.4_1$	N/A
Reactance X		0.0935		N/A	$3{,}6461_1$
Inverter Voltage	Point 1 v_{i1}	481.3∠-3.530°	-3.5301	$-95{,}000_1$*	$-2{,}900_1$
	Point 2 v_{i2}	485.9∠-3.576°	-3.5756	$-90{,}000_2$	$6{,}500_2$
	Point 3 v_{i3}	506.2∠0.655°	0.655	$10{,}000_3$	$-10{,}800_3$

Figure 5-9: System Characterization Result.

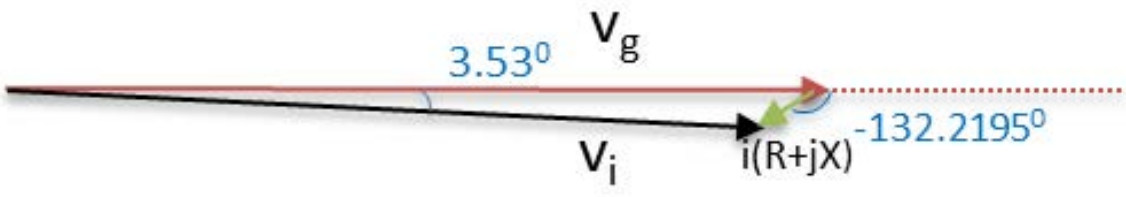

Figure 5-10: Vector Representation of Grid Voltage and Inverter Voltage.

	Real Power			Reactive Power		
	1	2	3	1	2	3
Grid	-99750	-94200	9897	-9217.6	-913	10937
Inverter	-95000	-90000	10000	-2900	6500	-10800
Line (loss)	2741.4	2424.4	59.44	3646.1	3224.5	79.05
Efficiency	95.24%	95.54%	98.97%			

Figure 5-11: Power Chart. Arrow shows power flow direction, red arrow indicates battery charging, blue arrow indicates battery discharging.

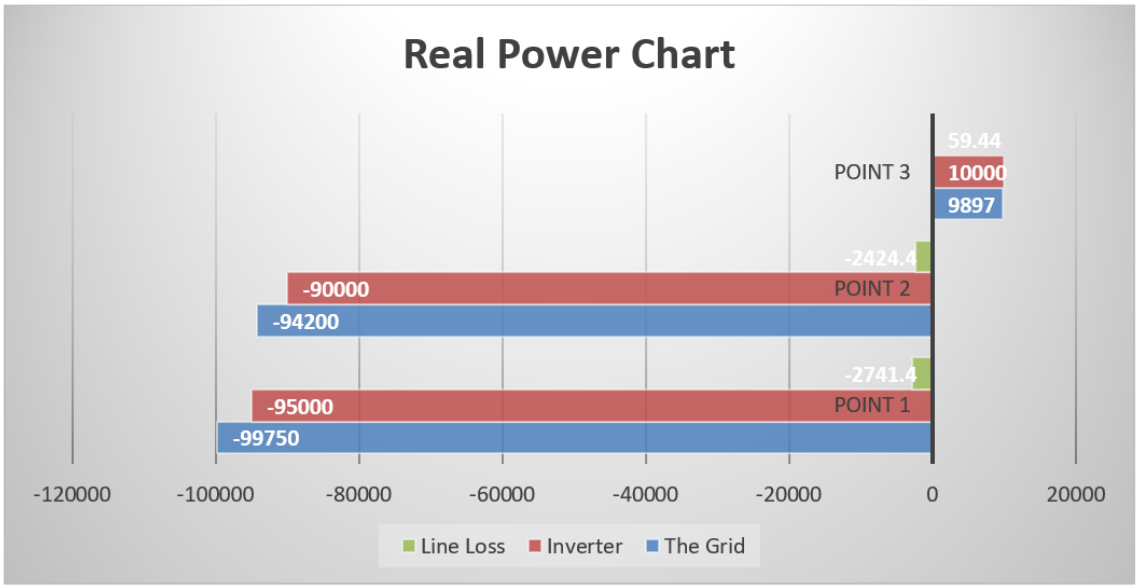

Figure 5-12: Real Power Chart.

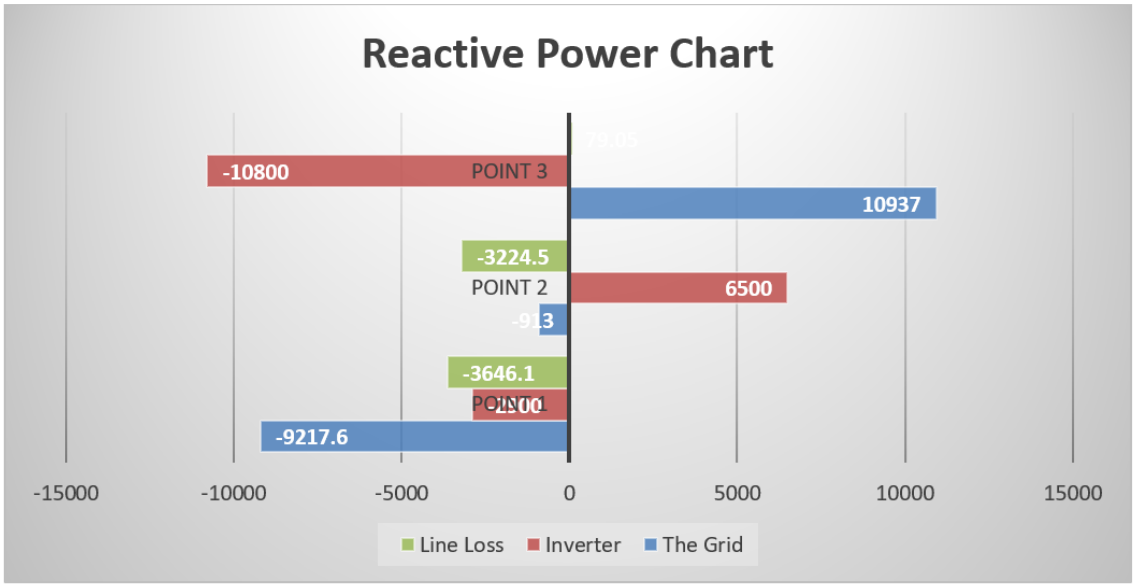

Figure 5-13: Reactive Power Chart.

5.2 Operation analysis

This section describes modeling of optimal scheduling for the Stone Edge Farm MCESS. Power flow diagram of the Stone Edge Farm MCESS, coupling of electric, natural gas, heating, cooling, and hydrogen systems, is illustrated in Fig. 5-14. The overall optimal scheduling can be modeled as an optimization problem with Eq. (5.17) as the objective function and subject to system constraints as in Eq. (5.18) to Section 5.2 plus MCESS components constraints Eqs. (5.1) to (5.7) as introduced in Section 2.

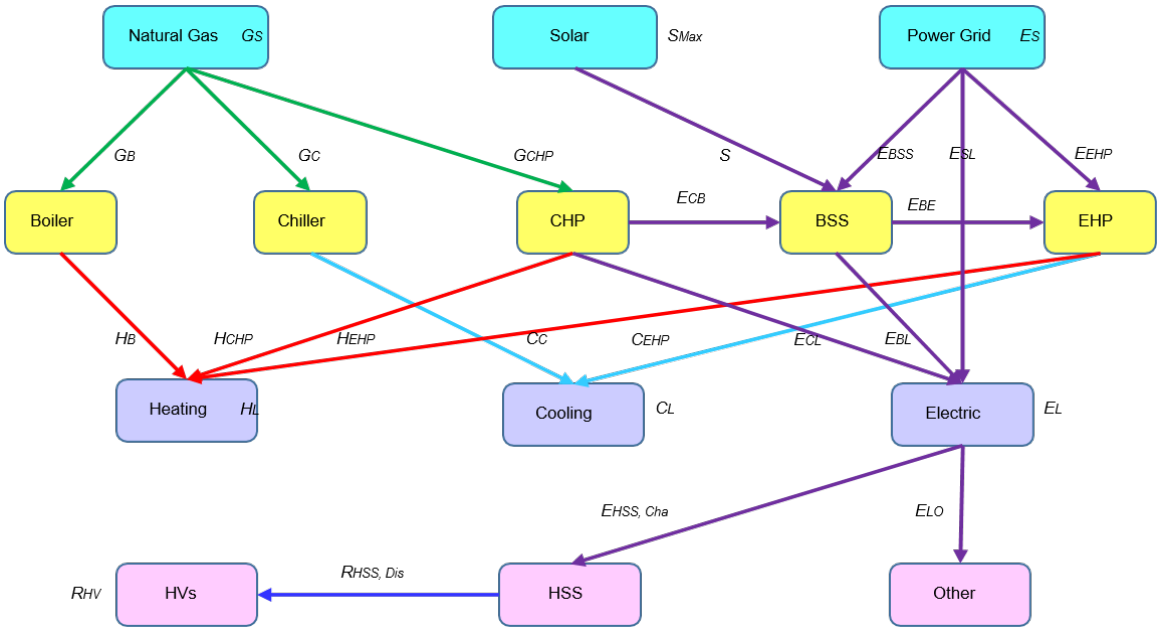

Figure 5-14: Power flow diagram of Stone Edge Farm MCESS.

Minimizing the total cost of purchased natural gas from local pipe line and electric power from distributed power grid within optimal scheduling horizon is treated as the objective function:

$$\min TC = \sum_{t \in T} \rho_E(t) E_S(t) \Delta T + \sum_{t \in T} \rho_G(t) + G_S(t) \Delta T \tag{5.17}$$

Purchased natural gas is supplied to CHP, boiler, and chiller as in Eq. (5.18) and corresponding power flow is drawn with green arrow in Fig. 8. On the load side, cooling power demand is satisfied by chiller and EHP as in Eq. (5.19), the

corresponding cooling power flow in the diagram is drawn with light blue arrow. Heating power demand from load side is satisfied by boiler, CHP, and EHP as shown in Eq. (5.20), and corresponding power flow is drawn with red arrow in the figure.

$$G_S(t) = G_B(t) + G_C(t) + G_{CHP}(t) \tag{5.18}$$

$$G_L(t) = G_C(t) = C_{EHP}(t) \tag{5.19}$$

$$H_L(t) = H_B(t) + H_{CHP}(t) + H_{EHP}(t) \tag{5.20}$$

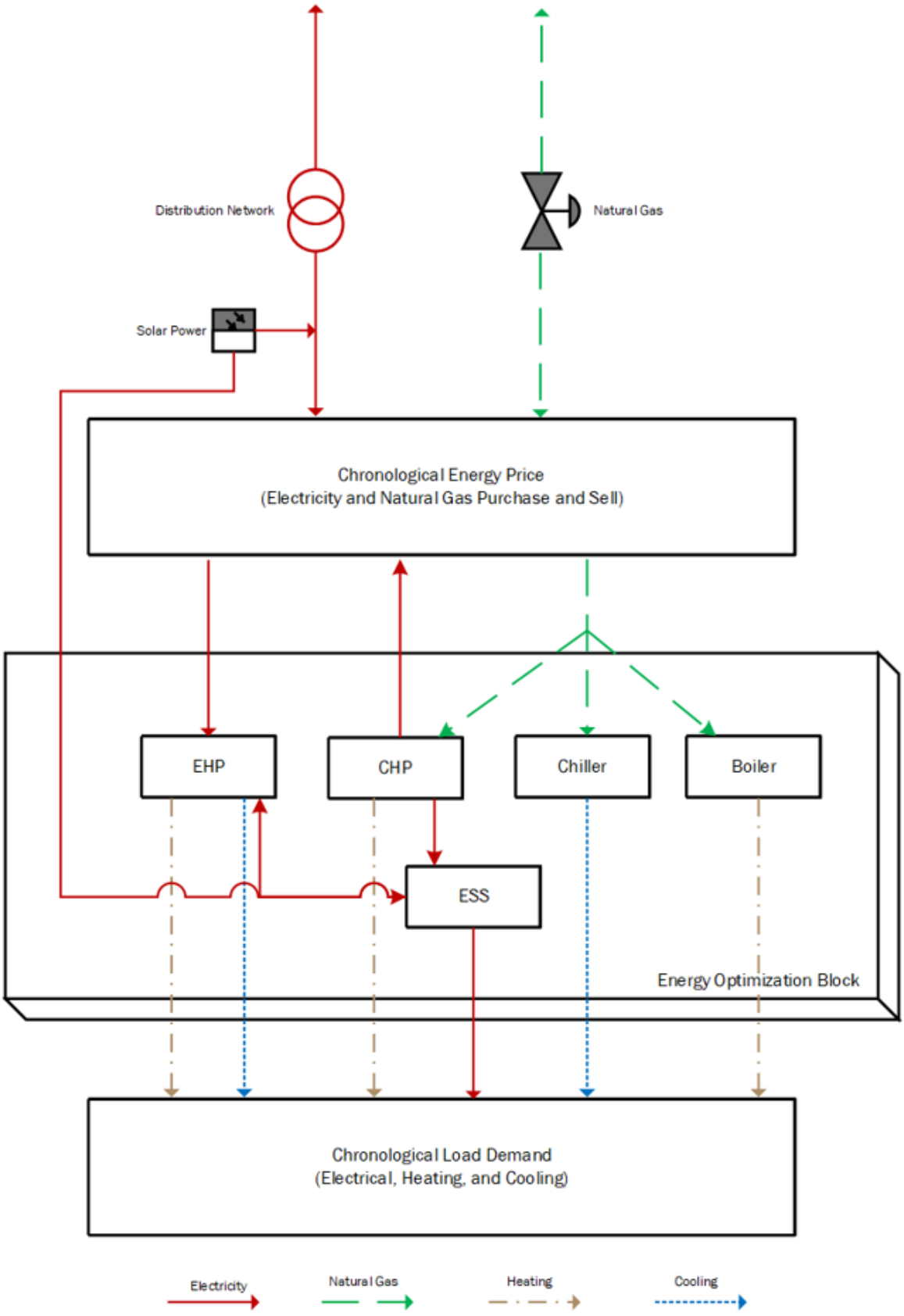

Figure 5-15: System Diagram.

All the electric power flow in the MCESS is drawn with purple arrow in Fig. 8. The electric power demand, consist of required HSS charging power and other kinds of electric load, are meet with the power supplied from CHP, BSS, and local distribution power grid as in Eq. (5.21) and Eq. (5.22). Electric power from CHP is supplied to load and BSS as Eq. (5.23). The electric power from CHP, solar photovoltaic arrays, and local distribution power grid can be used to charge BSS as formulated in Eq. (5.24). Discharging electric power from BSS are used to supply load electric power demand and EHP as Eq. (5.25). Equations Eq. (5.26) and Eq. (5.27) describes the electric power sources for EHP. Except the BSS discharging electric power, its remaining required input electric power is bought from local distribution power grid directly. Equation Eq. (5.28) summarizes the usage of electric power bought from local distribution power grid. In addition, in order to show the merits of the storage in MCESS later in the simulation, the initial and final stored power in BSS are set to zero as in Eq. (5.29).

$$E_L(t) = E_{CL}(t) + G_{BL}(t) + E_{SL}(t) \tag{5.21}$$

$$E_L(t) = E_{HSS,Cha}(t) + E_{LO}(t) \tag{5.22}$$

$$E_{CHP}(t) = E_{CL}(t) + E_{CB}(t) \tag{5.23}$$

$$E_{BSS,Cha}(t) = E_{CB}(t) + S(t) + E_{BSS}(t) \tag{5.24}$$

$$E_{BSS,Dis} = E_{BE}(t) + E_{BL}(t) \tag{5.25}$$

$$H_{EHP}(t) = [E_{EHP}(t) + E_{BE}(t)]\eta_{EHP,H} \tag{5.26}$$

$$C_{EHP}(t) = [E_{EHP}(t) + E_{BE}(t)]\eta_{EHP,C} \tag{5.27}$$

$$E_S(t) = E_{BSS}(t) + E_{SL}(t) + E_{EHP}(t) \tag{5.28}$$

$$E_{BSS,Si} = E_{BSS,Sf} = 0 \tag{5.29}$$

The hydrogen power flow in the system is marked with deep blue arrow in the figure. The discharging power from HSS are all supplied to meet HVs' hydrogen power demand as in Section 5.2. Similar with BSS, the initial and final stored power in HSS

are set to zero for further simulation.

$$R_{HV}(t) = R_{HSS,Dis}(t) \tag{5.30}$$

$$R_{HSS,Si} = R_{HSS,Sf} = 0 \tag{5.31}$$

Price of Electricity P electricity, the electricity price in Sonoma country is in a range of \$0.08 – \$0.3 per kWh on the business rate depending on the specific type, and we analyze the difference on the price rate between peak time and off-peak time. Information source is from PG&E. With the system data from various sources, we generate the plot shown in Fig. 5-16a.

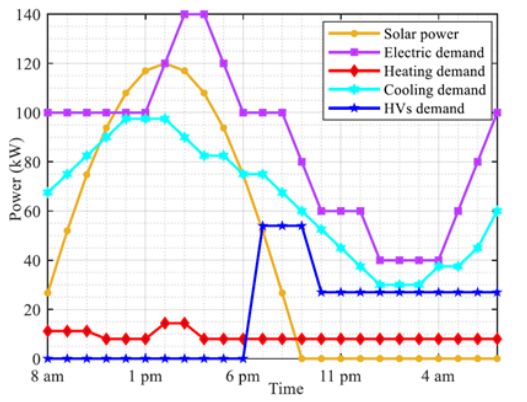

Demanded power and available solar power (Jul)

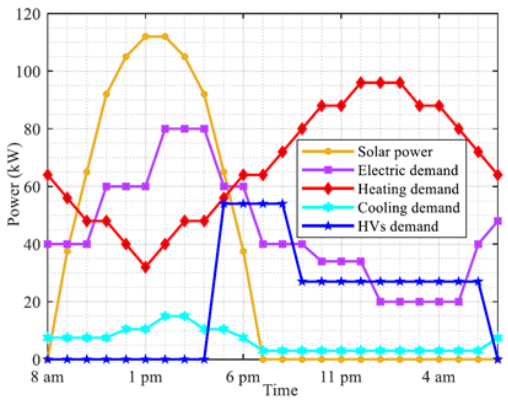

Demanded power and available solar power (Dec)

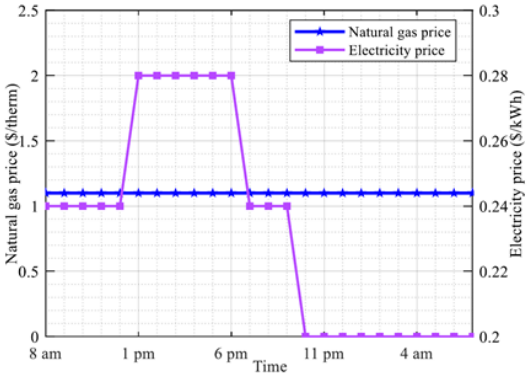

Natural gas and electricity price (Jul)

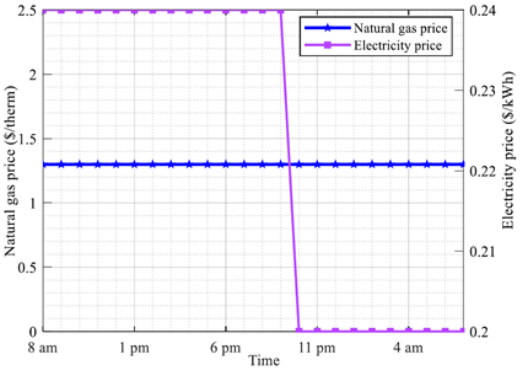

Natural gas and electricity price (Dec)

(a) Demanded Power and Natural Gas.

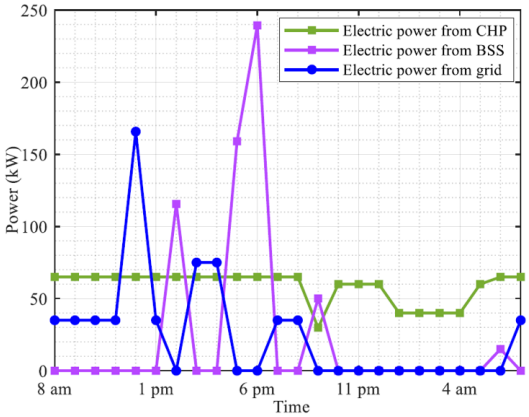

Generated electric power for load (Jul)

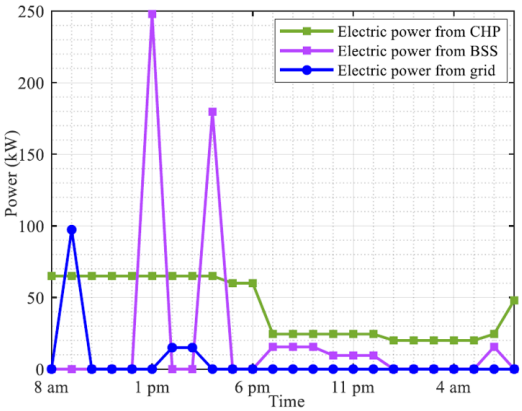

Generated electric power for load (Dec)

(b) Generated Electric Power.

Figure 5-16: Economic Analysis of System Operation.

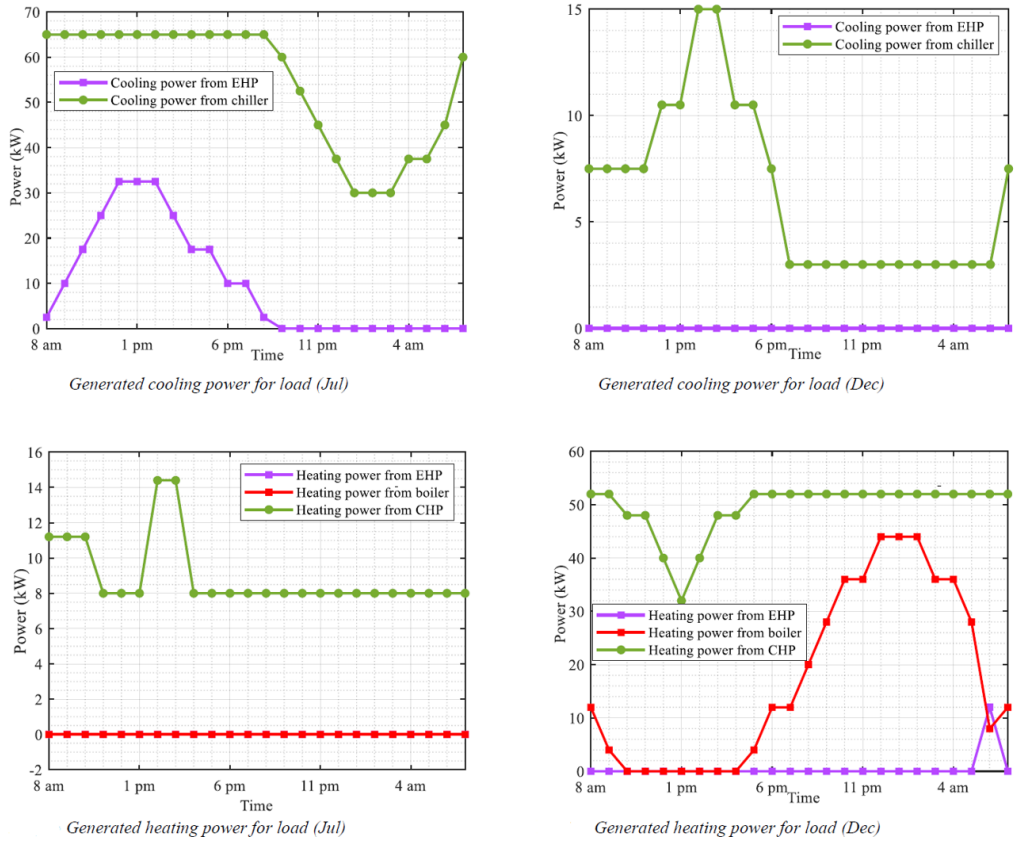

(c) Generated Cooling and Heating Power.

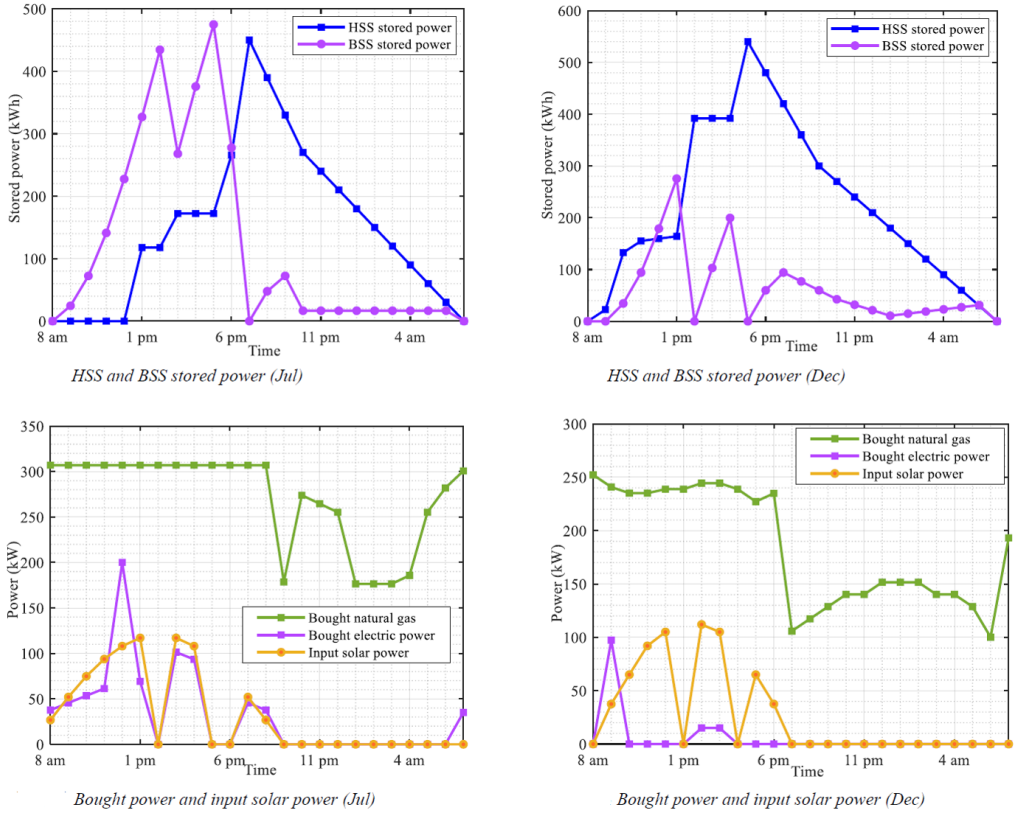

(d) Stored Power at BSS and HSS, Bought Power, and Solar Power.

Figure 5-16: Economic Analysis of System Operation.

Recalling power flows in the three-component network (Solar arrays, EV, and the grid) described in Chapter 3, our proposed method introduce two more paths - solar charging and super charging indicated in Fig. 5-17, this forms a decision map from the operation research standpoint. Inside this map, we have five events, four events are independent besides super charging, which is the intersection of EV charging and solar charging, the goal is to optimize the system performance from economic viewpoint, odds for each event varies depends on the environment situation, e.g. suppose event 1 is normal charging day - late afternoon time when solar power is away from its peak generation, it's more likely to do EV charging as noted in orange described in Fig. 5-18, meaning 40% of the time we should consider EV charging, 18%of the time for solar charging, and 20% of the time for super charging, 12% of the time for solar back-feeding power to the grid. event 2 is electricity shortage during sunny days, it's most likely to do V2G as noted in green, meaning 60% of the time we should consider V2G described in Fig. 5-18, 40% of the time we should consider solar charging. This work can be further developed using advanced machine learning methods such as deep learning and neural nets, which is discussed in the future section in Chapter 6.

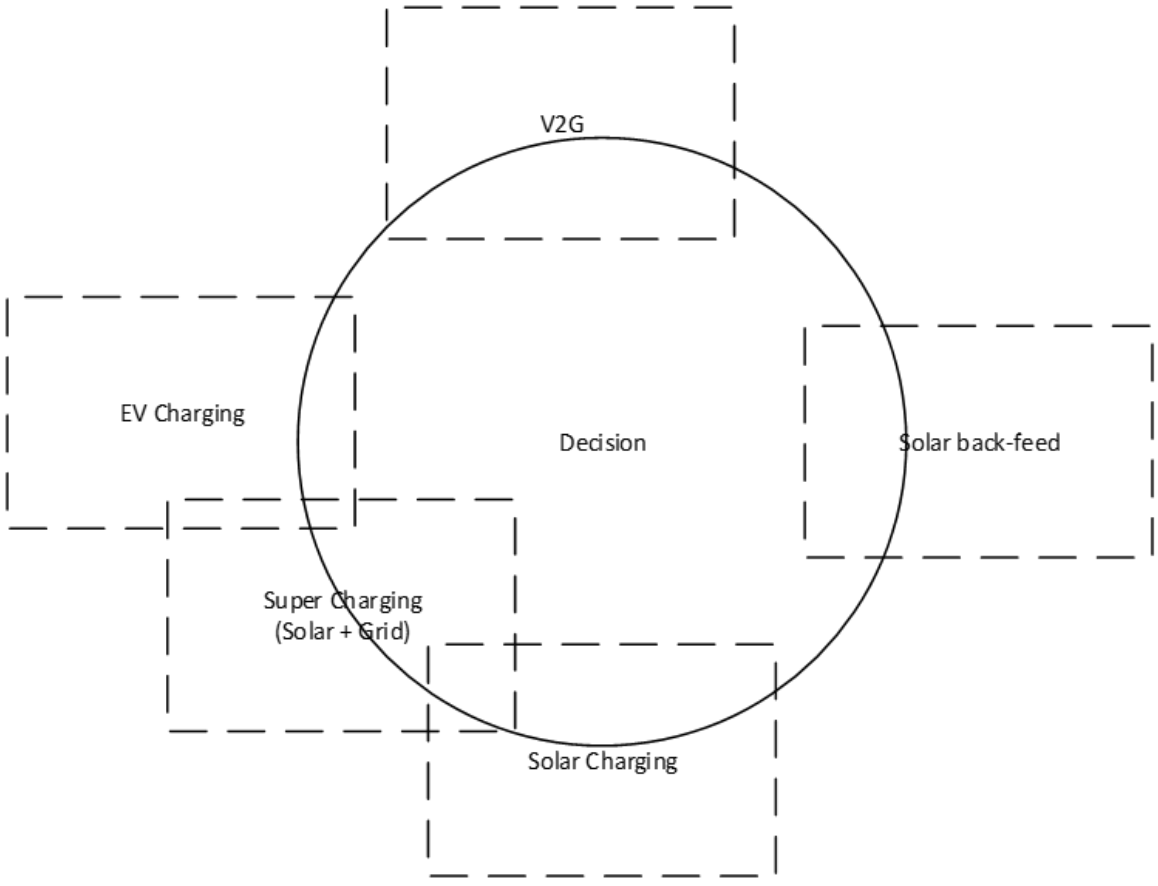

Figure 5-17: Decision Map.

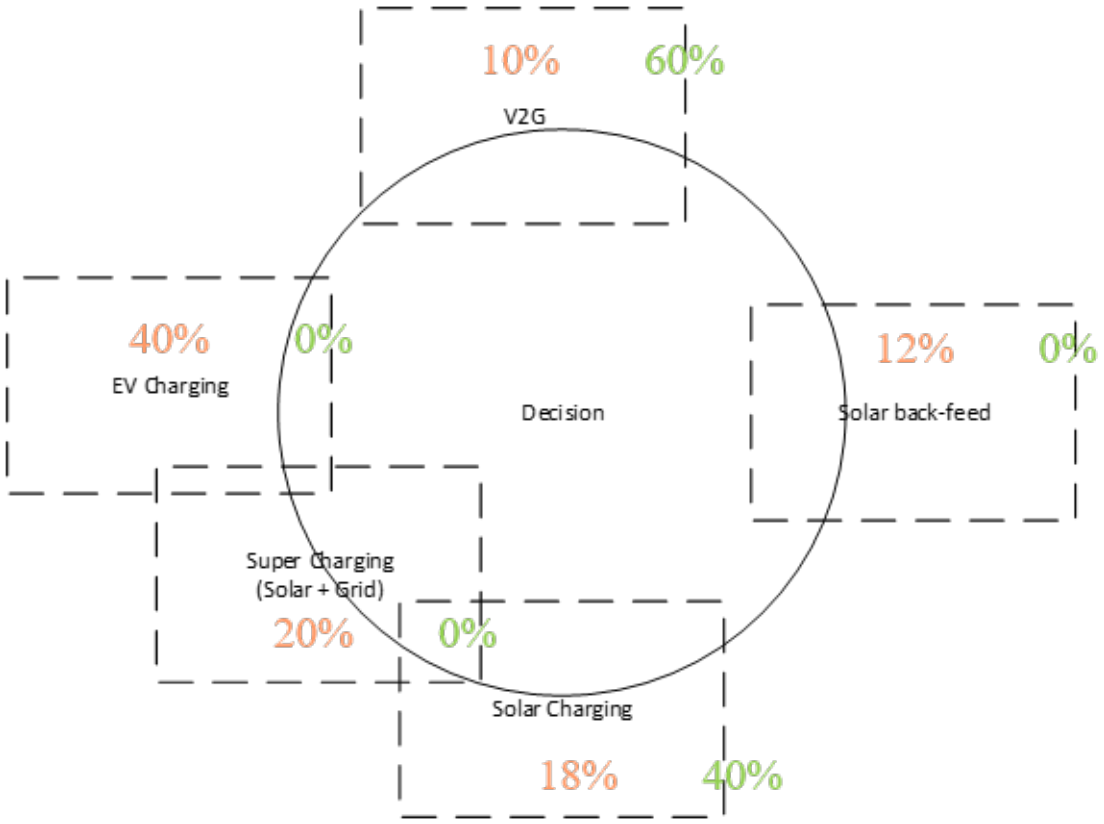

Figure 5-18: Decision Map With Stochastic Process.

In recent years, due to the growing concerns of environmental problems and energy crisis [93], more efficient scheduling and management of energy production and consumption has been encouraged policy makers and industry advisors. Researchers have developed the concept of smart grid, which includes a variety of operation and energy measures including smart meters, smart appliances, renewable energy resources, and energy efficient resources. Because of this new power grid concept, lots of studies have focused on electrical technical issues. In response to challenge of improving energy utilizing efficiency, multi-carrier energy storage systems (MCESSs), composed of electrical power networks, natural gas networks, heating networks, and other energy networks are attracting more attention and developing rapidly in recent years [94, 95]. Traditionally, different energy infrastructures in a system are commonly planned and operated independently, which results in less efficient energy usage and resource wasting [96, 97]. Through integrating as MCESS, defined as system with units where multiple energy carriers can be converted, conditioned and stored to meet energy demands, different energy infrastructures can be coupled and optimized as one unit [98–100]. Because of the strong coupling among these different energy infrastructures in a MCESS, their interactions should be studied and optimal scheduling and management of power flow should be carried out so as to improve the overall energy utilization efficiency while meeting various energy demands. The initial concept and structure of MCESS are presented in [101, 102]. Authors in [103–105] have proposed power flow management methods for MCESS with natural gas and electricity integrated. A multi-agent and integrated model for long-term planning for MCESS has been presented in [106]. Authors in [107] have developed a multi-period optimal power flow scheduling for large-scale MCESS. A mixed integer linear programming (MILP) model has been proposed to solve the optimal optimization problem for MCESS operation in [108]. The method is extended in [109–112], evaluating the potential of integrating renewable energies into MCESS. In [113], a genetic algorithm based method is proposed to solve the optimal power flow scheduling and management problem for MCESS considering non-linear system characteristics. A few more works have recently explored the merits of demand response applications in

the operation of MCESS [114–117].

The electric and heating systems are coupled by CHP as noted in Section 5.1.1 in the MCESS, which uses natural gas to produce electricity, and the waste heat from the turbine is a power generation source for balancing the heat loads in the heating system [25], [26]. CHP can meet heating power demand with less cost than EHP (Electric and Heat Pump) when local natural gas price is relatively lower than electricity price. CHP in Stone Edge Farm MCESS is mainly driven by a Capstone Gas turbine C65 natural gas-fired variable external combustion engine as shown in Fig.1 below. The combined heat and power efficiency is up to 90%. Among the converted power from natural gas, 68% goes to heating power and the remaining becomes electric power, which would be the maximum available heating and electric power from CHP at different time point given certain amount of natural gas input. Considering CHP limitations, the maximum output heating power is 52kW and maximum output electric power is 65kW as in (1) below.

With the bi-directional EV charging technology using solar power developed in Chapter 3, we discuss several operation situations to quantitatively show its advantages on economic saving. In Table 5.3 below, assuming the power not produced by the solar arrays was purchased from the utility, the total costs of MCESS operation for the two selected dates with and without solar photovoltaic arrays and storages are listed to show their corresponding economic merits. To show the completeness of operation data, we analyze two different seasons - summer and winter. Picking a date in summer - Jul 25th, 2017, the optimal operation cost is $440.9. If without the solar photovoltaic arrays and BSS, the optimal operation cost would be $599.1, suggesting a cost increase of 35.9%. On the other hand, if there is no HSS in the system, the cost would be increased to $460.3, equivalent to a cost increase of 4.4%. Similarly, picking a date in winter - Dec 6th, 2017, the optimal operation cost is $226.7. If there are no solar photovoltaic arrays and BSS in the MCESS, the optimal operation cost would be $343.6, suggesting a cost increase of 51.5%. If there is no HSS in the system, the cost would be increased to $242.9, equivalent to a cost increase of 7.1%. The results can actually explain the benefits that the solar photovoltaic arrays and storages bring

to MCESS. With BSS, solar power from photovoltaic arrays can be utilized to the greatest extent. Moreover, based on reasonable charging and discharging scheduling for the storages according to the expected energy price, operating cost of the system can be further reduced. From the above calculations, it is obvious that with the application of our smart and efficient EV charger, the cost saving can be enhanced further up to 27.2% for summer and 33.0% for winter against the traditional method which has no solar power involved.

Table 5.3: Economic Benefits of Solar Energy Source and Battery Storage System.

*	Summer (July 2017)	Winter (Dec. 2017)
Without Solar Power and BSS	\$599.1	\$343.6
With Solar Power and BSS	\$460.3 (23.0%)	\$242.9(29.3%)
With Solar Power and BSS (smart charger)	\$436.3(27.2%)	\$230.2(33.0%)

We propose optimal scheduling for a real multi-carrier energy storage system with vehicles (EV and HV) applications is proposed from an economic point of view. The main contribution of this work is twofold: 1) besides traditional battery storage system in multi-carrier energy storage system, storage system (BSS and HSS) is also considered in this research for vehicle applications. 2) The proposed optimal scheduling is simulated and analyzed based on data collected from real multi-carrier energy storage system. Therefore, real system characteristics have been fully considered. As the simulation results suggest, the proposed optimal scheduling can help quantify the daily operation cost and achieve considerably operation cost saving by reasonably arranging and utilizing the components in multi-carrier energy storage system. For the Stone Edge Farm multi-carrier energy storage system, the local electricity and gas price are fixed, solar power can be predicted with high accuracy due to the local weather condition, and load demand can be effectively managed.

To conclude, the proposed optimal scheduling can help quantify the daily operation cost and achieve considerably operation cost saving up to 23% in summer and 29.3% in winter further to 27.2% and 33.0% with smart EV charger developed in Chapter 3, by reasonably arranging and utilizing all the components in the MCESS.

Since the micro-grid site was still under construction while the research was carried, optimization strategy was not fully developed on details, such as arranging electric vehicle charging time, prioritizing sources, keeping battery levels in certain ranges, etc, thus these would be future work once the site is fully operational. By looking back at Fig. 2-1, the operation analysis has validated the effectiveness on the efficiency improvement and cost saving of a centralized structure, which is redesigning a EV charger that serves as the power hub connecting solar power and the grid with the EV shown in Fig. 2-3b.

Chapter 6

Conclusion and Future Work

This thesis presents a centralization methodology to tackle the complicated structure, cost and low efficiency issues existing in current energy networks, by designing a bi-directional EV charger that uses all wide-bandgap semiconductor devices to electric network and an uniform multi-user wireless power transfer system to electronic network. In the electric network describing in Chapter 3, this work reduces up to 50% cost on hardware in Section 2.2 and 50% on power conversion loss in Chapter 3. In the electronic network describing in Chapter 4, our work achieves uniform efficiency delivery in 2-D and quasi uniform in 3-D, allowing multiple electronic loads moving in the relatively fixed space while being charged. In Chapter 5, quantitative analysis of the system operation on electric network shows an optimal strategy can further prove a combination of solar power and EV (or battery storage system) can offer significant saving up to 33% on overall purchased energy cost equipped with smart and efficient EV charger at the Stone Edge Farm micro-grid site.

Centralization methodology means we build a hub serving as the center of its network, which simplifies the system architecture therefore improving efficiency and reducing cost overall. For electric network, our proposed method - bi-directional EV charger in Chapter 3 connecting solar power and the grid to achieve maximum efficiency and minimal cost has been validated through experiments and operation data. For electronics network, our proposed method - a 3-D quasi-uniform wireless power transfer system in Chapter 4 connecting multiple battery-powered devices has

been validated as the most convenient solution offering the easiness of use.

With this centralization methodology in smart grid, the system structure is simplified to meet the increasing need of renewable source such as solar power for the electric vehicle application and the flexibility of charging multiple electronic devices for the mobile phone application in 5G. We have seen these papers [69,82,83] to follow our ideas, and we firmly believe this centralized structure would provide an easy access for the efficient data mining process, which can optimize the system performance in the long run.

Future work can include advanced machine learning such as deep learning and game theory methods to optimize the system performance further [118–133].

Appendix A

System Modeling

An easy example of data classification and clustering is shown in Fig. A-1, where data is divided into 5 categories: Capstone Turbine, Aquion Battery, Tesla battery, Electrolyzer, and Solar. For the sake of brevity, let us assume the net profit of the farm is a function of just two features, the value of power x and the time factor theta. The data can be presented in a two-dimensional frame, x-axis and y-axis shows the value of x and theta after standardization, respectively.

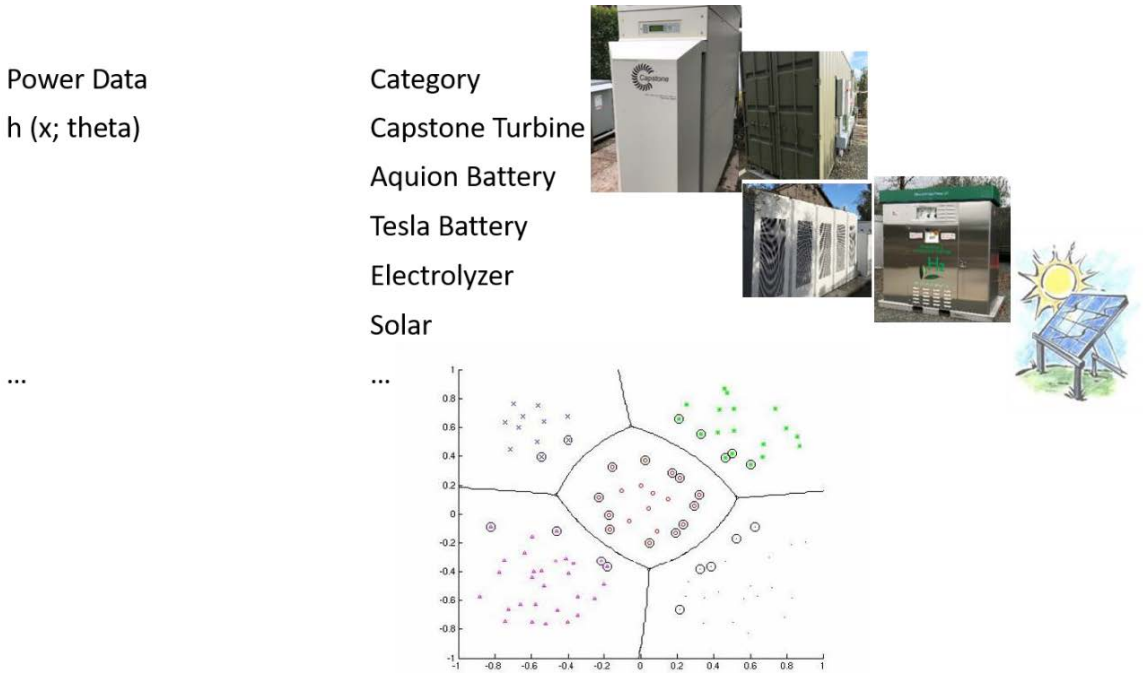

Figure A-1: Mathematical Representation of the Collected Data.

Three sets of data points are extracted to build the 15 non-linear equations with 15 unknown variables.

$$
\begin{bmatrix}
\frac{1}{\sqrt{3}} & 0 & 0 & 0 & 0 & -R & X & 0 & 0 & 0 \\
0 & -\frac{1}{\sqrt{3}} & 0 & 0 & & & & & & \\
0 & \frac{1}{\sqrt{3}} & 0 & 0 & 0 & 0 & -X & -R & 0 & 0 \\
0 & 0 & 0 & 0 & 0 & & & & & \\
V_{id1} & V_{iq1} & 0 & 0 & 0 & 0 & 0 & 0 & 0 & 0 \\
0 & 0 & 0 & 0 & 0 & & & & & \\
\sqrt{3}I_{d1} & \sqrt{3}I_{q1} & 0 & 0 & 0 & 0 & 0 & 0 & 0 & 0 \\
0 & 0 & 0 & 0 & 0 & & & & & \\
\sqrt{3}I_{q1} & \sqrt{3}I_{d1} & 0 & 0 & 0 & 0 & 0 & 0 & 0 & 0 \\
0 & 0 & 0 & 0 & 0 & & & & & \\
0 & 0 & \frac{1}{\sqrt{3}} & 0 & 0 & 0 & 0 & 0 & -R & X \\
0 & 0 & -\frac{1}{\sqrt{3}} & 0 & 0 & & & & & \\
0 & 0 & 0 & -\frac{1}{\sqrt{3}} & 0 & 0 & 0 & 0 & -X & -R \\
0 & 0 & 0 & 0 & 0 & & & & & \\
0 & 0 & V_{id2} & V_{iq2} & 0 & 0 & 0 & 0 & 0 & 0 \\
0 & 0 & 0 & 0 & 0 & & & & & \\
0 & 0 & \sqrt{3}I_{d2} & \sqrt{3}I_{q2} & 0 & 0 & 0 & 0 & 0 & 0 \\
0 & 0 & 0 & 0 & 0 & & & & & \\
0 & 0 & -\sqrt{3}I_{q2} & \sqrt{3}I_{d2} & 0 & 0 & 0 & 0 & 0 & 0 \\
0 & 0 & 0 & 0 & 0 & & & & & \\
0 & 0 & 0 & 0 & \frac{1}{\sqrt{3}} & 0 & 0 & 0 & 0 & 0 \\
-R & X & -\frac{1}{\sqrt{3}} & 0 & 0 & & & & & \\
0 & 0 & 0 & 0 & 0 & \frac{1}{\sqrt{3}} & 0 & 0 & 0 & 0 \\
-X & -R & 0 & 0 & 0 & & & & & \\
0 & 0 & 0 & 0 & V_{id3} & V_{iq3} & 0 & 0 & 0 & 0 \\
0 & 0 & 0 & 0 & 0 & & & & & \\
0 & 0 & 0 & 0 & \sqrt{3}I_{d3} & \sqrt{3}I_{q3} & 0 & 0 & 0 & 0 \\
0 & 0 & 0 & 0 & 0 & & & & & \\
0 & 0 & 0 & 0 & -\sqrt{3}I_{q3} & \sqrt{3}I_{d3} & 0 & 0 & 0 & 0 \\
0 & 0 & 0 & 0 & 0 & & & & &
\end{bmatrix}
\begin{bmatrix}
V_{id1} \\ v_{iq1} \\ V_{id2} \\ V_{iq2} \\ V_{id3} \\ V_{iq3} \\ I_{d1} \\ I_{q1} \\ I_{d2} \\ I_{q2} \\ I_{d3} \\ I_{q3} \\ V_{gd} \\ R \\ X
\end{bmatrix}
=
\begin{bmatrix}
0 \\ 0 \\ V_{i1}^2 \\ P_1 \\ Q_1 \\ 0 \\ 0 \\ V_{i2}^2 \\ P_2 \\ Q_2 \\ 0 \\ 0 \\ V_{i3}^2 \\ P_3 \\ Q
\end{bmatrix}
\tag{A.1}
$$

Appendix B

Operation Data of Stone Edge Farm Micro-Grid Site

Time [sec]	Battery Real Power [W]	Battery Reactive Power [VAr]	SOC [%]	Real Power [W]	Reactive Power [VAr]	Apparent Power [VA]	Average Voltage [V]	Frequency [Hz]	S
2	0	0	20.12051	0	0	0	499	59.99	0
3	0	0	20.12178	0	0	0	499.2	60	0
4	0	0	20.12129	0	0	0	498.8	60.029	0
5	0	0	20.12043	0	0	0	499.4	59.99	0
6	0	0	20.12043	0	0	0	499	59.99	0
7	0	0	20.12183	0	0	0	499.2	60.029	0
8	0	0	20.11965	0	0	0	499.2	60.02	0
9	0	0	20.11916	0	0	0	499.1	60.06	0
10	0	0	20.12039	0	0	0	499.4	60.02	0
11	0	0	20.12039	0	0	0	499.2	60.06	0
12	0	0	20.12137	0	0	0	499.1	60	0
13	0	0	20.12035	0	0	0	499.3	60.04	0
14	0	0	20.12035	0	0	0	499.1	60.029	0
15	0	0	20.12129	0	0	0	499.1	60.02	0
16	0	0	20.12129	0	0	0	498.5	60.04	0
17	0	0	20.12133	0	0	0	499.1	60	0
18	0	0	20.12133	0	0	0	499.6	60	0
19	0	0	20.12125	0	0	0	499.3	60.029	0
20	0	0	20.12125	0	0	0	499.5	60.02	0
21	0	0	20.12072	0	0	0	499	60.029	0
22	0	0	20.12072	0	0	0	499	60	0
23	0	0	20.12101	0	0	0	498.9	60	0
24	0	0	20.12101	0	0	0	498.9	60	0
27	0	0	20.12088	0	0	0	498.9	60.029	0
28	0	0	20.12023	0	0	0	499.1	60.029	0
29	0	0	20.12023	0	0	0	498.8	60.02	0
30	0	0	20.12035	0	0	0	499.3	59.99	0
31	0	0	20.12035	0	0	0	498.9	59.99	0
32	0	0	20.12146	0	0	0	499.1	60.02	0
33	0	0	20.12146	0	0	0	498.6	59.99	0
34	0	0	20.12088	0	0	0	499.1	60	0
35	0	0	20.12088	0	0	0	499.3	60	0
36	0	0	20.12121	0	0	0	499.2	59.99	0
37	0	0	20.12121	0	0	0	499.4	60.02	0
38	0	0	20.12101	0	0	0	499.6	59.99	0
39	0	0	20.12051	0	0	0	499.1	59.99	0
40	0	0	20.11998	0	0	0	499.5	59.99	0
41	0	0	20.12027	0	0	0	499.8	60	0
42	0	0	20.12084	0	0	0	499.7	60.029	0
43	0	0	20.12051	0	0	0	499	60.029	0
44	0	0	20.12039	0	0	0	499.4	60	0
45	0	0	20.12039	0	0	0	499.6	60	0
46	0	0	20.12019	0	0	0	499.9	60	0
47	0	0	20.12002	0	0	0	499.5	60	0
48	0	0	20.12068	0	0	0	499.5	60.04	0
49	0	0	20.12068	0	0	0	499.5	60.04	0
54	0	0	20.12002	0	0	0	500.1	60.02	0
55	0	0	20.12051	0	0	0	499.7	60.06	0

56	0	0	20.12051	0	0	0	499.9	60.02	0
57	0	0	20.12051	0	0	0	500.2	60.02	0
58	0	0	20.12117	0	0	0	499.5	60.029	0
59	0	0	20.1215	0	0	0	499.7	60.02	0
60	0	0	20.12043	0	0	0	499.7	60.029	0
61	0	0	20.12043	0	0	0	499.7	60.029	0
62	0	0	20.12043	0	0	0	499.3	60	0
63	0	0	20.12068	0	0	0	499.5	60.029	0
64	0	0	20.12068	0	0	0	499.3	60.029	0
65	0	0	20.12084	0	0	0	499.6	60.02	0
66	0	0	20.12084	0	0	0	499.1	60	0
67	0	0	20.12068	0	0	0	499.7	60	0
68	0	0	20.12068	0	0	0	499.7	60	0
69	0	0	20.12068	0	0	0	499.1	60.02	0
70	0	0	20.12047	0	0	0	499.7	60.029	0
71	0	0	20.12047	0	0	0	499.3	60.029	0
72	0	0	20.12113	0	0	0	499.3	60	0
73	0	0	20.12113	0	0	0	499.5	60.029	0
74	0	0	20.12088	0	0	0	499.7	60	0
75	0	0	20.12088	0	0	0	499.6	60	0
76	0	0	20.12088	0	0	0	499.6	60	0
77	0	0	20.12096	0	0	0	500	60	0
78	0	0	20.12096	0	0	0	500	60.029	0
79	0	0	20.12064	0	0	0	499.9	60	0
80	0	0	20.12084	0	0	0	499.8	60.02	0
81	0	0	20.12068	0	0	0	500.1	60.02	0
82	0	0	20.12047	0	0	0	499.8	60.02	0
83	0	0	20.12047	0	0	0	499.8	60.02	0
84	0	0	20.12096	0	0	0	499.6	60.02	0
85	0	0	20.12051	0	0	0	499.7	60.029	0
86	0	0	20.12039	0	0	0	500.1	60.02	0
87	0	0	20.12084	0	0	0	500	60.029	0
88	0	0	20.12039	0	0	0	500	60.029	0
89	0	0	20.12039	0	0	0	500.2	60	0
90	0	0	20.12101	0	0	0	500.1	60.029	0
91	0	0	20.12101	0	0	0	500.2	60.029	0
92	0	0	20.12105	0	0	0	500.1	60.029	0
93	0	0	20.12125	0	0	0	500.1	60.02	0
94	0	0	20.12142	0	0	0	500.2	60.04	0
95	0	0	20.12142	0	0	0	500	60.02	0
96	0	0	20.12142	0	0	0	500	60.02	0
97	0	0	20.12133	0	0	0	500	60.02	0
98	0	0	20.12113	0	0	0	500	60.029	0
99	0	0	20.12166	0	0	0	500.3	60.02	0
100	0	0	20.12166	0	0	0	500.2	60.02	0
101	0	0	20.12117	0	0	0	500.5	60.02	0
102	0	0	20.12068	0	0	0	500.4	60.029	0
103	0	0	20.12035	0	0	0	500.1	60.02	0
104	0	0	20.12084	0	0	0	500.2	60.02	0
105	0	0	20.12084	0	0	0	500.2	60.02	0
106	0	0	20.12084	0	0	0	500.2	60.02	0
109	0	0	20.12133	0	0	0	500.4	60.04	0
110	0	0	20.12039	0	0	0	500.7	60.029	0

111	0	0	20.12039	0	0	0	500.4	60.02	0
112	0	0	20.12084	0	0	0	500.7	60.029	0
113	0	0	20.12084	0	0	0	500.6	60.04	0
114	0	0	20.12113	0	0	0	500.6	60.029	0
115	0	0	20.12113	0	0	0	500.4	60.04	0
116	0	0	20.12101	0	0	0	500.7	60.029	0
117	0	0	20.12101	0	0	0	500.8	60.04	0
118	0	0	20.12072	0	0	0	500.5	60.029	0
119	0	0	20.12072	0	0	0	500.2	60.04	0
120	0	0	20.12092	0	0	0	500.4	60.04	0
121	0	0	20.12092	0	0	0	500.7	60.04	0
122	0	0	20.12133	0	0	0	500.9	60.029	0
123	0	0	20.12084	0	0	0	500.4	60.029	0
124	0	0	20.12084	0	0	0	500.7	60.029	0
125	0	0	20.12133	0	0	0	500.9	60.029	0
126	0	0	20.1208	0	0	0	500.4	60.029	0
127	0	0	20.1208	0	0	0	500.3	60.029	0
128	0	0	20.12101	0	0	0	500.2	60.029	0
129	0	0	20.12051	0	0	0	500.8	60.029	0
130	0	0	20.1208	0	0	0	500.6	60.029	0
131	0	0	20.12129	0	0	0	500.5	60.029	0
132	0	0	20.12043	0	0	0	500.6	60.02	0
133	0	0	20.12043	0	0	0	500.7	60.02	0
134	0	0	20.12088	0	0	0	500.7	60.02	0
135	0	0	20.12109	0	0	0	500.7	60.029	0
136	0	0	20.12043	0	0	0	500.7	60.029	0
137	0	0	20.12023	0	0	0	500.7	60.029	0
138	0	0	20.12125	0	0	0	500.6	60.029	0
139	0	0	20.12125	0	0	0	500.8	60.02	0
140	-9055	0	20.12092	0	0	0	500.7	60.029	0
141	-10055	0	20.12092	0	0	0	500.8	60.02	0
142	-11098	0	20.12183	4691	319	9234	500.9	59.99	4701.834
143	-11089	0	20.12183	-11840	-4450	15028	496.3	60.02	12648.64
144	-10916	0	20.12178	-11564	-4377	14172	496.5	60.029	12364.64
145	-10746	0	20.12178	-11456	-4546	14891	496.8	60.029	12325.02
146	-10609	0	20.12133	-11234	-4279	13881	496.6	60.029	12021.34
147	-10485	0	20.12154	-11186	-4619	14512	496.5	60.02	12102.14
148	-10376	0	20.12158	-10969	-4239	13708	496.8	60.029	11759.6
149	-10277	0	20.12137	-10911	-4600	14095	496.5	60.02	11841.03
150	-10180	0	20.12088	-10764	-4306	13777	496.6	60.02	11593.33
151	-10100	0	20.12088	-10689	-4496	13683	497	60	11596.07
152	-10031	0	20.12211	-10696	-4434	14053	496.9	60.02	11578.63
153	-9968	0	20.12166	-10541	-4493	13437	496.7	60.02	11458.61
154	-9910	0	20.12318	-10540	-4555	14159	497	60.02	11482.14
155	-9856	0	20.12363	-10429	-4372	13315	497.1	60.02	11308.33
156	-9808	0	20.124	-10393	-4640	13971	496.8	60.02	11381.74
157	-9770	0	20.124	-10319	-4323	13231	497.2	60.029	11187.94
158	-9732	0	20.12376	-10344	-4601	13679	497.1	60.029	11321.11
159	-9704	0	20.12376	-10229	-4324	13240	496.9	60.029	11105.38
160	-9672	0	20.12417	-10248	-4698	13469	497.4	60.02	11273.54
161	-9643	0	20.12417	-10256	-4427	13565	497	60.02	11170.67
162	-9624	0	20.12585	-10122	-4641	13146	497.3	60.02	11135.25
163	-9606	0	20.12585	-10205	-4494	13842	497.4	60.029	11150.7

164	-9588	0	20.12646	-10125	-4466	13092	496.9	60.02	11066.2
165	-9568	0	20.12618	-10200	-4632	13866	497	60.029	11202.47
166	-9552	0	20.12659	-10108	-4392	13061	497	60.02	11020.95
167	-9537	0	20.12663	-10073	-4809	13690	497.2	60.029	11162.07
168	-9531	0	20.12721	-10021	-4334	13032	497.2	60.029	10918.06
169	-9522	0	20.12716	-10037	-4666	13341	497.4	60.02	11068.56
170	-9516	0	20.1286	-10018	-4391	13250	497.1	60.02	10938.06
171	-9508	0	20.1286	-10018	-4765	13242	497.3	60.02	11093.49
172	-9501	0	20.12983	-10084	-4507	13686	497	60.02	11045.37
173	-9494	0	20.12983	-9995	-4525	13010	497.2	60.029	10971.58
174	-9486	0	20.12917	-10115	-4662	13843	497.3	60.029	11137.66
175	-9478	0	20.12922	-10003	-4466	12981	497.6	60.04	10954.69
176	-9470	0	20.13045	-10096	-4780	13812	497.7	60.04	11170.39
177	-9463	0	20.1309	-10018	-4423	13019	497.4	60.029	10950.95
178	-9454	0	20.13176	-10056	-4775	13511	497.5	60.04	11132.1
179	-9448	0	20.13127	-10005	-4410	13106	497.7	60.029	10933.81
180	-9448	0	20.13291	-9926	-4739	13138	497.9	60.029	10999.25
181	-9452	0	20.13291	-10029	-4538	13379	497.6	60.04	11007.92
182	-9446	0	20.13246	-9936	-4782	13045	497.7	60.029	11026.86
183	-9450	0	20.13295	-10013	-4660	13655	497.6	60.029	11044.26
184	-9446	0	20.13402	-9927	-4524	12904	497.7	60.04	10909.26
185	-9450	0	20.13353	-10017	-4824	13792	497.3	60.04	11118.06
186	-9447	0	20.13439	-9918	-4474	12928	497.8	60.029	10880.41
187	-9450	0	20.13439	-9954	-4847	13594	497.7	60.06	11071.38
188	-9447	0	20.1339	-9997	-4392	12972	497.9	60.04	10919.23
189	-9448	0	20.13439	-9918	-4759	13219	497.9	60.04	11000.67
190	-9448	0	20.1359	-10029	-4467	13213	497.6	60.029	10978.84
191	-9449	0	20.1359	-9906	-4666	12954	497.2	60.029	10949.9
192	-9448	0	20.13693	-10072	-4584	13540	497.2	60.029	11066.09
193	-9449	0	20.13697	-9903	-4758	12918	497.1	60.029	10986.72
194	-9448	0	20.13779	-10108	-4749	13823	496.9	60.04	11168.02
195	-9448	0	20.13779	-9910	-4637	12913	497.1	60.029	10941.2
196	-9451	0	20.13775	-9982	-4907	13715	497	60.029	11122.9
197	-9447	0	20.13755	-10023	-4496	13064	496.4	60.029	10985.2
198	-9447	0	20.13923	-9946	-4828	13409	497.3	60.04	11055.88
199	-9452	0	20.13923	-9931	-4475	13039	497.1	60.04	10892.68
200	-9446	0	20.14005	-9970	-4893	13313	497.7	60.04	11105.96
201	-9449	0	20.13972	-9974	-4583	13353	497.6	60.029	10976.55
202	-9448	0	20.13993	-10030	-4777	13045	497.6	60.04	11109.48
203	-9449	0	20.13993	-10022	-4708	13657	497.4	60.029	11072.75
204	-9447	0	20.14017	-10016	-4615	12962	497.4	60.029	11028.08
205	-9447	0	20.14067	-9992	-4894	13795	497.3	60.029	11126.15
206	-9451	0	20.1419	-9925	-4653	12994	497.6	60.04	10961.57
207	-9446	0	20.14173	-9972	-4929	13590	497.1	60.029	11123.66
208	-9450	0	20.14235	-9924	-4476	13011	497.5	60.04	10886.71
209	-9447	0	20.14251	-10035	-4945	13461	497.3	60.04	11187.24
210	-9448	0	20.14305	-9941	-4558	13211	497.1	60.029	10936.13
211	-9450	0	20.14288	-9949	-4821	13143	497.4	60.029	11055.53
212	-9448	0	20.14399	-9971	-4714	13562	496.9	60.02	11029.17
213	-9451	0	20.14399	-9902	-4791	12928	497.5	60.04	11000.15
214	-9447	0	20.14535	-10114	-4866	13862	497.2	60.02	11223.68
215	-9448	0	20.14485	-9919	-4627	12964	497.4	60.04	10945.12
216	-9449	0	20.14596	-9994	-4955	13771	497.3	60.029	11154.91

217	-9448	0	20.14613	-9985	-4526	13027	497.2	60.029	10962.89
218	-9448	0	20.1465	-9938	-5030	13487	497.8	60.029	11138.44
219	-9451	0	20.14682	-9987	-4588	13139	497.7	60.02	10990.45
220	-9446	0	20.14658	-9944	-4954	13264	497.5	60.02	11109.69
221	-9449	0	20.14654	-9957	-4655	13397	497.4	60.029	10991.4
222	-9450	0	20.14715	-9985	-4844	13080	497.7	60.029	11097.95
223	-9446	0	20.1467	-10002	-4796	13710	497.7	60.04	11092.41
224	-9450	0	20.14818	-9904	-4660	12890	498	60.029	10945.54
225	-9448	0	20.14904	-10118	-4966	13902	497.7	60.029	11270.98
226	-9448	0	20.14859	-9918	-4708	12994	498.1	60.029	10978.71
227	-9451	0	20.14838	-10022	-5051	13751	497.8	60.029	11222.88
228	-9448	0	20.15048	-9919	-4615	13040	497.5	60.029	10940.05
229	-9450	0	20.14982	-9965	-5028	13515	497.7	60.029	11161.63
230	-9446	0	20.14974	-9937	-4672	13259	497.4	60.02	10980.51
231	-9449	0	20.14974	-9921	-4984	13224	497.6	60.04	11102.54
232	-9447	0	20.15146	-10106	-4750	13727	497.5	60.029	11166.63
233	-9448	0	20.15212	-9926	-4894	13013	497.7	60.02	11066.92
234	-9449	0	20.15167	-10101	-4915	13903	497.6	60.04	11233.32
235	-9447	0	20.1515	-9923	-4726	12964	497.7	60.029	10990.95
236	-9450	0	20.15298	-9972	-5110	13757	497.2	60.029	11205.04
237	-9447	0	20.15298	-9945	-4690	13036	497.5	60.029	10995.41
238	-9450	0	20.15319	-9943	-5066	13566	497.3	60.02	11159.19
239	-9447	0	20.15319	-10045	-4704	13261	497.3	60.029	11091.87
240	-9447	0	20.15421	-9937	-4985	13334	497.1	60.04	11117.29
241	-9449	0	20.15462	-9976	-4743	13492	497.2	60.029	11046.11
242	-9448	0	20.15528	-9942	-4986	13125	497.1	60.029	11122.21
243	-9450	0	20.15507	-10016	-4789	13786	496.9	60.029	11102.02
244	-9447	0	20.15499	-9926	-4934	13066	497.4	60.029	11084.67
245	-9450	0	20.15499	-10084	-4992	13895	496.7	60.029	11251.98
246	-9449	0	20.15647	-9921	-4839	13053	497.5	60.029	11038.21
247	-9451	0	20.15618	-10039	-5102	13754	497	60.029	11261.08
248	-9447	0	20.15635	-9933	-4708	13088	497.5	60.02	10992.26
249	-9450	0	20.15635	-9927	-5066	13421	496.8	60.02	11144.94
250	-9447	0	20.157	-10055	-4709	13432	497.6	60.029	11103.05
251	-9448	0	20.1575	-9941	-5015	13256	497.7	60.029	11134.35
252	-9451	0	20.15832	-10050	-4853	13727	497.7	60.029	11160.38
253	-9446	0	20.15832	-9940	-5010	13060	497.8	60.02	11131.2
254	-9449	0	20.15869	-10022	-5030	13862	497.3	60.029	11213.45
255	-9450	0	20.15869	-10029	-4772	13125	497.9	60.029	11106.43
256	-9447	0	20.15979	-9982	-5158	13834	497.5	60.029	11235.89
257	-9450	0	20.15979	-9953	-4704	13091	497.5	60.04	11008.63
258	-9445	0	20.16078	-9961	-5173	13661	497.7	60.029	11224.15
259	-9448	0	20.16078	-9955	-4765	13243	497.7	60.02	11036.63
260	-9450	0	20.16185	-9940	-5113	13434	497.9	60.029	11177.94
261	-9446	0	20.16185	-10088	-4817	13639	497.6	60.029	11179.05
262	-9447	0	20.16226	-9938	-5057	13138	497.6	60.029	11150.65
263	-9449	0	20.16226	-10030	-4998	13871	497.4	60.029	11206.29
264	-9447	0	20.16259	-10029	-4940	13124	497.9	60.029	11179.64
265	-9447	0	20.16214	-10013	-5133	13911	497.6	60.029	11252.02
266	-9449	0	20.16259	-9935	-4892	13104	497.7	60.02	11074.11
267	-9447	0	20.16255	-10080	-5115	13780	497.6	60.02	11303.52
268	-9447	0	20.16398	-9931	-4717	13188	497.8	60.029	10994.31
269	-9448	0	20.16419	-9944	-5171	13530	497.3	60.02	11208.14

270	-9448	0	20.16501	-10019	-4834	13488	497.2	60	11124.2
271	-9449	0	20.1655	-9950	-5166	13311	497.7	60.029	11211.16
272	-9447	0	20.16612	-10121	-4920	13837	497.5	60.02	11253.49
273	-9448	0	20.16632	-9920	-5048	13089	497.7	60.02	11130.53
274	-9449	0	20.1671	-10097	-5102	14029	496.8	60.02	11312.82
275	-9448	0	20.1671	-9931	-4869	13075	497.6	60.02	11060.38
276	-9450	0	20.1671	-10078	-5189	13939	497	60	11335.42
277	-9448	0	20.1671	-9933	-4823	13091	497.5	60	11042
278	-9450	0	20.16751	-9942	-5247	13650	497.1	60.02	11241.64
279	-9447	0	20.16751	-9945	-4874	13244	497.9	60	11075.15
280	-9449	0	20.16841	-9948	-5183	13402	498	60.02	11217.23
281	-9449	0	20.16841	-10059	-4921	13658	497.6	60.02	11198.2
282	-9448	0	20.16924	-9910	-5124	13187	498	60	11156.32
283	-9450	0	20.16944	-10051	-5054	13900	497.7	60.02	11250.13
284	-9447	0	20.16985	-9943	-5086	13164	498.2	60.02	11168.29
285	-9450	0	20.16985	-9999	-5116	13862	497.5	60	11231.81
286	-9446	0	20.17084	-10037	-4959	13214	497.7	60.02	11195.22
287	-9448	0	20.17084	-9948	-5283	13811	497.5	60.02	11263.78
288	-9451	0	20.1708	-10003	-4925	13230	497.8	60	11149.69
289	-9445	0	20.1708	-9970	-5240	13566	497.7	60.02	11263.15
290	-9448	0	20.17182	-9968	-4933	13411	497.6	60.02	11121.85
291	-9450	0	20.17203	-9958	-5191	13367	497.4	60.02	11229.79
292	-9446	0	20.17309	-10013	-5014	13770	497.3	60.04	11198.23
293	-9449	0	20.17309	-9909	-5069	13129	497.6	60.029	11130.28
294	-9448	0	20.17355	-10123	-5167	13991	497.4	60.029	11365.43
295	-9448	0	20.17375	-9949	-4998	13150	497.7	60.029	11133.85
296	-9450	0	20.17371	-9984	-5287	13863	497.7	60.029	11297.46
297	-9447	0	20.17371	-10023	-4993	13237	497.6	60.029	11197.79
298	-9447	0	20.17474	-9945	-5299	13633	497.5	60.04	11268.65
299	-9450	0	20.17474	-9974	-4906	13313	497.5	60.029	11115.28
300	-9445	0	20.17535	-9959	-5297	13418	497.2	60.029	11280.07
301	-9448	0	20.17556	-9986	-5009	13622	497.6	60.029	11171.85
302	-9451	0	20.17638	-9942	-5204	13302	497.1	60.04	11221.63
303	-9446	0	20.17638	-10047	-5124	13995	497.1	60.029	11278.19
304	-9448	0	20.17699	-9952	-5028	13154	497.6	60.029	11150.03
305	-9447	0	20.17699	-10128	-5267	14019	497	60.029	11415.68
306	-9448	0	20.1774	-9942	-4995	13180	497.7	60.029	11126.25
307	-9449	0	20.1774	-10012	-5354	13846	497.1	60.029	11353.65
308	-9448	0	20.17863	-9946	-4910	13241	497.6	60.029	11091.93
309	-9450	0	20.17863	-9933	-5318	13566	496.9	60.04	11267.01
310	-9447	0	20.17946	-10069	-4970	13551	497.5	60.029	11228.79
311	-9448	0	20.17946	-9936	-5274	13285	497.7	60.029	11248.96
312	-9451	0	20.17946	-10023	-5113	13802	497.3	60.04	11251.81
313	-9446	0	20.17946	-9949	-5227	13224	497.5	60.029	11238.51
314	-9449	0	20.18069	-10037	-5250	13954	497.5	60.04	11327.13
315	-9448	0	20.18089	-9963	-5070	13204	497.7	60.06	11178.83
316	-9451	0	20.18192	-9983	-5362	13871	497.6	60.029	11331.87
317	-9447	0	20.18192	-10060	-4962	13242	497.6	60.029	11217.18
318	-9446	0	20.18253	-9962	-5345	13718	497.1	60.04	11305.33
319	-9451	0	20.18274	-9971	-4917	13409	497	60.029	11117.45
320	-9446	0	20.18315	-9938	-5310	13477	497.3	60.04	11267.65
321	-9449	0	20.18315	-10004	-5071	13682	497	60.029	11215.84
322	-9450	0	20.18438	-10047	-5240	13397	497.1	60.029	11331.36

323	-9445	0	20.18438	-10057	-5217	13965	497.3	60.029	11329.62
324	-9449	0	20.18479	-9929	-5144	13224	497.7	60.04	11182.39
325	-9447	0	20.185	-10131	-5331	14065	497	60.029	11448
326	-9448	0	20.185	-9952	-5005	13193	497.1	60.029	11139.67
327	-9450	0	20.185	-9967	-5379	13767	496.9	60.029	11325.84
328	-9447	0	20.18602	-9951	-5004	13276	497	60.029	11138.33
329	-9449	0	20.18602	-9950	-5362	13582	497.2	60.029	11302.81
330	-9447	0	20.18664	-10056	-4989	13600	497.3	60.02	11225.56
331	-9450	0	20.18684	-9946	-5333	13414	497	60.029	11285.56
332	-9445	0	20.18746	-10028	-5165	13885	497.1	60.029	11279.98
333	-9449	0	20.18746	-9961	-5255	13339	497.2	60.02	11262.17
334	-9450	0	20.18828	-10138	-5314	14098	497.3	60.029	11446.29
335	-9448	0	20.18869	-9932	-5078	13227	497.1	60.029	11154.85
336	-9448	0	20.18951	-10118	-5428	14013	497.1	60.02	11482.03
337	-9449	0	20.18972	-9940	-5074	13237	497.3	60.02	11160.16
338	-9448	0	20.19054	-10057	-5443	13847	497.2	60.029	11435.45
339	-9448	0	20.19054	-9955	-5052	13389	497.5	60.02	11163.54
340	-9451	0	20.19115	-9949	-5426	13506	497.6	60.02	11332.43
341	-9447	0	20.19115	-9997	-5117	13706	497.6	60.029	11230.48
342	-9450	0	20.19115	-9923	-5299	13309	497.3	60.029	11249.24
343	-9447	0	20.19115	-10175	-5252	14081	497.4	60.029	11450.51
344	-9448	0	20.19197	-9936	-5188	13233	497.6	60.029	11208.9
345	-9450	0	20.19218	-10079	-5420	14042	497.6	60.02	11443.89
346	-9449	0	20.1928	-9937	-5117	13265	497.2	60.04	11177.1
347	-9450	0	20.1928	-10072	-5490	13920	497.4	60.029	11471.06
348	-9446	0	20.19341	-9950	-5077	13279	497.4	60.029	11170.43
349	-9449	0	20.19362	-9938	-5378	13547	497.6	60.029	11299.86
350	-9448	0	20.19444	-10082	-5136	13647	497.4	60.029	11314.82
351	-9449	0	20.19444	-9938	-5357	13415	497.8	60.02	11289.88
352	-9447	0	20.19505	-10147	-5226	14002	497.3	60.029	11413.71
353	-9448	0	20.19505	-9969	-5311	13307	497.3	60.02	11295.47
354	-9450	0	20.19628	-10063	-5377	14032	497.4	60	11409.47
355	-9447	0	20.19628	-9999	-5182	13324	497.6	60.02	11262.02
356	-9448	0	20.19711	-9995	-5512	13891	497.2	60.02	11414.12
357	-9451	0	20.19711	-9966	-5066	13283	497.3	60.02	11179.69
358	-9446	0	20.19711	-9983	-5510	13762	497.5	60	11402.65
359	-9450	0	20.19711	-9960	-5123	13409	497.7	60.02	11200.3
360	-9446	0	20.19813	-10036	-5425	13634	497.5	60.02	11408.41
361	-9449	0	20.19813	-10003	-5199	13691	497.6	60.02	11273.4
362	-9449	0	20.19834	-10064	-5377	13447	497.4	60	11410.36
363	-9448	0	20.19834	-10055	-5303	13992	497.5	60.02	11367.71
364	-9452	0	20.19936	-9965	-5258	13318	497.6	60.02	11267.11
365	-9447	0	20.19936	-10040	-5465	14048	497.8	59.99	11431
366	-9450	0	20.19957	-9972	-5146	13318	497.6	60.02	11221.5
367	-9446	0	20.19957	-9952	-5486	13822	497.4	60	11363.91
368	-9450	0	20.20059	-9962	-5096	13358	497.5	60	11189.76
369	-9446	0	20.201	-9960	-5513	13658	497.3	60	11383.97
370	-9449	0	20.20183	-9994	-5153	13611	497.4	60	11244.26
371	-9449	0	20.20183	-10077	-5417	13551	497.9	59.99	11440.71
372	-9447	0	20.20183	-10030	-5265	13945	497.9	60.02	11327.89
373	-9451	0	20.20183	-9971	-5325	13369	498.2	60.02	11303.83
374	-9447	0	20.20203	-10060	-5380	14032	495.9	60	11408.24
375	-9450	0	20.20244	-9972	-5176	13307	495.9	60.02	11235.29

376	-9447	0	20.20388	-10022	-5478	13964	496.1	60	11421.43
377	-9451	0	20.20388	-9977	-5127	13354	496	59.99	11217.25
378	-9447	0	20.20388	-9941	-5481	13724	496.3	60	11351.87
379	-9450	0	20.20429	-9966	-5132	13470	496.2	60.02	11209.75
380	-9446	0	20.20552	-10055	-5430	13616	496.5	60.02	11427.51
381	-9447	0	20.20573	-10012	-5196	13828	495.9	60.02	11280.01
382	-9450	0	20.20614	-9970	-5323	13360	495.8	60	11302
383	-9445	0	20.20614	-10106	-5304	14033	496.2	60.02	11413.31
384	-9449	0	20.20696	-9952	-5274	13322	496.1	60	11263.1
385	-9446	0	20.20716	-10137	-5452	14110	495.8	59.99	11510.13
386	-9449	0	20.20778	-9929	-5166	13266	496.1	60.02	11192.52
387	-9448	0	20.20778	-10072	-5525	13923	495.7	60	11487.85
388	-9449	0	20.20778	-9952	-5119	13293	496	60.02	11191.36
389	-9449	0	20.20778	-10045	-5482	13676	496.1	60.02	11443.53
390	-9448	0	20.2086	-9993	-5154	13583	495.7	60	11243.83
391	-9451	0	20.2086	-9969	-5418	13457	495.6	60	11346.17
392	-9446	0	20.21024	-10040	-5269	13859	495.9	60	11338.6
393	-9451	0	20.21045	-9961	-5323	13308	495.9	60	11294.06
394	-9445	0	20.21106	-10103	-5397	14044	496	60	11454.18
395	-9448	0	20.21106	-9974	-5198	13318	495.7	60	11247.22
396	-9448	0	20.21106	-9974	-5198	13318	495.7	60	11247.22
399	-9451	0	20.21307	-9971	-5133	13224	496	60	11214.66
400	-79951	0	20.21307	-28067	-4239	41198	496.2	59.99	28385.31
401	-79843	0	20.2143	-83156	-4288	83566	477.1	60	83266.48
402	-79546	0	20.2143	-82890	-4311	83460	476.7	59.99	83002.03
403	-79278	0	20.2143	-82570	-4133	83014	476.9	60	82673.37
404	-79033	0	20.2143	-82402	-4312	83039	477	60.02	82514.74
405	-78793	0	20.21533	-82041	-3999	82508	476.8	60.02	82138.41
406	-78602	0	20.21595	-81856	-4314	82496	476.9	60.02	81969.6
407	-78432	0	20.2221	-81648	-4017	82129	476.8	60	81746.76
408	-78278	0	20.22231	-81532	-4253	82034	477.1	60	81642.85
409	-78139	0	20.22986	-81320	-4086	81841	476.8	60.02	81422.59
410	-78001	0	20.23109	-81204	-4256	81680	477	59.99	81315.45
411	-77892	0	20.23729	-81063	-4212	81676	476.7	60.02	81172.35
412	-77794	0	20.23811	-80948	-4211	81408	476.9	59.99	81057.46
413	-77705	0	20.2496	-80896	-4287	81543	476.6	60	81009.51
414	-77626	0	20.25022	-80808	-4062	81258	477.1	59.99	80910.03
415	-77547	0	20.25781	-80723	-4326	81370	476.8	59.99	80838.83
416	-77487	0	20.25863	-80564	-4042	81028	476.9	59.99	80665.33
417	-77431	0	20.25904	-80594	-4286	81208	476.5	59.99	80707.88
418	-77382	0	20.25945	-80483	-4056	80984	476.9	60.02	80585.14
419	-77334	0	20.26664	-80509	-4281	81021	477.1	60	80622.74
420	-77290	0	20.26725	-80370	-4177	80933	477	60	80478.47
421	-77257	0	20.27772	-80356	-4216	80836	477	60.02	80466.52
422	-77224	0	20.27834	-80327	-4283	80984	476.8	59.99	80441.1
423	-77199	0	20.28552	-80299	-4111	80765	477.1	60	80404.16
424	-77174	0	20.28593	-80290	-4286	80921	477.3	59.99	80404.32
425	-77144	0	20.29291	-80284	-4042	80750	477.2	59.99	80385.69
426	-77126	0	20.29352	-80187	-4368	80801	477.1	59.99	80305.88
427	-77113	0	20.30444	-80166	-4057	80640	477.2	59.99	80268.59
428	-77097	0	20.30506	-80207	-4295	80772	477.1	60	80321.91
429	-77082	0	20.31265	-80182	-4099	80733	476.9	59.99	80286.7
430	-77064	0	20.31368	-80204	-4254	80697	476.9	60	80316.74

431	-77049	0	20.3202	-80181	-4246	80804	476.8	60	80293.35
432	-77039	0	20.32082	-80077	-4214	80555	476.6	60	80187.8
433	-77034	0	20.32143	-80105	-4330	80744	477.2	59.959	80221.94
434	-77028	0	20.32184	-80083	-4071	80534	477.3	60.02	80186.41
435	-77022	0	20.32821	-80089	-4322	80741	476.8	59.99	80205.53
436	-77018	0	20.32903	-80066	-4050	80540	477.2	60.02	80168.37
437	-77012	0	20.33949	-80077	-4346	80683	476.7	60	80194.85
438	-77008	0	20.34011	-80062	-4091	80551	477.3	60	80166.45
439	-77002	0	20.34705	-80083	-4274	80607	477.1	59.99	80196.97
440	-76997	0	20.34807	-80084	-4187	80680	477.2	60	80193.38
441	-76993	0	20.3553	-80076	-4231	80553	477.3	60	80187.7
442	-76988	0	20.35591	-80085	-4303	80751	477.3	60	80200.52
443	-76983	0	20.36626	-80087	-4152	80563	477	60.02	80194.56
444	-76978	0	20.36728	-80117	-4333	80769	476.8	60.02	80234.09
445	-76971	0	20.37402	-80068	-4063	80531	477	60	80171.02
446	-76965	0	20.37422	-80094	-4342	80725	477.2	59.99	80211.61
447	-76961	0	20.38284	-80060	-4060	80553	477	60.02	80162.88
448	-76956	0	20.38366	-80083	-4315	80641	477.4	60	80199.17
449	-76951	0	20.38407	-80090	-4130	80616	476.9	60.02	80196.42
450	-76951	0	20.38469	-79960	-4256	80444	477.5	60	80073.19
451	-76950	0	20.39372	-80070	-4257	80690	477.4	60.02	80183.08
452	-76952	0	20.39433	-79977	-4186	80453	477.8	60.02	80086.47
453	-76950	0	20.40152	-80105	-4307	80765	476.8	60.02	80220.7
454	-76952	0	20.40234	-79962	-4103	80415	477.2	60	80067.2
455	-76951	0	20.40891	-80107	-4340	80767	476.9	59.99	80224.48
456	-76950	0	20.40952	-79968	-4042	80425	477.4	59.99	80070.09
457	-76951	0	20.41752	-80084	-4349	80684	477.4	59.99	80202
458	-76951	0	20.41835	-79942	-4084	80442	477.2	60.02	80046.25
459	-76950	0	20.42902	-80061	-4289	80578	477.3	60	80175.8
460	-76951	0	20.42963	-79937	-4178	80531	477	60	80046.11
461	-76950	0	20.43661	-80073	-4248	80562	477.6	60.02	80185.6
462	-76951	0	20.43764	-79976	-4287	80636	477.1	60	80090.82
463	-76949	0	20.43805	-80071	-4129	80539	477.9	60.02	80177.39
464	-76951	0	20.43825	-79992	-4357	80666	477.7	60.02	80110.57
465	-76949	0	20.44601	-80064	-4062	80543	477.6	60.02	80166.98
466	-76952	0	20.44704	-79991	-4351	80632	477.7	60	80109.25
467	-76949	0	20.45529	-80090	-4044	80602	477.4	60.02	80192.03
468	-76950	0	20.45549	-80000	-4312	80573	477.6	60.02	80116.12
469	-76952	0	20.46325	-80067	-4069	80611	477.4	60	80170.33
470	-76949	0	20.46407	-79960	-4272	80462	477.3	60	80074.04
471	-76953	0	20.47146	-80045	-4248	80708	477.5	60.02	80157.64
472	-76949	0	20.47187	-80012	-4227	80494	477.7	60.02	80123.58
473	-76952	0	20.48168	-80117	-4308	80777	477.2	59.99	80232.74
474	-76949	0	20.4825	-79978	-4091	80437	477.3	59.99	80082.56
475	-76950	0	20.49075	-80088	-4322	80739	477.2	60	80204.53
476	-76952	0	20.49116	-79932	-4012	80406	477.3	60	80032.62
477	-76950	0	20.49732	-80084	-4330	80682	477.5	60.02	80200.97
478	-76951	0	20.49814	-79975	-4041	80497	476.8	60	80077.03
479	-76948	0	20.49855	-80028	-4277	80552	477.1	60	80142.21
480	-76953	0	20.49896	-79976	-4153	80552	477.1	60	80083.76
481	-76952	0	20.50635	-80081	-4220	80563	477.3	60	80192.11
482	-76949	0	20.50758	-80026	-4271	80659	477.1	59.99	80139.89
483	-76952	0	20.51829	-80081	-4101	80568	477.2	60	80185.94

484	-76948	0	20.5187	-80035	-4309	80692	477.2	59.99	80150.91
485	-76952	0	20.52634	-79957	-4018	80438	477.2	60	80057.89
486	-76951	0	20.52716	-80067	-4286	80700	477.1	59.959	80181.63
487	-76949	0	20.53348	-79969	-4019	80453	476.6	59.97	80069.93
488	-76952	0	20.5341	-80047	-4262	80610	477	59.97	80160.38
489	-76948	0	20.54456	-79983	-4071	80511	477	60	80086.54
490	-76952	0	20.54518	-80090	-4223	80594	476.8	60	80201.26
491	-76949	0	20.55154	-79988	-4206	80627	476.4	59.97	80098.51
492	-76952	0	20.55195	-80063	-4142	80549	477.1	59.97	80170.07
493	-76948	0	20.55914	-80012	-4253	80675	476.9	59.97	80124.95
494	-76952	0	20.55996	-80051	-4033	80520	477.2	59.97	80152.53
495	-76949	0	20.56078	-79985	-4296	80632	477.1	59.959	80100.29
496	-76952	0	20.56139	-80076	-4031	80547	476.8	59.97	80177.4
497	-76949	0	20.57272	-79991	-4282	80595	476.9	59.97	80105.53
498	-76953	0	20.57334	-80055	-4060	80591	477.2	59.97	80157.89
499	-76948	0	20.57863	-80032	-4224	80534	477.1	59.99	80143.39
500	-76953	0	20.57925	-79964	-4086	80566	476.8	59.97	80068.33
501	-76950	0	20.58635	-80084	-4167	80563	477.1	59.99	80192.34
502	-76952	0	20.58758	-79975	-4224	80642	476.7	59.97	80086.47
503	-76950	0	20.59497	-80061	-4066	80542	477.7	60	80164.18
504	-76951	0	20.59517	-79986	-4252	80642	477.1	59.97	80098.94
505	-76949	0	20.60568	-80072	-3983	80540	477.2	60	80171
506	-76953	0	20.60691	-79973	-4283	80613	477.2	59.99	80087.61
507	-76950	0	20.61414	-80079	-4010	80574	477.6	59.99	80179.34
508	-76951	0	20.61496	-79983	-4258	80519	477	60	80096.26
509	-76949	0	20.61557	-80056	-4041	80610	477.1	59.99	80157.92
510	-76951	0	20.61598	-79960	-4185	80458	477	59.99	80069.44
511	-76949	0	20.62235	-80073	-4199	80713	476.8	59.99	80183.02
512	-76952	0	20.62317	-79950	-4114	80430	476.9	59.99	80055.78
513	-76949	0	20.63347	-80110	-4240	80778	477.1	59.97	80222.13
514	-76953	0	20.63409	-79942	-4002	80404	476.9	59.99	80042.11
515	-76952	0	20.64045	-80081	-4201	80736	477.1	59.99	80191.12
516	-76950	0	20.64086	-79966	-3940	80432	476.9	59.97	80063
517	-76952	0	20.64898	-80084	-4245	80685	476.8	59.99	80196.43
518	-76949	0	20.65001	-79985	-3983	80472	477.4	59.99	80084.11
519	-76952	0	20.66043	-80067	-4145	80582	477	59.97	80174.22
520	-76950	0	20.66146	-79965	-4145	80561	477.2	59.99	80072.36
521	-76953	0	20.66828	-80039	-4099	80526	477.1	59.97	80143.89
522	-76949	0	20.66869	-80053	-4170	80692	477.5	59.97	80161.54
523	-76952	0	20.67591	-80094	-4035	80560	477.1	59.99	80195.57
524	-76952	0	20.67673	-80001	-4247	80644	477.4	59.97	80113.65
525	-76951	0	20.67735	-80051	-3912	80518	477.3	60	80146.53
526	-76950	0	20.67796	-79979	-4230	80619	477.6	59.97	80090.78
527	-76952	0	20.68392	-80049	-4011	80545	477.4	60	80149.43
528	-76951	0	20.68474	-79974	-4237	80492	477.2	59.99	80086.16
529	-76950	0	20.69573	-80064	-4050	80606	477.5	60	80166.37
530	-76951	0	20.69594	-79949	-4161	80436	477.9	60.02	80057.21
531	-76950	0	20.70234	-80080	-4167	80735	477.6	60.029	80188.34
532	-76952	0	20.70337	-79940	-4049	80426	477.6	60	80042.48
533	-76951	0	20.71101	-80063	-4214	80733	477.6	60.02	80173.82
534	-76950	0	20.71142	-79968	-3937	80435	478.1	60.02	80064.85
535	-76952	0	20.72102	-80093	-4205	80742	477.6	60	80203.31
536	-76949	0	20.72164	-79982	-4002	80479	477.7	60.02	80082.06

2137	-96452	0	26.97402	-100014	-2677	100279	473.1	60.04
2138	-96451	0	26.97807	-99915	-2934	100290	472.7	60.04
2139	-96455	0	26.98285	-100002	-2637	100257	472.7	60.069
2140	-96454	0	26.98757	-100012	-2920	100359	472.2	60.09
2141	-96456	0	26.99311	-100022	-2679	100307	472.4	60.06
2142	-96454	0	26.99886	-100025	-2884	100331	472.2	60.069
2143	-96452	0	27.00425	-100007	-2753	100376	472.3	60.069
2144	-96451	0	27.00861	-100010	-2836	100299	472.3	60.06
2145	-96452	0	27.01313	-99916	-2904	100322	472.2	60.06
2146	-96452	0	27.01703	-100000	-2740	100288	472.5	60.06
2147	-96449	0	27.02251	-100047	-2932	100423	472.8	60.029
2148	-96454	0	27.02785	-99898	-2692	100187	472.8	60.06
2149	-96455	0	27.03154	-99998	-2872	100371	472.8	60.069
2150	-96455	0	27.04037	-100009	-2705	100305	472.7	60.069
2151	-96452	0	27.04098	-100029	-2869	100351	472.9	60.06
2152	-96450	0	27.04652	-99916	-2742	100259	473.3	60.069
2153	-96453	0	27.05222	-100008	-2886	100311	472.9	60.06
2154	-96452	0	27.05735	-100013	-2886	100415	472.7	60.029
2155	-96451	0	27.06192	-99999	-2776	100298	472.8	60.04
2156	-96450	0	27.06541	-100038	-3093	100444	472.8	60.029
2157	-96454	0	27.06951	-99992	-2722	100280	472.7	60.069
2158	-96452	0	27.07526	-100034	-3132	100418	472.6	60.06
2159	-96451	0	27.07977	-100034	-2656	100307	472.6	60.06
2160	-96449	0	27.08531	-99958	-3039	100306	473.2	60.06
2161	-96452	0	27.08988	-100044	-2832	100351	473	60.069
2162	-96450	0	27.09029	-100038	-3071	100363	473.2	60.06
2163	-96453	0	27.10003	-99920	-2969	100278	473	60.069
2164	-96453	0	27.10599	-100017	-2985	100314	473.2	60.06
2165	-96452	0	27.10942	-100014	-3064	100429	472.9	60.06
2166	-96451	0	27.11393	-99954	-2880	100215	473	60.06
2167	-96449	0	27.11845	-100056	-3051	100443	472.9	60.06
2168	-96454	0	27.12461	-99912	-2799	100191	472.8	60.069
2169	-96453	0	27.12845	-100036	-3206	100421	472.3	60.04
2170	-96451	0	27.12927	-100034	-2852	100329	472.6	60.04
2171	-96451	0	27.13882	-99933	-3146	100271	473.1	60.04
2172	-96452	0	27.13923	-100008	-2959	100337	472.9	60.069
2173	-96450	0	27.14826	-99963	-3083	100242	473.1	60.06
2174	-96453	0	27.15489	-100004	-3098	100400	472.9	60.069
2175	-96451	0	27.15817	-99999	-2879	100298	473.4	60.06
2176	-96449	0	27.15838	-99953	-3165	100358	472.9	60.06
2177	-96452	0	27.16737	-100058	-2981	100327	473.2	60.069
2178	-96450	0	27.1725	-100018	-3204	100416	472.8	60.04
2179	-96451	0	27.17634	-100027	-2819	100305	473.4	60.069
2180	-96450	0	27.18368	-99938	-3220	100321	472.9	60.069
2181	-96454	0	27.18716	-100023	-3005	100320	472.7	60.06
2182	-96451	0	27.19271	-100030	-3151	100338	472.4	60.09
2183	-96454	0	27.19696	-99925	-3147	100303	472.8	60.069
2184	-96451	0	27.2025	-100021	-3064	100328	472.6	60.069
2185	-96450	0	27.20681	-100065	-3167	100485	472.8	60.04
2186	-96455	0	27.21256	-99938	-3073	100229	473.1	60.069
2187	-96454	0	27.21523	-100041	-3160	100443	472.8	60.04
2188	-96451	0	27.21625	-100023	-2999	100304	472.4	60.069
2189	-96451	0	27.22482	-99932	-3206	100325	472.5	60.04

2190	-96454	0	27.23138	-100015	-3011	100313	471.9	60.069
2191	-96451	0	27.23426	-100028	-3224	100371	472.6	60.09
2192	-96450	0	27.24205	-99968	-3050	100303	472.3	60.069
2193	-96453	0	27.24663	-100025	-3216	100342	471.7	60.06
2194	-96451	0	27.25222	-100047	-3292	100448	472.3	60.06
2195	-96451	0	27.25469	-99925	-3115	100230	471.6	60.09
2196	-96453	0	27.26023	-100022	-3346	100433	471.9	60.06
2197	-96452	0	27.26275	-99996	-3038	100288	471.6	60.069
2198	-96451	0	27.27013	-100053	-3266	100433	471.6	60.04
2199	-96450	0	27.27336	-99971	-3028	100259	471.1	60.09
2200	-96454	0	27.28105	-100041	-3174	100402	471.6	60.069
2201	-96451	0	27.28366	-100047	-3085	100353	472.5	60.069
2202	-96450	0	27.29316	-99973	-3284	100307	472	60.06
2203	-96454	0	27.29392	-100032	-3209	100434	471.9	60.069
2204	-96452	0	27.29993	-100017	-3228	100314	472.1	60.06
2205	-96451	0	27.30219	-100047	-3300	100475	471.7	60.06
2206	-96449	0	27.30834	-99956	-3138	100251	471.8	60.06
2207	-96454	0	27.31168	-100055	-3283	100440	471.9	60.06
2208	-96451	0	27.31851	-100041	-3114	100334	471.6	60.06
2209	-96450	0	27.32118	-99979	-3408	100350	472	60.04
2210	-96452	0	27.32898	-100066	-3092	100362	471.4	60.06
2211	-96449	0	27.33232	-100040	-3272	100344	472	60.06
2212	-96453	0	27.33273	-100041	-3228	100380	471.6	60.06
2213	-96451	0	27.34212	-100061	-3428	100374	471.8	60.04
2214	-96451	0	27.34915	-99949	-3212	100362	471.7	60.02
2215	-96454	0	27.3512	-100033	-3346	100344	471.5	60.029
2216	-96452	0	27.35838	-100073	-3408	100500	471.8	60.04
2217	-96451	0	27.36059	-99968	-3131	100256	472.2	60.04
2218	-96454	0	27.36674	-100039	-3326	100413	472.7	60.029
2219	-96452	0	27.369	-100044	-3135	100337	471.9	60.04
2220	-96451	0	27.37742	-100033	-3263	100385	472.3	60.06
2221	-96450	0	27.38008	-99999	-3192	100305	472	60.04
2222	-96452	0	27.38111	-100072	-3450	100375	472.3	60.029
2223	-96450	0	27.39131	-99963	-3340	100338	471.8	60.04
2224	-96454	0	27.3985	-100049	-3384	100353	472	60.029
2225	-96454	0	27.40014	-100074	-3428	100499	471.7	60.04
2226	-96452	0	27.40076	-100050	-3115	100312	471.9	60.04
2227	-96450	0	27.40902	-99975	-3500	100385	471.6	60.029
2228	-96453	0	27.41805	-100032	-3268	100314	471.5	60.04
2229	-96453	0	27.4182	-100018	-3540	100409	471.6	60
2230	-96452	0	27.426	-100047	-3291	100346	472	60.069
2231	-96451	0	27.42867	-100017	-3524	100359	472	60.029
2232	-96451	0	27.42969	-99958	-3312	100311	471.9	60.029
2233	-96451	0	27.43908	-100024	-3510	100337	472.2	60.04
2234	-96451	0	27.43949	-100017	-3442	100416	471.7	60.06
2235	-96451	0	27.44785	-100033	-3384	100339	472.2	60.04
2236	-96450	0	27.44826	-100033	-3549	100459	472	60.04
2237	-96454	0	27.45611	-100040	-3331	100330	472.4	60.069
2238	-96453	0	27.45714	-100044	-3589	100456	472	60.029
2239	-96452	0	27.46649	-100042	-3266	100321	472.4	60.06
2240	-96451	0	27.47341	-100068	-3615	100456	472.2	60.04
2241	-96451	0	27.47546	-100000	-3248	100324	472.2	60.029
2242	-96450	0	27.48311	-99973	-3499	100272	472.5	60.069

2243	-96454	0	27.48666	-100046	-3491	100439	472.4	60.06
2244	-96453	0	27.49425	-100058	-3464	100359	472.2	60.04
2245	-96453	0	27.4961	-100057	-3593	100494	472.2	60.069
2246	-96450	0	27.50369	-100060	-3300	100334	472.5	60.04
2247	-96451	0	27.50574	-99980	-3568	100392	471.8	60.04
2248	-96453	0	27.51169	-100057	-3362	100356	472.5	60.06
2249	-96452	0	27.51416	-100047	-3337	100349	472.6	60.069
2250	-96452	0	27.52154	-100016	-3340	100340	472.9	60.06
2251	-96450	0	27.52339	-100053	-3590	100407	472.4	60.069
2252	-96455	0	27.53207	-99913	-3458	100281	472.5	60.06
2253	-96456	0	27.53447	-100031	-3584	100348	472	60.06
2254	-96454	0	27.54494	-100006	-3576	100417	472.3	60.06
2255	-96455	0	27.5455	-100033	-3515	100342	471.9	60.069
2256	-96454	0	27.54632	-100051	-3679	100452	472.3	60.029
2257	-96454	0	27.55488	-100013	-3403	100312	471.9	60.069
2258	-96454	0	27.56166	-100014	-3709	100422	472.3	60.04
2259	-96454	0	27.56371	-100000	-3428	100307	472	60.069
2260	-96454	0	27.57104	-100025	-3663	100410	472.3	60.069
2261	-96455	0	27.57315	-100006	-3510	100321	472.4	60.06
2262	-96453	0	27.58054	-100035	-3677	100344	472.2	60.06
2263	-96453	0	27.58321	-100030	-3626	100417	472.5	60.069
2264	-96454	0	27.58403	-100027	-3642	100331	472.2	60.06
2265	-96454	0	27.59435	-100026	-3669	100450	472.4	60.06
2266	-96454	0	27.59455	-100041	-3520	100336	472.4	60.06
2267	-96454	0	27.60364	-100039	-3814	100444	472.4	60.069
2268	-96455	0	27.60425	-100018	-3472	100316	472.4	60.09
2269	-96456	0	27.61235	-100041	-3836	100419	472.6	60.099
2270	-96457	0	27.61979	-100021	-3466	100319	472.2	60.069
2271	-96457	0	27.62185	-100030	-3768	100366	472.1	60.069
2272	-96457	0	27.62246	-100027	-3594	100376	472.1	60.09
2273	-96458	0	27.63129	-100023	-3661	100321	472.4	60.069
2274	-96459	0	27.63914	-100015	-3770	100430	472.3	60.06
2275	-96460	0	27.64114	-99998	-3492	100300	472.3	60.09
2276	-96460	0	27.64914	-100002	-3717	100413	471.4	60.069
2277	-96459	0	27.65078	-100018	-3446	100307	472.6	60.06
2278	-96461	0	27.6594	-100023	-3842	100410	471.7	60.06
2279	-96462	0	27.66105	-100010	-3515	100314	471.8	60.04
2280	-96462	0	27.66166	-100025	-3780	100384	471.8	60.069
2281	-96463	0	27.66967	-100042	-3583	100359	471.7	60.06
2282	-96463	0	27.67008	-100018	-3670	100320	472	60.069
2283	-96464	0	27.6789	-100002	-3712	100388	471.7	60.069
2284	-96466	0	27.67972	-100007	-3652	100307	471.4	60.06
2285	-96468	0	27.68978	-100011	-3803	100442	471.9	60.06
2286	-96469	0	27.69799	-100007	-3481	100294	471.7	60.06
2287	-96470	0	27.69881	-100027	-3865	100439	472.2	60.069
2288	-96471	0	27.69984	-100049	-3561	100359	471.9	60.04
2289	-96472	0	27.70922	-100015	-3838	100399	472.2	60.029
2290	-96475	0	27.70984	-100015	-3593	100330	472.3	60.06
2291	-96475	0	27.71749	-100026	-3799	100363	472.3	60.04
2292	-96475	0	27.71769	-100014	-3690	100378	471.9	60.06
2293	-96477	0	27.72693	-100017	-3718	100330	472.1	60.069
2294	-96477	0	27.72836	-100019	-3823	100448	471.9	60.029
2295	-96480	0	27.73821	-100023	-3759	100330	472	60.06

2296	-96481	0	27.73883	-100006	-3893	100444	471.5	60.06
2297	-96483	0	27.74807	-100019	-3640	100317	472.4	60.04
2298	-96484	0	27.75607	-100038	-3908	100449	471.5	60.02
2299	-96486	0	27.75756	-100013	-3561	100315	472.3	60.06
2300	-96487	0	27.75797	-99996	-3887	100388	471.9	60.06
2301	-96488	0	27.767	-100018	-3635	100349	472.2	60.06
2302	-96488	0	27.77516	-100015	-3847	100351	472.1	60.04
2303	-96490	0	27.77715	-100007	-3807	100398	471.9	60.06
2304	-96491	0	27.77777	-100033	-3713	100351	472.3	60.06
2305	-96491	0	27.7865	-100041	-3926	100481	472	60.04
2306	-96492	0	27.79486	-100045	-3777	100337	471.8	60.04
2307	-96493	0	27.79542	-100027	-3976	100449	472.3	60.02
2308	-96495	0	27.79603	-100022	-3607	100299	472	60.04
2309	-96497	0	27.80583	-99997	-3967	100402	471.8	60.029
2310	-96501	0	27.80644	-100008	-3724	100324	472.1	60.06
2311	-96502	0	27.81471	-100012	-3973	100374	472	60.06
2312	-96502	0	27.81594	-100013	-3782	100385	471.8	60.06
2313	-96503	0	27.82415	-100045	-3899	100367	472.4	60.029
2314	-96505	0	27.82456	-100018	-3968	100442	471.6	60.06
2315	-96507	0	27.83262	-100032	-3770	100349	471.5	60.04
2316	-96509	0	27.83344	-100045	-3998	100474	472	60.029
2317	-96511	0	27.84329	-100046	-3733	100347	472.1	60.06
2318	-96513	0	27.84432	-100032	-3927	100435	471.8	60.029
2319	-96516	0	27.85417	-100017	-3710	100319	472	60.029
2320	-96518	0	27.85499	-100035	-3978	100416	472.4	60.069
2321	-96520	0	27.86279	-100019	-3755	100348	472.2	60.06
2322	-96522	0	27.863	-100024	-3944	100366	471.9	60.04
2323	-96526	0	27.87229	-100017	-3920	100448	472	60.029
2324	-96529	0	27.88193	-99996	-4095	100441	472.5	60.04
2325	-96531	0	27.88346	-100019	-4032	100469	472.1	60.06
2326	-96533	0	27.88346	-100011	-3819	100324	471.9	60.06
2327	-96535	0	27.89229	-100056	-4086	100489	472.7	60.06
2328	-96535	0	27.89311	-100000	-3753	100312	472.6	60.04
2329	-96538	0	27.90255	-100006	-4073	100414	472.7	60.069
2330	-96540	0	27.90337	-100023	-3780	100363	472.8	60.06
2331	-96541	0	27.91158	-99998	-3974	100367	472.2	60.09
2332	-96543	0	27.9124	-100005	-3948	100388	473	60.09
2333	-96546	0	27.92199	-99981	-3982	100325	472.3	60.09
2334	-96550	0	27.92363	-100009	-4029	100450	472.8	60.069
2335	-96547	0	27.93087	-100058	-3929	100373	472.6	60.04
2336	-96549	0	27.93128	-100014	-4117	100452	472.7	60.029
2337	-96549	0	27.94031	-100093	-3824	100415	472.1	60.04
2338	-96543	0	27.94093	-100026	-4138	100440	472.3	60.029
2339	-96546	0	27.95001	-99999	-3837	100302	472.2	60.04
2340	-96547	0	27.95022	-99977	-4037	100341	472.1	60.04
2341	-96549	0	27.95951	-99979	-3874	100307	472.2	60.029
2342	-96548	0	27.96115	-100116	-4070	100440	472.2	60.04
2343	-96546	0	27.97054	-99999	-4049	100393	472	60.04
2344	-96550	0	27.97177	-99991	-4035	100299	472.2	60.02
2345	-96547	0	27.97998	-100094	-4109	100526	472	60.04
2346	-96548	0	27.98039	-100021	-3897	100325	472.5	60.069
2347	-96550	0	27.98778	-100004	-4108	100436	472.8	60.06
2348	-96546	0	27.98819	-99999	-3829	100312	472.6	60.06

2349	-96550	0	27.99763	-99981	-4046	100364	472.3	60.06
2350	-96547	0	27.99845	-100068	-3869	100380	472.4	60.029
2351	-96549	0	28.00757	-99997	-4107	100358	472.7	60.06
2352	-96550	0	28.01598	-100072	-3998	100444	472.4	60.04
2353	-96548	0	28.01722	-99982	-4014	100300	472.8	60.04
2354	-96548	0	28.01722	-99982	-4014	100300	472.8	60.04
2357	-96550	0	28.04568	-100103	-4085	100423	472.7	60.04
2358	0	0	28.04651	-78922	-4836	75841	481.1	60.04
2359	0	0	28.04733	-226	-5674	8490	502.7	60.04
2360	0	0	28.05554	-199	-5480	8363	502.6	60.06
2361	0	0	28.05615	-248	-5608	8328	502.8	60.029
2362	0	0	28.06518	-243	-5625	8718	502.6	60.06
2363	0	0	28.06641	-199	-5516	8083	502.6	60.06
2364	0	0	28.0714	-264	-5724	8896	502.4	60.069
2365	0	0	28.0714	-201	-5497	8019	502.3	60.04
2366	0	0	28.0714	-237	-5733	8883	502.1	60.04
2367	0	0	28.07119	-227	-5422	8105	502.5	60.06
2368	0	0	28.07099	-208	-5691	8660	502.4	60.04
2369	0	0	28.07099	-224	-5423	8305	502.8	60.04
2370	0	0	28.07058	-200	-5655	8532	502.6	60.04
2371	0	0	28.07058	-251	-5578	8598	502.8	60.06
2372	0	0	28.07037	-218	-5576	8266	502.7	60.04
2373	0	0	28.07037	-271	-5693	8904	502.2	60.069
2374	0	0	28.06996	-190	-5491	8018	502.7	60.069
2375	0	0	28.06996	-275	-5726	8934	502.5	60.06
2376	0	0	28.06955	-216	-5488	8066	502.7	60.04
2377	0	0	28.06955	-239	-5724	8854	502.8	60.06
2378	0	0	28.06929	-223	-5427	8191	502.8	60.069
2379	0	0	28.06929	-228	-5687	8639	502.6	60.06
2380	0	0	28.06908	-234	-5512	8460	503	60.06
2381	0	0	28.06908	-206	-5638	8419	502.6	60.069
2382	0	0	28.06826	-261	-5652	8804	502.5	60.04
2383	0	0	28.06806	-203	-5569	8205	502.5	60.04
2384	0	0	28.06806	-259	-5765	9001	502.7	60.06
2385	0	0	28.06806	-208	-5504	8143	502.6	60.09
2386	0	0	28.06785	-219	-5712	8994	502.7	60.069
2387	0	0	28.06785	-211	-5431	8265	502.5	60.069
2388	0	0	28.06744	-224	-5719	8953	502.6	60.09
2389	0	0	28.06744	-214	-5434	8448	502.8	60.069
2390	0	0	28.06682	-228	-5642	8600	502.7	60.06
2391	0	0	28.06662	-242	-5581	8778	502.9	60.06
2392	0	0	28.06621	-194	-5578	8479	502.5	60.069
2393	0	0	28.06621	-282	-5728	9163	502.8	60.06
2394	0	0	28.0658	-198	-5557	8361	502.6	60.069
2395	0	0	28.0658	-291	-5721	9130	502.8	60.09
2396	0	0	28.0658	-197	-5472	8387	502.8	60.04
2397	0	0	28.0658	-259	-5746	9096	502.8	60.09
2398	0	0	28.06559	-201	-5421	8345	502.9	60.06
2399	0	0	28.06559	-220	-5703	8794	502.9	60.06
2400	0	0	28.06553	-235	-5513	8675	503	60.04
2401	0	0	28.06553	-216	-5623	8530	502.9	60.04
2402	0	0	28.06492	-282	-5689	9141	502.7	60.069
2403	0	0	28.06492	-186	-5590	8422	502.7	60.06

2404	0	0	28.06471	-278	-5746	9351	502.4	60.04
2405	0	0	28.06471	-203	-5503	8290	502.7	60.06
2406	0	0	28.06451	-284	-5743	9141	502.4	60.04
2407	0	0	28.06451	-211	-5428	8279	502.3	60.04
2408	0	0	28.0643	-236	-5727	8915	502.6	60.04
2409	0	0	28.0641	-203	-5472	8498	502.6	60.06
2410	0	0	28.06389	-225	-5677	8660	502.6	60.029
2411	0	0	28.06389	-264	-5569	8911	502.7	60.04
2412	0	0	28.06369	-203	-5584	8565	502.5	60.04
2413	0	0	28.06369	-278	-5742	9329	502.4	60.029
2414	0	0	28.06369	-203	-5545	8413	502.6	60.04
2415	0	0	28.06369	-285	-5741	8858	502.7	60.04
2416	0	0	28.06369	-193	-5472	8333	502.8	60.04
2417	0	0	28.06369	-240	-5699	9108	502.6	60.04
2418	0	0	28.06348	-795	9083	11385	506.4	60.04
2419	0	0	28.06348	0	0	0	504	60.04
2420	0	0	28.06348	0	0	0	503.9	60.04
2421	0	0	28.06348	0	0	0	504	60.06
2422	0	0	28.06266	0	0	0	503.9	60.04
2423	0	0	28.06266	0	0	0	504	60.04
2424	0	0	28.06266	0	0	0	504.2	60.04
2425	0	0	28.06266	0	0	0	504.2	60.04
2426	0	0	0	0	0	0	0	0

Time [sec]	Battery Real Power [W]	Battery Reactive Power [VAr]	SOC [%]	Real Power [W]	Reactive Power [VAr]	Apparent Power [VA]	Average Voltage [V]	Frequency [Hz]	eff
0.0	0	0	27.938642	0	0	0	504.9	60.029	#DIV/0!
0.5	0	0	27.939158	0	0	0	503.6	60.029	
1.5	0	0	27.939043	0	0	0	503.9	60.029	
2.5	0	0	27.939248	0	0	0	503.6	60.04	
3.5	0	0	27.939306	0	0	0	503.8	60.04	
4.5	0	0	27.939306	0	0	0	504	60.029	
5.5	0	0	27.939248	0	0	0	504	60.029	
6.5	0	0	27.939248	0	0	0	503.9	60.029	
7.5	0	0	27.938648	0	0	0	503.8	60.029	
8.5	0	0	27.938041	0	0	0	503.7	60.029	
9.5	0	0	27.938041	0	0	0	503.8	60.029	
10.5	0	0	27.9385	0	0	0	504.2	60.029	
11.5	0	0	27.939158	0	0	0	504	60.029	
13.5	0	0	27.939158	0	0	0	504	60.029	
14.5	0	0	NaN	0	0	0	0	0	
15.5	0	0	NaN	0	0	0	0	0	
16.5	0	0	NaN	0	0	0	0	0	
17.5	0	0	NaN	0	0	0	0	0	
18.5	0	0	NaN	0	0	0	0	0	
19.5	0	0	NaN	0	0	0	0	0	
21.0	0	0	NaN	0	0	0	0	0	
21.5	0	0	27.938953	0	0	0	504.4	60.02	
22.5	-1850	0	27.938953	0	0	0	504.7	60.02	
23.5	-2350	0	27.93901	0	0	0	504.2	60.02	
24.5	-2850	0	27.938756	0	0	0	504.6	60.02	
25.5	-3350	0	27.938756	0	0	0	504.4	60.02	
26.5	-3850	0	27.938699	0	0	0	504.7	60.02	
27.5	-4350	0	27.938699	0	0	0	504.6	60.02	
28.5	-4913	0	27.939019	-3377	-3414	8834	504.6	60.02	1.454842
29.5	-4894	0	27.939019	-5325	-4351	9589	501.7	60.029	0.919061
30.5	-4865	0	27.939019	-5241	-4159	9150	501.8	60.02	0.928258
31.5	-4835	0	27.939019	-5195	-4405	9405	502.1	60.029	0.930703
32.5	-4817	0	27.938871	-5141	-3909	9011	501.7	60.02	0.936977
33.5	-4797	0	27.938871	-5100	-4425	9330	502.1	60.029	0.940588
34.5	-4777	0	27.938814	-5145	-4022	9079	502.2	60.029	0.928474
35.5	-4756	0	27.938642	-5132	-4337	9319	502	60.04	0.926734
36.5	-4738	0	27.938642	-5087	-4142	9273	501.8	60.02	0.931394
37.5	-4730	0	27.938814	-5010	-4281	9169	502	60.02	0.944112
38.5	-4721	0	27.938814	-5102	-4297	9419	502	60.029	0.925323
39.5	-4712	0	27.938814	-5035	-4258	9108	502.2	60.029	0.935849
40.5	-4702	0	27.939224	-5112	-4423	9417	502.1	60.04	0.919797
41.5	-4693	0	27.939167	-5054	-4113	8956	502.4	60.04	0.928571
43.5	-4693	0	27.939167	-5054	-4113	8956	502.4	60.04	0.928571
44.5	0	0	NaN	0	0	0	0	0	#DIV/0!
60.3	0	0	NaN	0	0	0	0	0	#DIV/0!
60.8	-4648	0	27.941276	-5082	-5800	10643	503.5	60.029	0.914601
61.5	0	0	27.941276	-3538	-5711	9436	503.7	60.029	0
62.5	0	0	27.942097	-167	-4611	8296	504.9	60.029	0
63.5	0	0	27.942097	-126	-4239	7928	505.1	60.02	0
64.5	0	0	27.942154	-145	-4605	8139	505.4	60.029	0
65.5	0	0	27.942211	-165	-4333	8096	505.4	60.029	0
66.5	0	0	27.942622	-151	-4488	8189	505.9	60.029	0
67.5	0	0	27.94245	-196	-4490	8338	505.3	60.02	0
68.5	0	0	27.942598	-152	-4443	7993	505.3	60.029	0
69.5	0	0	27.942598	-199	-4577	8389	504.9	60.029	0
70.5	0	0	27.942392	-173	-4357	7772	505.2	60.04	0
71.5	0	0	27.942679	-198	-4629	8280	505.1	60.04	0
72.5	0	0	27.942531	-145	-4230	7696	505.1	60.04	0
73.5	0	0	27.942359	-149	-4553	8005	505	60.029	0
74.5	0	0	27.942302	-155	-4326	7810	505.2	60.04	0
76.5	0	0	27.942302	-155	-4326	7810	505.2	60.04	0
77.5	0	0	NaN	0	0	0	0	0	#DIV/0!
78.5	0	0	NaN	0	0	0	0	0	#DIV/0!
79.5	0	0	NaN	0	0	0	0	0	#DIV/0!
80.5	0	0	NaN	0	0	0	0	0	#DIV/0!
81.5	0	0	NaN	0	0	0	0	0	#DIV/0!
82.5	0	0	NaN	0	0	0	0	0	#DIV/0!
83.5	0	0	NaN	0	0	0	0	0	#DIV/0!
84.5	0	0	NaN	0	0	0	0	0	#DIV/0!
85.5	0	0	NaN	0	0	0	0	0	#DIV/0!
86.5	0	0	NaN	0	0	0	0	0	#DIV/0!
91.0	0	0	NaN	0	0	0	0	0	#DIV/0!
91.5	0	0	27.940307	-126	-4539	7795	503.3	60.02	0
92.5	-4921	0	27.940102	-1665	-4205	8024	502.8	60.029	2.955556
93.5	-4916	0	27.940102	-5182	-4626	9436	502.2	60.02	0.948668
94.5	-4886	0	27.939988	-5257	-4203	9234	501.8	60.029	0.929427
95.5	-4855	0	27.939988	-5195	-4448	9336	501.8	60.02	0.934552
96.5	-4827	0	27.940102	-5188	-4372	9400	501.8	60.029	0.930416

97.5	-4809	0	27.940102	-5083	-4511	9266	502.5	60.029	0.946095
98.5	-4788	0	27.940102	-5214	-4492	9552	502	60.029	0.918297
99.5	-4769	0	27.940102	-5133	-4426	9251	502.7	60.029	0.929086
100.5	-4749	0	27.940307	-5183	-4640	9583	502.3	60.029	0.916265
101.5	-4736	0	27.940479	-5046	-4314	9060	502.1	60.029	0.938565
102.5	-4727	0	27.940685	-5015	-4672	9468	502.6	60.04	0.942572
103.5	-4719	0	27.940455	-5043	-4205	9084	502.3	60.029	0.935753
104.5	-4710	0	27.940455	-5010	-4617	9364	502.6	60.029	0.94012
105.5	-4700	0	27.940685	-5070	-4322	9219	501.6	60.029	0.927022
106.5	-4691	0	27.941505	-5019	-4499	9256	502.5	60.029	0.934648
107.5	-4681	0	27.941333	-5082	-4466	9459	502.4	60.02	0.921094
425.3	0	0	0	0	0	0	0	0	#DIV/0!
425.8	0	0	27.936237	0	0	0	503	60	#DIV/0!
426.5	-4948	0	27.936237	0	0	0	502.6	60.02	#DIV/0!
427.5	-5248	0	27.936237	0	0	0	502.9	60	#DIV/0!
428.5	-5748	0	27.936237	0	0	0	502.9	60.02	#DIV/0!
429.5	-6298	0	27.936237	0	0	0	502.6	59.99	#DIV/0!
430.5	-6748	0	27.936237	0	0	0	502.6	59.99	#DIV/0!
431.5	-7298	0	27.936237	0	0	0	502.6	60	#DIV/0!
432.5	-7848	0	27.936237	0	0	0	503.1	60	#DIV/0!
434.5	-7848	0	27.936237	0	0	0	503.1	60	#DIV/0!
435.5	0	0	NaN	0	0	0	0	0	#DIV/0!
436.5	0	0	NaN	0	0	0	0	0	#DIV/0!
438.5	0	0	NaN	0	0	0	0	0	#DIV/0!
439.0	-8246	0	27.936237	-8988	-3923	11712	499.2	60	0.917445
439.5	0	0	27.936237	-2509	-4263	8594	499.6	59.99	0
440.5	0	0	27.936032	-162	-4388	7757	501.8	60.029	0
441.5	0	0	27.936032	-166	-4061	7399	501.6	60	0
442.5	0	0	27.936032	-152	-4391	7696	501.5	60	0
443.5	0	0	27.936032	-169	-4093	7503	501.4	60	0
444.5	0	0	27.936032	-107	-4330	7572	502	59.99	0
446.5	0	0	27.936032	-107	-4330	7572	502	59.99	0
447.5	0	0	NaN	0	0	0	0	0	#DIV/0!
448.5	0	0	NaN	0	0	0	0	0	#DIV/0!
463.8	0	0	NaN	0	0	0	0	0	#DIV/0!
464.5	0	0	27.935211	-270	-5491	8640	501.3	60	0
465.5	0	0	27.935211	-165	-4192	7743	501.1	60.02	0
466.5	0	0	27.935006	-121	-4211	7564	501.7	60	0
467.5	0	0	27.935006	-190	-4300	7940	501.1	60.029	0
469.5	0	0	27.935006	-190	-4300	7940	501.1	60.029	0
470.5	0	0	NaN	0	0	0	0	0	#DIV/0!
471.5	0	0	NaN	0	0	0	0	0	#DIV/0!
542.9	0	0	NaN	0	0	0	0	0	#DIV/0!
543.5	0	0	27.930287	0	0	0	502	60.029	#DIV/0!
544.5	0	0	27.930287	0	0	0	502.2	60.02	#DIV/0!
545.5	0	0	27.930287	0	0	0	502.4	60.029	#DIV/0!
546.5	0	0	27.930287	0	0	0	501.8	60.029	#DIV/0!
547.5	0	0	27.930287	0	0	0	501.9	60.029	#DIV/0!
548.5	0	0	27.930081	0	0	0	502.1	60.029	#DIV/0!
549.5	0	0	27.930081	0	0	0	502.1	60.02	#DIV/0!
550.5	0	0	27.930081	0	0	0	502.1	60.029	#DIV/0!
551.5	0	0	27.930081	0	0	0	502.3	60.029	#DIV/0!
552.5	0	0	27.930081	0	0	0	502.5	60.029	#DIV/0!
553.5	0	0	27.930081	0	0	0	502.4	60.029	#DIV/0!
554.5	0	0	27.930081	0	0	0	502.5	60.02	#DIV/0!
555.5	0	0	27.930081	0	0	0	502.3	60.02	#DIV/0!
556.5	0	0	27.930081	0	0	0	502.3	60.029	#DIV/0!
557.5	0	0	27.930081	0	0	0	502.4	60.02	#DIV/0!
558.5	0	0	27.930081	0	0	0	501.9	60.029	#DIV/0!
562.5	0	0	27.930081	0	0	0	501.9	60.029	#DIV/0!
563.5	0	0	NaN	0	0	0	0	0	#DIV/0!
564.5	0	0	NaN	0	0	0	0	0	#DIV/0!
736.8	0	0	NaN	0	0	0	0	0	#DIV/0!
737.5	0	0	27.92803	0	0	0	504.4	60.029	#DIV/0!
738.5	-4326	0	27.92803	0	0	0	504.5	60.04	#DIV/0!
739.5	-4416	0	27.92803	0	0	0	504.9	60.06	#DIV/0!
740.5	-4445	0	27.92803	-4792	-5278	9918	502.6	60.04	0.927588
741.5	-4067	0	27.92803	-4649	-4992	9219	502.4	60.04	0.874812
744.5	-4067	0	27.92803	-4649	-4992	9219	502.4	60.04	0.874812
745.5	0	0	NaN	0	0	0	0	0	#DIV/0!
746.5	0	0	NaN	0	0	0	0	0	#DIV/0!
749.0	0	0	NaN	0	0	0	0	0	#DIV/0!
749.5	-2050	0	27.927619	-2370	-5253	8641	502	60.06	0.864979
750.5	-1968	0	27.927619	-2313	-5122	8263	503	60.06	0.850843
751.5	-1830	0	27.927619	-2184	-5344	8720	503.2	60.06	0.837912
752.5	-1721	0	27.927824	-2062	-5091	8265	503.5	60.06	0.834627
753.5	-1630	0	27.927824	-1971	-5414	8614	503	60.069	0.826991
754.5	-1540	0	27.927824	-1884	-5168	8433	502.8	60.06	0.81741
755.5	-1460	0	27.927824	-1746	-5255	8452	503	60.06	0.836197
756.5	-1374	0	27.927824	-1702	-5325	8709	503	60.04	0.807286
757.5	-1311	0	27.927824	-1561	-5263	8314	503.1	60.04	0.839846
758.5	-1261	0	27.927619	-1619	-5344	8702	502.8	60.06	0.778876

759.5	-1203	0	27.927619	-1476	-5179	8149	503.2	60.06	0.815041
760.5	-1157	0	27.927619	-1498	-5394	8537	503.2	60.06	0.772363
761.5	-1116	0	27.927619	-1344	-5077	8098	503.1	60.06	0.830357
762.5	-1081	0	27.927414	-1355	-5343	8537	502.9	60.069	0.797786
763.5	-1043	0	27.927414	-1370	-5120	8347	502.8	60.04	0.761314
764.5	-1015	0	27.927414	-1243	-5336	8488	503.3	60.04	0.816573
765.5	-991	0	27.927414	-1279	-5321	8571	503.1	60.06	0.774824
766.5	-967	0	27.927209	-1214	-5274	8354	503.3	60.06	0.79654
767.5	-946	0	27.927209	-1314	-5416	8702	502.9	60.06	0.719939
768.5	-925	0	27.927004	-1137	-5258	8216	503	60.06	0.813544
769.5	-911	0	27.927004	-1195	-5506	8704	503.2	60.06	0.762343
770.5	-896	0	27.926388	-1135	-5146	8098	503.3	60.069	0.789427
771.5	-882	0	27.926388	-1165	-5468	8598	503.3	60.06	0.757082
772.5	-871	0	27.926388	-1146	-5165	8173	503.4	60.06	0.760035
773.5	-857	0	27.926388	-1146	-5348	8509	502.8	60.069	0.747818
774.5	-842	0	27.926388	-1076	-5266	8373	503.2	60.06	0.782528
775.5	-838	0	27.926388	-1035	-5385	8472	503.3	60.06	0.809662
776.5	-836	0	27.926388	-1075	-5452	8682	503.6	60.06	0.777674
777.5	-834	0	27.926388	-1017	-5362	8240	503.1	60.06	0.820059
778.5	-831	0	27.926388	-1124	-5519	8705	503.5	60.06	0.739324
779.5	-828	0	27.926388	-1026	-5260	8191	503.4	60.06	0.807018
780.5	-823	0	27.926388	-1067	-5498	8555	503	60.069	0.771321
781.5	-820	0	27.926388	-1031	-5190	8138	502.9	60.06	0.795344
782.5	-817	0	27.925978	-1022	-5418	8450	503.5	60.06	0.799413
783.5	-815	0	27.925773	-1048	-5244	8269	503.2	60.06	0.777672
784.5	-811	0	27.925773	-1048	-5404	8389	503.6	60.06	0.773855
785.5	-806	0	27.925773	-1094	-5369	8505	503.1	60.04	0.736746
786.5	-802	0	27.925773	-1031	-5397	8370	503.3	60.06	0.777886
787.5	-798	0	27.925773	-1120	-5468	8597	503.3	60.04	0.7125
788.5	-796	0	27.925362	-1057	-5376	8167	503.5	60.06	0.753075
789.5	-791	0	27.925362	-1107	-5578	8676	503.3	60.06	0.714544
790.5	-788	0	27.925362	-1047	-5217	8025	503.2	60.06	0.752627
791.5	-784	0	27.925362	-1048	-5494	8525	503.1	60.04	0.748092
792.5	-782	0	27.924952	-1034	-5182	8138	503.2	60.06	0.756286
793.5	-778	0	27.924952	-1027	-5496	8521	503.2	60.06	0.757546
794.5	-774	0	27.924747	-1059	-5355	8380	502.9	60.04	0.730878
795.5	-770	0	27.924747	-1049	-5404	8390	503.1	60.04	0.734032
796.5	-768	0	27.924541	-1094	-5482	8650	502.9	60.04	0.702011
797.5	-763	0	27.924541	-1034	-5429	8239	502.8	60.04	0.737911
798.5	-759	0	27.924541	-1102	-5603	8823	503.1	60.04	0.688748
799.5	-756	0	27.924541	-1050	-5361	8151	503	60.06	0.72
800.5	-752	0	27.924131	-1101	-5604	8787	503.1	60.04	0.683015
801.5	-748	0	27.924131	-1051	-5253	8132	502.8	60.06	0.711703
802.5	-753	0	27.923926	-961	-5573	8618	503.2	60.04	0.783559
803.5	-750	0	27.923926	-1050	-5298	8339	503.1	60.04	0.714286
804.5	-749	0	27.923926	-968	-5508	8481	503.1	60.04	0.77376
805.5	-750	0	27.923926	-1087	-5453	8620	503.2	60.04	0.689972
806.5	-748	0	27.923721	-948	-5469	8368	503	60.029	0.78903
807.5	-752	0	27.923721	-1118	-5533	8768	503	60.04	0.67263
808.5	-748	0	27.923516	-1022	-5336	8202	502.7	60.04	0.731898
809.5	-752	0	27.923516	-1120	-5670	8830	503.2	60.029	0.671429
810.5	-748	0	27.92331	-956	-5300	8148	503	60.04	0.782427
811.5	-751	0	27.92331	-1089	-5624	8804	503.2	60.06	0.689624
812.5	-749	0	27.92331	-1046	-5242	8287	503.1	60.06	0.716061
813.5	-751	0	27.92331	-936	-5601	8600	503.6	60.06	0.80235
814.5	-748	0	27.92331	-1077	-5434	8528	503.2	60.06	0.694522
815.5	-751	0	27.92331	-993	-5460	8377	502.8	60.029	0.756294
816.5	-749	0	27.923105	-1095	-5574	8746	503.3	60.029	0.684018
817.5	-751	0	27.923105	-964	-5426	8239	502.8	60.04	0.779046
818.5	-748	0	27.922695	-1117	-5606	8715	503.1	60.04	0.669651
819.5	-752	0	27.922695	-942	-5332	8178	503.3	60.04	0.798301
820.5	-750	0	27.922695	-1084	-5657	8688	503.8	60.04	0.691882
821.5	-749	0	27.922695	-937	-5309	8152	503.4	60.04	0.79936
822.5	-752	0	27.922284	-1041	-5554	8537	503.4	60.04	0.722382
823.5	-750	0	27.922284	-1046	-5362	8416	503.4	60.04	0.717017
824.5	-748	0	27.922284	-949	-5493	8464	503.7	60.06	0.788198
825.5	-751	0	27.922284	-1086	-5538	8682	503.4	60.029	0.691529
826.5	-749	0	27.921874	-1040	-5425	8237	503.7	60.06	0.720192
827.5	-753	0	27.921874	-1074	-5655	8855	503.5	60.04	0.701117
828.5	-748	0	27.921669	-1048	-5484	8275	503.6	60.04	0.71374
829.5	-753	0	27.921669	-1026	-5635	8796	503.6	60.04	0.733918
830.5	-750	0	27.921669	-1055	-5327	8156	503.8	60.06	0.7109
831.5	-749	0	27.921669	-961	-5652	8665	503.9	60.06	0.779396
832.5	-751	0	27.921053	-1053	-5377	8257	503.5	60.04	0.7132
833.5	-748	0	27.921053	-959	-5660	8556	503.5	60.06	0.779979
834.5	-752	0	27.921053	-1073	-5497	8566	503.4	60.04	0.700839
835.5	-749	0	27.921053	-963	-5557	8482	503.7	60.04	0.777778
836.5	-752	0	27.921053	-1117	-5614	8854	503.4	60.06	0.673232
837.5	-749	0	27.921053	-1043	-5505	8300	503.8	60.04	0.718121
838.5	-753	0	27.921053	-1052	-5681	8955	503.5	60.04	0.715779
839.5	-749	0	27.921053	-1061	-5436	8183	503.3	60.06	0.705938
840.5	-751	0	27.920233	-985	-5727	8762	503.4	60.04	0.762437

841.5	-750	0	27.920233	-1055	-5349	8245	503.4	60.06	0.7109
842.5	-750	0	27.920233	-961	-5669	8734	503.8	60.069	0.780437
843.5	-748	0	27.920233	-1044	-5412	8525	503.5	60.06	0.716475
844.5	-751	0	27.920233	-1056	-5618	8523	503.6	60.069	0.711174
845.5	-748	0	27.920233	-1006	-5581	8747	503.7	60.06	0.743539
846.5	-752	0	27.919822	-1038	-5521	8399	503.3	60.06	0.72447
847.5	-749	0	27.919822	-1126	-5704	8963	503.9	60.06	0.665187
848.5	-752	0	27.919822	-996	-5530	8294	503.5	60.06	0.75502
852.5	-752	0	27.919822	-996	-5530	8294	503.5	60.06	0.75502
853.5	0	0	NaN	0	0	0	0	0	#DIV/0!
854.5	0	0	NaN	0	0	0	0	0	#DIV/0!
855.5	0	0	NaN	0	0	0	0	0	#DIV/0!
856.5	0	0	NaN	0	0	0	0	0	#DIV/0!
857.5	0	0	NaN	0	0	0	0	0	#DIV/0!
858.5	0	0	NaN	0	0	0	0	0	#DIV/0!
859.5	0	0	NaN	0	0	0	0	0	#DIV/0!
860.5	0	0	NaN	0	0	0	0	0	#DIV/0!
861.5	0	0	NaN	0	0	0	0	0	#DIV/0!
862.5	0	0	NaN	0	0	0	0	0	#DIV/0!
863.5	0	0	NaN	0	0	0	0	0	#DIV/0!
864.5	0	0	NaN	0	0	0	0	0	#DIV/0!
868.5	0	0	NaN	0	0	0	0	0	#DIV/0!
869.5	0	0	NaN	0	0	0	0	0	#DIV/0!
870.5	0	0	NaN	0	0	0	0	0	#DIV/0!
871.5	0	0	NaN	0	0	0	0	0	#DIV/0!
872.5	0	0	NaN	0	0	0	0	0	#DIV/0!
873.5	0	0	NaN	0	0	0	0	0	#DIV/0!
874.5	0	0	NaN	0	0	0	0	0	#DIV/0!
1058.5	0	0	NaN	0	0	0	0	0	#DIV/0!
1059.0	0	0	27.909973	0	0	0	505	60.04	#DIV/0!
1059.5	-809	0	27.909973	0	0	0	504.8	60.04	#DIV/0!
1060.5	-859	0	27.909973	0	0	0	504.9	60.04	#DIV/0!
1061.5	-967	0	27.909973	-251	1627	5629	504.5	60.06	3.85259
1062.5	-1081	0	27.909973	-1320	-5198	7848	503.1	60.06	0.818939
1063.5	-1049	0	27.909973	-1336	-4859	7883	503.3	60.06	0.78518
1064.5	-1023	0	27.909973	-1222	-5054	7777	503.3	60.04	0.837152
1065.5	-1000	0	27.909973	-1253	-5141	8163	503.3	60.04	0.798085
1066.5	-978	0	27.909973	-1234	-4955	7838	503.2	60.04	0.792545
1067.5	-956	0	27.909973	-1262	-5127	8126	503.3	60.06	0.757528
1068.5	-935	0	27.909768	-1153	-4843	7701	503.5	60.069	0.810928
1069.5	-923	0	27.909768	-1144	-5216	7974	503.1	60.06	0.806818
1070.5	-914	0	27.909563	-1118	-4825	7733	503	60.04	0.817531
1071.5	-903	0	27.909563	-1092	-5158	7812	503.1	60.069	0.826923
1072.5	-891	0	27.909358	-1128	-4840	7785	503.4	60.06	0.789894
1073.5	-879	0	27.909358	-1124	-5090	7782	503.1	60.04	0.782028
1074.5	-869	0	27.909358	-1116	-4975	8127	503.2	60.04	0.778674
1075.5	-858	0	27.909358	-1115	-4959	7757	503.3	60.04	0.769507
1076.5	-848	0	27.908537	-1115	-5011	8078	503.3	60.04	0.760538
1077.5	-844	0	27.908537	-1029	-4873	7667	503.5	60.04	0.820214
1078.5	-844	0	27.908332	-1034	-5097	7999	503.3	60.06	0.816248
1079.5	-842	0	27.908332	-1030	-4855	7698	503.3	60.06	0.817476
1080.5	-841	0	27.908127	-1017	-5163	7826	503.2	60.04	0.826942
1081.5	-842	0	27.908127	-1005	-4733	7628	503.2	60.04	0.837811
1082.5	-842	0	27.908127	-996	-5183	7857	503.1	60.04	0.845382
1083.5	-841	0	27.908127	-1018	-4844	7935	503.2	60.04	0.82613
1084.5	-841	0	27.908127	-1018	-4844	7935	503.2	60.04	0.82613
1085.5	0	0	NaN	0	0	0	0	0	#DIV/0!
1086.5	0	0	NaN	0	0	0	0	0	#DIV/0!
1087.5	0	0	NaN	0	0	0	0	0	#DIV/0!
1088.5	0	0	NaN	0	0	0	0	0	#DIV/0!
1089.5	0	0	NaN	0	0	0	0	0	#DIV/0!
1090.5	0	0	NaN	0	0	0	0	0	#DIV/0!
1097.4	0	0	NaN	0	0	0	0	0	#DIV/0!
1097.9	-830	0	27.907101	-967	-4163	7313	503	60.04	0.858325
1098.5	-1890	0	27.907101	-1750	-4375	7393	503.3	60.04	1.08
1099.5	-1886	0	27.907101	-2172	-4622	7850	503	60.06	0.868324
1100.5	-1870	0	27.907101	-2158	-5042	7945	503	60.04	0.866543
1101.5	-1857	0	27.907101	-2158	-4610	7865	503	60.06	0.860519
1102.5	-1842	0	27.906485	-2069	-5020	7953	502.6	60.06	0.890285
1103.5	-1838	0	27.906485	-2048	-4614	7884	503.1	60.04	0.897461
1104.5	-1832	0	27.906485	-2047	-4915	8206	502.7	60.04	0.894968
1105.5	-1826	0	27.906485	-2085	-4994	8579	504.7	60.06	0.875779
1106.5	-1821	0	27.906485	-2072	-4802	8156	504.5	60.04	0.878861
1107.5	-1815	0	27.906485	-2103	-5059	8494	504.2	60.06	0.863053
1108.5	-1808	0	27.90628	-2081	-4640	8024	504.6	60.069	0.868813
1109.5	-1801	0	27.90628	-2086	-5104	8348	504.6	60.06	0.863375
1110.5	-1796	0	27.906075	-2055	-4575	8020	504.7	60.06	0.873966
1111.5	-1790	0	27.906075	-2058	-4909	8151	504.7	60.04	0.869776
1112.5	-1784	0	27.906075	-2065	-4656	8190	505	60.06	0.863923
1113.5	-1779	0	27.906075	-2060	-4928	8188	504.9	60.04	0.863592
1114.5	-1773	0	27.906075	-2096	-4719	8445	504.5	60.06	0.845897
1115.5	-1767	0	27.906075	-2062	-4793	8181	504.9	60.04	0.856935

19651.0	-77446	0	28.659888	-79978	-2631	80243	483.9	60	0.968341
19651.5	-77447	0	28.660503	-79967	-2633	80283	483.7	60.02	0.968487
19652.0	-77447	0	28.660914	-79977	-2861	80386	484.3	59.99	0.968366
19652.5	-77447	0	28.661324	-79959	-2785	80256	484.3	60.02	0.968584
19653.0	-77449	0	28.668915	-79930	-2596	80206	484	60.02	0.96896
19653.5	-77450	0	28.669736	-79971	-2738	80359	484.1	60.02	0.968476
19654.0	-77451	0	28.670352	-79951	-2878	80336	484.2	59.99	0.968731
19654.5	-77451	0	28.670557	-80064	-2710	80348	484.1	60.02	0.967364
19655.0	-77446	0	28.680346	-80044	-2599	80324	483.9	60	0.967543
19655.5	-77445	0	28.680757	-79988	-2809	80407	484.2	60.02	0.968208
19656.0	-77445	0	28.680962	-79962	-2818	80297	484.2	60.029	0.968523
19656.5	-77447	0	28.681167	-79950	-2580	80209	483.9	60	0.968693
19657.0	-77448	0	28.681372	-79932	-2578	80256	483.9	60.02	0.968924
19657.5	-77449	0	28.682457	-79968	-2860	80374	484	60	0.9685
19658.0	-77450	0	28.682662	-79992	-2733	80267	484	60	0.968222
19658.5	-77450	0	28.682867	-79943	-2562	80211	484.2	60	0.968815
19659.0	-77452	0	28.690253	-79975	-2775	80403	484.2	60.02	0.968453
19659.5	-77449	0	28.690459	-80049	-2812	80413	483.9	59.99	0.96752
19660.0	-77448	0	28.690664	-79969	-2658	80248	484.1	60.02	0.968475
19660.5	-77449	0	28.690664	-79927	-2558	80222	484.2	60.02	0.968997
19661.0	-77449	0	28.700102	-80015	-2891	80428	484.3	59.99	0.967931
19661.5	-77449	0	28.700658	-79954	-2775	80272	484	60	0.968669
19662.0	-77450	0	28.701069	-79960	-2553	80223	483.6	60	0.968609
19662.5	-77450	0	28.701274	-79954	-2684	80308	484.2	60	0.968682
19663.0	-77451	0	28.707429	-79993	-2844	80381	484.1	60	0.968222
19663.5	-77450	0	28.708045	-80056	-2713	80338	484.2	59.99	0.967448
19664.0	-77449	0	28.708455	-79965	-2520	80237	484.1	60.02	0.968536
19664.5	-77449	0	28.708865	-79991	-2867	80428	484.3	60	0.968221
19665.0	-77450	0	28.719534	-79939	-2783	80305	484.4	60.02	0.968864
19665.5	-77451	0	28.72015	-79992	-2637	80284	484	59.99	0.968234
19666.0	-77449	0	28.720355	-80012	-2585	80292	484.1	60	0.967967
19666.5	-77448	0	28.720765	-80008	-2825	80415	484	60	0.968003
19667.0	-77448	0	28.720971	-79961	-2749	80263	484.2	59.99	0.968572
19667.5	-77448	0	28.721996	-79950	-2539	80220	484	60	0.968705
19668.0	-77450	0	28.721996	-79941	-2615	80318	484	60	0.96884
19668.5	-77451	0	28.721996	-79992	-2842	80384	483.9	59.97	0.968234
19669.0	-77451	0	28.726656	-80009	-2668	80301	484.1	60	0.968029
19669.5	-77449	0	28.726656	-80019	-2466	80300	484.2	60.02	0.967883
19670.0	-77448	0	28.727067	-79962	-2768	80393	483.6	60	0.96856
19670.5	-77449	0	28.727067	-79947	-2777	80291	484.3	59.99	0.968754
19671.0	-77450	0	28.738	-79974	-2578	80225	484.2	60	0.96844
19671.5	-77450	0	28.738615	-79943	-2587	80263	484.3	60	0.968815
19672.0	-77452	0	28.739231	-79971	-2796	80385	484.1	60	0.968501
19672.5	-77449	0	28.739641	-80046	-2743	80344	483.7	60.02	0.967556
19673.0	-77445	0	28.746207	-79956	-2480	80220	483.5	60	0.968595
19673.5	-77447	0	28.746822	-79941	-2722	80350	483.7	59.99	0.968802
19674.0	-77448	0	28.747028	-79964	-2770	80336	483.9	60	0.968536
19674.5	-77449	0	28.747233	-79961	-2667	80264	483.9	60	0.968585
19675.0	-77450	0	28.756466	-79932	-2512	80211	483.6	60.02	0.968949
19675.5	-77451	0	28.757286	-79983	-2791	80401	484	60	0.968343
19676.0	-77449	0	28.757491	-80052	-2715	80394	484.2	60	0.967484
19676.5	-77447	0	28.757697	-79949	-2552	80205	484.1	60.02	0.968705
19677.0	-77447	0	28.757902	-79926	-2671	80291	483.7	60.02	0.968984
19677.5	-77449	0	28.758722	-79967	-2847	80367	484.1	59.99	0.968512
19678.0	-77449	0	28.758928	-79947	-2707	80234	484.4	60.02	0.968754
19678.5	-77450	0	28.759133	-79935	-2518	80226	483.6	60.029	0.968912
19679.0	-77451	0	28.766519	-79975	-2725	80378	484.1	60.02	0.96844
19679.5	-77449	0	28.766519	-80070	-2779	80446	483.9	60	0.967266
19680.0	-77447	0	28.766724	-79925	-2624	80224	483.9	60.02	0.968996
19680.5	-77448	0	28.766929	-79943	-2473	80251	483.3	60.02	0.96879
19681.0	-77449	0	28.777129	-79981	-2777	80391	483.8	60.02	0.968342
19681.5	-77449	0	28.77795	-79974	-2704	80282	483.7	60.02	0.968427
19682.0	-77449	0	28.77795	-79969	-2484	80230	484.2	60.02	0.968488
19682.5	-77450	0	28.77795	-79917	-2630	80298	484.3	60.02	0.96913
19683.0	-77452	0	28.784369	-80001	-2790	80398	483.8	60	0.968138
19683.5	-77449	0	28.784985	-80032	-2671	80305	483.8	60.02	0.967725
19684.0	-77447	0	28.78519	-79943	-2459	80214	483.9	60	0.968778
19684.5	-77448	0	28.7856	-79956	-2698	80374	483.5	60.029	0.968633
19685.0	-77449	0	28.795918	-79945	-2773	80288	483.9	60.02	0.968779
19685.5	-77449	0	28.796533	-79953	-2560	80217	483.6	60.02	0.968682
19686.0	-77450	0	28.797149	-79942	-2526	80239	484	60.02	0.968827
19686.5	-77451	0	28.797559	-79953	-2796	80361	484	59.99	0.968707
19687.0	-77450	0	28.797559	-80041	-2714	80339	484.1	60.029	0.967629
19687.5	-77447	0	28.79838	-79968	-2464	80226	483.7	60.02	0.968475
19688.0	-77447	0	28.79838	-79962	-2624	80315	483.8	60.02	0.968548
19688.5	-77449	0	28.798585	-79948	-2804	80334	483.9	60	0.968742
19689.0	-77449	0	28.806236	-79954	-2680	80242	484	60.02	0.968669
19689.5	-77451	0	28.806236	-79949	-2444	80224	483.6	60.02	0.968755
19690.0	-77451	0	28.806441	-80056	-2702	80476	483.9	60	0.96746
19690.5	-77447	0	28.806646	-80052	-2740	80379	484.2	60.02	0.967459
19691.0	-77445	0	28.817051	-79941	-2506	80202	483.9	60	0.968777
19691.5	-77446	0	28.817256	-79944	-2501	80270	483.7	60	0.968753

19692.0	-77447	0	28.817666	-79940	-2790	80338	484	60	0.968814
19692.5	-77447	0	28.817666	-79969	-2697	80264	484.1	60	0.968463
19693.0	-77449	0	28.824642	-79916	-2468	80191	484	59.99	0.96913
19693.5	-77450	0	28.825668	-79965	-2620	80345	483.9	60.02	0.968549
19694.0	-77451	0	28.825873	-79940	-2749	80322	484.1	59.97	0.968864
19694.6	-77451	0	28.826284	-79951	-2607	80236	484.5	60.02	0.968731
19695.1	-77449	0	28.836747	-80045	-2510	80342	483.7	59.99	0.967568
19695.6	-77448	0	28.837158	-79956	-2700	80372	483.8	60.02	0.968633
19696.1	-77449	0	28.837568	-79953	-2674	80279	483.7	60	0.968682
19696.6	-77450	0	28.837773	-79945	-2490	80207	483.7	60	0.968791
19697.1	-77451	0	28.838038	-79974	-2472	80313	483.5	60	0.968452
19697.6	-77447	0	28.838653	-80035	-2758	80404	483.4	60	0.967664
19698.1	-77447	0	28.838653	-79949	-2653	80216	483.6	60.02	0.968705
19698.6	-77449	0	28.838858	-79945	-2411	80208	482.9	60	0.968779
19699.1	-77449	0	28.843167	-79970	-2641	80357	483.2	60.02	0.968476
19699.6	-77451	0	28.843167	-79940	-2716	80294	483	60.02	0.968864
19700.1	-77452	0	28.843372	-79932	-2532	80217	482.7	60.029	0.968974
19700.6	-77450	0	28.843372	-80022	-2425	80319	482.1	60.029	0.967859
19701.1	-77446	0	28.854392	-79987	-2709	80370	482.2	60	0.968232
19701.6	-77447	0	28.855829	-79947	-2647	80251	481.7	60.02	0.968729
19702.1	-77449	0	28.856034	-79935	-2455	80190	481.7	60.02	0.9689
19702.6	-77450	0	28.856444	-79925	-2529	80284	481.7	60.02	0.969033
19703.1	-77452	0	28.861984	-79973	-2723	80376	481.5	60	0.968477
19703.6	-77449	0	28.862599	-80055	-2572	80326	481.8	60	0.967447
19704.1	-77448	0	28.862804	-79932	-2386	80191	481.9	60.04	0.968924
19704.6	-77450	0	28.86301	-79968	-2649	80376	481.9	60.02	0.968512
19705.1	-77451	0	28.873004	-79925	-2680	80272	482	60.04	0.969046
19705.6	-77451	0	28.873619	-80035	-2484	80305	481.7	60.02	0.967714
19706.1	-77447	0	28.873619	-80032	-2478	80342	482.1	60.02	0.9677
19706.6	-77448	0	28.873825	-79964	-2699	80353	481.9	60.02	0.968536
19707.1	-77449	0	28.874235	-79936	-2608	80239	482.1	60.04	0.968888
19707.6	-77450	0	28.875056	-79930	-2370	80190	481.5	60.029	0.968973
19708.1	-77453	0	28.875056	-79948	-2592	80374	481.4	60.02	0.968792
19708.6	-77450	0	28.875261	-80046	-2687	80415	481.1	60.06	0.967569
19709.1	-77448	0	28.882237	-80016	-2537	80271	480.8	60.029	0.967906
19709.6	-77449	0	28.882647	-79925	-2386	80195	480.8	60.02	0.969021
19710.1	-77450	0	28.882647	-79961	-2577	80382	481.4	59.99	0.968597
19710.6	-77451	0	28.882852	-79928	-2625	80270	480.6	60	0.96901
19711.1	-77451	0	28.893608	-80043	-2450	80298	481.1	60	0.967617
19711.6	-77447	0	28.894018	-79999	-2425	80289	481.4	60	0.9681
19712.1	-77448	0	28.894223	-79979	-2670	80361	481.7	59.99	0.968354
19712.6	-77450	0	28.894223	-79901	-2594	80183	481.8	60.029	0.969325
19713.1	-77452	0	28.900702	-79978	-2403	80260	481.6	60	0.968416
19713.6	-77449	0	28.901728	-80021	-2597	80396	481.5	60	0.967858
19714.1	-77449	0	28.901933	-79944	-2748	80300	481.6	60	0.968791
19714.6	-77450	0	28.902139	-79942	-2898	80253	482.2	60.06	0.968827
19715.1	-77451	0	28.911576	-79982	-2438	80304	481.7	60.02	0.968355
19715.6	-77447	0	28.912602	-80032	-2653	80432	481.8	60.02	0.9677
19716.1	-77448	0	28.912602	-79937	-2611	80253	482.1	60.029	0.968863
19716.6	-77448	0	28.912808	-79949	-2443	80205	481.9	60	0.968718
19717.1	-77450	0	28.913218	-79935	-2441	80264	482.2	60.02	0.968912
19717.6	-77452	0	28.914039	-79937	-2694	80342	481.6	60	0.968913
19718.1	-77450	0	28.914244	-80037	-2571	80316	481.6	60.02	0.967677
19718.6	-77448	0	28.914449	-79981	-2365	80232	481.3	60	0.96833
19719.1	-77449	0	28.922451	-79939	-2643	80373	481.2	60	0.968851
19719.6	-77451	0	28.922656	-79965	-2631	80319	480.5	59.99	0.968561
19720.1	-77453	0	28.922656	-79933	-2464	80233	480.1	60.02	0.968974
19720.6	-77450	0	28.922656	-80033	-2343	80313	480.3	60	0.967726
19721.1	-77447	0	28.932034	-79971	-2600	80364	480.1	59.99	0.968439
19721.6	-77448	0	28.932445	-79958	-2571	80267	479.5	59.97	0.968609
19722.1	-77451	0	28.932445	-79882	-2341	80139	479.2	60	0.969568
19722.6	-77452	0	28.93265	-79942	-2467	80297	478.9	60.029	0.968852
19723.1	-77450	0	28.939626	-80020	-2588	80398	479.5	60.02	0.967883
19723.6	-77448	0	28.941062	-79998	-2511	80258	478.9	59.99	0.968124
19724.1	-77450	0	28.941472	-79911	-2318	80200	478.5	60.02	0.969203
19724.6	-77452	0	28.941472	-79910	-2558	80309	478.9	60.02	0.96924
19725.1	-77453	0	28.950354	-80001	-2604	80349	479.1	59.99	0.96815
19725.6	-77451	0	28.950765	-80013	-2392	80279	478.6	60	0.96798
19726.1	-77447	0	28.95097	-80025	-2365	80304	478.5	60.02	0.967785
19726.6	-77448	0	28.95138	-79925	-2581	80324	478.4	59.97	0.969008
19727.1	-77451	0	28.95179	-79909	-2523	80199	478.3	59.99	0.96924
19727.6	-77453	0	28.952611	-79935	-2314	80208	478.6	60	0.96895
19728.1	-77452	0	28.952611	-80035	-2487	80410	478.4	60	0.967727
19728.6	-77449	0	28.952611	-80011	-2597	80379	478.3	59.99	0.967979
19729.1	-77450	0	28.960613	-79919	-2486	80183	478.4	59.99	0.969106
19729.6	-77452	0	28.960613	-79935	-2302	80202	478.3	60	0.968937
19730.1	-77451	0	28.960613	-80026	-2534	80433	478.3	59.99	0.967823
19730.6	-77448	0	28.960818	-79998	-2570	80314	478.3	59.99	0.968124
19731.1	-77450	0	28.970461	-79913	-2344	80151	477.9	59.97	0.969179
19731.6	-77452	0	28.971487	-79954	-2348	80267	478.3	60.02	0.968707
19732.1	-77449	0	28.971692	-80012	-2595	80400	478.8	59.959	0.967967
19732.6	-77449	0	28.972103	-79941	-2498	80203	478.8	59.97	0.968827

19733.1	-77452	0	28.978317	-79932	-2291	80183	478.3	59.99	0.968974
19733.6	-77451	0	28.979138	-80018	-2500	80384	478.1	59.97	0.96792
19734.1	-77449	0	28.979343	-80021	-2586	80393	478.7	59.99	0.967858
19734.6	-77450	0	28.979548	-79905	-2427	80186	478.5	59.99	0.969276
19735.1	-77452	0	28.990952	-79913	-2279	80189	478.4	59.99	0.969204
19735.6	-77451	0	28.991567	-80055	-2582	80441	477.9	60	0.967472
19736.1	-77447	0	28.991567	-80019	-2524	80306	478.3	60	0.967858
19736.6	-77449	0	28.991773	-79937	-2341	80190	478.7	59.97	0.968875
19737.1	-77450	0	28.992123	-79941	-2425	80296	479	60	0.96884
19737.6	-77451	0	28.992944	-79966	-2583	80342	478.8	59.959	0.968549
19738.1	-77451	0	28.993149	-80025	-2485	80294	479.3	59.99	0.967835
19738.6	-77448	0	28.993354	-80026	-2283	80280	478.9	59.97	0.967785
19739.1	-77449	0	28.998835	-79915	-2555	80318	479.2	59.97	0.969142
19739.6	-77451	0	28.99904	-79936	-2591	80285	478.9	59.95	0.968913
19740.1	-77452	0	28.99904	-80013	-2422	80274	479.2	59.97	0.967993
19740.6	-77449	0	28.999245	-80021	-2322	80289	478.8	59.99	0.967858
19741.1	-77449	0	29.009444	-79953	-2587	80341	479.4	59.95	0.968682
19741.6	-77451	0	29.010265	-79930	-2523	80214	479.2	59.97	0.968985
19742.1	-77454	0	29.01047	-79928	-2331	80179	478.7	60	0.969047
19742.6	-77451	0	29.010675	-80017	-2441	80373	478.9	60	0.967932
19743.1	-77449	0	29.017386	-80028	-2604	80402	478.9	59.99	0.967774
19743.6	-77451	0	29.018002	-79897	-2485	80157	478.8	59.99	0.969386
19744.1	-77453	0	29.018002	-79944	-2302	80224	478.8	59.99	0.968841
19744.6	-77451	0	29.018207	-80030	-2563	80430	478.9	59.99	0.967775
19745.1	-77448	0	29.02791	-79998	-2577	80323	478.8	59.99	0.968124
19745.6	-77450	0	29.02873	-79923	-2376	80183	478.7	60	0.969058
19746.1	-77453	0	29.028936	-79930	-2353	80257	478.7	59.97	0.96901
19746.6	-77450	0	29.029141	-80070	-2581	80462	478.7	59.99	0.967279
19747.1	-77447	0	29.029551	-79988	-2548	80250	479.1	59.97	0.968233
19747.6	-77449	0	29.030372	-79919	-2317	80177	479.2	60	0.969094
19748.1	-77452	0	29.030577	-79915	-2487	80296	478.6	59.99	0.96918
19748.6	-77451	0	29.030577	-80042	-2590	80393	479.2	59.99	0.967629
19749.1	-77449	0	29.037758	-80008	-2467	80280	479.1	60	0.968016
19749.6	-77450	0	29.038168	-79915	-2323	80195	479.1	60.02	0.969155
19750.1	-77453	0	29.038168	-79951	-2544	80379	479.4	59.97	0.968756
19750.6	-77451	0	29.038168	-80003	-2553	80322	479.1	59.99	0.968101
19751.1	-77448	0	29.048427	-80030	-2359	80281	479.1	59.99	0.967737
19751.6	-77449	0	29.049043	-79908	-2375	80212	479.3	60	0.969227
19752.1	-77451	0	29.049043	-79952	-2598	80334	479.1	60	0.968719
19752.6	-77453	0	29.049453	-79961	-2484	80253	479.4	59.99	0.968635
19753.1	-77451	0	29.053967	-80019	-2288	80284	478.3	60	0.967908
19753.6	-77449	0	29.054993	-79987	-2517	80347	478.7	60	0.96827
19754.1	-77450	0	29.055198	-79927	-2604	80288	479.3	60	0.969009
19754.6	-77453	0	29.055608	-79950	-2434	80247	479	60	0.968768
19755.1	-77450	0	29.066893	-80002	-2314	80274	478.3	59.99	0.968101
19755.6	-77449	0	29.067918	-79968	-2581	80365	478.6	60	0.9685
19756.1	-77451	0	29.067918	-79910	-2555	80230	478.7	60	0.969228
19756.6	-77452	0	29.068124	-80015	-2328	80265	478.7	60	0.967969
19757.1	-77449	0	29.068329	-80005	-2375	80321	478.4	60.029	0.968052
19757.6	-77449	0	29.06915	-79940	-2604	80334	478.5	60	0.968839
19758.1	-77452	0	29.06915	-79908	-2480	80181	478.8	60.02	0.969265
19758.6	-77452	0	29.069355	-80008	-2286	80273	479.1	60	0.968053
19759.1	-77449	0	29.077356	-80053	-2544	80462	478.6	60	0.967472
19759.6	-77448	0	29.077562	-79941	-2591	80298	479	59.99	0.968815
19760.1	-77450	0	29.077562	-79932	-2422	80204	479.3	60	0.968949
19760.6	-77451	0	29.077562	-79936	-2322	80230	479.3	60.02	0.968913
19761.1	-77452	0	29.085769	-79975	-2622	80383	480.2	59.97	0.968453
19761.6	-77448	0	29.086179	-80047	-2580	80326	480.6	59.99	0.967532
19762.1	-77448	0	29.086384	-79939	-2336	80196	480.2	60	0.968839
19762.6	-77449	0	29.086589	-79911	-2494	80257	480.6	59.99	0.969191
19763.1	-77451	0	29.094796	-79920	-2651	80270	482	60	0.969107
19763.6	-77453	0	29.095617	-79981	-2537	80270	480.6	60	0.968392
19764.1	-77450	0	29.095822	-80029	-2339	80288	481.6	59.99	0.967774
19764.6	-77448	0	29.096027	-79961	-2592	80357	482	60.02	0.968572
19765.1	-77449	0	29.106286	-79915	-2623	80236	481.6	60.029	0.969142
19765.6	-77451	0	29.107107	-79953	-2420	80221	481.7	60.02	0.968707
19766.1	-77448	0	29.107107	-80011	-2425	80292	482	60	0.967967
19766.6	-77448	0	29.107517	-79953	-2653	80348	481.8	60	0.968669
19767.1	-77449	0	29.107722	-79945	-2854	80241	481.6	60.02	0.968779
19767.6	-77451	0	29.108543	-79915	-2390	80168	481.8	60.02	0.969167
19768.1	-77453	0	29.108748	-80027	-3129	80462	481.4	60	0.967836
19768.6	-77450	0	29.108953	-80019	-2671	80394	481.5	59.99	0.967895
19769.1	-77448	0	29.114903	-79965	-2535	80217	481.5	60.02	0.968524
19769.6	-77449	0	29.115108	-79977	-3144	80412	481.7	60.029	0.968391
19770.1	-77451	0	29.115108	-79933	-2628	80344	482.1	60	0.968949
19770.6	-77451	0	29.115108	-80028	-2905	80349	481.4	60	0.967799
19771.1	-77447	0	29.126188	-80022	-2875	80334	481.3	60	0.967821
19771.6	-77447	0	29.126598	-79960	-3157	80401	481.2	59.99	0.968572
19772.1	-77449	0	29.126598	-79944	-3059	80263	481.7	60.02	0.968791
19772.6	-77450	0	29.126803	-79961	-2824	80246	481.2	60	0.968597
19773.1	-77451	0	29.134189	-80002	-3021	80429	481.5	60.02	0.968113
19773.6	-77448	0	29.13542	-80011	-3180	80408	481.8	59.99	0.967967

19774.1	-77449	0	29.135626	-79956	-3003	80271	481.6	60	0.968645
19774.6	-77450	0	29.136036	-79924	-2898	80254	481.9	60.02	0.969046
19775.1	-77452	0	29.144363	-79947	-2353	80247	481.9	60	0.968792
19775.6	-77448	0	29.145183	-80019	-3089	80377	482.1	60	0.96787
19776.1	-77448	0	29.145388	-79944	-2889	80223	482	60	0.968778
19776.6	-77449	0	29.145594	-79964	-2954	80326	482.1	60	0.968548
19777.1	-77450	0	29.145944	-79934	-2479	80258	481.8	60.02	0.968924
19777.6	-77452	0	29.146765	-79999	-3114	80331	482.6	60	0.968162
19778.1	-77449	0	29.146765	-80045	-2818	80339	482.1	60.02	0.967568
19778.6	-77448	0	29.14697	-79945	-3095	80385	482.3	60.02	0.968766
19779.1	-77450	0	29.154561	-79961	-3107	80360	482.1	59.99	0.968597
19779.6	-77452	0	29.154561	-79964	-2959	80301	482.6	60	0.968586
19780.1	-77450	0	29.154561	-80036	-2844	80344	482.1	60	0.96769
19780.6	-77448	0	29.154561	-79994	-3135	80420	482.6	60	0.968173
19781.1	-77449	0	29.16441	-79941	-3008	80283	482.1	60	0.968827
19781.6	-77450	0	29.165436	-79957	-2864	80230	482.3	60	0.968646
19782.1	-77452	0	29.165641	-79945	-2944	80319	482.1	60	0.968816
19782.6	-77452	0	29.166051	-80029	-3144	80453	481.4	59.99	0.967799
19783.1	-77449	0	29.171591	-80039	-2976	80335	481.9	59.99	0.967641
19783.6	-77450	0	29.172412	-79909	-2836	80234	481.8	59.99	0.969227
19784.1	-77453	0	29.172617	-79957	-2987	80394	481	60	0.968683
19784.6	-77450	0	29.172822	-80043	-3040	80440	480.9	60	0.967605
19785.1	-77447	0	29.18267	-79957	-2900	80251	481.3	60	0.968608
19785.6	-77449	0	29.183696	-79931	-2855	80259	480.2	59.99	0.968948
19786.1	-77451	0	29.183696	-79961	-3003	80399	480.2	60	0.96861
19786.6	-77453	0	29.183901	-79987	-3072	80308	480.4	60.02	0.96832
19787.1	-77450	0	29.184312	-80060	-2794	80340	480	60	0.967399
19787.6	-77448	0	29.184927	-79962	-3013	80376	479.9	59.99	0.96856
19788.1	-77450	0	29.185132	-79942	-2960	80350	480	60	0.968827
19788.6	-77452	0	29.185337	-80025	-2902	80325	480	60.02	0.967848
19789.1	-77449	0	29.192253	-80036	-2738	80328	479.5	60	0.967677
19789.6	-77449	0	29.192253	-79944	-3065	80389	479.1	60	0.968791
19790.1	-77452	0	29.192253	-79905	-2957	80284	479.6	59.99	0.969301
19790.6	-77453	0	29.192253	-80044	-2830	80332	479.9	60.02	0.96763
19791.1	-77451	0	29.202922	-80011	-2806	80342	479.9	60.04	0.968004
19791.6	-77447	0	29.203948	-80016	-3031	80419	479.5	59.97	0.967894
19792.1	-77449	0	29.204154	-79911	-2954	80220	480.2	60	0.969191
19792.6	-77451	0	29.204359	-79942	-2706	80228	479.9	59.97	0.96884
19793.1	-77453	0	29.210719	-80024	-2902	80418	479.3	59.99	0.967872
19793.6	-77449	0	29.21154	-80051	-3006	80447	479.7	60	0.967496
19794.1	-77450	0	29.21154	-79913	-2866	80204	479.9	60	0.969179
19794.6	-77453	0	29.211745	-79968	-2687	80267	479.8	60.029	0.96855
19795.1	-77452	0	29.221593	-80045	-2974	80474	479.6	60	0.967606
19795.6	-77449	0	29.222209	-80029	-2944	80372	479.8	60.029	0.967762
19796.1	-77450	0	29.222414	-79964	-2796	80233	479.8	60	0.968561
19796.6	-77451	0	29.222414	-79928	-2818	80268	479.3	60.029	0.96901
19797.1	-77453	0	29.222824	-80015	-3082	80449	479.6	59.99	0.967981
19797.6	-77451	0	29.22344	-80035	-2885	80334	479.7	60	0.967714
19798.1	-77449	0	29.223645	-79953	-2733	80246	479.3	60.02	0.968682
19798.6	-77451	0	29.223645	-79943	-2843	80358	479.2	60.029	0.968828
19799.1	-77453	0	29.230416	-79984	-2978	80377	479.4	59.99	0.968356
19799.6	-77452	0	29.230621	-80021	-2785	80317	479.4	60.02	0.967896
19800.1	-77450	0	29.230621	-80018	-2675	80325	479.1	60.029	0.967907
19800.6	-77450	0	29.230826	-79960	-2880	80387	479.4	59.97	0.968609
19801.1	-77452	0	29.242316	-79914	-2917	80241	478.6	60.02	0.969192
19801.6	-77452	0	29.243547	-80026	-2658	80308	478.3	60.029	0.967835
19802.1	-77450	0	29.243752	-80032	-2787	80394	478.4	60.02	0.967738
19802.6	-77449	0	29.243957	-79953	-2989	80361	478.8	60	0.968682
19803.1	-77452	0	29.249086	-79903	-2883	80197	478.6	60	0.969325
19803.6	-77453	0	29.249497	-80038	-2709	80332	478.4	60.029	0.967703
19804.1	-77450	0	29.249702	-80020	-2869	80443	478.4	60.02	0.967883
19804.6	-77449	0	29.249907	-79950	-2940	80336	478.3	59.99	0.968718
19805.1	-77451	0	29.260166	-79906	-2751	80197	478.2	60.02	0.969276
19805.6	-77454	0	29.261192	-79992	-2615	80317	478	60.02	0.968272
19806.1	-77451	0	29.261192	-80041	-2915	80461	478.2	60	0.967642
19806.6	-77447	0	29.261397	-80007	-2905	80309	479	60.02	0.968003
19807.1	-77449	0	29.261807	-79898	-2696	80185	478.2	60	0.969348
19807.6	-77452	0	29.262628	-79945	-2912	80382	477.8	60.02	0.968816
19808.1	-77452	0	29.262833	-80041	-2912	80440	478.6	60	0.967654
19808.6	-77449	0	29.263038	-80016	-2793	80304	478.3	60.02	0.967919
19809.1	-77449	0	29.270895	-79937	-2609	80240	478.5	60.029	0.968875
19809.6	-77452	0	29.270895	-79940	-2870	80377	478.1	59.99	0.968877
19810.1	-77452	0	29.270895	-80018	-2884	80378	478.7	59.99	0.967932
19810.6	-77450	0	29.2711	-80017	-2687	80288	478.2	60	0.967919
19811.1	-77449	0	29.280478	-79918	-2693	80251	478.4	60	0.969106
19811.6	-77451	0	29.281299	-79947	-2944	80352	478.5	59.97	0.968779
19812.1	-77453	0	29.281504	-80002	-2801	80304	478.9	59.99	0.968138
19812.6	-77452	0	29.281709	-79979	-2691	80272	478.9	59.97	0.968404
19813.1	-77450	0	29.288275	-80034	-2798	80411	478	59.99	0.967714
19813.6	-77448	0	29.2893	-79975	-2951	80352	478.8	59.99	0.968403
19814.1	-77450	0	29.2893	-79885	-2734	80194	478.8	59.99	0.969519
19814.6	-77454	0	29.289506	-79990	-2642	80308	478.4	59.97	0.968296

19815.1	-77452	0	29.299559	-80028	-2828	80445	478.4	59.99	0.967811
19815.6	-77449	0	29.299969	-80036	-2829	80358	478.5	59.99	0.967677
19816.1	-77449	0	29.300175	-79903	-2598	80171	478.8	59.99	0.969288
19816.6	-77452	0	29.300585	-79956	-2673	80347	478	59.99	0.968683
19817.1	-77450	0	29.300995	-80016	-2879	80425	478.4	59.99	0.967931
19817.6	-77448	0	29.301816	-79959	-2803	80256	478.3	59.97	0.968596
19818.1	-77450	0	29.302021	-79906	-2572	80189	478.7	60	0.969264
19818.6	-77452	0	29.302021	-80016	-2772	80446	478	59.99	0.967956
19819.1	-77451	0	29.308176	-80022	-2877	80400	478.5	60	0.967871
19819.6	-77449	0	29.308382	-80004	-2705	80292	478.3	60.02	0.968064
19820.1	-77450	0	29.308382	-79937	-2528	80243	478.6	60	0.968888
19820.6	-77452	0	29.308587	-79919	-2886	80339	479.1	59.97	0.969131
19821.1	-77452	0	29.31823	-80030	-2801	80353	478.5	59.99	0.967787
19821.6	-77450	0	29.319051	-80033	-2605	80306	478.8	60	0.967726
19822.1	-77448	0	29.319051	-79918	-2722	80273	478.9	59.99	0.969093
19822.6	-77452	0	29.319051	-79908	-2884	80307	479.3	59.99	0.969265
19823.1	-77453	0	29.326907	-80043	-2812	80328	478.7	59.99	0.967642
19823.6	-77452	0	29.327728	-79990	-2558	80279	479.1	60.02	0.968271
19824.1	-77450	0	29.327933	-80033	-2827	80466	478.5	60.02	0.967726
19824.6	-77450	0	29.328344	-79907	-2864	80289	479	60.02	0.969252
19825.1	-77453	0	29.338542	-79976	-2619	80275	478.5	59.99	0.968453
19825.6	-77452	0	29.339158	-80017	-2554	80325	478.5	60	0.967944
19826.1	-77449	0	29.339158	-80053	-2840	80466	478.7	60	0.967472
19826.6	-77449	0	29.339363	-79919	-2726	80223	478.8	60.02	0.969094
19827.1	-77451	0	29.339773	-79903	-2561	80177	478.8	60	0.969313
19827.6	-77453	0	29.340799	-80012	-2656	80392	478.1	60	0.968017
19828.1	-77451	0	29.341004	-80020	-2840	80413	478.8	60	0.967896
19828.6	-77448	0	29.341004	-80005	-2732	80279	479.4	60	0.968039
19829.1	-77450	0	29.34804	-79931	-2507	80220	478.6	60	0.968961
19829.5	-77452	0	29.348245	-79908	-2775	80341	479.4	60	0.969265
19830.1	-77452	0	29.348245	-79908	-2775	80341	479.4	60	0.969265
19830.6	-77451	0	29.348245	-80039	-2633	80307	480.2	59.99	0.967666
19831.1	-77447	0	29.357478	-79945	-2615	80266	480.3	60	0.968754
19831.6	-77448	0	29.358094	-79952	-2911	80365	480.8	59.99	0.968681
19832.1	-77451	0	29.358094	-79917	-2871	80221	481.5	60.029	0.969143
19832.6	-77453	0	29.358299	-80000	-2608	80282	481.9	60.02	0.968163
19833.1	-77450	0	29.364394	-80047	-2844	80460	482	60.029	0.967557
19833.6	-77448	0	29.365625	-79948	-2691	80335	482.3	60.02	0.96873
19834.1	-77450	0	29.36583	-79939	-2782	80234	481.6	60	0.968864
19834.6	-77453	0	29.36624	-79917	-2606	80196	481.8	60.02	0.969168
19835.0	-77450	0	29.376439	-80068	-2895	80494	481.9	60.02	0.967303
19835.6	-77450	0	29.376439	-80068	-2895	80494	481.9	60.02	0.967303
19836.1	-77450	0	29.377465	-79930	-2589	80196	482	60	0.968973
19836.6	-77452	0	29.37767	-79969	-2637	80326	481.9	60.02	0.968525
19837.1	-77450	0	29.37814	-80016	-2914	80426	481.6	59.99	0.967931
19837.6	-77445	0	29.378961	-79940	-2796	80206	481.7	60	0.968789
19838.1	-77449	0	29.378961	-79886	-2673	80143	482.2	60	0.969494
19838.6	-77452	0	29.378961	-79918	-2791	80304	481.5	60.02	0.969143
19839.1	-77453	0	29.386553	-80012	-2849	80374	481.6	60	0.968017
19839.6	-77450	0	29.386963	-80007	-2688	80283	481.7	60	0.96804
19840.1	-77449	0	29.386963	-79898	-2633	80182	481.5	60.02	0.969348
19840.6	-77452	0	29.386963	-79914	-2507	80179	481.2	60	0.969192
19841.1	-77451	0	29.395375	-80008	-2787	80317	481.1	60.04	0.968041
19841.6	-77448	0	29.396196	-80001	-2582	80239	481	60.02	0.968088
19842.1	-77450	0	29.396401	-79896	-2734	80268	481	60.02	0.969385
19842.6	-77453	0	29.396811	-79982	-2845	80357	480.5	60.02	0.96838
19843.1	-77452	0	29.403787	-80034	-2736	80298	480.8	60	0.967739
19843.6	-77449	0	29.404403	-79986	-2539	80243	481	60.029	0.968282
19844.1	-77450	0	29.404608	-79907	-2860	80314	481.2	60	0.969252
19844.6	-77454	0	29.405018	-79958	-2821	80317	480.8	60.029	0.968684
19845.1	-77453	0	29.415747	-80003	-2628	80253	480.9	60.02	0.968126
19845.6	-77451	0	29.416773	-79998	-2561	80268	480.4	60.029	0.968162
19846.1	-77449	0	29.416773	-80037	-2832	80413	480.7	60	0.967665
19846.6	-77450	0	29.416979	-79882	-2756	80170	480.6	60.02	0.969555
19847.1	-77452	0	29.417329	-79945	-2709	80229	480.5	60.04	0.968816
19847.6	-77451	0	29.418149	-79971	-2704	80318	480	60.029	0.968489
19848.1	-77450	0	29.418354	-80017	-2835	80384	480.1	60	0.967919
19848.6	-77449	0	29.418354	-79900	-2711	80161	480.8	60.02	0.969324
19849.1	-77452	0	29.425535	-79939	-2663	80188	480.3	60.029	0.968889
19849.6	-77452	0	29.425741	-79990	-2521	80250	480.3	60.04	0.968271
19850.1	-77449	0	29.425741	-80033	-2782	80366	480.3	60	0.967713
19850.6	-77450	0	29.425946	-79944	-2604	80199	480.9	60.02	0.968803
19851.1	-77452	0	29.433537	-79940	-2659	80289	481.3	60	0.968877
19851.6	-77453	0	29.433742	-80049	-2794	80450	481.5	59.99	0.96757
19852.0	-77449	0	29.433948	-80019	-2739	80299	481.9	60.029	0.967883
19852.5	-77449	0	29.433948	-80019	-2739	80299	481.9	60.029	0.967883
19853.0	-77451	0	29.44236	-79965	-3828	80270	481.8	60.029	0.968561
19853.5	-77453	0	29.44318	-79993	-3526	80275	482.4	60.02	0.968247
19854.0	-77451	0	29.44318	-80083	-3807	80502	482.1	60	0.967134
19854.5	-77448	0	29.443591	-80030	-2740	80284	482.4	60.02	0.967737
19855.0	-77448	0	29.453439	-79951	-3529	80219	482.5	60.02	0.968693
19855.5	-77450	0	29.454055	-79958	-3606	80250	482.5	60.02	0.968634

19856.0	-77453	0	29.454465	-79986	-3750	80406	482.5	60	0.968332
19856.5	-77450	0	29.45467	-80095	-3844	80416	482.4	60.02	0.966977
19857.1	-77450	0	29.45467	-80095	-3844	80416	482.4	60.02	0.966977
19857.6	-77451	0	29.455491	-79920	-2893	80273	482.4	59.99	0.969107
19858.1	-77455	0	29.455696	-79983	-2739	80257	482.2	60.029	0.968393
19858.6	-77452	0	29.455901	-80005	-2753	80372	482.3	60.02	0.968089
19859.1	-77451	0	29.462877	-80029	-2827	80375	482	60.04	0.967787
19859.6	-77448	0	29.463287	-79970	-2639	80224	482.2	60.02	0.968463
19860.1	-77450	0	29.463287	-79930	-2672	80186	482	60.029	0.968973
19860.6	-77454	0	29.463287	-80016	-2744	80424	481.9	60.02	0.967981
19861.1	-77451	0	29.472725	-80029	-2758	80332	481.7	60.029	0.967787
19861.6	-77448	0	29.473751	-79992	-2493	80228	482.2	60.02	0.968197
19862.1	-77450	0	29.473751	-79910	-2624	80265	481.9	60.029	0.969215
19862.6	-77452	0	29.473956	-79949	-2731	80306	482	60.02	0.968768
19863.1	-77451	0	29.480522	-80028	-2704	80298	482.3	60.029	0.967799
19863.5	-77448	0	29.481343	-79937	-2530	80190	482.3	60.029	0.968863
19864.1	-77448	0	29.481343	-79937	-2530	80190	482.3	60.029	0.968863
19864.6	-77452	0	29.481753	-79949	-2861	80342	483	60	0.968768
19865.1	-77450	0	29.492217	-80038	-2607	80298	482.5	60.029	0.967665
19865.6	-77449	0	29.492832	-79913	-2570	80190	483.2	60.029	0.969166
19866.1	-77451	0	29.492832	-79936	-2851	80325	483.1	60.02	0.968913
19866.6	-77453	0	29.493243	-80028	-2726	80314	483.3	60.02	0.967824
19867.1	-77450	0	29.493653	-80003	-2532	80255	483.8	60.029	0.968089
19867.6	-77448	0	29.494474	-79965	-2624	80198	483.5	60.02	0.968524
19868.1	-77451	0	29.494474	-79918	-2889	80289	483.5	60.04	0.969131
19868.6	-77452	0	29.494474	-80027	-2710	80292	483.6	60.02	0.967823
19869.1	-77448	0	29.50145	-79998	-2532	80256	483.6	60.04	0.968124
19869.6	-77449	0	29.501655	-79973	-2790	80376	483.6	60.04	0.968439
19870.1	-77450	0	29.501655	-79958	-2769	80273	483.5	60.04	0.968634
19870.6	-77452	0	29.50186	-80007	-2580	80258	483.9	60.04	0.968065
19871.1	-77449	0	29.511648	-80029	-2558	80342	483.9	60	0.967762
19871.6	-77448	0	29.512468	-79956	-2818	80342	483.8	60.04	0.968633
19872.1	-77451	0	29.512468	-79936	-2715	80206	484.3	60.02	0.968913
19872.6	-77453	0	29.512879	-79992	-2545	80271	483.5	60.02	0.968259
19873.1	-77450	0	29.518745	-80015	-2650	80270	484.3	60.04	0.967944
19873.6	-77448	0	29.519771	-79958	-2790	80324	484.2	60.02	0.968609
19874.1	-77450	0	29.519976	-79951	-2670	80216	483.7	60.02	0.968718
19874.6	-77451	0	29.520181	-79916	-2547	80194	484	60.06	0.969155
19875.1	-77453	0	29.53085	-80004	-2789	80434	483.9	60	0.968114
19875.6	-77450	0	29.531671	-80064	-2954	80441	484.2	60.04	0.967351
19876.1	-77447	0	29.531876	-79958	-2555	80198	484	60.06	0.968596
19876.6	-77448	0	29.532081	-79927	-2615	80262	484	60.029	0.968984
19877.1	-77450	0	29.532081	-79910	-2804	80298	483.9	60.029	0.969215
19877.6	-77452	0	29.532902	-79971	-3003	80365	483.9	60.02	0.968501
19878.1	-77448	0	29.533107	-79998	-2473	80249	483.9	60.029	0.968124
19878.6	-77449	0	29.533312	-79954	-2728	80331	483.5	60.029	0.968669
19879.1	-77450	0	29.538586	-79908	-2813	80254	484	60.029	0.96924
19879.6	-77453	0	29.538586	-80020	-2650	80301	484.4	60.02	0.967921
19880.1	-77449	0	29.538586	-80024	-2535	80292	483.7	60.04	0.967822
19880.6	-77446	0	29.538586	-79990	-2803	80369	483.6	60.029	0.968196
19881.1	-77447	0	29.548845	-79936	-2738	80230	484.8	60.029	0.968863
19881.6	-77447	0	29.549665	-79969	-2569	80212	484.9	60.029	0.968463
19882.1	-77448	0	29.549665	-79962	-2658	80276	485.2	60.06	0.96856
19882.6	-77447	0	29.54987	-79982	-2853	80347	485.7	60.02	0.968305
19883.1	-77447	0	29.556231	-79976	-2713	80240	486.1	60.06	0.968378
19883.6	-77447	0	29.557462	-79947	-2545	80199	486.2	60.04	0.968729
19884.1	-77448	0	29.557667	-80002	-2804	80391	485.7	60.04	0.968076
19884.6	-77447	0	29.558077	-79941	-2824	80277	486.3	60.029	0.968802
19885.1	-77447	0	29.567721	-80009	-2655	80268	485.9	60.029	0.967979
19885.6	-77446	0	29.568131	-79957	-2646	80264	486.2	60.029	0.968596
19886.1	-77446	0	29.568131	-79994	-2810	80280	486.1	60.029	0.968148
19886.6	-77445	0	29.568541	-79958	-2779	80241	486.3	60.029	0.968571
19887.1	-77445	0	29.568746	-79967	-2522	80216	485.5	60.04	0.968462
19887.6	-77444	0	29.569567	-79976	-2751	80361	486	60.029	0.968341
19888.1	-77444	0	29.569772	-79990	-2864	80348	486.4	60.02	0.968171
19888.6	-77444	0	29.569977	-79969	-2692	80221	486.2	60.029	0.968425
19889.1	-77444	0	29.576133	-79970	-2572	80238	485.7	60.029	0.968413
19889.6	-77443	0	29.576543	-80003	-2800	80393	486.1	59.99	0.968001
19890.1	-77443	0	29.576543	-80007	-3050	80392	486.2	60.04	0.967953
19890.6	-77441	0	29.576543	-80003	-2617	80242	486.3	60.029	0.967976
19891.1	-77441	0	29.588648	-79979	-2630	80284	486.2	60.04	0.968267
19891.6	-77444	0	29.589674	-79999	-2826	80391	486.2	60.02	0.968062
19892.1	-77443	0	29.589674	-79965	-2749	80247	486.4	60.04	0.968461
19892.6	-77443	0	29.589879	-79952	-2513	80212	486.3	60.029	0.968619
19893.1	-77442	0	29.595009	-80008	-2724	80370	485.7	60.02	0.967928
19893.6	-77441	0	29.595829	-79957	-2835	80339	486.1	60.02	0.968533
19894.1	-77440	0	29.595829	-80000	-2688	80282	486.7	60.02	0.968
19894.6	-77440	0	29.596034	-79956	-2518	80249	486.5	60.029	0.968533
19895.1	-77439	0	29.605328	-80013	-2842	80417	486.3	60.029	0.96783
19895.6	-77437	0	29.606149	-79988	-2801	80317	486.4	60.06	0.968108
19896.1	-77435	0	29.606354	-79994	-2603	80249	486.7	60.02	0.96801
19896.6	-77435	0	29.606559	-79961	-2604	80277	486.7	60.06	0.96841

19897.1	-77434	0	29.606969	-79995	-2829	80390	486.5	60.029	0.967985
19897.6	-77433	0	29.60779	-79983	-2724	80258	487.3	60.02	0.968118
19898.1	-77433	0	29.60779	-79959	-2520	80234	486.7	60.04	0.968409
19898.6	-77433	0	29.60779	-80015	-2704	80420	486.6	60.029	0.967731
19899.1	-77431	0	29.615321	-79970	-2802	80347	486.6	60.029	0.968251
19899.6	-77431	0	29.615731	-79988	-2651	80270	486.7	60.029	0.968033
19900.1	-77429	0	29.615731	-79992	-2537	80285	486.9	60.029	0.967959
19900.6	-77428	0	29.615731	-80029	-2770	80424	487	60.029	0.967499
19901.1	-77426	0	29.626461	-80002	-2759	80305	486.8	60.02	0.967801
19901.6	-77425	0	29.627282	-79996	-2521	80241	486.8	60.029	0.967861
19902.1	-77424	0	29.627282	-79951	-2663	80313	486.8	60.02	0.968393
19902.6	-77423	0	29.627487	-80024	-2991	80374	486.4	60.04	0.967497
19903.1	-77422	0	29.634257	-79974	-2708	80234	486.4	60.02	0.96809
19903.6	-77421	0	29.635078	-79987	-2512	80267	486.3	60.029	0.96792
19904.1	-77421	0	29.635283	-79962	-2759	80361	486.6	60	0.968222
19904.6	-77420	0	29.635488	-79986	-2778	80338	486.3	60.029	0.967919
19905.1	-77420	0	29.64466	-79998	-2587	80251	486.5	60	0.967774
19905.6	-77418	0	29.645481	-80007	-2581	80291	486.4	60.02	0.96764
19906.1	-77417	0	29.645686	-80016	-2770	80402	486	60.029	0.967519
19906.6	-77416	0	29.645892	-80017	-2721	80280	486.2	59.99	0.967494
19907.1	-77415	0	29.646302	-79971	-2501	80243	486.1	60.02	0.968038
19907.6	-77414	0	29.646917	-79999	-2690	80358	485.5	60.029	0.967687
19908.1	-77414	0	29.646917	-79961	-2787	80341	485.8	60.02	0.968147
19908.6	-77413	0	29.647123	-79970	-2651	80245	486	60.029	0.968026
19909.1	-77413	0	29.654304	-79976	-2480	80246	486	60.02	0.967953
19909.6	-77413	0	29.654509	-79979	-2758	80387	485.2	59.99	0.967917
19910.1	-77413	0	29.654509	-79999	-2749	80318	485.4	60.02	0.967675
19910.6	-77412	0	29.654509	-79959	-2540	80230	485.5	60	0.968146
19911.1	-77411	0	29.664767	-79956	-2563	80274	485.4	60.02	0.96817
19911.6	-77411	0	29.665383	-79961	-2778	80351	485.4	60	0.968109
19912.1	-77411	0	29.665588	-79996	-2694	80283	485.1	60.02	0.967686
19912.6	-77410	0	29.665998	-79967	-2451	80224	485.7	60.02	0.968024
19913.1	-77410	0	29.672769	-79977	-2646	80352	485.2	60.02	0.967903
19913.6	-77410	0	29.674	-79978	-2755	80343	485.3	60	0.967891
19914.1	-77410	0	29.674205	-79960	-2612	80242	485.6	60.02	0.968109
19914.6	-77410	0	29.674205	-79973	-2504	80272	485.3	60.02	0.967952
19915.1	-77409	0	29.684464	-80009	-2728	80408	485.5	60.02	0.967504
19915.6	-77408	0	29.684874	-79991	-2719	80298	485	60	0.967709
19916.1	-77407	0	29.684874	-79961	-2504	80203	484.8	60.02	0.968059
19916.6	-77408	0	29.685285	-79974	-2547	80310	485.3	60.02	0.967915
19917.1	-77408	0	29.68549	-79959	-2786	80359	485	60.029	0.968096
19917.6	-77409	0	29.686311	-79948	-2655	80223	484.6	59.99	0.968242
19918.1	-77409	0	29.686516	-79962	-2443	80219	484.7	60.029	0.968072
19918.6	-77410	0	29.686721	-79999	-2670	80408	484.1	60.029	0.967637
19919.1	-77410	0	29.692876	-79948	-2732	80300	484.7	60	0.968254
19919.6	-77410	0	29.692876	-79966	-2544	80245	483.8	60	0.968036
19920.1	-77410	0	29.692876	-79926	-2477	80202	484.5	60.04	0.968521
19920.6	-77411	0	29.693081	-80005	-2740	80407	483.6	60.02	0.967577
19921.1	-77410	0	29.703135	-79956	-2663	80239	483.7	60.02	0.968157
19921.6	-77410	0	29.703956	-79952	-2446	80209	483.1	60	0.968206
19922.1	-77411	0	29.703956	-79913	-2539	80260	483.1	60.02	0.968691
19922.6	-77413	0	29.703956	-79953	-2696	80317	482.5	60.02	0.968231
19923.1	-77415	0	29.71005	-79950	-2553	80211	482.4	60.02	0.968293
19923.6	-77416	0	29.71087	-79905	-2381	80171	481.8	60.029	0.968851
19924.1	-77419	0	29.711076	-79978	-2650	80376	481.5	60.029	0.968004
19924.6	-77419	0	29.711486	-79923	-2657	80275	481.5	60.02	0.96867
19925.1	-77422	0	29.720924	-79936	-2459	80198	482	60.02	0.96855
19925.6	-77423	0	29.721745	-79961	-2425	80248	481.6	60.02	0.96826
19926.1	-77424	0	29.721745	-79960	-2691	80348	482.2	60.02	0.968284
19926.6	-77425	0	29.722155	-79958	-2613	80232	482.1	60.029	0.968321
19927.1	-77426	0	29.72236	-79947	-2400	80197	482.5	60.04	0.968467
19927.6	-77426	0	29.723181	-79952	-2571	80324	482.6	60	0.968406
19928.1	-77427	0	29.723386	-79952	-2727	80315	483.1	59.99	0.968419
19928.6	-77428	0	29.723386	-79958	-2580	80222	483.2	60.02	0.968358
19929.1	-77429	0	29.732475	-79942	-2412	80204	483.5	60.029	0.968565
19929.6	-77430	0	29.732885	-79975	-2707	80381	483.4	60.029	0.968178
19930.1	-77430	0	29.732885	-79996	-3228	80406	483.3	60	0.967923
19930.6	-77430	0	29.732885	-79952	-2464	80204	483.3	60	0.968456
19931.1	-77431	0	29.741092	-79961	-2486	80274	482.7	60.029	0.96836
19931.6	-77431	0	29.741913	-79952	-2680	80326	482.9	60.029	0.968469
19932.1	-77432	0	29.742323	-79970	-2604	80226	482.6	60.02	0.968263
19932.6	-77433	0	29.742528	-79935	-2409	80189	482.1	60.02	0.9687
19933.1	-77435	0	29.749216	-79945	-2553	80322	482	60.04	0.968603
19933.6	-77437	0	29.750242	-79933	-2667	80296	481.9	60.04	0.968774
19934.1	-77438	0	29.750447	-79914	-2515	80177	481.8	60	0.969017
19934.6	-77442	0	29.750857	-79927	-2392	80195	481.5	60.029	0.968909
19935.1	-77443	0	29.761526	-79956	-2645	80339	481.4	60.02	0.96857
19935.6	-77444	0	29.762142	-79951	-2629	80237	481.7	60.04	0.968643
19936.1	-77445	0	29.762142	-79914	-2418	80160	481.5	59.99	0.969104
19936.6	-77447	0	29.762552	-79939	-2472	80246	481	60.04	0.968826
19937.1	-77449	0	29.762757	-79927	-2647	80301	481.2	60.029	0.968997
19937.6	-77450	0	29.763578	-79928	-2565	80187	481	60.04	0.968997

19938.1	-77452	0	29.763578	-79974	-2340	80222	481.2	60.02	0.968465
19938.6	-77451	0	29.763578	-80028	-2561	80395	480.9	60.029	0.967799
19939.1	-77447	0	29.769467	-79976	-2656	80309	481	60	0.968378
19939.6	-77449	0	29.769467	-79944	-2492	80207	481.6	60.029	0.968791
19940.1	-77450	0	29.769467	-79911	-2353	80177	481.1	60.02	0.969203
19940.6	-77452	0	29.769467	-80028	-2629	80416	481.2	60.029	0.967811
19941.1	-77448	0	29.779931	-80001	-2604	80293	481.2	60.02	0.968088
19941.6	-77448	0	29.780957	-79939	-2381	80192	481.2	60.04	0.968839
19942.1	-77450	0	29.781162	-79908	-2502	80240	481.4	60.02	0.96924
19942.6	-77452	0	29.781572	-80028	-2680	80412	481	60.02	0.967811
19943.1	-77449	0	29.790189	-80009	-2544	80277	481.3	60.029	0.968004
19943.6	-77448	0	29.79101	-79914	-2339	80168	481.3	60.02	0.969142
19944.1	-77452	0	29.791215	-79924	-2587	80330	480.7	60.02	0.969071
19944.6	-77452	0	29.79142	-80007	-2631	80338	480.4	60.029	0.968065
19945.1	-77450	0	29.801208	-80041	-2413	80310	480.5	60.04	0.967629
19945.6	-77448	0	29.802234	-79876	-2375	80155	479.6	60.02	0.969603
19946.1	-77451	0	29.802234	-79964	-2624	80328	479.3	60	0.968573
19946.6	-77452	0	29.802234	-79987	-2534	80268	478.8	60.02	0.968307
19947.1	-77450	0	29.802644	-80019	-2313	80270	478.8	60	0.967895
19947.6	-77449	0	29.803054	-79924	-2483	80283	478.3	60.02	0.969033
19948.1	-77453	0	29.803054	-79981	-2608	80348	478.7	60.04	0.968392
19948.6	-77451	0	29.803259	-80002	-2451	80282	477.6	60.02	0.968113
19949.1	-77449	0	29.808245	-80005	-2310	80283	478.7	60	0.968052
19949.6	-77449	0	29.808245	-79924	-2558	80318	478	60.029	0.969033
19950.1	-77451	0	29.808245	-79982	-2557	80308	477.6	60.029	0.968355
19950.6	-77450	0	29.80845	-80018	-2339	80262	478	60	0.967907
19951.1	-77448	0	29.820084	-79920	-2360	80224	477.5	60.029	0.969069
19951.6	-77450	0	29.820904	-79947	-2592	80322	477.8	59.99	0.968767
19952.1	-77451	0	29.821109	-79967	-2518	80238	478	60.029	0.968537
19952.6	-77450	0	29.821315	-80029	-2300	80291	477.1	60.02	0.967774
19953.1	-77448	0	29.827059	-79916	-2483	80262	477.9	60.029	0.969118
19953.6	-77451	0	29.82788	-79927	-2574	80283	477.6	59.99	0.969022
19954.1	-77453	0	29.828085	-79992	-2410	80258	478	60	0.968259
19954.6	-77451	0	29.828291	-80030	-2283	80309	477.4	60.029	0.967775
19955.1	-77448	0	29.837523	-79987	-2577	80353	477.3	60.029	0.968257
19955.6	-77450	0	29.838754	-79915	-2537	80202	477.5	60	0.969155
19956.1	-77452	0	29.838754	-79984	-2322	80236	477.7	60	0.968344
19956.6	-77450	0	29.839165	-79994	-2425	80328	478.3	60.029	0.968198
19957.1	-77449	0	29.83937	-79943	-2621	80306	478.2	59.99	0.968803
19957.5	-77451	0	29.839985	-79918	-2510	80194	477.6	60.02	0.969131
19957.5	-77451	0	29.839985	-79918	-2510	80194	477.6	60.02	0.969131
19958.0	-77452	0	29.840191	-80046	-4177	80469	478.1	60.02	0.967594
19958.5	-77450	0	29.840191	-80062	-3017	80327	478	60.02	0.967375
19959.0	-77448	0	29.847782	-80001	-3932	80305	478.5	60.029	0.968088
19959.5	-77450	0	29.847721	-79950	-3243	80327	477.8	60.02	0.96873
19960.0	-77453	0	29.847721	-79942	-3022	80236	477.8	60.02	0.968865
19960.5	-77451	0	29.847926	-80035	-3033	80324	477.8	60.02	0.967714
19961.0	-77448	0	29.857774	-80088	-3980	80412	477.9	60	0.967036
19961.5	-77449	0	29.858595	-79954	-3182	80258	477.6	60.02	0.968669
19962.0	-77452	0	29.859005	-79960	-2959	80238	476.5	60	0.968634
19962.5	-72164	0	29.85921	-76706	-3333	76620	477.7	60	0.940787
19963.0	-72152	0	29.865099	-74492	-3408	74895	479.1	59.99	0.968587
19963.5	-72177	0	29.86592	-74551	-4255	75031	479	60	0.968156
19964.0	-72199	0	29.866125	-74577	-3093	74885	479.1	60.02	0.968113
19964.5	-72220	0	29.866535	-74586	-3351	75027	479.2	60	0.968278
19965.0	-72241	0	29.877676	-74571	-3360	74943	478.4	59.99	0.968755
19965.5	-72262	0	29.878291	-74582	-3041	74866	478.8	60.02	0.968893
19966.0	-72279	0	29.878702	-74688	-3170	75001	478.6	60.02	0.967746
19966.5	-72295	0	29.878907	-74679	-3404	75092	479.1	59.99	0.968077
19967.0	-72311	0	29.878907	-74677	-3311	74979	478.6	60.029	0.968317
19967.5	-72331	0	29.879523	-74667	-3098	74951	478.7	60.029	0.968714
19968.0	-72347	0	29.879523	-74689	-3287	75078	478.1	60.02	0.968643
19968.5	-72362	0	29.879728	-74705	-3407	75118	478.7	60	0.968637
19969.0	-72374	0	29.886149	-74797	-3208	75106	479	60.029	0.967606
19969.5	-72384	0	29.886149	-74772	-3070	75071	478.9	60.06	0.968063
19970.0	-72395	0	29.886355	-74814	-3369	75241	477.8	60.029	0.967666
19970.5	-72405	0	29.886355	-74792	-3370	75130	478.6	60.029	0.968085
19971.0	-72415	0	29.895854	-74782	-3050	75055	478	60.029	0.968348
19971.5	-72426	0	29.896675	-74772	-3193	75144	478.9	60.029	0.968625
19972.0	-72435	0	29.897085	-74805	-3351	75189	478.5	60.02	0.968318
19972.5	-72449	0	29.89729	-74800	-4317	75268	479.2	59.99	0.96857
19973.0	-72459	0	29.90365	-74790	-3030	75081	478.9	60	0.968833
19973.5	-72467	0	29.904266	-74915	-3388	75314	479.1	60	0.967323
19974.0	-72472	0	29.904676	-74924	-4229	75398	479.4	60.029	0.967274
19974.5	-72478	0	29.904881	-74889	-3271	75198	479.1	60.029	0.967806
19975.0	-72484	0	29.913355	-74855	-3140	75156	479.4	60.02	0.968325
19975.5	-72489	0	29.913765	-74917	-3440	75319	479.1	60.02	0.967591
19976.0	-72494	0	29.914176	-74897	-3318	75191	479.8	60.04	0.967916
19976.5	-72499	0	29.914381	-74924	-4218	75310	479.9	60.029	0.967634
19977.0	-72503	0	29.914791	-74874	-3277	75232	480.3	60	0.968333
19977.5	-72510	0	29.915407	-74900	-3450	75308	480	60.02	0.968091
19978.0	-72516	0	29.915612	-74875	-3318	75169	480	60.02	0.968494

19978.5	-72521	0	29.915817	-74871	-3201	75163	480.8	60.029	0.968613
19979.0	-72527	0	29.922177	-74909	-3408	75336	480.7	60.029	0.968201
19979.5	-72532	0	29.922177	-74903	-3478	75286	480.6	60.02	0.968346
19980.0	-72537	0	29.922383	-74897	-3180	75169	480.7	60	0.96849
19980.5	-72542	0	29.922588	-74880	-3248	75186	480.6	60	0.968777
19981.0	-72549	0	29.931759	-74891	-3481	75315	480.8	60.02	0.968728
19981.5	-72554	0	29.93217	-74920	-3321	75241	480.5	60.02	0.96842
19982.0	-72555	0	29.932375	-74999	-3280	75288	480.6	60.029	0.967413
19982.5	-72555	0	29.932375	-74952	-3401	75339	480.1	60.029	0.96802
19983.0	-72557	0	29.939494	-75018	-3475	75415	481.1	60.02	0.967195
19983.5	-72556	0	29.940315	-74970	-3309	75263	480.4	60.02	0.9678
19984.0	-72557	0	29.940931	-74988	-3148	75284	480.9	60.04	0.967581
19984.5	-72558	0	29.941136	-74956	-3484	75382	480.8	60.04	0.968008
19985.0	-72559	0	29.949958	-75002	-3479	75390	480.8	60.02	0.967428
19985.5	-72560	0	29.950635	-74983	-3245	75260	480.3	60	0.967686
19986.0	-72560	0	29.951251	-75000	-3259	75330	480.5	60.02	0.967467
19986.5	-72561	0	29.951661	-74983	-3556	75395	480.9	60	0.967699
19987.0	-72561	0	29.951866	-75011	-3376	75297	481.4	60	0.967338
19987.5	-72562	0	29.952482	-74965	-3242	75251	480.5	60.029	0.967945
19988.0	-72563	0	29.952687	-74991	-3418	75391	480.9	60.02	0.967623
19988.5	-72564	0	29.952892	-75014	-3619	75408	480.7	60.02	0.967339
19989.0	-72564	0	29.958432	-74974	-3359	75276	480.6	60.02	0.967856
19989.5	-72566	0	29.958637	-74963	-3291	75272	481	60.029	0.968024
19990.0	-72565	0	29.958637	-75036	-3515	75462	480.9	60.029	0.967069
19990.5	-72565	0	29.958637	-75010	-3594	75362	481.1	60	0.967404
19991.0	-72565	0	29.967808	-75005	-3291	75281	481	60.02	0.967469
19991.5	-72565	0	29.968424	-74982	-3320	75356	481.4	60.02	0.967766
19992.0	-72566	0	29.968629	-74999	-3622	75419	481.2	60	0.96756
19992.5	-72566	0	29.968834	-75012	-3430	75324	481.5	60.029	0.967392
19993.0	-72566	0	29.974784	-74956	-3185	75239	481.3	60.029	0.968115
19993.5	-72567	0	29.9754	-75012	-3558	75428	481.4	60.029	0.967405
19994.0	-72566	0	29.976015	-74982	-3565	75379	481.4	60.02	0.967779
19994.5	-72567	0	29.97622	-74968	-3377	75276	481.3	60.029	0.967973
19995.0	-72567	0	29.985248	-74962	-3233	75267	481.5	60.029	0.96805
19995.5	-72568	0	29.985658	-75017	-3584	75443	481	60.02	0.967354
19996.0	-72568	0	29.985864	-75001	-3529	75334	481.5	60	0.96756
19996.5	-72568	0	29.986274	-74973	-3207	75257	481	60.02	0.967922
19997.0	-72569	0	29.986479	-74974	-3448	75333	480.9	60.02	0.967922
19997.5	-72570	0	29.987095	-75039	-3623	75444	481.4	60	0.967097
19998.0	-72570	0	29.9873	-74984	-3489	75305	481	60.029	0.967806
19998.5	-72570	0	29.9873	-74975	-3260	75266	480.6	60	0.967923
19999.0	-72571	0	29.994624	-74983	-3529	75425	481	60.02	0.967833
19999.5	-72571	0	29.994624	-74973	-3542	75347	480.7	60.029	0.967962
20000.0	-72572	0	29.994624	-74987	-3291	75279	480.8	60.029	0.967794
20000.5	-72573	0	29.994624	-74945	-3325	75258	480.5	60.02	0.96835
20001.0	-72574	0	30.003857	-75017	-3531	75434	480.8	59.97	0.967434
20001.5	-72574	0	30.004883	-74973	-3431	75306	480.6	59.99	0.968002
20002.0	-72575	0	30.005088	-74992	-3203	75262	480.5	60.029	0.96777
20002.5	-72576	0	30.005293	-74974	-3463	75370	480.5	60.02	0.968016
20003.0	-72577	0	30.011038	-74978	-3645	75388	480.4	60.029	0.967977
20003.5	-72578	0	30.011859	-74948	-3470	75255	480.7	59.99	0.968378
20004.0	-72580	0	30.012269	-74988	-3350	75283	480.3	59.99	0.967888
20004.5	-72581	0	30.012475	-74987	-3589	75405	480.2	60	0.967914
20005.0	-72582	0	30.021564	-74986	-3541	75358	480.6	60.02	0.967941
20005.5	-72583	0	30.021769	-74982	-3303	75264	480.1	60	0.968006
20006.0	-72583	0	30.021974	-74991	-3343	75327	480.9	60.04	0.967889
20006.5	-72584	0	30.021974	-74999	-3636	75419	480.1	60	0.9678
20007.0	-72584	0	30.022384	-74997	-3526	75324	480.2	60.02	0.967825
20007.5	-72585	0	30.023	-74970	-3280	75241	480.7	60.02	0.968187
20008.0	-72586	0	30.023205	-74992	-3563	75384	480.1	59.99	0.967917
20008.5	-72587	0	30.023205	-74977	-3702	75383	480.4	60.029	0.968124
20009.0	-72588	0	30.030797	-74963	-3401	75274	480	60	0.968318
20009.5	-72588	0	30.031207	-74965	-3371	75282	481.8	60.029	0.968292
20010.0	-72589	0	30.031207	-74991	-3564	75405	482	59.99	0.967969
20010.5	-72590	0	30.031412	-74993	-3632	75328	482.1	60	0.967957
20011.0	-72591	0	30.04044	-74973	-3371	75264	482	60.06	0.968229
20011.5	-72592	0	30.041055	-74977	-3522	75340	481.8	60.02	0.96819
20012.0	-72595	0	30.041055	-74875	-3733	75309	482	60	0.969549
20012.5	-72597	0	30.041466	-74988	-3530	75279	480.6	60.02	0.968115
20013.0	-72599	0	30.04721	-74965	-3312	75256	480.6	60.02	0.968439
20013.5	-72599	0	30.048031	-75010	-3568	75429	480.6	60.02	0.967858
20014.0	-72601	0	30.048236	-74966	-3583	75377	480.4	60.02	0.968452
20014.5	-72601	0	30.048236	-74999	-3418	75290	480.4	59.99	0.968026
20015.0	-72602	0	30.058762	-74974	-3327	75288	480.4	60.04	0.968362
20015.5	-72601	0	30.059788	-75029	-3653	75452	480.7	60.029	0.967639
20016.0	-72602	0	30.059788	-74968	-3703	75301	480.3	60.06	0.96844
20016.5	-72603	0	30.060198	-75024	-3348	75301	479.7	60	0.96773
20017.0	-72603	0	30.060403	-74977	-3499	75373	480.4	60.029	0.968337
20017.5	-72604	0	30.061019	-75002	-3714	75399	480.8	60.02	0.968028
20018.0	-72604	0	30.061224	-75018	-3552	75337	480.4	60.02	0.967821
20018.5	-72605	0	30.061429	-74963	-3431	75256	480.5	60	0.968544
20019.0	-72606	0	30.067236	-75044	-3580	75485	480.4	60.02	0.967512

20019.5	-72607	0	30.067441	-74963	-3700	75365	481.6	60	0.968571
20020.0	-72607	0	30.067441	-75019	-3493	75320	481	60.02	0.967848
20020.5	-72607	0	30.067646	-74991	-3446	75314	481.5	60.029	0.96821
20021.0	-72607	0	30.076325	-75027	-3722	75459	481.7	60	0.967745
20021.5	-72606	0	30.07694	-75016	-3663	75342	481.4	60.029	0.967874
20022.0	-72607	0	30.077146	-75000	-3413	75299	482	60.04	0.968093
20022.5	-72606	0	30.077556	-75001	-3592	75393	482.1	60.02	0.968067
20023.1	-72605	0	30.084737	-75048	-3762	75443	483.2	60.02	0.967448
20023.6	-72604	0	30.085968	-75019	-3727	75335	483.1	60.06	0.967808
20024.1	-72603	0	30.085968	-75026	-3506	75339	483.9	60.029	0.967705
20024.6	-72602	0	30.085968	-75035	-3794	75486	484.4	60.04	0.967575
20025.1	-72601	0	30.094872	-75031	-3696	75393	485.5	60.029	0.967613
20025.6	-72599	0	30.095693	-75055	-3472	75327	485.8	60.029	0.967277
20026.1	-72595	0	30.095898	-75052	-3603	75408	486.5	60.06	0.967263
20026.6	-72593	0	30.095898	-75048	-3871	75471	486.7	60.04	0.967288
20027.1	-72591	0	30.096103	-75045	-3728	75368	486.5	60.06	0.9673
20027.6	-72588	0	30.096719	-75048	-3625	75342	487.2	60.06	0.967221
20028.1	-72585	0	30.096924	-75081	-3807	75495	486.8	60.02	0.966756
20028.6	-72583	0	30.097129	-75033	-3891	75444	487.3	60.029	0.967348
20029.1	-72581	0	30.102812	-75058	-3691	75371	486.8	60.06	0.966999
20029.6	-72579	0	30.102812	-75026	-3607	75334	486.8	60.06	0.967385
20030.1	-72576	0	30.102812	-75081	-3833	75498	486.9	60.04	0.966636
20030.6	-72575	0	30.103017	-75030	-3870	75384	487.3	60.06	0.96728
20031.1	-72572	0	30.1134	-75060	-3702	75348	487.1	60.029	0.966853
20031.6	-72570	0	30.114631	-75038	-3678	75408	487.2	60.06	0.96711
20032.1	-72566	0	30.114836	-75096	-3959	75503	487.1	60	0.96631
20032.6	-72563	0	30.114836	-75038	-3808	75347	486.8	60.04	0.967017
20033.1	-72561	0	30.120314	-75048	-3571	75340	486.7	60.06	0.966861
20033.6	-72558	0	30.120519	-75069	-3846	75495	486.8	60	0.966551
20034.1	-72556	0	30.120519	-75060	-3950	75446	486.4	60.06	0.96664
20034.6	-72554	0	30.120929	-75044	-3682	75341	486.7	60.029	0.966819
20035.1	-72552	0	30.129895	-75035	-3608	75336	486.4	60.04	0.966909
20035.6	-72550	0	30.131126	-75089	-3875	75505	486.6	60.02	0.966187
20036.1	-72548	0	30.131126	-75003	-3563	75299	486.7	60.02	0.967268
20036.6	-72551	0	30.131331	-74934	-3586	75212	486.8	60.04	0.968199
20037.1	-72551	0	30.131537	-75038	-3778	75418	486.7	60.04	0.966857
20037.6	-72549	0	30.132152	-75038	-3921	75452	486.9	59.99	0.96683
20038.1	-72548	0	30.132357	-75003	-3879	75284	486.3	60	0.967268
20038.6	-72551	0	30.132562	-74933	-3605	75224	487	60	0.968212
20039.1	-72552	0	30.139743	-75046	-3822	75484	486.1	59.99	0.966767
20039.6	-72550	0	30.139743	-75041	-3898	75433	486.4	60	0.966805
20040.1	-72548	0	30.139743	-75051	-3729	75332	486.4	60	0.966649
20040.6	-72549	0	30.139743	-74948	-3680	75279	486.4	60	0.967991
20041.1	-72551	0	30.148566	-74971	-3923	75394	486.7	60	0.967721
20041.6	-72550	0	30.148976	-75058	-3816	75386	486.4	60.02	0.966586
20042.1	-72547	0	30.148976	-75055	-3639	75332	486.6	60	0.966585
20042.6	-72548	0	30.149387	-74941	-3819	75343	486.8	60	0.968068
20043.1	-72552	0	30.156978	-74927	-3980	75330	486.8	59.99	0.968302
20043.6	-72552	0	30.157799	-75052	-3811	75381	486.6	60	0.96669
20044.1	-72550	0	30.157799	-75027	-3518	75327	486.4	60	0.966985
20044.6	-72548	0	30.158209	-75075	-3946	75518	486.1	59.99	0.96634
20045.1	-72549	0	30.168057	-74945	-3927	75299	486.7	59.97	0.96803
20045.6	-72551	0	30.168468	-74992	-3693	75294	486.5	60.02	0.96745
20046.1	-72550	0	30.168673	-75030	-3710	75390	486.8	60.02	0.966947
20046.6	-72547	0	30.168673	-75061	-3999	75467	486.5	59.99	0.966507
20047.1	-72551	0	30.168673	-74948	-3825	75248	487.3	60.02	0.968018
20047.6	-72551	0	30.169494	-75030	-3637	75323	486.9	60.029	0.96696
20048.1	-72550	0	30.169494	-75058	-3808	75460	486.8	59.99	0.966586
20048.5	-72549	0	30.169699	-75019	-4051	75427	486.9	60	0.967075
20048.5	-72549	0	30.169699	-75019	-4051	75427	486.9	60	0.967075
20049.0	-72549	0	30.175792	-74971	-3884	75279	486.5	60.02	0.967694
20049.5	-72551	0	30.175792	-74956	-3711	75277	487.4	60.02	0.967915
20050.0	-72551	0	30.175792	-75070	-3949	75515	487.1	60.029	0.966445
20050.5	-72548	0	30.175997	-75053	-3994	75404	487	60.04	0.966624
20051.0	-72548	0	30.185292	-74954	-3719	75223	487.6	60.029	0.9679
20051.5	-72551	0	30.185907	-74929	-3832	75323	487.4	59.97	0.968263
20052.0	-93695	0	30.186523	-89654	-3360	91436	487.6	60	1.045073
20052.5	-93719	0	30.186728	-96783	-3611	97042	481	60.029	0.968342
20053.0	-93628	0	30.192678	-96793	-3337	96984	481.2	60.029	0.967301
20053.5	-93542	0	30.193294	-96695	-3671	97024	481.1	59.97	0.967392
20054.0	-93459	0	30.193909	-96570	-3644	96892	481.4	60.02	0.967785
20054.5	-93381	0	30.193909	-96528	-3466	96752	481.2	60.02	0.967398
20055.0	-93307	0	30.203963	-96499	-3492	96740	480.9	59.97	0.966922
20055.5	-93236	0	30.204373	-96430	-3696	96790	481.6	60	0.966878
20056.0	-93166	0	30.204783	-96283	-3632	96553	482	60.029	0.967627
20056.5	-93101	0	30.205194	-96285	-3504	96508	481.3	59.97	0.966932
20057.0	-93028	0	30.205604	-96196	-3574	96514	481.2	60	0.967067
20057.5	-92971	0	30.20663	-96111	-3720	96413	482.3	60.029	0.967329
20058.0	-92918	0	30.206835	-96072	-3592	96311	481.7	59.99	0.96717
20058.5	-92867	0	30.206835	-95980	-3446	96207	481.7	60.029	0.967566
20059.0	-92820	0	30.213463	-95969	-3709	96316	481.9	59.99	0.967187
20059.5	-92775	0	30.213463	-95884	-3593	96172	482	60	0.967575

20060.0	-92732	0	30.213463	-95898	-3508	96137	481.9	60.029	0.966986
20060.5	-92690	0	30.213463	-95771	-3513	96037	481.6	60	0.96783
20061.0	-92652	0	30.226245	-95807	-3791	96140	481.2	59.97	0.967069
20061.5	-92614	0	30.226656	-95733	-3754	95994	482.1	60.04	0.96742
20062.0	-92573	0	30.227271	-95688	-3449	95917	481.7	60	0.967446
20062.5	-92540	0	30.227682	-95642	-3634	95969	482.1	60.04	0.967567
20063.0	-92509	0	30.236299	-95595	-3773	95927	481.9	59.99	0.967718
20063.5	-92481	0	30.237325	-95552	-3540	95798	481.9	60	0.96786
20064.0	-92454	0	30.237735	-95585	-3492	95836	481.8	60.04	0.967244
20064.5	-92426	0	30.238146	-95499	-3704	95863	481.7	60.04	0.967822
20065.0	-92403	0	30.250046	-95479	-3821	95780	482.2	60.04	0.967783
20065.5	-92381	0	30.250866	-95462	-3414	95697	481.6	60	0.967725
20066.0	-92358	0	30.250866	-95507	-3569	95780	481.9	60.029	0.967029
20066.5	-92335	0	30.251072	-95484	-3822	95832	481.9	60.029	0.967021
20067.0	-92310	0	30.251277	-95336	-3799	95597	481.8	60	0.96826
20067.5	-92294	0	30.251892	-95367	-3514	95610	481.4	60	0.967777
20068.0	-92276	0	30.252097	-95357	-3673	95699	481.9	60.04	0.96769
20068.5	-92259	0	30.252303	-95377	-3832	95717	481.9	60.029	0.967309
20069.0	-92242	0	30.259011	-95332	-3577	95600	481.4	60.04	0.967587
20069.5	-92228	0	30.259011	-95264	-3481	95524	481.6	60.04	0.968131
20070.0	-92216	0	30.259216	-95260	-3707	95609	482	60.029	0.968045
20070.5	-92203	0	30.259216	-95299	-3759	95581	481.8	60.029	0.967513
20071.0	-92190	0	30.271322	-95246	-3488	95461	481.7	60	0.967915
20071.5	-92178	0	30.271937	-95286	-3576	95591	481.4	60.029	0.967382
20072.0	-92163	0	30.272553	-95261	-3864	95603	481.7	60.04	0.967479
20072.5	-92151	0	30.272963	-95247	-3363	95496	481.8	60	0.967495
20073.0	-92139	0	30.282749	-95170	-3602	95414	481.5	60.04	0.968152
20073.5	-92132	0	30.283775	-95147	-3745	95501	482	60.02	0.968312
20074.0	-92126	0	30.28398	-95146	-3855	95475	481.3	60.029	0.968259
20074.5	-92119	0	30.28398	-95166	-3552	95415	482.2	59.99	0.967982
20075.0	-92112	0	30.295675	-95144	-3556	95413	481.3	60	0.968133
20075.5	-92105	0	30.296291	-95204	-3797	95563	481.6	60.02	0.967449
20076.0	-92097	0	30.297111	-95159	-3674	95426	481.8	60	0.967822
20076.5	-92089	0	30.297317	-95166	-3448	95390	481.6	60.029	0.967667
20077.0	-92080	0	30.297522	-95160	-3663	95491	481.9	60.029	0.967633
20077.5	-92073	0	30.298342	-95166	-3847	95524	481.7	60.02	0.967499
20078.0	-92065	0	30.298548	-95175	-3637	95419	481.2	59.99	0.967323
20078.5	-92058	0	30.298753	-95137	-3607	95380	481.7	59.99	0.967636
20079.0	-92051	0	30.306344	-95167	-3791	95536	481.8	59.97	0.967258
20079.5	-92044	0	30.306344	-95094	-3788	95421	481.9	59.97	0.967926
20080.0	-92041	0	30.306344	-95071	-3668	95308	481.7	59.99	0.968129
20080.5	-92039	0	30.306344	-95032	-3610	95304	482.2	59.99	0.968505
20081.0	-92037	0	30.318039	-95068	-3855	95440	482.1	59.97	0.968118
20081.5	-92035	0	30.318655	-95053	-3772	95332	481.3	60	0.968249
20082.0	-92032	0	30.319065	-95050	-3627	95292	482	59.99	0.968248
20082.5	-92031	0	30.31927	-95047	-3733	95400	481.7	59.99	0.968268
20083.0	-92029	0	30.327682	-95048	-3956	95385	481.7	60.02	0.968237
20083.5	-92029	0	30.328298	-95085	-3714	95348	481.5	60	0.96786
20084.0	-92026	0	30.328913	-95047	-3637	95306	481.5	59.97	0.968216
20084.5	-92025	0	30.329324	-95052	-3856	95419	481.7	59.97	0.968154
20085.0	-92022	0	30.342455	-95076	-3807	95368	482.1	60	0.967878
20085.5	-92020	0	30.343275	-95069	-3649	95330	481.7	60.02	0.967929
20086.0	-92019	0	30.343686	-95036	-3641	95325	481.6	60.02	0.968254
20086.5	-92017	0	30.344096	-95086	-3853	95439	482	59.97	0.967724
20087.0	-92014	0	30.344506	-95019	-3893	95296	481.9	60.02	0.968375
20087.5	-92012	0	30.345122	-95073	-3679	95314	482	59.99	0.967804
20088.0	-92011	0	30.345327	-95049	-3774	95411	481.5	59.97	0.968038
20088.5	-92008	0	30.345532	-95074	-3805	95402	482.3	60.029	0.967751
20089.0	-92006	0	30.352303	-95079	-3806	95345	481.6	60	0.96768
20089.5	-92003	0	30.352303	-95050	-3642	95323	482	60.02	0.967943
20090.0	-92001	0	30.352303	-95087	-3903	95458	482.5	60.029	0.967546
20090.5	-91999	0	30.352303	-95050	-3948	95354	481.6	60	0.967901
20091.0	-91996	0	30.364676	-95090	-3658	95313	481.7	60.02	0.967462
20091.5	-91995	0	30.365907	-95050	-3660	95381	482.1	60.02	0.967859
20092.0	-91993	0	30.365907	-95066	-3875	95438	481.8	59.959	0.967675
20092.5	-91991	0	30.366112	-95037	-3841	95311	481.8	60.02	0.967949
20093.0	-91990	0	30.373971	-95061	-3690	95307	481.4	59.99	0.967694
20093.5	-91989	0	30.375202	-95017	-3899	95388	482.1	60.029	0.968132
20094.0	-91987	0	30.375407	-95077	-3915	95433	481.9	60.02	0.9675
20094.5	-91987	0	30.375817	-95032	-3741	95312	481.3	60.02	0.967958
20095.0	-91985	0	30.388538	-95044	-3702	95308	481.4	59.97	0.967815
20095.5	-91984	0	30.389359	-95084	-3904	95442	481.8	60	0.967397
20096.0	-91982	0	30.389564	-95058	-3872	95349	481.6	60.02	0.967641
20096.5	-91980	0	30.389974	-95096	-3645	95342	481.2	60.029	0.967233
20097.0	-91976	0	30.39018	-95048	-3786	95373	481.5	60	0.967679
20097.5	-91975	0	30.391205	-95056	-3886	95397	481.7	60.02	0.967588
20098.0	-91972	0	30.391411	-95067	-3880	95324	481.7	60.02	0.967444
20098.5	-91971	0	30.391411	-95051	-3644	95303	481.6	59.99	0.967596
20099.0	-91969	0	30.398797	-95045	-3960	95425	481.7	59.97	0.967636
20099.5	-91968	0	30.398797	-95062	-3901	95381	482	60.029	0.967453
20100.0	-91965	0	30.398797	-95090	-3776	95345	482.5	59.99	0.967136
20100.5	-91962	0	30.399002	-95060	-3731	95336	481.9	60	0.96741

20101.0	-91960	0	30.411393	-95095	-3974	95472	482.1	60	0.967033
20101.5	-91958	0	30.412624	-95053	-3875	95317	481.4	60.029	0.967439
20102.0	-91957	0	30.412624	-95062	-3671	95313	482	60	0.967337
20102.5	-91954	0	30.412829	-95064	-3842	95409	482.2	60.029	0.967285
20103.1	-91952	0	30.421098	-95079	-3981	95440	482.3	60.029	0.967112
20103.6	-91950	0	30.422124	-95040	-3916	95311	482.4	60.029	0.967487
20104.1	-91949	0	30.422329	-94993	-3716	95246	482.5	60.04	0.967956
20104.6	-91953	0	30.42274	-94964	-3968	95345	482.2	59.99	0.968293
20105.1	-91952	0	30.434167	-95086	-3995	95382	481.9	60.04	0.96704
20105.6	-91950	0	30.434988	-95045	-3720	95283	482	59.99	0.967436
20106.1	-91949	0	30.435193	-94994	-3796	95283	482	60	0.967945
20106.6	-91953	0	30.435603	-94929	-3999	95300	481.9	60.02	0.96865
20107.1	-91954	0	30.436014	-95030	-3844	95277	481.5	60.06	0.967631
20107.6	-91954	0	30.436834	-95035	-3685	95280	481.1	60.02	0.96758
20108.1	-91952	0	30.436834	-95047	-3875	95397	481.3	60.04	0.967437
20108.6	-91953	0	30.436834	-95013	-3998	95364	480.3	60.02	0.967794
20109.1	-91952	0	30.444015	-95036	-3878	95290	480.3	60.029	0.967549
20109.6	-91949	0	30.444221	-95001	-3666	95245	479.8	60.04	0.967874
20110.1	-91951	0	30.444221	-94967	-3897	95298	479.7	60	0.968242
20110.6	-91955	0	30.444221	-94983	-3938	95266	479.5	60.029	0.968121
20111.1	-91956	0	30.457209	-95032	-3670	95268	479.4	60.029	0.967632
20111.6	-91957	0	30.458235	-94980	-3801	95282	479	60.04	0.968172
20112.1	-91958	0	30.45844	-95009	-4009	95332	477.6	60.02	0.967887
20112.6	-91959	0	30.45885	-95016	-3810	95270	478.4	60	0.967826
20113.1	-91960	0	30.466852	-94993	-3634	95232	477.7	60.02	0.968071
20113.6	-91962	0	30.467673	-95027	-3874	95384	477.4	60	0.967746
20114.1	-91963	0	30.468083	-95008	-3930	95342	476.7	60.04	0.96795
20114.6	-91965	0	30.468288	-95015	-3688	95244	477.8	60.029	0.9679
20115.1	-91965	0	30.47951	-95023	-3688	95281	477.3	60.029	0.967818
20115.6	-91967	0	30.480536	-95001	-3930	95351	477.8	60.02	0.968063
20116.1	-91968	0	30.480536	-95008	-3969	95291	477	60.029	0.968003
20116.6	-91969	0	30.480536	-95007	-3701	95239	478.4	60.029	0.968023
20117.1	-91969	0	30.480947	-95005	-3790	95329	478.5	60.029	0.968044
20117.6	-91970	0	30.481767	-95015	-4001	95366	478.7	60	0.967952
20118.1	-91970	0	30.481972	-95015	-3862	95264	479.2	60.029	0.967952
20118.6	-91970	0	30.482178	-95059	-3710	95295	479.4	60.06	0.967504
20119.1	-91969	0	30.489359	-95028	-4022	95398	480.1	60.02	0.967809
20119.6	-91970	0	30.489564	-95033	-3935	95340	479.6	60.04	0.967769
20120.1	-91969	0	30.489564	-95043	-3802	95278	479.8	60	0.967657
20120.6	-91969	0	30.489769	-95014	-3760	95297	480	60.04	0.967952
20121.1	-91970	0	30.502758	-95008	-4048	95368	479.4	60.04	0.968024
20121.6	-91970	0	30.503578	-95027	-3924	95285	479.6	60.02	0.96783
20122.1	-91971	0	30.503783	-94977	-3794	95214	479	60.029	0.96835
20122.6	-91971	0	30.504194	-95031	-3862	95377	479.3	60.04	0.9678
20123.1	-91973	0	30.51199	-94943	-4034	95279	478.9	60	0.968718
20123.6	-91974	0	30.512606	-95028	-3873	95291	478.6	60.029	0.967862
20124.1	-91977	0	30.512811	-94975	-3728	95229	478.2	60.029	0.968434
20124.6	-91977	0	30.513221	-95009	-4023	95360	477.8	60	0.968087
20125.1	-91979	0	30.52588	-94999	-3921	95295	478	60.029	0.96821
20125.6	-91980	0	30.527316	-94996	-3730	95228	478	60.04	0.968251
20126.1	-91983	0	30.527316	-94971	-3734	95260	476.7	60.04	0.968538
20126.6	-91984	0	30.527316	-95014	-4051	95373	477.4	60	0.96811
20127.1	-91986	0	30.527789	-94996	-3887	95253	477.9	60.04	0.968314
20127.6	-91987	0	30.528815	-95009	-3760	95238	477.7	60.029	0.968192
20128.1	-91989	0	30.528815	-94990	-3915	95350	477.8	60.029	0.968407
20128.6	-91990	0	30.52902	-94999	-3949	95316	477.5	60.02	0.968326
20129.1	-91991	0	30.535648	-95037	-3818	95295	478	60.02	0.967949
20129.6	-91992	0	30.536058	-95009	-3798	95263	478.5	60.029	0.968245
20130.1	-91992	0	30.536058	-95054	-4071	95411	478.6	60.029	0.967787
20130.6	-91992	0	30.536058	-95027	-4010	95307	478.6	60.02	0.968062
20131.1	-91993	0	30.548716	-95009	-3822	95252	479.2	60.02	0.968256
20131.6	-91992	0	30.549332	-95003	-3883	95313	479.7	60.04	0.968306
20132.1	-91993	0	30.549332	-95039	-4082	95384	480.3	60.02	0.96795
20132.6	-91993	0	30.549742	-95022	-4007	95279	480.1	60.04	0.968123
20133.1	-91994	0	30.558297	-95032	-3771	95270	480.4	60.02	0.968032
20133.6	-91993	0	30.559323	-95020	-4014	95385	480.1	60.029	0.968144
20134.1	-91993	0	30.559528	-95052	-4080	95387	481.2	60	0.967818
20134.6	-91993	0	30.559528	-95027	-3914	95275	481.2	60.02	0.968072
20135.1	-91993	0	30.571428	-95054	-3818	95316	480.6	60.04	0.967797
20135.6	-91992	0	30.572659	-95016	-3707	95338	481.9	60	0.968174
20136.1	-91991	0	30.572864	-95048	-4086	95339	481.2	60	0.967837
20136.6	-91990	0	30.573069	-95053	-3850	95295	481	60.029	0.967776
20137.1	-91989	0	30.573275	-95014	-3998	95354	481.1	60	0.968163
20137.6	-91989	0	30.574095	-95018	-4104	95358	481.5	60.02	0.968122
20138.1	-91988	0	30.574506	-95056	-4007	95321	481.7	60.02	0.967724
20138.6	-91987	0	30.574506	-95015	-3866	95266	481.2	60.02	0.968131
20139.1	-91986	0	30.581687	-95064	-4095	95425	481.2	60.02	0.967622
20139.6	-91985	0	30.582097	-95027	-4058	95330	481.4	60.029	0.967988
20140.1	-91983	0	30.582097	-95071	-4012	95309	481.5	60.029	0.967519
20140.6	-91983	0	30.582302	-95019	-3914	95291	481.2	60.04	0.968048
20141.1	-91980	0	30.593256	-95077	-4085	95409	481.1	60.029	0.967426
20141.6	-91980	0	30.593872	-95040	-4148	95323	481.1	60.029	0.967803

20142.1	-91978	0	30.594282	-95035	-3917	95279	481.1	60.029	0.967833
20142.6	-91978	0	30.594487	-95044	-4061	95379	481	60.02	0.967741
20143.1	-91976	0	30.602346	-95043	-4206	95385	481.3	59.97	0.96773
20143.6	-91975	0	30.603577	-95069	-3934	95332	481.2	60.02	0.967455
20144.1	-91975	0	30.603577	-95011	-3874	95273	481	60.029	0.968046
20144.6	-91973	0	30.603577	-95073	-4182	95450	481	60	0.967393
20145.1	-91972	0	30.616219	-95059	-4058	95348	481.4	60.02	0.967525
20145.6	-91971	0	30.617244	-95039	-3838	95273	480.8	60.02	0.967719
20146.1	-91970	0	30.617655	-95031	-3990	95309	480.7	60	0.967789
20146.6	-91969	0	30.61786	-95074	-4223	95428	481.9	59.99	0.967341
20147.1	-91967	0	30.61827	-95050	-4107	95317	481.1	60.02	0.967564
20147.6	-91965	0	30.619091	-95078	-3791	95330	481	60.02	0.967258
20148.1	-91965	0	30.619501	-95007	-4065	95367	481	60	0.967981
20148.6	-91963	0	30.619501	-95082	-4212	95421	481.4	60	0.967197
20149.1	-91963	0	30.627503	-95037	-4024	95305	481.4	59.99	0.967655
20149.6	-91961	0	30.627708	-95042	-3920	95296	481.2	60	0.967583
20150.1	-91960	0	30.627708	-95115	-4133	95477	481.4	59.99	0.96683
20150.6	-91959	0	30.627913	-95041	-4163	95321	481.5	60.02	0.967572
20151.1	-91958	0	30.639198	-95069	-3918	95308	481.2	59.99	0.967276
20151.6	-91957	0	30.640224	-95034	-4032	95345	480.8	60	0.967622
20152.1	-91955	0	30.640224	-95064	-4185	95422	481.3	59.99	0.967296
20152.6	-91955	0	30.640429	-95032	-4141	95298	481.5	60.029	0.967621
20153.1	-91955	0	30.647673	-95042	-3898	95295	481.2	60.02	0.96752
20153.6	-91953	0	30.648904	-95040	-4188	95408	481.2	60.029	0.967519
20154.1	-91953	0	30.648904	-95057	-4185	95383	481.2	59.99	0.967346
20154.6	-91952	0	30.648904	-95040	-4052	95286	481.5	60	0.967508
20155.1	-91951	0	30.662035	-95035	-3917	95295	481.6	60.029	0.967549
20155.6	-91949	0	30.662856	-95068	-4201	95428	481.2	60.04	0.967192
20156.1	-91950	0	30.663266	-94962	-4141	95239	481.2	60.02	0.968282
20156.6	-91954	0	30.663471	-94942	-3906	95184	481.4	60.02	0.968528
20157.1	-91954	0	30.663882	-95069	-4097	95390	481.5	60.04	0.967234
20157.6	-91953	0	30.664702	-95019	-4188	95374	481.6	60.029	0.967733
20158.1	-91952	0	30.665113	-95060	-4163	95333	481.1	60.04	0.967305
20158.6	-91952	0	30.665113	-95026	-3870	95283	481.3	60.02	0.967651
20159.1	-91950	0	30.672846	-95103	-4222	95484	481.7	60.04	0.966846
20159.6	-91951	0	30.673052	-94962	-4187	95304	481.6	60.04	0.968293
20160.1	-91951	0	30.673052	-95060	-4023	95312	481.4	60.02	0.967294
20160.6	-91951	0	30.673257	-95054	-4037	95334	481.1	60.04	0.967355
20161.1	-91949	0	30.685772	-95037	-4214	95367	482	60.029	0.967507
20161.6	-91954	0	30.686798	-94962	-4152	95257	481.7	60.06	0.968324
20162.1	-91953	0	30.686798	-95061	-3859	95305	481.8	60.06	0.967305
20162.6	-91952	0	30.687003	-95078	-4155	95432	481.8	60.06	0.967122
20163.1	-91951	0	30.693096	-95061	-4196	95391	482.1	60.02	0.967284
20163.6	-91950	0	30.694122	-95032	-4143	95292	482.1	60.02	0.967569
20164.1	-91952	0	30.694532	-94930	-4025	95195	481.9	60.02	0.96863
20164.6	-91953	0	30.694532	-95003	-3117	95286	481.8	60.02	0.967896
20165.1	-91952	0	30.7067	-95050	-4253	95355	481.9	60.04	0.967407
20165.6	-91950	0	30.707931	-95069	-4037	95324	482.1	60.06	0.967192
20166.1	-91949	0	30.708342	-94974	-4059	95258	481.8	60.069	0.968149
20166.6	-91954	0	30.708547	-94918	-3082	95163	482.4	60.02	0.968773
20167.1	-91955	0	30.708752	-95053	-4231	95320	482.5	60.04	0.967408
20167.6	-91954	0	30.709573	-95043	-3968	95288	482	60.029	0.967499
20168.1	-91953	0	30.709778	-95060	-4198	95413	481.9	60.06	0.967315
20168.6	-91952	0	30.709778	-95049	-4227	95393	481.9	60.04	0.967417
20169.1	-91951	0	30.718679	-95065	-4108	95321	481.6	60.04	0.967243
20169.6	-91950	0	30.718885	-95041	-3983	95282	481.9	60.029	0.967477
20170.1	-91954	0	30.718885	-94945	-4294	95322	481.8	60.04	0.968498
20170.6	-91954	0	30.71909	-95074	-4201	95381	481.4	60.02	0.967183
20171.1	-91952	0	30.731463	-95082	-3999	95322	481.5	60.02	0.967081
20171.6	-91951	0	30.732284	-95070	-4061	95396	481.6	60.029	0.967193
20172.1	-91949	0	30.732489	-95053	-4260	95405	481.6	60.02	0.967345
20172.6	-91952	0	30.732694	-94960	-4136	95231	481.9	60.02	0.968324
20173.1	-91953	0	30.73967	-95048	-3930	95309	481.4	60.029	0.967438
20173.6	-91951	0	30.740901	-95077	-4195	95452	482	60.029	0.967121
20174.1	-91950	0	30.741311	-95022	-4248	95364	481.6	60.04	0.967671
20174.6	-91952	0	30.741311	-94980	-4074	95258	481.1	60.02	0.96812
20175.1	-91952	0	30.752801	-95031	-4032	95308	481	60.02	0.9676
20175.6	-91949	0	30.753827	-95092	-4284	95465	481.9	60	0.966948
20176.1	-91949	0	30.754237	-94975	-4224	95285	481.7	60	0.968139
20176.6	-91953	0	30.754443	-94969	-3975	95236	481.3	60	0.968242
20177.1	-91953	0	30.754853	-95044	-3150	95357	481	60.02	0.967478
20177.6	-91951	0	30.755468	-95062	-4266	95426	481.9	60	0.967274
20178.1	-91950	0	30.755468	-95019	-4177	95297	481.5	60	0.967701
20178.6	-91951	0	30.755468	-94982	-4006	95241	481.2	60	0.968089
20179.1	-91952	0	30.763265	-95027	-3193	95332	481.3	60.02	0.967641
20179.6	-91950	0	30.76347	-95061	-3054	95277	480.9	60.029	0.967274
20180.1	-91949	0	30.76347	-95008	-4103	95263	482	60.02	0.967803
20180.6	-91952	0	30.763675	-94962	-4048	95256	481.2	60.04	0.968303
20181.1	-91952	0	30.777012	-95031	-3132	95277	481.7	60.02	0.9676
20181.6	-91951	0	30.778037	-95037	-4189	95323	482.2	60.029	0.967528
20182.1	-91949	0	30.778448	-95078	-3940	95332	481.6	60.029	0.96709
20182.6	-91949	0	30.778653	-94972	-4202	95324	481.4	60.029	0.96817

20183.1	-91953	0	30.785834	-94974	-4246	95330	481.9	59.99	0.968191
20183.6	-91952	0	30.786655	-95084	-4112	95362	481.4	60.02	0.967061
20184.1	-91950	0	30.787065	-95051	-3279	95393	481.6	60	0.967375
20184.6	-91949	0	30.787065	-95023	-4282	95414	481.4	60.04	0.96765
20185.1	-91952	0	30.799297	-94954	-3015	95175	482	60.02	0.968385
20185.6	-91952	0	30.800528	-95002	-3011	95255	481.3	60.02	0.967895
20186.1	-91951	0	30.800528	-95060	-4122	95390	482	60	0.967294
20186.6	-91949	0	30.800733	-95010	-4298	95384	482.2	60.029	0.967782
20187.1	-91952	0	30.800938	-94975	-4222	95247	481.6	60.029	0.968171
20187.6	-91952	0	30.801554	-95008	-3186	95316	481.7	60.06	0.967834
20188.1	-91950	0	30.801964	-95064	-3330	95380	482.1	60	0.967243
20188.6	-91950	0	30.801964	-94925	-3227	95154	481.8	60	0.968659
20189.1	-91953	0	30.810171	-95008	-3040	95251	481.6	60.02	0.967845
20189.6	-91953	0	30.810376	-95042	-3260	95384	481.6	60.029	0.967499
20190.1	-91950	0	30.810376	-95095	-4323	95465	481.9	59.99	0.966928
20190.6	-91950	0	30.810581	-95003	-4269	95303	481.8	60.04	0.967864
20191.1	-91952	0	30.822687	-94981	-4033	95228	482.2	60.04	0.968109
20191.6	-91953	0	30.823507	-95048	-4143	95389	481.4	60.029	0.967438
20192.1	-91950	0	30.823918	-95032	-3246	95265	482.1	60.02	0.967569
20192.6	-91950	0	30.824123	-94999	-4189	95266	481.9	60.029	0.967905
20193.1	-91953	0	30.831651	-94939	-4022	95207	481.6	60.04	0.968548
20193.6	-91954	0	30.832882	-95062	-4284	95460	481.9	60.029	0.967306
20194.1	-91953	0	30.833292	-94991	-3209	95219	482	60	0.968018
20194.6	-91951	0	30.833292	-95117	-4141	95379	481.4	60.029	0.966715
20195.1	-91950	0	30.84655	-95024	-4065	95299	481.8	60.04	0.96765
20195.6	-91952	0	30.847371	-95005	-4328	95393	481.4	60	0.967865
20196.1	-91951	0	30.847371	-95020	-3131	95229	481.7	60.029	0.967702
20196.6	-91950	0	30.847576	-95079	-4057	95334	481.4	60.02	0.967091
20197.1	-91947	0	30.847718	-95011	-3972	95367	481.3	60.029	0.967751
20197.6	-91951	0	30.848538	-94948	-4305	95317	481.7	60	0.968435
20198.1	-91953	0	30.848949	-95010	-3051	95220	481.6	60.04	0.967824
20198.6	-91952	0	30.848949	-95045	-4019	95323	481.8	60.02	0.967458
20199.1	-91951	0	30.856067	-95008	-3430	95309	481.7	60.02	0.967824
20199.6	-91949	0	30.856272	-95102	-4305	95445	481.6	60	0.966846
20200.1	-91949	0	30.856272	-94924	-3051	95169	481.3	60.04	0.968659
20200.6	-91952	0	30.856477	-94997	-3304	95328	481.5	60.02	0.967946
20201.1	-91951	0	30.868456	-95057	-4351	95435	481.9	60	0.967325
20201.6	-91949	0	30.869481	-95093	-4245	95380	481.3	60	0.966938
20202.1	-91949	0	30.869687	-94934	-3244	95237	481	60	0.968557
20202.6	-91952	0	30.869892	-94918	-3337	95222	481.8	60.04	0.968752
20203.1	-91954	0	30.877546	-95067	-4340	95433	481.5	60.04	0.967255
20203.6	-91951	0	30.878777	-95067	-4196	95347	481.5	60.04	0.967223
20204.1	-91951	0	30.878777	-95061	-4045	95343	481.6	60.02	0.967284
20204.6	-91948	0	30.879188	-94975	-3378	95256	481.9	60.069	0.968128
20205.1	-91951	0	30.892256	-94958	-4312	95278	481.4	60.02	0.968333
20205.6	-91953	0	30.893281	-95043	-4044	95292	481	60.02	0.967488
20206.1	-91952	0	30.893281	-95053	-3418	95382	481.8	60	0.967376
20206.6	-91950	0	30.893487	-95066	-4356	95448	481.3	60.029	0.967223
20207.1	-91950	0	30.893897	-95016	-4216	95286	481.4	60.029	0.967732
20207.6	-91953	0	30.894718	-94951	-3317	95279	481.6	60.029	0.968426
20208.1	-91953	0	30.894923	-95065	-4255	95425	481.8	60.04	0.967265
20208.6	-91952	0	30.895128	-95028	-3233	95258	481.4	60.02	0.967631
20209.1	-91950	0	30.90313	-95050	-3098	95274	481.1	60.029	0.967386
20209.6	-91949	0	30.90313	-94954	-3495	95278	481.5	60.02	0.968353
20210.1	-91952	0	30.90313	-94960	-3374	95240	481.7	60.02	0.968324
20210.6	-91952	0	30.90313	-95059	-4301	95365	481.5	60.04	0.967315
20211.1	-91950	0	30.91503	-95054	-4039	95305	481.3	60.029	0.967345
20211.6	-91950	0	30.91585	-94952	-3533	95256	481.5	60.02	0.968384
20212.1	-91954	0	30.916466	-94999	-4373	95389	481.4	60.029	0.967947
20212.6	-91953	0	30.916671	-95030	-4274	95308	481.4	60	0.967621
20213.1	-91952	0	30.923852	-95073	-4036	95341	481.1	60	0.967173
20213.6	-91949	0	30.924468	-95001	-3412	95296	481.9	60.02	0.967874
20214.1	-91951	0	30.924878	-94996	-4338	95349	481.5	60.029	0.967946
20214.6	-91953	0	30.925288	-95032	-4196	95302	481	59.99	0.9676
20215.1	-91951	0	30.937599	-95042	-3445	95376	481.7	60.029	0.967478
20215.6	-91950	0	30.938214	-94974	-3403	95215	481.3	60	0.96816
20216.1	-91951	0	30.938625	-94968	-4294	95269	481.6	60.069	0.968231
20216.6	-91951	0	30.939035	-95050	-3327	95348	480.7	60.04	0.967396
20217.1	-91949	0	30.93924	-94974	-3399	95266	481.6	60.02	0.968149
20217.6	-91953	0	30.940266	-94956	-3393	95213	481.9	60.02	0.968375
20218.1	-91953	0	30.940676	-95070	-4237	95348	481.6	60.04	0.967214
20218.6	-91952	0	30.940676	-95056	-4067	95349	480.8	60.02	0.967346
20219.1	-91951	0	30.948615	-95027	-3421	95333	481.7	60.029	0.96763
20219.6	-91950	0	30.948615	-94984	-3282	95195	481.3	60	0.968058
20220.1	-91952	0	30.94882	-94983	-4142	95239	481.3	60.02	0.968089
20220.6	-91951	0	30.94882	-95109	-4133	95409	481.6	60.02	0.966796
20221.1	-91949	0	30.960783	-94955	-3436	95198	481.6	60.029	0.968343
20221.6	-91953	0	30.961399	-94943	-3119	95162	481.2	60	0.968507
20222.1	-91954	0	30.961809	-95039	-3389	95346	481.5	60.04	0.96754
20222.6	-91952	0	30.962014	-95071	-4260	95431	481.6	60	0.967193
20223.1	-91951	0	30.970695	-95027	-3425	95265	481.5	60	0.96763
20223.6	-91951	0	30.971516	-94982	-3210	95230	481.6	60.029	0.968089

20224.1	-91950	0	30.972131	-95066	-3508	95404	481.1	60.029	0.967223
20224.6	-91949	0	30.972542	-94960	-3381	95219	481.7	60.029	0.968292
20225.1	-91952	0	30.984647	-94925	-3314	95136	481.5	60.04	0.968681
20225.6	-91953	0	30.985057	-95043	-3286	95304	481.7	60.04	0.967488
20226.1	-91952	0	30.985468	-95039	-3427	95353	481.9	60.029	0.967519
20226.6	-91950	0	30.985878	-95031	-3515	95286	481.8	60.06	0.967579
20227.1	-91949	0	30.986083	-94915	-3210	95144	481.6	60	0.968751
20227.6	-91953	0	30.986904	-94976	-3450	95303	481.3	60.029	0.968171
20228.1	-91954	0	30.987109	-95032	-4322	95433	481.6	60.029	0.967611
20228.6	-91953	0	30.987109	-95057	-3403	95297	481.8	60	0.967346
20229.1	-91951	0	30.99429	-95027	-3285	95262	481.6	60	0.96763
20229.6	-91950	0	30.99429	-95050	-3576	95391	481.2	60.04	0.967386
20230.1	-91950	0	30.994495	-94965	-3520	95219	481.6	59.99	0.968251
20230.6	-91952	0	30.994495	-94966	-3321	95195	481.7	60	0.968262
20231.1	-91953	0	31.00728	-95025	-3377	95303	481.5	60.02	0.967672
20231.6	-91951	0	31.008511	-95054	-3558	95393	481.3	59.97	0.967355
20232.1	-91949	0	31.008511	-95001	-3394	95212	481	60.029	0.967874
20232.6	-91952	0	31.008716	-94929	-3207	95134	481.2	60.029	0.96864
20233.1	-91953	0	31.016859	-95082	-4083	95359	481.7	60.04	0.967092
20233.6	-91952	0	31.01809	-95015	-3556	95349	481.3	60.029	0.967763
20234.1	-91950	0	31.018295	-95045	-3470	95281	481.4	60.02	0.967436
20234.6	-91951	0	31.018706	-94940	-3385	95177	481.9	60.02	0.968517
20235.1	-91952	0	31.029785	-95057	-4111	95347	481.7	60.04	0.967335
20235.6	-91951	0	31.030195	-95035	-3507	95319	481.7	60.029	0.967549
20236.1	-91949	0	31.030811	-94985	-3292	95205	481.8	60.029	0.968037
20236.6	-91952	0	31.031221	-94926	-3399	95231	482.1	60	0.96867
20237.1	-91954	0	31.031221	-95062	-4257	95410	482.2	60.02	0.967306
20237.6	-91953	0	31.032042	-95045	-3492	95302	481.6	59.99	0.967468
20238.1	-91952	0	31.032247	-95079	-3965	95289	481.7	60.029	0.967112
20238.6	-91952	0	31.032247	-95050	-3543	95398	480.9	60.029	0.967407
20239.1	-91950	0	31.040044	-95048	-4341	95435	481.7	60	0.967406
20239.6	-91950	0	31.040044	-95025	-3314	95249	481.6	60.04	0.96764
20240.1	-91950	0	31.040249	-94925	-3390	95177	481.6	60.02	0.968659
20240.6	-91954	0	31.040249	-95059	-3597	95381	481.7	60.02	0.967336
20241.1	-91952	0	31.053585	-95014	-3583	95257	482	60.04	0.967773
20241.6	-91952	0	31.054201	-95070	-3389	95290	481.6	60	0.967203
20242.1	-91950	0	31.054611	-95001	-3529	95299	481.7	60	0.967885
20242.6	-91953	0	31.054816	-94964	-3625	95303	481.7	60.029	0.968293
20243.1	-91953	0	31.062549	-95032	-3564	95269	481.4	60.029	0.9676
20243.6	-91951	0	31.063575	-95054	-4265	95349	481.9	60.04	0.967355
20244.1	-91950	0	31.063985	-95059	-3660	95416	482.1	60.02	0.967294
20244.6	-91950	0	31.06419	-94956	-3615	95265	481.9	60.029	0.968343
20245.1	-91953	0	31.074859	-94949	-3312	95173	482.5	60.02	0.968446
20245.6	-91953	0	31.07527	-95067	-3442	95319	482	60.029	0.967244
20246.1	-91952	0	31.075885	-95045	-3690	95406	481.7	60.02	0.967458
20246.6	-91950	0	31.076501	-95033	-3599	95290	481.9	60	0.967559
20247.1	-91950	0	31.076706	-94947	-3450	95177	481.2	60.02	0.968435
20247.6	-91953	0	31.077732	-94965	-3642	95288	481.8	60.02	0.968283
20248.1	-91953	0	31.077732	-95045	-3691	95384	482.1	60	0.967468
20248.6	-91952	0	31.077937	-95044	-4384	95427	481.8	60.029	0.967468
20249.1	-91952	0	31.086554	-95043	-3459	95286	481.9	60.029	0.967478
20249.6	-91950	0	31.086759	-95037	-3743	95392	482.1	60.02	0.967518
20250.1	-91949	0	31.086759	-94973	-3637	95266	481.8	60.029	0.968159
20250.6	-91953	0	31.086759	-94946	-3442	95173	481.9	60	0.968477
20251.1	-91954	0	31.09989	-95049	-3520	95324	481.9	60.04	0.967438
20251.6	-91953	0	31.100301	-95033	-3713	95367	482.1	60.029	0.96759
20252.1	-91951	0	31.100711	-95051	-3700	95306	482.1	60.02	0.967386
20252.6	-91949	0	31.100916	-95076	-4292	95368	482.1	60.04	0.967111
20253.1	-91952	0	31.108303	-94948	-3707	95291	482	60.02	0.968446
20253.6	-91953	0	31.109328	-95073	-3673	95375	481.9	60.04	0.967183
20254.1	-91951	0	31.109944	-95040	-3531	95291	482.3	60.02	0.967498
20254.6	-91949	0	31.110354	-95023	-4118	95273	481.8	60.029	0.96765
20255.1	-91953	0	31.121844	-94994	-3755	95359	482	60.029	0.967987
20255.6	-91952	0	31.122254	-95039	-3632	95289	482	60.029	0.967519
20256.1	-91951	0	31.122665	-95058	-3314	95278	482.1	60.02	0.967315
20256.6	-91949	0	31.123075	-94937	-3517	95231	482.2	60.06	0.968526
20257.1	-91953	0	31.12369	-95047	-3768	95401	481.9	60.02	0.967448
20257.6	-91952	0	31.124511	-95031	-3713	95282	482.2	60.029	0.9676
20258.1	-91950	0	31.124716	-95059	-3492	95287	482.5	60.04	0.967294
20258.6	-91950	0	31.124922	-94966	-3789	95332	481.9	60.04	0.968241
20259.1	-91953	0	31.132987	-94973	-3748	95295	482.2	60.029	0.968201
20259.6	-91953	0	31.132987	-95078	-3521	95332	481.8	60.04	0.967132
20260.1	-91951	0	31.133192	-95044	-3544	95297	482.4	60.029	0.967457
20260.6	-91949	0	31.133192	-95005	-3693	95334	482.2	60.029	0.967833
20261.1	-91952	0	31.146118	-94941	-3521	95197	481.8	60.04	0.968517
20261.6	-91954	0	31.146323	-95056	-3458	95285	481.9	60.029	0.967367
20262.1	-91952	0	31.146734	-95033	-3635	95353	481.8	60.04	0.96758
20262.6	-91951	0	31.146939	-95042	-3841	95377	481.8	60.02	0.967478
20263.1	-91950	0	31.15412	-95039	-3668	95290	482.1	60.06	0.967498
20263.6	-91950	0	31.155146	-94951	-3479	95200	482.2	60.04	0.968394
20264.1	-91954	0	31.155761	-94972	-3784	95350	482.4	60.04	0.968222
20264.6	-91954	0	31.156172	-95041	-3778	95351	482.5	60.04	0.967519

20265.1	-91953	0	31.168687	-95039	-3559	95280	482.4	60.04	0.967529
20265.6	-91952	0	31.169508	-95044	-3611	95324	481.7	60.06	0.967468
20266.1	-91951	0	31.169918	-95058	-3832	95416	482.1	60	0.967315
20266.6	-91950	0	31.170329	-95010	-3656	95241	482.3	60.04	0.967793
20267.1	-91953	0	31.170944	-94942	-3517	95187	482.5	60	0.968518
20267.6	-91953	0	31.171765	-95047	-3716	95375	482.3	60.04	0.967448
20268.1	-91952	0	31.17197	-95028	-3772	95359	482.2	60.069	0.967631
20268.6	-91952	0	31.172175	-95067	-3614	95328	482	60.04	0.967234
20269.1	-91951	0	31.179625	-95030	-3607	95287	482.4	60.02	0.9676
20269.6	-91950	0	31.179625	-94989	-3803	95346	482.3	60.04	0.968007
20270.1	-91952	0	31.179625	-94967	-3661	95258	482.3	60.02	0.968252
20270.6	-91952	0	31.179625	-95027	-3565	95268	482.5	60.029	0.967641
20271.1	-91951	0	31.191051	-95020	-3670	95329	481.9	60.02	0.967702
20271.6	-91950	0	31.191462	-95035	-3803	95381	482.4	60	0.967538
20272.1	-91951	0	31.192077	-94931	-3728	95197	482	60.029	0.968609
20272.6	-91953	0	31.192282	-95052	-3530	95303	482.3	60.029	0.967397
20273.1	-91952	0	31.199874	-95016	-3688	95380	482.1	60.029	0.967753
20273.6	-91951	0	31.200694	-95076	-3830	95428	481.9	60.02	0.967132
20274.1	-91949	0	31.201105	-94948	-3695	95203	482	60.02	0.968414
20274.6	-91953	0	31.201515	-94989	-3510	95273	481.8	60.029	0.968038
20275.1	-91952	0	31.214646	-95024	-3729	95364	482.3	59.99	0.967671
20275.6	-91951	0	31.215262	-95062	-3775	95331	481.9	60.029	0.967274
20276.1	-91950	0	31.215877	-94958	-3557	95202	482.2	60.02	0.968323
20276.6	-91952	0	31.215877	-94964	-3663	95298	481.8	60.02	0.968283
20277.1	-91954	0	31.216082	-95037	-3865	95402	482.1	60	0.96756
20277.6	-91952	0	31.217108	-95062	-3649	95305	481.8	60.02	0.967285
20278.1	-91951	0	31.217313	-95047	-3538	95298	482.2	60.02	0.967427
20278.6	-91950	0	31.217519	-95066	-3803	95433	481.9	60.029	0.967223
20279.0	-91950	0	31.22552	-94954	-3785	95261	482.3	60.04	0.968364
20279.0	-91950	0	31.22552	-94954	-3785	95261	482.3	60.04	0.968364
20279.5	-91954	0	31.22552	-94948	-3462	95343	482.2	60.029	0.968467
20280.0	-91955	0	31.22552	-95060	-4120	95346	482.4	59.99	0.967336
20280.5	-91953	0	31.225725	-95023	-4142	95337	482.4	60.02	0.967692
20281.0	-91953	0	31.236805	-95100	-4365	95494	482	60.02	0.966909
20281.5	13046	0	31.23742	-87954	-3794	86494	482.3	60.02	-0.14833
20282.0	13200	0	31.238036	11797	-5910	16299	510.4	60.04	1.118929
20282.5	13055	0	31.238446	13334	-5939	16396	512.5	60.02	0.979076
20283.0	12887	0	31.245973	13132	-6059	16173	511.9	60.04	0.981343
20283.5	12728	0	31.246999	13086	-5379	15929	512	60.029	0.972643
20284.0	12578	0	31.24741	12912	-5709	15615	511.8	60.02	0.974133
20284.5	12434	0	31.24782	12678	-6054	15640	511.7	60.029	0.980754
20285.0	12298	0	31.259925	12555	-5979	15458	511.8	60.029	0.97953
20285.5	12170	0	31.260541	12492	-5312	15117	511.8	60.029	0.974224
20286.0	12047	0	31.260746	12310	-5762	15208	511.7	60.02	0.978635
20286.5	11909	0	31.260746	12122	-6076	15135	511.5	60.029	0.982429
20287.0	11801	0	31.260746	12037	-5862	14986	511.2	60.029	0.980394
20287.5	11698	0	31.261156	11986	-5694	14781	511.4	60.029	0.975972
20288.0	11601	0	31.261156	11832	-5952	14918	511.9	60.029	0.980477
20288.5	11509	0	31.261156	11709	-6026	14730	511.8	60.04	0.982919
20289.0	11422	0	31.25972	11637	-5822	14593	511.5	60.029	0.981524
20289.5	11340	0	31.25972	11585	-5659	14541	511.2	60.029	0.978852
20290.0	11260	0	31.25972	11415	-6016	14612	511.6	60.029	0.986421
20290.5	11187	0	31.25972	11324	-5922	14423	511.3	60.029	0.987902
20291.0	11117	0	31.257668	11353	-5725	14267	511.2	60.029	0.979213
20291.5	11037	0	31.257668	11234	-5819	14359	511.4	60.029	0.982464
20292.0	10975	0	31.257668	11091	-6052	14248	511.4	60.029	0.989541
20292.5	10916	0	31.257668	11097	-5848	14182	511.8	60.029	0.983689
20293.0	10860	0	31.256232	11068	-5668	14015	511.1	60.04	0.981207
20293.5	10807	0	31.256027	10971	-5933	14242	511.4	60.06	0.985051
20294.0	10757	0	31.256027	10875	-5996	14055	511.6	60.029	0.989149
20294.5	10710	0	31.256027	10889	-5357	13838	511.6	60.04	0.983561
20295.0	10666	0	31.253565	10853	-5697	13954	511	60.04	0.98277
20295.5	10622	0	31.253565	10742	-6032	14004	511.2	60.02	0.988829
20296.0	10583	0	31.253565	10696	-5906	13854	511.4	60.029	0.989435
20296.5	10538	0	31.253565	10745	-5663	13760	511.1	60.029	0.980735
20297.0	10501	0	31.253565	10611	-5853	13881	511.2	60.02	0.989633
20297.5	10468	0	31.25336	10566	-6017	13846	510.9	60.06	0.990725
20298.0	10436	0	31.25336	10615	-5805	13772	511.1	60.04	0.983137
20298.5	10405	0	31.25336	10567	-5124	13426	511	60.04	0.984669
20299.0	10377	0	31.251923	10472	-5949	13819	511.3	60.04	0.990928
20299.5	10349	0	31.251923	10501	-5953	13706	511.3	60.029	0.985525
20300.0	10321	0	31.251923	10433	-5720	13524	510.8	60.029	0.989265
20300.5	10299	0	31.251923	10420	-5740	13678	511	60.04	0.988388
20301.0	10277	0	31.249256	10340	-5987	13675	510.9	60.029	0.993907
20301.5	10252	0	31.249256	10371	-5863	13628	510.9	60.029	0.988526
20302.0	10230	0	31.249256	10365	-5657	13415	510.6	60.04	0.986975
20302.5	10211	0	31.249256	10314	-5838	13643	511	60.04	0.990014
20303.0	10193	0	31.248436	10272	-6006	13550	511	60.02	0.992309
20303.5	10177	0	31.24823	10285	-5778	13478	511.2	60.02	0.989499
20304.0	10160	0	31.24823	10339	-5633	13465	510.5	60.029	0.982687
20304.5	10142	0	31.24823	10259	-5941	13625	511.5	60.04	0.988595
20305.0	10128	0	31.245358	10204	-5273	13333	511	60.029	0.992552

20305.5	10116	0	31.245358	10217	-5664	13345	510.9	60.04	0.990115
20306.0	10104	0	31.245358	10218	-5796	13479	510.5	60.029	0.988843
20306.5	10089	0	31.245358	10150	-5975	13477	510.9	60.04	0.99399
20307.0	10076	0	31.245358	10212	-5293	13273	510.9	60.02	0.986682
20307.5	10064	0	31.245153	10237	-5621	13299	510.6	60.04	0.983101
20308.0	10051	0	31.245153	10170	-5860	13588	511	60.029	0.988299
20308.5	10040	0	31.245153	10146	-5938	13418	511	60.02	0.989553
20309.0	10031	0	31.244127	10101	-5743	13313	511.2	60.02	0.99307
20309.5	10024	0	31.244127	10144	-5625	13278	510.9	60.029	0.98817
20310.0	10016	0	31.244127	10054	-5940	13488	510.9	60.04	0.99622
20310.5	10009	0	31.244127	10082	-5880	13339	511.2	60.029	0.992759
20311.0	10002	0	31.24187	10110	-5635	13235	511.2	60.04	0.989318
20311.5	9993	0	31.24187	10093	-5792	13423	511.4	60.029	0.990092
20312.0	9986	0	31.24187	10030	-5965	13383	511.2	60.029	0.995613
20312.5	9979	0	31.24187	10090	-5796	13367	511.2	60.029	0.988999
20313.0	9972	0	31.241049	10113	-5610	13214	510.8	60.029	0.986058
20313.5	9964	0	31.240844	10056	-5896	13486	511.2	60.029	0.990851
20314.0	9957	0	31.240844	10059	-5935	13389	511.2	60.02	0.98986
20314.5	9950	0	31.240639	10095	-5693	13273	511.1	60.04	0.985636
20315.0	9943	0	31.238998	10050	-5673	13322	510.9	60.02	0.989353
20315.5	9941	0	31.238998	9960	-5976	13414	511.3	60.04	0.998092
20316.0	9939	0	31.238998	9965	-5853	13300	511.2	60.04	0.997391
20316.5	9937	0	31.238792	10028	-5626	13171	510.7	60.04	0.990925
20317.0	9935	0	31.238792	9974	-5803	13390	511.2	60.029	0.99609
20317.5	9933	0	31.238587	9952	-5937	13345	510.9	60.029	0.998091
20318.0	9932	0	31.238587	9996	-5762	13271	511	60.04	0.993597
20318.5	9929	0	31.238587	10033	-5597	13171	510.9	60.06	0.989634
20319.0	9927	0	31.237151	9959	-5890	13452	511.3	60.06	0.996787
20319.5	9925	0	31.237151	9958	-5908	13265	511.1	60.029	0.996686
20320.0	9924	0	31.236946	10018	-5687	13196	510.8	60.04	0.990617
20320.5	9921	0	31.236946	10010	-5675	13264	510.9	60.029	0.991109
20321.0	9919	0	31.234894	9959	-5963	13380	511.1	60.029	0.995984
20321.5	9917	0	31.234689	9976	-5810	13309	511.1	60.029	0.994086
20322.0	9916	0	31.234484	10026	-5586	13141	510.4	60.04	0.989029
20322.5	9914	0	31.234279	9989	-5837	13422	511	60.04	0.992492
20323.0	9912	0	31.233253	9944	-5982	13326	510.9	60.029	0.996782
20323.5	9910	0	31.233253	9979	-5726	13198	511.1	60.04	0.993085
20324.0	9909	0	31.233048	10040	-5552	13185	510.8	60.04	0.986952
20324.5	9906	0	31.233048	9951	-5886	13415	510.9	60.029	0.995478
20325.0	9904	0	31.230791	9974	-5906	13288	511.2	60.04	0.992982
20325.5	9902	0	31.230791	10023	-5665	13180	511.1	60.029	0.987928
20326.0	9900	0	31.23038	10017	-5712	13386	511.2	60.04	0.98832
20326.5	9897	0	31.23038	9950	-5980	13390	511	60.029	0.994673
20327.0	9895	0	31.23038	9984	-5774	13283	511.2	60.04	0.991086
20327.5	9893	0	31.23038	10040	-5604	13193	510.3	60.029	0.985359
20328.0	9890	0	31.23038	9971	-5783	13440	510.8	60.029	0.991876
20328.5	9889	0	31.23038	9962	-5921	13344	510.8	60.02	0.992672
20329.0	9887	0	31.229829	9995	-5701	13214	510.9	60.02	0.989195
20329.5	9885	0	31.229624	10029	-5664	13339	511	60	0.985642
20330.0	9883	0	31.229624	9940	-5938	13452	510.9	60.02	0.994266
20330.5	9881	0	31.229624	9968	-5855	13308	510.6	60.029	0.991272
20331.0	9879	0	31.227572	10018	-5587	13196	511	60	0.986125
20331.5	9877	0	31.227572	10000	-5728	13406	510.7	60.02	0.9877
20332.0	9875	0	31.227572	9950	-5935	13367	510.8	60.029	0.992462
20332.5	9873	0	31.227367	9976	-5757	13282	510.7	60.02	0.989675
20333.0	9871	0	31.225931	10050	-5552	13173	510.9	60.02	0.982189
20333.5	9869	0	31.225931	9954	-5813	13466	510.7	60.02	0.991461
20334.0	9867	0	31.225931	9968	-5899	13310	510.9	60.02	0.989868
20334.5	9866	0	31.225931	10001	-5659	13230	510.6	60.029	0.986501
20335.0	9864	0	31.2247	10048	-4901	12946	511	60.029	0.981688
20335.5	9862	0	31.2247	9923	-5878	13404	510.9	60.02	0.993853
20336.0	9860	0	31.2247	9992	-5770	13271	510.3	60.02	0.986789
20336.5	9858	0	31.224494	10026	-5548	13170	510.6	60.029	0.983244
20337.0	9856	0	31.224289	9977	-5770	13387	510.7	60	0.987872
20337.5	9854	0	31.224084	9955	-5902	13318	510.9	60	0.989854
20338.0	9852	0	31.224084	9986	-5740	13250	510.8	60.02	0.986581
20338.5	9850	0	31.224084	10046	-5556	13194	510.5	60.02	0.98049
20339.0	9847	0	31.223058	9957	-5865	13444	511.1	60	0.988952
20339.5	9849	0	31.223058	9880	-5840	13217	511.3	60.029	0.996862
20340.0	9852	0	31.223058	9949	-5600	13168	510.8	60	0.99025
20340.5	9851	0	31.223058	10010	-5570	13315	510.7	60.02	0.984116
20341.0	9849	0	31.221417	9943	-5878	13375	511.1	60.02	0.990546
20341.0	9849	0	31.221417	9943	-5878	13375	511.1	60.02	0.990546
20341.5	9850	0	31.221212	9934	-5759	13275	511	60	0.991544
20342.0	9851	0	31.221212	9992	-5511	13112	511	60.02	0.985889
20342.5	9850	0	31.221212	9985	-5782	13472	510.9	60.04	0.98648
20343.0	9848	0	31.21957	9954	-5903	13300	511.3	60.02	0.989351
20343.5	9848	0	31.219365	9877	-5672	13156	511	60.02	0.997064
20344.0	9851	0	31.219365	10016	-5564	13199	510.7	60.029	0.983526
20344.5	9849	0	31.219365	9963	-5898	13483	510.9	60.029	0.988558
20345.0	9849	0	31.217519	9938	-5800	13282	510.8	60.02	0.991044
20345.5	9851	0	31.217519	9968	-5605	13148	510.7	60.02	0.988262

20346.0	-75148	0	31.217519	-13183	-4567	25830	511	60.02	5.700372
20346.5	-75354	0	31.217519	-77050	-4362	77789	487.4	60.02	0.977988
20347.0	-75226	0	31.217519	-77800	-4271	78117	486.7	60.029	0.966915
20347.5	-75088	0	31.217313	-77711	-4062	78015	486.6	60.029	0.966247
20348.0	-74958	0	31.217108	-77587	-4267	78027	486.8	60.02	0.966115
20348.5	-74834	0	31.217108	-77402	-4325	77813	486.8	60.029	0.966823
20349.0	-74717	0	31.215467	-77298	-4163	77660	486.9	60.029	0.96661
20349.5	-74604	0	31.215467	-77179	-4080	77536	487.1	60.02	0.966636
20350.0	-74499	0	31.215467	-77116	-4345	77609	486.8	60	0.966064
20350.5	-74397	0	31.215467	-76977	-4265	77354	486.9	60.02	0.966483
20351.0	-74283	0	31.215672	-76875	-4101	77188	486.7	60.029	0.966283
20351.5	-74193	0	31.215467	-76770	-4209	77203	487.1	60	0.966432
20352.0	-74109	0	31.215467	-76680	-4350	77155	487.4	59.99	0.966471
20352.5	-74029	0	31.215672	-76555	-4196	76910	487	60.02	0.967004
20353.0	-73954	0	31.222994	-76474	-4018	76830	486.9	60.029	0.967048
20353.5	-73883	0	31.223404	-76397	-4286	76895	487.2	60.02	0.967093
20354.0	-73815	0	31.223815	-76376	-4315	76812	487.6	60	0.966469
20354.5	-73752	0	31.22402	-76247	-4102	76573	487.3	60	0.967277
20355.0	-73690	0	31.234484	-76191	-4154	76597	487	60.029	0.967175
20355.5	-73634	0	31.235099	-76149	-4338	76636	487.6	60	0.966973
20356.0	-73567	0	31.235304	-76081	-4238	76461	487.3	60.02	0.966956
20356.5	-73515	0	31.23551	-76009	-4034	76348	487.4	60.029	0.967188
20357.0	-73467	0	31.235715	-75971	-4193	76421	487.6	60.029	0.96704
20357.5	-73420	0	31.236125	-75937	-4337	76396	487.3	60.02	0.966854
20358.0	-73378	0	31.23633	-75858	-4179	76217	487.3	60.029	0.967307
20358.5	-73337	0	31.236536	-75837	-4067	76213	486.8	60.029	0.967035
20359.0	-73297	0	31.242075	-75750	-4290	76242	487.5	60.02	0.967617
20359.5	-73261	0	31.242075	-75775	-4312	76177	487.3	60.02	0.966823
20360.0	-73224	0	31.242486	-75686	-4058	76005	487.8	60.029	0.967471
20360.5	-73192	0	31.242691	-75646	-4091	76063	487.5	60.04	0.967559
20361.0	-73155	0	31.252334	-75665	-4329	76142	487.3	60.029	0.966827
20361.5	-73124	0	31.252744	-75568	-4265	75915	487.2	60.029	0.967658
20362.0	-73098	0	31.253155	-75494	-4001	75830	487	60.029	0.968262
20362.5	-73074	0	31.25336	-75572	-4246	76071	487	60.04	0.966945
20363.0	-73048	0	31.260336	-75535	-4329	75997	487.2	60.04	0.967075
20363.5	-73023	0	31.261156	-75442	-4121	75782	487.1	60	0.967936
20364.0	-73003	0	31.261156	-75444	-3989	75796	487.1	60.029	0.967645
20364.5	-72983	0	31.261567	-75433	-4323	75932	487	60.029	0.967521
20365.0	-72963	0	31.270594	-75437	-4229	75834	487	60.06	0.967204
20365.5	-72942	0	31.27121	-75428	-4019	75764	487.2	60.02	0.967041
20366.0	-72920	0	31.27162	-75289	-3087	75589	487.3	60.029	0.968535
20366.5	-72906	0	31.27162	-75357	-4320	75842	487.7	60	0.967475
20367.0	-72890	0	31.271825	-75311	-4218	75673	487.3	60.02	0.967853
20367.5	-72875	0	31.272441	-75334	-3949	75673	487	60.02	0.967359
20368.0	-72860	0	31.272646	-75318	-4258	75824	487.6	60	0.967365
20368.5	-72844	0	31.272851	-75335	-4275	75800	487.4	60	0.966934
20369.0	-72831	0	31.278801	-75228	-4120	75586	487	60.04	0.968137
20369.5	-72820	0	31.279006	-75209	-3982	75605	487.4	60.04	0.968235
20370.0	-72810	0	31.279006	-75252	-4226	75758	487.6	60.02	0.967549
20370.5	-72798	0	31.279211	-75221	-4229	75621	487.5	60.029	0.967788
20371.0	-72784	0	31.289265	-75221	-4006	75563	486.4	60.029	0.967602
20371.5	-72774	0	31.28988	-75229	-4153	75697	487.4	60.029	0.967366
20372.0	-72764	0	31.290291	-75222	-4297	75684	487	60.02	0.967323
20372.5	-72754	0	31.290291	-75223	-4170	75578	487	60.02	0.967178
20373.0	-72745	0	31.296856	-75201	-3948	75554	487.4	60.02	0.967341
20373.5	-72737	0	31.297882	-75132	-4169	75628	486.8	60.02	0.968123
20374.0	-72733	0	31.298293	-75114	-4223	75563	487.1	59.97	0.968302
20374.5	-72728	0	31.298703	-75138	-4056	75483	487.3	60.029	0.967926
20375.0	-72723	0	31.308628	-75126	-3984	75507	487.1	60.02	0.968014
20375.5	-72718	0	31.309038	-75119	-4325	75615	487.2	60	0.968037
20376.0	-72711	0	31.309243	-75145	-4188	75518	487.4	60.02	0.967609
20376.5	-72706	0	31.309243	-75118	-3981	75461	487.2	60.02	0.967891
20377.0	-72702	0	31.309449	-75128	-4110	75575	486.8	60.02	0.967708
20377.5	-72697	0	31.310064	-75131	-4249	75601	487.7	60.029	0.967603
20378.0	-72691	0	31.310064	-75124	-4109	75488	487.5	60.04	0.967614
20378.5	-72687	0	31.310064	-75088	-3879	75461	487	60.029	0.968024
20379.0	-72682	0	31.316143	-75138	-4243	75628	487.5	60.029	0.967313
20379.5	-72677	0	31.316143	-75105	-4203	75537	487.2	60.04	0.967672
20380.0	-72671	0	31.316553	-75128	-4037	75452	487.5	60	0.967296
20380.5	-72667	0	31.316758	-75095	-3930	75512	487.6	60.02	0.967668
20381.0	-72661	0	31.32585	-75143	-4253	75638	487.6	59.99	0.96697
20381.5	-72656	0	31.32626	-75116	-4112	75480	487.8	60.029	0.967251
20382.0	-72651	0	31.326876	-75122	-3899	75452	487.2	60	0.967107
20382.5	-72646	0	31.327286	-75118	-4156	75600	487.7	60.02	0.967092
20383.0	-72646	0	31.333852	-74996	-4167	75463	487.3	60	0.968665
20383.5	-72647	0	31.334467	-75014	-4082	75367	487.2	60.02	0.968446
20384.0	-72647	0	31.334672	-75020	-3972	75374	487.6	60.029	0.968368
20384.5	-72646	0	31.334878	-75048	-4243	75545	487.7	60.02	0.967994
20385.0	-72647	0	31.345201	-75004	-4232	75394	487.6	60.02	0.968575
20385.5	-72646	0	31.345611	-75044	-3961	75378	486.8	60.02	0.968045
20386.0	-72645	0	31.346021	-75000	-4059	75408	487.3	60.02	0.9686
20386.5	-72645	0	31.346226	-75029	-4304	75514	487.5	60.02	0.968226

20387.0	-72646	0	31.346432	-74992	-4124	75348	487.4	60.02	0.968717
20387.5	-72646	0	31.347252	-75002	-3921	75348	487.2	60.029	0.968588
20388.0	-72647	0	31.347252	-75016	-4150	75507	487.1	60.02	0.96842
20388.5	-72647	0	31.347457	-75011	-4173	75468	487.2	60.02	0.968485
20389.0	-72648	0	31.352382	-75003	-4039	75362	487.1	60	0.968601
20389.5	-72647	0	31.352382	-75010	-3917	75378	487.4	60	0.968498
20390.0	-72647	0	31.352382	-75056	-4196	75555	487.5	60.029	0.967904
20390.5	-72645	0	31.352587	-75043	-4185	75411	487.5	60.029	0.968045
20391.0	-72645	0	31.36223	-74994	-3881	75327	487.8	60.04	0.968677
20391.5	-72645	0	31.362435	-75018	-4031	75442	486.8	60.04	0.968368
20392.0	-72645	0	31.362846	-75037	-4227	75509	487.4	60	0.968122
20392.5	-72645	0	31.362846	-75001	-4099	75360	487.8	60.02	0.968587
20393.0	-72646	0	31.370847	-75025	-3830	75360	487.2	60.029	0.968291
20393.5	-72647	0	31.371668	-75004	-4156	75480	487.7	59.99	0.968575
20394.0	-72647	0	31.371873	-75016	-4172	75462	487.4	60	0.96842
20394.5	-72647	0	31.372284	-75007	-4003	75345	487.4	60.02	0.968536
20395.0	-72647	0	31.380901	-75038	-3956	75436	487.3	60.029	0.968136
20395.5	-72647	0	31.381311	-75016	-4263	75504	487.5	60.02	0.96842
20396.0	-72646	0	31.381516	-75020	-4101	75391	487.2	60.02	0.968355
20396.5	-72647	0	31.381721	-74994	-3878	75328	487.4	60.029	0.968704
20397.0	-72647	0	31.381927	-75012	-4136	75498	487.6	60	0.968472
20397.5	-72648	0	31.382747	-74999	-4254	75467	487.7	60.02	0.968653
20398.0	-72648	0	31.382953	-74997	-4023	75345	487.9	60.02	0.968679
20398.5	-72649	0	31.383158	-75003	-3880	75360	487.8	60.029	0.968615
20399.0	-72648	0	31.388838	-75050	-4206	75547	487.8	60	0.967995
20399.5	-72649	0	31.388838	-74979	-4120	75405	487.7	60.02	0.968925
20400.0	-72649	0	31.389043	-75013	-3921	75345	487.8	60.02	0.968485
20400.5	-72650	0	31.389249	-74993	-3954	75390	487.8	60.04	0.968757
20401.0	-72648	0	31.399507	-75102	-4204	75588	487.6	60.02	0.967324
20401.5	-72646	0	31.399918	-75028	-4101	75381	487.4	60	0.968252
20402.0	-72646	0	31.400328	-75008	-3790	75341	487.7	60.029	0.96851
20402.5	-72647	0	31.400328	-75038	-4051	75515	487.5	60.04	0.968136
20403.0	-72647	0	31.405047	-75004	-4198	75463	488.2	60.02	0.968575
20403.5	-72649	0	31.405662	-74992	-3958	75354	487.3	60	0.968757
20404.0	-72649	0	31.405868	-75021	-3844	75388	487.1	60.029	0.968382
20404.5	-72649	0	31.406073	-75024	-4156	75526	487.7	60.04	0.968343
20405.0	-72649	0	31.414702	-75012	-4092	75400	487.6	60.029	0.968498
20405.5	-72649	0	31.415317	-74995	-3863	75319	487.4	60.02	0.968718
20406.0	-72650	0	31.415933	-75000	-4073	75442	487.1	60.04	0.968667
20406.5	-72647	0	31.416138	-75121	-4147	75609	487.2	60	0.967066
20407.0	-72645	0	31.416343	-74995	-4034	75342	487.2	60.029	0.968665
20407.5	-72646	0	31.416754	-74986	-3841	75351	487.5	60.04	0.968794
20408.0	-72647	0	31.416754	-74975	-4025	75487	487.6	60.029	0.96895
20408.5	-72648	0	31.416754	-75012	-4117	75459	487.3	60.02	0.968485
20409.0	-72649	0	31.423935	-75003	-3926	75344	487.9	60.02	0.968615
20409.5	-72648	0	31.423935	-75002	-3789	75366	488	60.02	0.968614
20410.0	-72649	0	31.423935	-75026	-4118	75523	487.4	60.029	0.968318
20410.5	-72649	0	31.42414	-75010	-4067	75398	488.1	60.02	0.968524
20411.0	-72650	0	31.434527	-74982	-3910	75318	487.8	60	0.968899
20411.5	-72649	0	31.435553	-75097	-3942	75567	488	60.029	0.967402
20412.0	-72646	0	31.436169	-75039	-4172	75504	488.1	60.04	0.96811
20412.6	-72645	0	31.436579	-75002	-3985	75350	487.8	60	0.968574
20413.1	-72647	0	31.443145	-75000	-3795	75351	487.6	60.04	0.968627
20413.6	-72648	0	31.44376	-74986	-4002	75488	487.9	60.02	0.968821
20414.0	-72649	0	31.443965	-75019	-4100	75434	487.6	60.04	0.968408
20414.0	-72649	0	31.443965	-75019	-4100	75434	487.6	60.04	0.968408
20414.5	-72649	0	31.44417	-74997	-3840	75328	487.7	60.04	0.968692
20415.0	-72650	0	31.453057	-75018	-3835	75381	487.2	60.029	0.968434
20415.5	-93792	0	31.453468	-89559	-3722	91964	487.8	60	1.047265
20416.0	-93818	0	31.453673	-96847	-3816	97142	481.1	60.029	0.968724
20416.5	-93726	0	31.453878	-96768	-3075	97038	481	60.02	0.968564
20417.0	-93637	0	31.454083	-96703	-3747	97058	481.4	60.029	0.968295
20417.5	-93553	0	31.455314	-96610	-3827	96967	481.6	60.029	0.968357
20418.0	-93472	0	31.455519	-96580	-3682	96877	481.3	60.06	0.967819
20418.5	-93395	0	31.455725	-96489	-3505	96767	481.4	60.04	0.967934
20419.0	-93323	0	31.460238	-96437	-3866	96847	481.8	60	0.967709
20419.5	-93253	0	31.460238	-96348	-3776	96685	481.4	60.029	0.967877
20420.0	-93186	0	31.460649	-96273	-3586	96523	481.4	60.029	0.967935
20420.5	-93112	0	31.460649	-96224	-3471	96545	481.4	60.04	0.967659
20421.0	-93055	0	31.471523	-96113	-3752	96516	481.5	60.06	0.968183
20421.5	-92999	0	31.472139	-96034	-3736	96335	481.5	60.04	0.968397
20422.0	-92949	0	31.472549	-96002	-3476	96283	481.8	60.04	0.968199
20422.5	-92899	0	31.473164	-95904	-3841	96332	481.6	60.06	0.968667
20423.0	-92855	0	31.481166	-95893	-3779	96284	481.9	60.029	0.968319
20423.5	-92810	0	31.482192	-95824	-3637	96099	482.3	60.029	0.968547
20424.0	-92770	0	31.482602	-95817	-3476	96112	481.9	60.04	0.9682
20424.5	-92729	0	31.482808	-95814	-3700	96218	481.6	60.029	0.967802
20425.0	-92691	0	31.494913	-95714	-3718	96046	482	60.04	0.968416
20425.5	-92645	0	31.495733	-95704	-3535	95963	481.7	60.06	0.968037
20426.0	-92611	0	31.496144	-95594	-3594	95912	481.5	60.06	0.968795
20426.5	-92582	0	31.496349	-95580	-3704	95972	481.5	60.06	0.968634
20427.0	-92553	0	31.496554	-95570	-2604	95876	482	60.04	0.968432

20427.5	-92524	0	31.49758	-95534	-3407	95793	481.5	60.029	0.968493
20428.0	-92500	0	31.497785	-95489	-3724	95877	481.7	60.04	0.968698
20428.5	-92475	0	31.49799	-95510	-3794	95870	482	60.06	0.968223
20429.0	-92450	0	31.504761	-95501	-3625	95767	481.5	60.06	0.968053
20429.5	-92425	0	31.504966	-95400	-3456	95689	482	60.04	0.968816
20430.0	-92406	0	31.505171	-95402	-3797	95800	481.7	60.06	0.968596
20430.5	-92383	0	31.505377	-95381	-3615	95685	482.1	60.04	0.968568
20431.0	-92364	0	31.518367	-95391	-3405	95654	481.6	60.06	0.968267
20431.5	-92344	0	31.518983	-95358	-3620	95727	482.1	60.06	0.968393
20432.0	-92327	0	31.519393	-95305	-3754	95693	481.7	60.04	0.968753
20432.5	-92312	0	31.519598	-95244	-3676	95521	481.6	60.04	0.969216
20433.0	-92299	0	31.526984	-95315	-3431	95591	481.7	60.04	0.968358
20433.5	-92285	0	31.52801	-95265	-3725	95678	482	60.029	0.968719
20434.0	-92271	0	31.528626	-95298	-3650	95639	481.3	60.029	0.968236
20434.5	-92257	0	31.528831	-95272	-3513	95535	481.3	60.06	0.968354
20435.0	-92242	0	31.541141	-95292	-3397	95592	481.5	60.06	0.967993
20435.5	-92227	0	31.541962	-95207	-3660	95606	481.2	60.06	0.9687
20436.0	-92218	0	31.542372	-95166	-3590	95451	481.9	60.069	0.969023
20436.5	-92209	0	31.542783	-95180	-3427	95456	481.3	60.04	0.968785
20437.0	-92201	0	31.542988	-95170	-3602	95540	481.6	60.029	0.968803
20437.5	-92192	0	31.544014	-95177	-3764	95553	481.6	60.029	0.968637
20438.0	-92183	0	31.544219	-95196	-3607	95492	481.7	60.04	0.96835
20438.5	-92174	0	31.544424	-95156	-3453	95440	482.2	60.06	0.968662
20439.0	-92165	0	31.552156	-95227	-3695	95621	481.4	60.029	0.967845
20439.5	-92155	0	31.552156	-95178	-3758	95493	482.1	60.029	0.968238
20440.0	-92146	0	31.552361	-95219	-3549	95467	481.7	60.029	0.967727
20440.5	-92136	0	31.552566	-95065	-3533	95385	481.7	60.06	0.96919
20441.0	-92133	0	31.564466	-95086	-3686	95469	482	60.02	0.968944
20441.5	-92129	0	31.565082	-95074	-3611	95353	481.5	60.04	0.969024
20442.0	-92126	0	31.565492	-95079	-3419	95349	481.7	60.06	0.968942
20442.5	-92122	0	31.565492	-95085	-3637	95469	481.5	60.04	0.968838
20443.0	-92119	0	31.572058	-95047	-3676	95411	481.8	60.029	0.969194
20443.5	-92116	0	31.572879	-95048	-3531	95329	481.4	60.04	0.969152
20444.0	-92113	0	31.573289	-95065	-3295	95360	481.5	60.04	0.968948
20444.5	-92109	0	31.573699	-95085	-3668	95468	481.4	60.04	0.968702
20445.0	-92106	0	31.585189	-95070	-3632	95365	481.8	60.04	0.968823
20445.5	-92101	0	31.58601	-95054	-3467	95308	481.6	60.06	0.968933
20446.0	-92098	0	31.586625	-95066	-3393	95416	481.5	60.04	0.96878
20446.5	-92094	0	31.587036	-95066	-3671	95448	481.7	60.04	0.968738
20447.0	-92091	0	31.587241	-95066	-3556	95343	481.8	60.04	0.968706
20447.5	-92087	0	31.588472	-95085	-3445	95354	481.8	60.06	0.96847
20448.0	-92084	0	31.588677	-95075	-3605	95477	481.4	60.04	0.968541
20448.5	-92080	0	31.588882	-95066	-3629	95410	482	60.029	0.96859
20449.0	-92077	0	31.598255	-95100	-3446	95372	481.6	60.04	0.968212
20449.5	-92073	0	31.598255	-95039	-3507	95339	482.1	60.069	0.968792
20450.0	-92070	0	31.59846	-95133	-3669	95516	481.6	60.029	0.967803
20450.5	-92064	0	31.59846	-95047	-3659	95347	481.8	60.06	0.968616
20451.0	-92060	0	31.61063	-95077	-3347	95331	482.1	60.04	0.968268
20451.5	-92057	0	31.611451	-95058	-3626	95448	481.9	60.06	0.96843
20452.0	-92054	0	31.611656	-95062	-3634	95434	482.6	60.029	0.968357
20452.5	-92052	0	31.611861	-95047	-3474	95336	481.8	60.06	0.968489
20453.0	-92048	0	31.617606	-95069	-3320	95350	482.2	60.06	0.968223
20453.5	-92047	0	31.618427	-94986	-3583	95387	482	60.04	0.969059
20454.0	-92048	0	31.619043	-94982	-3669	95324	482.2	60.09	0.96911
20454.5	-92048	0	31.619453	-94983	-3475	95245	481.6	60.04	0.9691
20455.0	-92049	0	31.631213	-94935	-3493	95261	481.8	60.04	0.9696
20455.5	-92051	0	31.631828	-95064	-3618	95453	481.6	60.04	0.968306
20456.0	-92048	0	31.632239	-95067	-3586	95334	482.1	60.06	0.968243
20456.5	-92047	0	31.632649	-94956	-3257	95214	481.6	60.04	0.969365
20457.0	-92050	0	31.632854	-94966	-3478	95345	481.5	60.069	0.969294
20457.5	-92049	0	31.634085	-95069	-3674	95427	481.8	60.02	0.968234
20458.0	-92047	0	31.63429	-95020	-3470	95281	481.6	60.04	0.968712
20458.5	-92048	0	31.634495	-94939	-3225	95226	481.6	60.06	0.969549
20459.0	-92049	0	31.643933	-95023	-3615	95424	481.2	60.02	0.968702
20459.5	-92049	0	31.643933	-94988	-3543	95294	481.8	60.06	0.969059
20460.0	-92050	0	31.644139	-94998	-3364	95254	481.7	60.06	0.968968
20460.5	-92048	0	31.644139	-95084	-3402	95424	481.5	60.029	0.96807
20461.0	-92047	0	31.655974	-94994	-3616	95375	481.4	60.04	0.968977
20461.5	-92049	0	31.656589	-94947	-3508	95230	481.6	60.029	0.969478
20462.0	-92051	0	31.657	-94975	-3274	95238	481.5	60.06	0.969213
20462.5	-92050	0	31.657205	-95028	-3422	95433	482	60.04	0.968662
20463.0	-92047	0	31.663565	-95071	-3509	95421	481.5	60.029	0.968192
20463.5	-92048	0	31.664181	-94946	-3370	95215	481.6	60.06	0.969477
20464.0	-92049	0	31.664796	-94973	-3301	95249	481.8	60.06	0.969212
20464.5	-92051	0	31.665207	-95009	-3591	95431	481.5	60.02	0.968866
20465.0	-92046	0	31.677042	-95078	-3535	95372	482	60.029	0.96811
20465.5	-92045	0	31.678067	-94989	-3305	95241	481.6	60.04	0.969007
20466.0	-92046	0	31.678067	-94957	-3350	95282	481.6	60.04	0.969344
20466.5	-92046	0	31.678273	-94998	-3660	95375	481.5	60.02	0.968926
20467.0	-92047	0	31.678888	-94982	-3354	95247	481.7	60.04	0.969099
20467.5	-92048	0	31.679709	-94958	-3241	95232	482	60.04	0.969355
20468.0	-92050	0	31.679914	-94976	-3447	95356	481.5	60.029	0.969192

Bibliography

[1] S. Sergio, C. Lee, X. Wang, and J. Kirtley, "Electric Drives and Power Chargers: Recent Solutions to Improve Performance and Energy Efficiency for Hybrid and Fully Electric Vehicles," *IEEE Vehicular Technology Magazine*, vol. 15, pp. 73 – 83, March 2020.

[2] C. D. et al., "Energy management in fuel-cellvehicles: key issues identified in the IEEE vehicular technology society motor vehicle challenge 2017," *IEEE Vehicular Technology Magazine*, vol. 13, no. 3, pp. 144–151, 2018.

[3] A. M. El-Refaie, "Motors/generators for traction/propulsion applications: A review," *IEEE Vehicular Technology Magazine*, vol. 8, no. 1, pp. 90–99, 2013.

[4] A. T. et al., "Experimental characterization of a belt-driven multiphase induction machine for 48-V automotive applications: losses and temperatures assessments," *IEEE Trans. Industry Applications*, vol. 52, no. 2, pp. 1321–1330, 2016.

[5] R. B. et al., "Multiphase starter generator for a 48-V minihybrid powertrain: design and testing," *IEEE Trans. Industry Applications*, vol. 52, no. 2, pp. 1750–1758, 2016.

[6] S. C. et al., "Design and testing of a belt-driven induction starter–generator," *IEEE Trans. Industry Applications*.

[7] A. G. et al., "Energy storage in pennsylvania: SEPTA's novel and innovative integration of emerging smart grid technologies," *IEEE Vehicular Technology Magazine*, vol. 9, no. 2, pp. 76–86, 2014.

[8] S. N. et al., "A permanent-magnet double-stator integrated-startergenerator for hybrid electric vehicles," *IEEE VPPC 2008*, pp. 1–6, 2018.

[9] Y. D. D. Richard, "Valeo stars technology: A competitive solution for hybridization," *IEEE PCC 2007*, pp. 1601–1605, 2007.

[10] A. Kurs, A. Karalis, R. Moffatt, J. D. Joannopoulos, P. Fisher, and M. Soljacic, "Wireless Power Transfer via Strongly Coupled Magnetic Resonances," *Science*, vol. 317, no. 5834, pp. 83–86, 2017.

[11] O. Galinina, H. Tabassum, and et. al, "On feasibility of 5g-grade dedicated rf charging technology for wireless-powered wearables," *IEEE Wireless Communications*, vol. 23, 11 2015.

[12] J. L. K. Jr., *Electric Power Principles: Sources, Conversion, Distribution and Use*. John Wiley Sons, Inc, 2012.

[13] A. E. Fitzgerald, C. K. Jr., and S. Umans, *Electric Machinery*. McGraw-Hill Science, 2002.

[14] J. Heuer, P. Kiomarnicki, and Z. A. Styczynski, "Integration of electrical vehicles into the smart grid in the Harz.EE-mobility research project," in *2011 IEEE Power and Energy Society General Meeting*, 2011.

[15] S. Deilmani, A. S. Masoum, and P. S. Moses, "Real-Time Coordination of Plug-In Electric Vehicle Charging in Smart Grids to Minimize Power Losses and Improve Voltage Profile," *IEEE Transactions on Smart Grid*, vol. 2, no. 3, pp. 456–467, 2011.

[16] C. Pang, P. Dutta, and M. Kezunovic, "BEVs/PHEVs as Dispersed Energy Storage for V2B Uses in the Smart Grid," *IEEE Transactions on Smart Grid*, vol. 3, no. 1, pp. 473–482, 2012.

[17] W. Tushar, W. Saad, and etc., "Economics of Electric Vehicle Charging: A Game Theoretic Approach," *IEEE Transactions on Smart Grid*, vol. 3, no. 4, pp. 1767–1778, 2012.

[18] Y. Xing, J. Jin, and etc., "Overloading of distribution transformers in smart grid due to uncoordinated charging of plug-In electric vehicles," in *2012 IEEE PES Innovative Smart Grid Technologies (ISGT)*, 2012.

[19] G. Brusaglino, "Integration of Road Electric Vehicles into the Smart Grid System," in *2013 International Conference on Clean Electrical Power*, 2013.

[20] C. Liu, K. T. Chau, D. Wu, and S. Gao, "Opportunities and Challenges of Vehicle-to-Home, Vehicle-to-Vehicle, and Vehicle-to-Grid Technologies," *Proceedings of the IEEE*, vol. 101, no. 11, pp. 2409–2424, 2013.

[21] R. C. Green, L. Wang, and M. Alam, "Applications and Trends of High Performance Computing for Electric Power Systems: Focusing on Smart Grid," *IEEE Transactions on Smart Grid*, vol. 4, no. 2, pp. 922–931, 2013.

[22] Z. Tan, P. Yang, and A. Nehorai, "An Optimal and Distributed Demand Response Strategy With Electric Vehicles in the Smart Grid," *IEEE Transactions on Smart Grid*, vol. 5, no. 2, pp. 861–869, 2014.

[23] J. Donadee and M. D. llic, "Stochastic Optimization of Grid to Vehicle Frequency Regulation Capacity Bids," *IEEE Transactions on Smart Grid*, vol. 5, no. 2, pp. 1061–1069, 2014.

[24] R. Das, K. Thuirugnanam, and etc., "Mathematical Modeling for Economic Evaluation of Electric Vehicle to Smart Grid Interaction," *IEEE Transactions on Smart Grid*, vol. 5, no. 2, pp. 712–721, 2014.

[25] Y. Mou, H. Xing, Z. Lin, and M. Fu, "Decentralized Optimal Demand-Side Management for PHEV Charging in a Smart Grid," *IEEE Transactions on Smart Grid*, vol. 6, no. 2, pp. 726–736, 2015.

[26] R. A. V. E. Veldman, "Distribution Grid Impacts of Smart Electric Vehicle Charging From Different Perspectives," *IEEE Transactions on Smart Grid*, vol. 6, no. 1, pp. 333–342, 2015.

[27] V. Monteiro, J. G. Pinto, and J. L. Afonso, "Operation Modes for the Electric Vehicle in Smart Grids and Smart Homes: Present and Proposed Modes," *IEEE Transactions on Vehicular Technology*, vol. 65, no. 3, pp. 1007–1020, 2016.

[28] J. Dai, M. Dong, and etc., "A review on electric vehicles and renewable energy synergies in smart grid," in *2016 China International Conference on Electricity Distribution (CICED)*, 2016.

[29] L. Y. et al., "NOx control technologies for Euro 6 diesel passenger cars," *Int. Council Clean Transportation, white paper*, pp. 1–22, 2015.

[30] S. S. et al., "HV-CMOS design and characterization of a smart rotor coil driver for automotive alternators," *IEEE Trans. on Industrial Electronics*, vol. 60, no. 6, pp. 2309–2317, 2013.

[31] V. Handbook, *From stop-start to hybridization.* 2017.

[32] L. Mihet-Popa and S. Saponara, "Toward green vehicles digitalization for the next generation of connected and electrified transport systems," *Energies*, vol. 11, no. 11, 2018.

[33] F. Lambert, "Vw unveils meb platform for electric vehicles, launches 'electric for all' campaign to have 'affordable' evs," 2019.

[34] S. L. Ho, J. Wang, W. N. Fu, and M. Sun, "A Comparative Study Between Novel Witricity and Traditional Inductive Magnetic Coupling in Wireless Charging," *IEEE Trans. Magnetics*, vol. 47, no. 5, pp. 1522–1525, 2011.

[35] Z. Dang, Y. Cao, and J. A. Qahouq, "Reconfigurable Magnetic Resonance-Coupled Wireless Power Transfer system," *IEEE Trans. Power Electron.*, vol. 30, no. 11, pp. 6057–6069, 2015.

[36] J. Kim, G. Wei, M. Kim, J. Jong, and C. Zhu, "A Comprehensive Study on Composite Resonant Circuit-Based Wireless Power Transfer Systems," *IEEE Trans. Ind. Electron.*, vol. 65, no. 6, pp. 4670–4680, 2017.

[37] Carobolante, P. Menegoli, F. Marino, and N. Jeong, "A Novel Charger Architecture for Resonant Wireless Power Transfer," *IEEE Journal of Emerging and Selected Topics in Power Electronics*, vol. 6, no. 2, pp. 571–580, 2018.

[38] M. R. Basar, M. Y. Ahmad, J. Cho, and F. B. Ibrahim, "An Improved Wearable Resonant Wireless Power Transfer System for Biomedical Capsule Endoscope," *IEEE Journal of Emerging and Selected Topics in Power Electronics*, vol. 65, no. 10, pp. 7772–7781, 2018.

[39] h. K. Song, Y. Kim, D. Kim, S. Jeong, Y. Cho, S. Lee, S. Ahn, and J. Kim, "EMI Reduction Methods in Wireless Power Transfer System for Drone Electrical Charger using Tightly-coupled Three-phase Resonant Magnetic Field," *IEEE Trans. Ind. Electron.*, vol. 65, no. 9, pp. 6839–6849, 2018.

[40] C. Cai, J. Wang, R. Liu, Z. Fang, P. Zhang, M. Long, M. Hu, and Z. Lin, "Resonant Wireless Charging System Design for 110kV High Voltage Transmission Line Monitoring Equipment," *IEEE Trans. Ind. Electron.*, vol. 66, no. 5, pp. 4118–4129, 2018.

[41] A. Abdolkhani and A. P. H. and. C. Nair, "A Double Stator Through-hole Type Contactless Slipring for Rotary Wireless Power Transfer Applications," *IEEE Trans. Energy Convers.*, vol. 29, no. 2, pp. 426–434, 2014.

[42] M. Liu, K. W. Chan, J. Hu, Q. Lin, J. Liu, and W. Xu, "Design and Realization of a Coreless and Magnetless Electric Motor Using Magnetic Resonant Coupling Technology," *IEEE Trans. Energy Convers.*, vol. 34, pp. 1200–1212, 2019.

[43] H. Zeng and F. Z. Peng, "SiC-Based Z-Source Resonant Converter with Constant Frequency and Load Regulation for EV Wireless Charger," *IEEE Trans. Energy Convers.*, vol. 32, no. 11, pp. 8813–8822, 2016.

[44] B. H. Choi, V. X. Thai, E. S. LEE, J. H. Kim, and C. T. Rim, "Dipole-Coil-Based Wide-Range Inductive Power Transfer Systems for Wireless Sensors," *IEEE Trans. Energy Convers.*, vol. 63, no. 5, pp. 3158–3167, 2016.

[45] L. Shi, Z. Kabelac, D. Katabi, and et al, "Wireless Power Hotspot that Charges All of Your Devices," *MobiCom*, 2015.

[46] H. Yin, M. Fu, M. Liu, J. Song, and C. Ma, "Autonomous Power Control in A Reconfigurable 6.78 Megahertz Multiple-receiver Wireless Charging System," *IEEE Trans. on Ind. Electron.*, vol. 65, no. 8, pp. 6177–6187, 2017.

[47] A. Berger, M. Agostinelli, S. Vesti, J. A. Oliver, J. A. Cobos, and M. Huemer, "A Wireless Charging System Applying Phase-Shift and Amplitude Control to Maximize Efficiency and Extractable Power," *IEEE Trans. Power Electron.*, vol. 30, no. 11, pp. 6338 – 6348, 2015.

[48] Y. Cao, Z. Dang, J. A. Dahouq, and E.Philips, "Dynamic Efficiency Tracking Controller for Reconfigurable Four-Coil Wireless Power Transfer System," *IEEE Applied Power Electronics Conference and Exposition (APEC)*, pp. 3684 – 3689, 2016.

[49] D. N. D. K. X. Lu, P. Wang and Z. Han, "Wireless Charger Networking for Mobile Devices: Fundamentals, Standards, and Network Applications," *IEEE Communications Surveys and Tutorials*, vol. 22, no. 2, pp. 126 – 135, 2015.

[50] D. N. D. K. X. Lu, P. Wang and Z. Han, "Wireless Charging Technologies: Fundamentals, Standards, and Network Applications," *IEEE Communications Surveys and Tutorials*, vol. 18, no. 2, pp. 1413 – 1452, 2015.

[51] J. Jadidian and D. Katabi, "Magnetic MIMO: How to charge your phone in your pocket," *Proceedings of the 20th Annual International Conference on Mobile Computing and Networking, ACM 2014*, 2014.

[52] G. Yang, M. R. V. Moghadam, and R. Zhang, "Magnetic MIMO Signal Processing and Optimization for Wireless Power Transfer," *IEEE Trans. Signal Process*, vol. 65, no. 11, pp. 2860–2874, 2017.

[53] P. Sun, Y. Dong, H. YE, and H. Zhao, "A Wireless Power Transfer CPS Based on 2D Omni-Directional Rotating Magnetic Field," Software Quality, Reliability and Security Companion (QRS-C)," *IEEE International Conference*, pp. 252–258, 2016.

[54] J. Zhao, X. Huang, and W. Wang, "Wireless power transfer with twodimensional resonators," *IEEE Trans Magn.*, vol. 50, no. 1, 2014.

[55] J. A. Wheeler and R. P. Feynman, "Classical electrodynamics in terms of direct interparticle action," *IEEE Communications Surveys and Tutorials*, vol. 21, no. 3, pp. 180 – 181, 1949.

[56] P. C. Krause, O. Wasynczuk, T. C. O'Connell, and M. Hasan, "Tesla's Contribution to Electric Machine Analysis," *IEEE Trans. Energy Convers.*, vol. 32, no. 2, pp. 591 – 598, 2017.

[57] S. D. Sudhoff and R. Sahu, "Metamodeling of Rotating Electric Machinery," *IEEE Trans. Energy Convers.*, vol. 33, no. 3, pp. 1058 – 1071, 2018.

[58] O. Laldin, S. D. Sudhoff, and S. Pekarek, "An Analytical Design Model for Wound Rotor Synchronous Machines," *IEEE Trans. Energy Convers.*, vol. 30, no. 4, pp. 1299 – 1309, 2015.

[59] J. A. Krizan and S. D. Sudhoff, "Design Model for Salient Permanent-Magnet Machines with Investigation of Saliency and Wide-Speed-Range Performance," *IEEE Trans. Energy Convers.*, vol. 28, no. 1, pp. 95 – 105, 2013.

[60] M. G. G. G. Inventory, "GHG Emissions and Mitigation Policies," in *https://www.mass.gov/info-details/ghg-emissions-and-mitigation-policies*, 2019.

[61] K. Afridi, *A Methodology for the Design and Evaluation of Advanced Automotive Electrical Power Systems*. PhD thesis, Department of Electrical Engineering and Computer Science, Massachusetts Institute of Technology, 1998.

[62] X. Wang, H. Bai, J. Kirtley, and etc., "Power-Loss Analysis and Efficiency Maximization of a Silicon-Carbide MOSFET-Based Three-Phase 10-kW Bidirectional EV Charger Using Variable-DC-Bus Control," *IEEE Journal of Emerging and Selected Topics in Power Electronics*, vol. 4, pp. 880–892, September 2016.

[63] J. Sears, D. Roberts, and K. Glitman, "A comparison of electric vehicle Level 1 and Level 2 charging efficiency," *IEEE Conference on Technologies for Sustainability.*, 2014.

[64] B. Whitaker, A. Barkley, and et al., "A High-Density, High-Efficiency, Isolated On-Board Vehicle Battery Charger Utilizing Silicon Carbide Power Devices," *IEEE Transactions on Power Electronics*, vol. 29, no. 5, pp. 2606–2617, 2014.

[65] E. Asa, K. Colak, and D. Czarkowski, "Analysis of A Novel Interleaved CLL Resonant Converter for EV Battery Charger Applications," *2014 IEEE Energy Conversion Congress and Exposition (ECCE)*, pp. 2031–2036, 2014.

[66] M. Li, Q. Chen, X. Ren, Y. Zhang, K. Jin, and B. Chen, "The integrated LLC resonant converter using center-tapped transformer for on-board EV charger," *2015 IEEE Energy Conversion Congress and Exposition (ECCE)*, pp. 6293–6298.

[67] M. Kwon, S. Jung, and S. Choi, "A high efficiency bi-directional EV charger with seamless mode transfer for V2G and V2H application," *2015 IEEE Energy Conversion Congress and Exposition (ECCE)*, pp. 5394–5399.

[68] J. Lai, L. Zhang, and et al., "A high-efficiency 3.3-kW bidirectional on-board charger," *2015 IEEE 2nd International Future Energy Electronics Conference (IFEEC)*, pp. 1–5.

[69] R. Ullah, A. Ali, and Z. Ullah, "Zero Voltage Switched Full Bridge Converters for the Battery Charger of Electric Vehicle," *International Journal of Electrical, Computer, Energetic, Electronic and Communication Engineering*, vol. 10, pp. 1046–1055, 08 2016.

[70] P. Jain and T. Jain, "Impacts of G2V and V2G power on electricity demand profile," *Proc. IEEE Int. Electric Vehicle Conf.*, pp. 1–8, 2014.

[71] "Technology roadmap: Solar photovoltaic energy," 2014.

[72] S. Kim and F.-S. Kang, "Multifunctional onboard battery charger for plug-in electric vehicles," *IEEE Trans. Ind. Electron.*, vol. 62, no. 6, pp. 3460–3472, 2014.

[73] Y. S. Dow, H. I. Son, and H.-D. Lee, "A study on half bridge LLC resonant converter for battery charger on board," *Proc. IEEE 8th Int. Conf. Power Electron., ECCE Asia (ICPEECCE)*, pp. 2694–2698, 2011.

[74] H. Wang, S. Dusmez, and A. Khaligh, "High-power modular multilevel converters with SiC JFETs," *Proc. IEEE Appl. Power Electron. Conf. Expo. (APEC)*, pp. 1683–1689, 2014.

[75] J. L. Hudgins, "Power electronic devices in the future," *IEEE J. Emerg. Sel. Topics Power Electron.*, vol. 1, no. 1, pp. 1–17, 2013.

[76] D. P. et al., "High-power modular multilevel converters with SiC JFETs," *IEEE Trans. Power Electron.*, vol. 27, no. 1, pp. 28–36, 2012.

[77] E. de Oliveira, S. Araujo, B. Dombert, and P. Zacharias, "Onboard battery chargers in electric cars: Benchmarking a novel 5-level hybrid converter with a full SiC-based approach," *Proc. Int. Exhibit. Conf. Power Electron., Intell. Motion, Renew. Energy Energy Manage*, pp. 1–8, 2014.

[78] B. W. et al., "A high-density, high-efficiency, isolated on-board vehicle battery charger utilizing silicon carbide power devices," *IEEE Trans. Power Electron.*, vol. 29, no. 5, pp. 2606–2617, 2014.

[79] F. Krismer and J. W. Kolar, "Accurate power loss model derivation of a high-current dual active bridge converter for an automotive application," *IEEE Trans. Ind. Electron.*, vol. 57, no. 3, pp. 881–891, 2010.

[80] L. Xue, Z. S. D. Diaz, F. Luo, P. Mattavelli, and D. Boroyevich, "Dual active bridge based battery charger for plug-in hybrid electric vehicle with charging current containing low frequency ripple," *Proc. 28th Annu. IEEE Appl. Power Electron. Conf. Expo. (APEC)*, pp. 1920–1925, 2013.

[81] M. Arias, D. G. Lamar, F. F. Linera, D. Balocco, A. A. Diallo, and J. N. Sebastián, "Design of a soft-switching asymmetrical halfbridge converter as second stage of an LED driver for street lighting application," *IEEE Trans. Power Electron.*, vol. 27, no. 3, pp. 1608–1621, 2012.

[82] G. R. C. Mouli, J. Schijffelen, and et al., "A high-efficiency 3.3-kW bidirectional on-board charger," *IEEE Transactions on Power Electronics*, vol. 34, no. 2, pp. 1082–1098, 2019.

[83] H. Li, S. Wang, , and et al., "A SiC Bidirectional LLC On-Board Charger," *2019 IEEE Applied Power Electronics Conference and Exposition (APEC)*, pp. 3353–3360, 2019.

[84] Y. Zhang, T. Lu, and etc., "Quasi-Uniform Magnetic Field Generated by Multiple Transmitters of Magnetically-Coupled Resonant Wireless Power Transfer," *IEEE ICEMS 2015*, 2015.

[85] L. Xie, Y. Shi, Y. T. Hou, and W. Lou, "Wireless Power Transfer and Applications to Sensor Networks," *IEEE Wireless Communications*, pp. 140 – 145, 2013.

[86] Y. Wang, J. Song, L. Lin, X. Wu, and W. Zhang, "Research on magnetic coupling resonance wireless power transfer system with variable coil structure," *2017 IEEE PELS Workshop on Emerging Technologies: Wireless Power Transfer (WoW)*, 2017.

[87] F. Hattori, J. Imaoka, M. Yamamoto, and M. Masuda, "Fundamental Experiment of 3-phase Electric Resonant Coupling Wireless Power Transfer," *2018 7th International Conference on Renewable Energy Research and Applications (ICRERA)*, 2018.

[88] M. R. Basar, M. Y. Ahmad, J. Cho, and F. Ibrahim, "A 3-coil wireless power transfer system with fine tuned power amplifier for biomedical capsule," *2017 IEEE Asia Pacific Microwave Conference (APMC)*, 2017.

[89] S. Y. Tan, H. J. Lee, K. Y. Lau, and P. J. Ker, "Simulation of 4-coils Magnetic Resonance Coupling for Multiple Receivers Wireless Power Transfer at Various Transmission Distance," *2018 IEEE Student Conference on Research and Development (SCOReD),*, 2018.

[90] C. Xu, Y. Zhuang, H. Han, C. Song, Y. Huang, and J. Zhou, "Multi-coil high efficiency wireless power transfer system against misalignment," *2018 IEEE Student Conference on Research and Development (SCOReD)*, 2018.

[91] X. Liu, J. Wu, N. Jenkins, and et al., "Combined analysis of electricity and heat networks," *Appl. Energy*, vol. 162, pp. 1238–1250, 2016.

[92] M. Geidl, G. Koeppel, P. Favre-Perrod, and et al., "Energy hubs for the future," *Appl. Energy*, vol. 5, 2007.

[93] M. I. Qureshi, A. M. Rasli, and K. Zaman, "Energy crisis, greenhouse gas emissions and sectoral growth reforms: repairing the fabricated mosaic," *Journal of Cleaner Production*, vol. 112, pp. 3657 – 3666, 2016.

[94] Z. Pan, Q. Guo, and H. Sun, "Feasible region method based integrated heat and electricity dispatch considering building thermal inertia," *Appl. Energy*, vol. 192, pp. 395–407, 2017.

[95] X. J. X. Xu, H. Jia, and et al., "Hierarchical management for integrated community energy systems," *Appl. Energy*, vol. 160, pp. 231–243, 2015.

[96] M. Geidl and G. Andersson, "Optimal power flow of multiple energy carriers," *IEEE Trans. Power Syst.*, vol. 22, no. 1, pp. 145–155, 2007.

[97] G. Li, R. Zhang, T. Jiang, and et al., "Security-constrained bi-level economic dispatch model for integrated natural gas and electricity systems considering wind power and power-to-gas process," *Appl. Energy*, vol. 194, pp. 696–704, 2017.

[98] T. Krause, G. Andersson, K. Frohlich, and et al., "Multiple-energy carriers: modeling of production, delivery, and consumption," *Proc. IEEE*, vol. 99, pp. 15–27, 2011.

[99] M. Geidl, "Integrated modeling and optimization of multi-carrier energy systems," *Ph.D. thesis, Swiss Federal Institute of Technology Zurich*, 2007.

[100] M. Geidl and G. Andersson, "Optimal coupling of energy infrastructure," *Proc. IEEE Power Tech Conf., Lausanne*, pp. 1398 – 1403, 2007.

[101] K. Hemmes, J. Zachariah-Wolf, M. M. Geidl, and G. Andersson, "Towards multi-source multi-product energy systems," *Int. J. Hydrog. Energy*, vol. 32, pp. 1332 – 1338, 2007.

[102] R. Frik and P. Favre-Perrod, "Proposal for a multifunctional energy bus and its interlink with generation and consumption," *High voltage Laboratory, ETH, Zurich.*

[103] M. Chaudry, N. Jenkins, M. Qadrdan, and et al., "Combined gas and electricity network expansion planning," *Appl. Energy*, vol. 113, pp. 1171 – 1187, 2014.

[104] L. Bai, F. Li, H. Cui, and et al., "Interval optimization based operating strategy for gas-electricity integrated energy systems considering demand response and wind uncertainty," *Appl. Energy*, vol. 167, pp. 270 – 279, 2016.

[105] L. Wu and M. Shahidehpour, "Optimal coordination of stochastic hydro and natural gas supplies in midterm operation of power systems," *IET Gener. Transm. Distrib.*, vol. 5, pp. 577 – 587, 2011.

[106] C. Unsihuay-Vila, J. W. Marangon-Lima, and et al., "A model to longterm, multiarea, multistage, and integrated expansion planning of electricity and natural gas systems," *IEEE Trans. Power Syst.*, vol. 25, pp. 1154 – 1168, 2010.

[107] F. Barati, H. Seifi, M. Sepasian, and et al., "Multi-period integrated framework of generation, transmission, and natural gas grid expansion planning for largescale systems," *IEEE Trans. Power Syst.*, vol. 30, pp. 2527 – 2537, 2015.

[108] J. Qiu, Z. Y. Dong, J. H. Zhao, and et al., "Low carbon oriented expansion planning of integrated gas and power systems," *IEEE Trans. Power Syst.*, vol. 30, pp. 1035 – 1046, 2015.

[109] A. Martinez-Mares and C. Fuerte-Esquivel, "A robust optimization approach for the interdependency analysis of integrated energy systems considering wind power uncertainty," *IEEE Trans. Power Syst.*, vol. 28, pp. 3964–3976, 2013.

[110] J. Li, J. Fang, Q. Zeng, and et al.:, "Optimal operation of the integrated electrical and heating systems to accommodate the intermittent renewable sources," *Appl. Energy*, vol. 167, pp. 244–254, 2016.

[111] M. Moeini-Aghtaie, P. Dehghanian, M. Fotuhi-Firuzabad, and et al.:, "Multi agent genetic algorithm: an online probabilistic view on economic dispatch of energy hubs constrained by wind availability," *IEEE Trans. Sustain. Energy,*, vol. 5, pp. 699–708, 2014.

[112] L. Bai, F. Li, T. Jiang, and et al., "Robust scheduling for wind integrated energy systems considering gas pipeline and power transmission N–1 contingencies," *IEEE Trans. Power Syst.*, vol. 32, pp. 1582–1584, 2017.

[113] M. Moeini-Aghtaie, A. Abbaspour, Fotuhi-Firuzabad, and et al., "A decomposed solution to multiple-energy carriers optimal power flow," *IEEE Trans. Power Syst.*, vol. 29, pp. 706–716, 2013.

[114] S. S. Bahrami and A. Sheikhi, "From demand response in smart grid toward integrated demand response in smart energy hub," *IEEE Trans. Smart Grid*, vol. 7, pp. 650–658, 2016.

[115] M. Alipour, K. Zare, and M. Abapour, "MINLP probabilistic scheduling model for demand response programs integrated energy hubs," *IEEE Trans. Ind. Inf.*, vol. 14, pp. 79–88, 2018.

[116] S. Pazouki and M. R. Haghifam, "Optimal planning and scheduling of energy hub in presence of wind, storage and demand response under uncertainty," *Elsevier J. Electr. Power Energy Syst.,*, vol. 80, pp. 219–239, 2016.

[117] X. Li, R. Zhang, L. Bai, and et al., "Stochastic low-carbon scheduling with carbon capture power plants and coupon-based demand response," *Appl. Energy*, vol. 210, pp. 1219–1228, 2018.

[118] A. Sheikhi, M. Rayati, and A. M. Ranjbar, "Energy Hub Optimal Sizing in the Smart Grid: Machine Learning Approach," *ISGT*, 2015.

[119] S. Ali, K. Wu, K. Weston, and D. Marinakis, "A Machine Learning Approach to Meter Placement for Power Quality Estimation in Smart Grid," *IEEE Transactions on Smart Grid*, 2016.

[120] M. Ozay, I. Esnaola, F. T. Y. Vural, S. R. KULKARNI, and h. V. Poor, "Machine Learning Methods for Attack Detection in the Smart Grid," *IEEE Transactions on Neural Networks and Learning Systems*, 2016.

[121] W. Zhang, G. Chen, Z. Dong, J. Li, and Z. Wu, "An Efficient Algorithm for Optimal Real-Time Pricing Strategy in Smart Grid," *2014 IEEE PES General Meeting*, 2014.

[122] F. Guo, C. Wen, and Z. Li, "Distributed Optimal Energy Scheduling Based on a Novel PD Pricing-Feedback Strategy in Smart Grid," *2015 IEEE ICIEA*, 2015.

[123] V. R. E and V. A, "Distribution Grid Impacts of Smart Electric Vehicle Charging From Different Perspectives," *IEEE Trans. on Smart Grid*, vol. 6, pp. 333–342, 2015.

[124] S. L. Arun and M. P. Selvan, "Dynamic Demand Response in Smart Buildings Using An Intelligent Residential Load Management System," *IET Generation*, vol. 11, pp. 4348–4357, 2017.

[125] L. Zhao, Z. Yang, and W. Lee, "Effectiveness of Zero Pricing in TOU Demand Responses at the Residential Level," *2017 IEEE/IAS ICPS*, 2017.

[126] N. Yaagoubi and H. T. Mouftah, "Energy Trading in the Smart Grid: A Distributed Game - Theoretic Approach," *Canadian Journal of Electrical and Computer Engineering*, vol. 40, pp. 57–65, 2017.

[127] L. Piao, Q. Ai, and S. Fan, "Game Theoretic Based Pricing Strategy for Electric Vehicle Charging Stations, journal = RPG 2015 year = 2015,"

[128] N. Yaagoubi and H. T. Mouftah, "Game Theory and Pricing Strategies for Demand-Side Management in the Smart Grid," *2014 CSNDSP*, 2014.

[129] Y. Park and S. Kim, "Game Theory-Based Bi-Level Pricing Scheme for Smart Grid Scheduling Control Algorithm," *Journal of Communication and Network*, vol. 18, pp. 484–492, 2016.

[130] M. Alamaniotis and L. H. Tsoukalas, "Implementing Smart Energy Systems: Integrating Load and Price Forecasting for Single Parameter Based Demand Response," *2016 IEEE PES ISGT-Europe*, 2016.

[131] T. Jiang, Y. Cao, L. Yu, and Z. Wang, "Load Shaping Strategy Based on Energy Storage and Dynamic Pricing in Smart Grid," *IEEE Trans. on Smart Grid*, vol. 4, pp. 2868–2876, 2014.

[132] G. E. Rahi, S. R. Etesami, W. Saad, N. Mandayam, and H. V. Poor, "Managing Price Uncertainty in Prosumer-Centric Energy Trading - A Prospect-Theoretic Stackelberg Game Approach," *IEEE Trans. on Smart Grid*, 2017.

[133] M. G. Flammini, G. Prettico, G. Fulli, E. bompard, and G. Chicco, "Interaction of Consumers, Photovoltaic Systems and EV Energy Demand in a Reference Network Model," *2017 ICEETA*, 2017.